CRANFIELD UNIVERSITY

HUSSAIN J. HUSSAIN

Development of a Hybrid Powerplant for Kuwait: The Simultaneous Production of Power, Fresh Water and Cooling

SCHOOL OF ENGINEERING

PhD THESIS

CRANFIELD UNIVERSITY

SCHOOL OF ENGINEERING

PhD THESIS

Academic Year 2009-2010

HUSSAIN J. HUSSAIN

Development of a Hybrid Powerplant for Kuwait: The Simultaneous Production of Power, Fresh Water and Cooling

Supervisor: Dr Ossama Badr

March 2010

This thesis is submitted for the degree of PhD

ABSTRACT

The harsh summer months of Kuwait combined with massive urbanisation projects, population growth and generous subsidies resulted in a rapid increase in electricity and freshwater consumption over the past 30 years. This led the government to invest heavily in large and capital intensive cogeneration powerplants that generate electricity via steam turbines and produce desalinated seawater through the utilisation of the multi-stage flash (MSF) desalination process. Air-conditioning (A/C) load accounts for about 70% of electric peak-load during summer. As a result, Kuwait consumes annually millions of barrels of oil and tons of natural gas that can be otherwise exported or saved for the future as a strategic commodity.

The main objective of this research is to develop, model and recommend an optimum hybrid powerplant configuration and operation strategy for Kuwait that can simultaneously satisfy the demand for electricity, freshwater and cooling based on minimum fuel consumption. This is achieved by modelling and simulation of steam Rankine cycle, MSF water desalination and absorption refrigeration systems (ARSs) in Matlab to estimate their steam consumption. Reverse osmosis (RO) desalination and vapour-compression A/C are linked to the hybrid simulation program via their electricity consumption.

Simulations show that during the hybrid configuration power-RO-AR is the most viable for Kuwait. During the winter months of January, February and December the optimum operation strategy with minimum fuel cost is the power-RO. On the other hand, operating the powerplant in the power-RO-AR hybrid mode during summer results in minimum fuel cost. The total annual fuel cost savings resulting from modifying the Doha West (DW) powerplant configuration and operation strategy are estimated to be about $363 million. This amounts to savings of about 8 million barrels of oil and 114 million m^3 of natural gas per year. Furthermore, the payback period of hybridising the DW powerplant by adding RO desalination and AR system is one year with net savings of $127 million in the second year of operation.

ACKNOWLEDGMENTS

I wish to express my sincere thanks and gratitude to my supervisor Dr. Ossama Badr for his support, valuable and continuous advice, guidance, and assistance throughout the duration of the research work.

My thanks also go to the Kuwait Institute for Scientific Research (KISR) for the scholarship and financial support for the duration of my study at Cranfield University.

The support and understanding of Dr Adel Hussain, the manager of the Buildings and Energy Technology (BET) department at KISR and my colleagues is highly appreciated. Special thanks are due for my colleague and dear friend Dr. Mohammed Sebzali for his advice and support whenever I needed him.

My gratitude belongs to my father and my mother, whose love, encouragement, support and faith meant a very great deal to me. I would like to express my appreciation for all the kind support they have offered. It would have been much harder without such support. I also thank my sisters and all my family members for their words of kindness and encouragement.

Thanks to my lovely kids Fatmah and Mohammed.

Last but not least, I would like to express my gratefulness and gratitude to my wife Eman for her unconditional support, encouragement and tolerance over the life of this PhD. Without her love and care, it would simply not have been possible.

Table of Contents

List of Figures

List of Tables

NOTATIONS

B, B_0, B_1, …, B_7	Coefficients of Equations 3.16 and 3.18, defined in Equation 3.19
BPE	Boiling point elevation
C_{barrel}	Price of heavy oil barrel in $US
$C_{gas,total}$	Monthly cost of natural gas at DW in $US
C_{oil}	Monthly cost of oil in $US
C_{gas}	Price of natural gas in $/M. Btu
C_P	Specific heat (kJ/kg.°C)
$Ca_{AR,unit}$	Refrigeration capacity of one AR unit (MW)
$Ca_{MSF,H}$	High MSF unit capacity in m^3/day
$Ca_{MSF,L}$	Low MSF unit capacity in m^3/day
Ca_{RO}	Capacity of one RO unit, 110,000 m^3/day
CC	Carbon content coefficient in kg carbon/kJ
CV_{gas}	Calorific value of natural gas of 38302 kJ/m^3
CV_{oil}	Calorific value of heavy oil of 43,959 kJ/kg
d	discount rate (%)
$days$	Days of the month
D, E, F', G	Coefficients on Equation 3.22, defined in Equation 3.23
E	Energy consumption (kWh/m^3)
$E_{gas,total}$	Total natural gas energy consumed at DW
$E_{RO,total}$	Monthly electricity consumed by RO, kWh
$E_{RO,unit}$	Estimated specific energy consumption of one RO unit, kWh/m^3
F	Fraction of fuel oxidised
F, F_0	Coefficients of Equation 3.16, defined in Equation 3.19
FS	Fuel savings (million US dollars)

H	Height of the brine pool (m)
$h_{MSF,liquid}$	Enthalpy of liquid water leaving brine heater of MSF units into condensed water line (kJ/kg)
$n_1, n_2, \ldots, n_{10}$	Coefficients of Equation 3.22, defined in Table 3.1
L	Flash chamber length (m)
$m_{AR,total}$	Mass flowrate of steam to run *N* number of AR units for a s*ingle* turbine-set
$m_{AR,unit}$	Mass flowrate of steam required by one AR unit (kg/s)
$m_{MSF,H}$	Production capacity of a single high capacity MSF unit
$m_{MSF,L}$	Production capacity of a single low capacity MSF unit, 313.25 kg/s
$m_{oil,MSF,L}$	Mass flowrate of residual oil consumed by low capacity MSF in kg/month
n	Number of feed water heaters
N	A function of temperature in Equation 3.34, defined in Equation 3.35
NB_{oil}	Total number of heavy oil barrels consumed at DW per month
$N_{MSF,L}$	Number of low capacity MSF units
$N_{MSF,H}$	Number of high capacity MSF units
N_{RO}	Number of RO units to satisfy demand
NT	Number of steam turbines in operation
NEA	Non-equilibrium allowance
Pr	Power (kW)
p	Pressure (N/m^2)
p^*	Pressure in Equation 3.21, defined in Equation 3.23
q	Specific amount of heat transferred (J/kg)
$\dot{Q}$	Volumetric flowrate of water (m^3/s)
$\dot{Q}_b$	Flashing brine flowrate per chamber width (kg/m s)
Q_{boiler}	Heat input into boiler in kJ/kg

$Q_{bh,H}$	Heat input to the brine heater section of high capacity MSF in kJ/kg
$Q_{bh,L}$	Heat input to the brine heater section of low capacity MSF in kJ/kg
RF	Refrigeration capacity (kW_R)
R_{CO_2}	The quantity of CO_2 released to the atmosphere in million tonnes per unit of fuel consumed
s	Specific entropy (J/kg K)
S	Salt concentration (ppm)
t	year in payback period calculations, Equation 7.5
T	Temperature
T^*	Temperature in Equation 3.22, defined in Equation 3.23
$Unit_{AR}$	The total number of AR units to replace AC load at DW
V	Reduced specific volume in Equation 3.29, defined in Equation 3.30
$V_{gas,total}$	Monthly natural gas consumed at DW in m^3
$V_{gas,MSF}$	Volume of natural gas consumed by MSF units in m^3/month
w	Specific work (J/kg)
W	Work (kW)
W_{demand}	Expected monthly distilled-water demand in m^3
WW	Distilled water (m^3)
x	Steam quality
y	Maximum number of years to offset capital investment

Subscripts

AR	Absorption refrigeration
B	Boiler
bd	Blowdown stream
bh	Brine heater

c	Condenser
cw	Cooling water in condenser tubes of heat rejection section
d	Distillate
e	extracted steam
f	Saturated water phase
fb	Flashing brine
g	Saturated vapour phase
H	Feed-water heater
i	Number of stages in heat recovery section
j	Number of stages in heat rejection section
mant	Maintenance
n	Total number of flashing stages
net	Net output
P	Pump
r	Reheat
rec	Recirculation brine in heat recovery section
RO	Reverse osmosis
s	Saturated state
T	Turbine
T-HP	High-pressure turbine
T-LP	Low pressure turbine
v	Vapour

Greek letters

a_{oil}	Percentage of oil consumption at DW which equals 90%
ε	Efficiency (%)
λ	Latent heat of vaporisation (kJ/kg)
ΔT	Stage temperature drop (°C)

b	Coefficient in Equation 15, defined in Equation 17
b'	Coefficient defined in Equation 21
t	Coefficient of Equation 34
k	Conversion factor of 1.63×10^{-4} barrel oil equivalent (bboe)
Γ	A function of temperature in Equation 27, defined in Equation 30
w	A factor to convert energy from kJ to Btu, 0.948
h_{boiler}	Efficiency of auxiliary boiler
h_P	Isentropic efficiency of a pump (%)
h_T	Isentropic efficiency of a turbine (%)
h_{th}	Thermal efficiency (%)
Δh_{lat}	Latent heat of vaporisation (J/kg)
ΔP	Pump head (kPa)
Δs_{lat}	Entropy of vaporisation (J/kg K)
ΔT_{opt}	Optimal temperature rise
v	Specific volume (m^3/kg)
c	A function of temperature in Equation 23, defined in Equation 24

ABBREVIATIONS

A/C	Air-conditioning
ARS	Absorption refrigeration system
COP	Coefficient of performance
DC	Degrees of subcooling
DW	Doha West
GT	Gas turbine
GDP	Gross domestic product
GNI	Gross national income
ICE	Internal combustion engine
KISR	Kuwait Institute for Scientific Research
MEW	Ministry of Electricity and Water, Kuwait
MSF	Multi-stage flash
PR	Power rating
RO	Reverse osmosis
ST	Steam turbine
TTD	Terminal temperature difference
VC	Vapour-compression

1. Introduction and Thesis Overview

1.1. Background

Kuwait is located in a hot and dry desert region with typical summer average daily temperatures in the range 42°C to 46°C. This harsh climate has deprived the country of large-scale natural freshwater resources. To be able to further develop the country socially and economically, and to meet the growing demand for electricity and freshwater, the government decided to invest in central cogeneration (i.e. dual-purpose) powerplants, where electricity and distilled water are produced simultaneously via the steam cycle and multistage flash (MSF) desalination process, respectively. Advantages of such plants include fuel savings and lower capital and maintenance costs compared with separate production of electricity and water.

Kuwait, however, since commissioning the first cogeneration powerplant in the 1950s (MEW, 2002a) has failed to curb the continuing rapid growth in consumer electricity and freshwater demands. This trend may be attributed to the boom in the economy during the past three decades, population increase and the generous subsidies of electricity and water unit prices by the government, reaching around 75%-80% of actual production cost. The extremely high temperatures during summer months, coupled with cheap electricity prices, have also lead to the widespread use of air-conditioning (A/C) in every household. The extensive use of A/C systems during summer, with peak loads of around 45 - 70% of generation capacity, has lead to power shortages and blackouts around the country as the total demand frequently exceeds installed capacity (Al-Fuzai, 2007). Kuwait depends on MSF desalination to satisfy more than 90% of its freshwater demand (Darwish et al., 2008). An inherent disadvantage of the MSF desalination technology is its high

energy consumption and the inflexible water-to-power production ratio when coupled with steam power generation in a cogeneration plant (El-Sayed, 2001). Another cause for concern is the faster rate of growth of freshwater demand compared with that for power (Darwish et al., 2008), which may lead to freshwater shortage in the future.

The reduction or negation of the generous subsidies can help curb the annual and peak growth in electricity and water consumption. However, it is not an option at the moment since the elected members of parliament refuse to agree to any government proposal in this direction.

1.2. Hybrid Powerplants

Cogeneration powerplants operating in Kuwait, which incorporate the high-energy consuming MSF desalination process suffer a fuel penalty due to the additional production of steam in separate boilers in order to satisfy freshwater demand (El-Sayed, 2001). Such plants use commonly oil – the strategically and economically vital commodity for Kuwait – as a fuel. To continue satisfying power and freshwater needs and slow the rate of consumption of oil, the government needs to look at alternative solutions. The Ministry of Electricity and water (MEW) can invest in new efficient plants such combined-cycle (CC) power plants coupled with efficient desalination processes such as reverse osmosis (RO). Alternatively, it can retrofit existing cogeneration powerplants with more efficient and flexible technologies. These plants can be turned into "hybrid" plants which include MSF and RO desalination, and may also include absorption refrigeration (AR) systems to satisfy the demand for cooling during summer months (Abdel-Jawad et al., 2001; El-Sayed, 2001; Darwish, 2001; Hamed, 2005; Al-Katheeri and Agashichev, 2008; Darwish et al., 2008 & 2009; Fois et al., 2008; and Kamal, 2008). Benefits of such hybrid plants include fuel savings, reduced harmful emissions to the environment,

greater flexibility in dealing with demand, and delayed rate of commissioning of new powerplants.

This research study investigates operation strategy, fuel consumption and associated CO_2 emissions of cogeneration plants currently operating in Kuwait. Different hybrid powerplant configurations that include MSF and RO desalination to satisfy potable water demand, and vapour-compression (VC) and AR systems to satisfy A/C cooling demand will be modelled, simulated and analysed. Fuel consumption comparisons will be drawn to be able to recommend the most feasible configuration(s) for Kuwait.

1.3. Aim and Objectives

The aim of this study is to develop efficient hybrid powerplant configurations and operation strategy for the simultaneous production of power, freshwater and cooling for Kuwait. This is achieved through the modelling and simulation of the main thermally-driven processes within the plant, namely, the Rankine steam cycle, MSF desalination and AR cooling system in order to estimate their steam consumption. The energy consumption of the electrically-driven RO desalination process and VC A/C systems are also estimated. Hence, this research is only concerned with the feasibility of energy and cooling production systems within the powerplant. Electricity transmission and chilled-water distribution networks (i.e. district cooling schemes) are not studied in this work. These are not included because it adds a new dimension to the research which does not conform to the stated objective above.

The Doha West (DW) is used as the reference and typical powerplant in this study. Different configurations of the plant when operating as a hybrid system are simulated with the aim of satisfying the demand for power, freshwater and cooling with the least consumption of fuel and CO_2 emissions.

The simulations are performed on a monthly basis to account for seasonal changes in demand. The consumption and production data used in this study are taken from MEW statistical year book for 2001.

1.4. Thesis Overview

The thesis comprises eight chapters:

- *Chapter 1* is an introduction which describes the background and aims.

- *Chapter 2* gives a general background on the State of Kuwait. The electricity and freshwater production and consumption profiles are presented to demonstrate the current situation regarding the power generation sector in Kuwait and the imminent problems facing it.

- *Chapter 3* describes the steam Rankine cycle in detail and the different improvements added to increase its efficiency. Then the different modelling techniques used by researchers are studied to help in the selection of a suitable model for this research work. The final part presents the mathematical model used to simulate the steam Rankine cycle and a validation of the model using performance data from an existing powerplant in Kuwait.

- *Chapter 4* presents a detailed description of the two most popular desalination processes today, namely, the MSF and RO. Section 4.1 starts with describing the MSF desalination process and introduces the steady-state mathematical model developed to simulate its performance. The model is validated using available data from a MSF desalination plant currently operating in Kuwait. Section 4.2 describes RO desalination and its benefit in regard to energy consumption. The specific energy consumption of RO desalination plants is then estimated using experimental data from a pilot plant operating in Kuwait, and the result is then compared to published energy consumption data from literature.

- *Chapter 5* describes the VC refrigeration cycle, which is the most common cycle utilised for A/C systems in Kuwait and around the world. The average coefficient of performance (COP) from the different types of A/C systems operating in Kuwait is then estimated using data collected by the Buildings and Energy Technologies Department at the Kuwait Institute for Scientific Research (KISR). The single- and double-effect AR systems are both described in Section 5.2. The mathematical model for the double-effect system, based on a literature review of developed models, is then presented and validated.

- *Chapter 6* introduces the hybrid powerplant configurations developed for performance evaluation, and then selection based on its performance. The assumptions and constraints for the models are presented. In addition, the equations for the estimation of steam flows and consumption, fuel consumption and CO_2 emissions are developed and presented in the chapter. The details of each hybrid configuration with corresponding flow diagrams are also presented.

- *Chapter 7* presents the simulation results of the original cogeneration powerplant and for the hybrid configurations discussed in the previous chapter. The performance parameter selected to compare results of the different models is the fuel cost, which includes the cost of both heavy oil and natural gas utilised at Kuwait's powerplants. The results are based on monthly fuel consumption to study the effects of seasonal variations on the type of hybrid configuration selected. The final recommendation for the most feasible hybrid configuration and operation strategy for Kuwait is then given based on the minimum fuel cost for each month of the year. The monthly and total fuel cost savings are estimated and presented. Finally, a cost analysis is presented to justify the investment in the selected hybrid powerplant configuration.

- The conclusions are given in *Chapter 8*. Also, Recommendations for future work are suggested in this chapter.

- Finally, *Appendix A* includes a MSF rigorous model and RO energy consumption data from the pilot plant. *Appendix B* presents power consumption data for A/C units in Kuwait, and the single-effect ARS mathematical model with its validation. *Appendix C* gives detailed results for all hybrid models in tabulated form including CO_2 emissions.

Chapter 2

2. Kuwait: Background and Electricity & Water Profiles

2.1 Introduction

With start of the energy crisis of the 1970s, industrialised countries have started the process of searching for new energy producing technologies. Many researchers and scientists developed systems that depend on renewable energy resources. Others modified and improved conventional systems to make them more energy efficient. Cogeneration of heat and power using a number of prime movers was one option that stood out, especially with the advancement of gas turbine systems. Since then, cogeneration has been increasingly becoming popular in industrialised countries, especially in Western Europe. Cogeneration systems not only save energy due to the simultaneous use of power and heat, they generally have a lower capital cost than conventional powerplants and their construction lead-time is shorter.

For the Gulf council Countries (GCC), Saudi Arabia, Kuwait, Oman, Qatar, Bahrain, and United Arab Emirates, business continues to be as usual. To meet the growing demand for electricity and water, the governments of these countries decided to invest heavily in central power stations, where electricity and distilled seawater are produced. However, due to the global concern over the depletion of oil and natural gas reserves and the environment, these countries must start looking for other viable power generation options.

In Kuwait, all powerplants are dual-purpose plants, where electricity is generated via steam turbines, and potable water is produced by the distillation of seawater. All of the plants are fuelled either by oil products or natural gas. Looking at the electricity and freshwater demand trends, Kuwait has failed to curb or slow the growing consumer demand. This trend may be attributed to the boom in the economy during

the past three decades, population increase and the generous subsidy of electricity and water by the government, reaching around 75%-80% of actual cost. Also, the extremely high temperatures during the summer months lead to the widespread use of air-conditioning in every household, regardless of level of income because of the cheap electricity prices.

This chapter gives a background on Kuwait in regard to its location, climate, population and energy consumption. The chapter also explores the main reasons for the rapid increase of electricity and water consumption in the country. An overview of the power generation and water desalination sectors is given with corresponding production and consumption data.

Further more the freshwater resources are discussed. Seawater desalination by the multi-stage flash (MSF) technique is the main source of freshwater in Kuwait. Hence, the number of desalination units and their capacities are focussed on and discussed.

2.2 Topography and Climate

Kuwait is located at the far north-western corner of the Persian Gulf, known locally as the Arabian Gulf (Figure 2.1). It is a small state with an area of about 17,818 km^2. At its most distant points, it is about 200 km north to south and 170 km east to west. Shaped roughly like a triangle, Kuwait borders the gulf to the east, with 195 km of coast line, bounded to the south, west and North by Saudi Arabia and Iraq.

Kuwait has a desert climate; typically hot and dry. It is also entirely flat. Average annual rainfall varies from 75 to 150 mm across the country with a range of between 25 to as much as 325 mm per year. In summer, average daily temperatures range from 42°C to 46°C; the highest recorded temperature is 51.5°C. The summers are long, punctuated mainly by dust storms in June and July when north-westerly winds cover the cities in sand. In late summer, which is more humid, there are occasional

sharp, brief thunderstorms. By November, summer is over, and colder winter weather sets in, dropping temperatures to as low as 3°C at night; daytime temperature is in the upper 20s°C range (Library of Congress, 2003).

2.3 Population Growth

During the 1950s and 1960s, Kuwait's population rose dramatically on account of massive immigration from surrounding countries. The influx of migrants was due in part to Kuwait's rapid expansion as a modern state with a flourishing economy and massive employment opportunities. The result is a multi-national mixture of people from other Arab countries, East Asian and South Asian countries, and some Europeans and North Americans. In 1957, when the first official census was carried out, Kuwait had 206,000 inhabitants. By the end of June 2008, the total population had reached approximately 3.3 million, with only 1.04 million Kuwaitis (Kuwait Information Office, 2009). In the early 2000's, the population growth rate was at 3.5% (World Fact Book, 2009). Figure 2.2 shows the population trend for the years 1985 to 2008. The decrease in population between 1990 and 1991 is due to the Gulf war, and the subsequent return of most foreign workers to their countries.

2.4 Economy

2.4.1. Oil Sector

Kuwait's economy is dominated by its oil industry. In the 1990s, the unexpected decline in oil prices reduced government revenues, and placed constraints on government spending. As the country continues to depend on this one natural resource, fluctuations in the demand for oil directly affects the country's development plans. Recently, the oil revenues have started to rise, due in part, to the lower OPEC quotas of the member countries and growing demand from emerging economies. There is new awareness among Kuwaitis that they need to diversify their sources of income. Accordingly, the Kuwaiti Government has been taking some measures to encourage private-sector investments.

Figure 2.1. Map of the State of KuwaitMap of the State of Kuwait

Kuwait's crude oil production is currently running at 2.78 million barrels per day, which is close to the maximum production capacity. In the oil sector, crude production may remain constant for some time, in conformance with OPEC quotas. However, Kuwait plans to increase its capacity to 4 million barrels per day by 2020 (DOE, 2009).

2.4.2. Non-Oil Sector

Kuwait's non-oil economy grew by an estimated 7% in 1995 and 1996 as domestic demand increased because of the return of the number of expatriate workers to early pre-Gulf War levels. In 1952, the Kuwait Investment Board was established

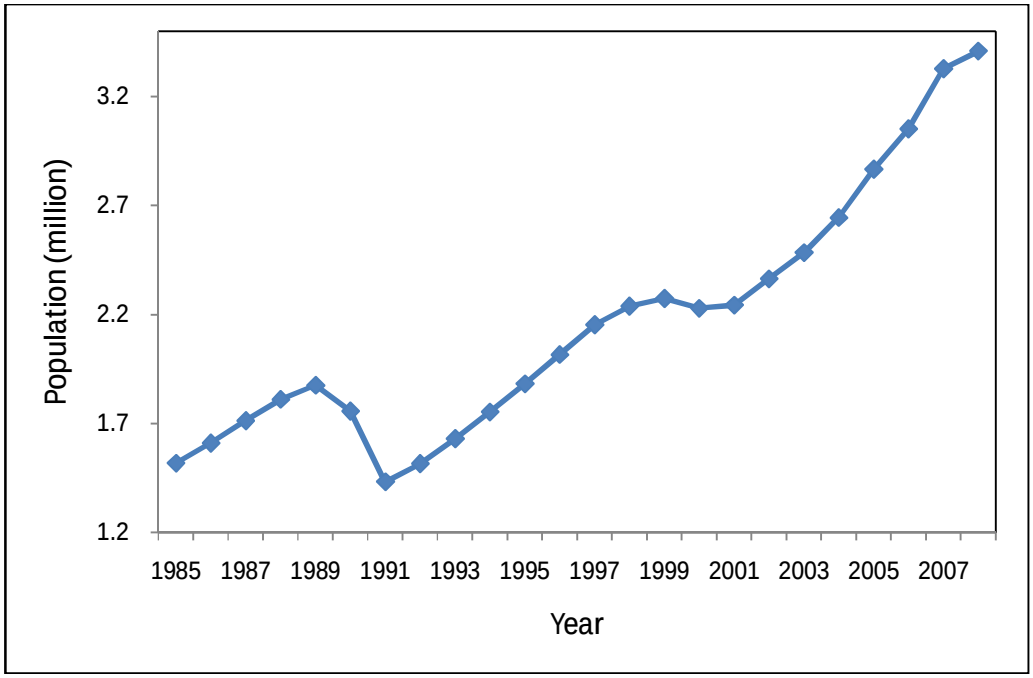

Figure 2.2 Population trend for the State of Kuwait from 1985-2008

in London to manage Kuwait's portfolio of foreign investments. In 1958, the Kuwaiti Investment Board became the Kuwait Investment Office (KIO), managed by Kuwaiti nationals. Kuwait's investments were prudent, combining safety with capital appreciation and income.

In the 1980s, Kuwait began diversifying its overseas investments, placing more investments in Japanese firms. By the late 1980s, Kuwait was earning more from these overseas investments than it was from the direct sale of oil: in 1987 foreign investments generated US$6.3 billion, while oil revenues were US$5.4 billion. The *Financial Times* of London estimated Kuwait's overseas investments in early 1990 at more than US$100 billion, most of it in the Reserve Fund for Future Generations (Library of Congress, 2003).

2.4.3. Labour Force

Kuwait's total labour force has increased from 1.248 million in the middle of 1999 to about 2 million in 2008. Of this current total, approximately 20% are Kuwaiti nationals. Kuwaiti female workers make up about 42% of the total Kuwaiti labour force, but when calculated against the total labour force in Kuwait, this number declines to 23%. In 2006, Kuwaiti workers in the public sector amounted to a total of 285,257, equal to about 84% of the Kuwaiti labour force. In the private sector, the Kuwaiti labour force amounts to approximately 42,440, representing only 12% of the Kuwaiti work force, 2.7% of the total labour force in the private sector, and about 2% of the entire labour force (KIBS, 2009 and World Fact Book, 2009).

2.4.4. Economic Indicators

According to World Fact Book (2009), the Gross Domestic Product (GDP) was $149.1 billion in 2008 with an increase of 8.5% from 2007 figure of $137.5 billion. The contribution of oil and gas sectors is about 50%. This increase is due mostly to the increase in the average price of a barrel of oil from $64.20 per barrel in 2007 to $91.48 per barrel in 2008. Figure 2.3 shows the trends in GDP for the years 1985 to 2007. The figure shows that there was a drop in GDP during the years 1997-1999 because of the drop in oil prices.

The per capita gross national income (GNI) reflects the average income of a country's citizens and is an indication of the general standard of living. The per capita GNI for Kuwait rose steadily following the Gulf war in 1991 up to 1998 when the price of oil fell to around $10 as shown in Figure 2.4. The per capita GNI increased to $38,227 in 2006, an increase of 19% from the 2005 figure of $32,001. The sharp increase was due to the record increase in the price of oil during 2006-2007.

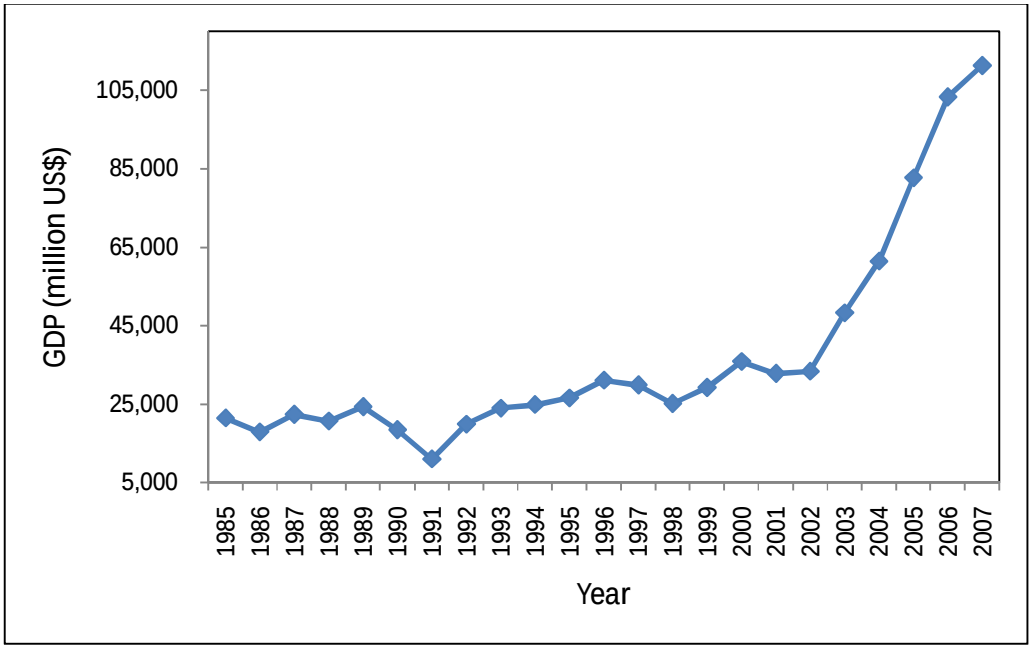

Figure 2.3 Trends in GDP for the period 1985-2007

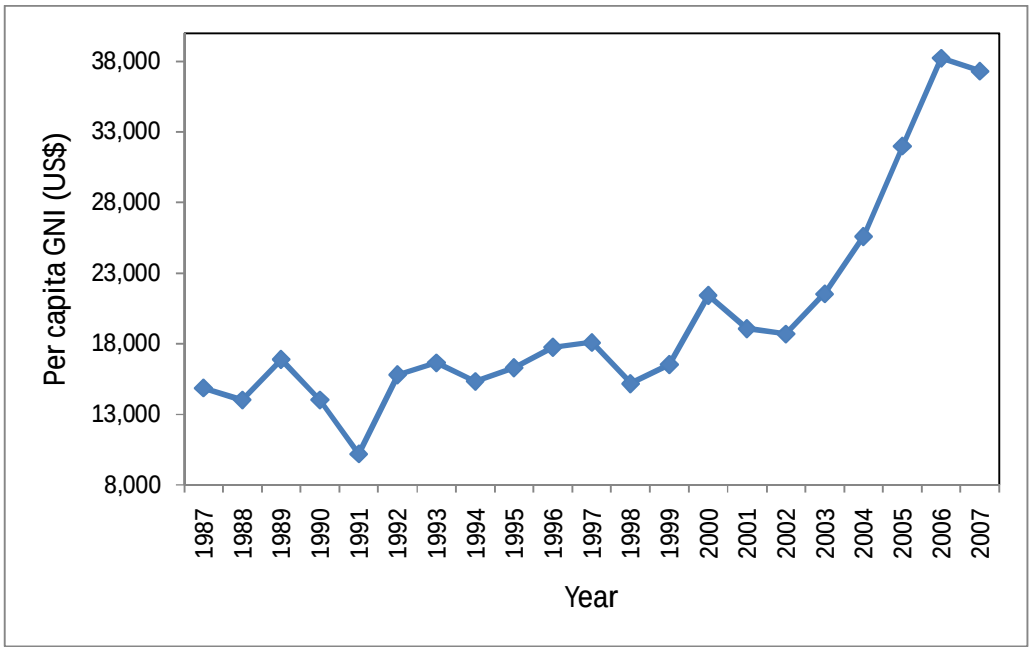

Figure 2.4 Trends in per capita GNI for the period 1987-2007

(IMF, 2009)

2.5. Energy

Petroleum and natural gas represent the two main natural resources of energy and national income for Kuwait. They have been a priority in development projects depending on the balance between production levels and consumption rationalisation. According to EIA (2009), the fuel share of energy consumption in Kuwait is 59% for oil and 41% for natural gas. Figures 2.5 and 2.6 show oil and natural gas consumption trends, respectively, for the period 1980-2008.

2.5.1. Oil

Kuwait has an estimated 104 billion barrels of proven oil reserves, which is between 8% and 9% of the world total. The Neutral Zone area, which Kuwait shares with Saudi Arabia, holds 5 billion barrels of reserves, half of which belongs to Kuwait. Most of the oil fields in Kuwait have been producing since the 1950s, and in 2008 it produced around 2.8 million barrels per day (EIA, 2009). Figure 2.7 shows the trend in oil production for the period 1980-2008. From the figure we can see that production went back to normal in 1993, following the sharp drop due to the Gulf War during 1990-1991.

2.5.2. Natural Gas

Kuwait produces a relatively modest volume of natural gas, the vast majority of which is "associated gas" (i.e., found and produced in conjunction with oil). Kuwait hopes to increase its use of natural gas (both domestic and imported) significantly, especially in electricity generation, water desalination, and petrochemicals. A switch to natural gas (from diesel oil) would free up a substantial amount of oil for export (EIA, 2003). Kuwait also hopes to reduce flaring of associated gas by tying together gathering centres. Finally, Kuwait continues to seek both associated and non-associated gas supplies. The increased use of natural gas in electricity generation has

caused consumption to outpace production during the summer months. Figure 2.8 shows the production of natural gas for the period 1980-2008.

In March 2009, Kuwait and Qatar singed an agreement whereby Kuwait would import liquefied natural gas each summer for the next 5 years (EIA, 2009). The pipeline is to run from Qatar's port of Ras Laffan to the LPG terminal at Ahmadi port. Kuwait and The Islamic Republic of Iran signed a memorandum of understanding in 2005 for the import of natural gas from its Pars gas field (EIA, 2009).

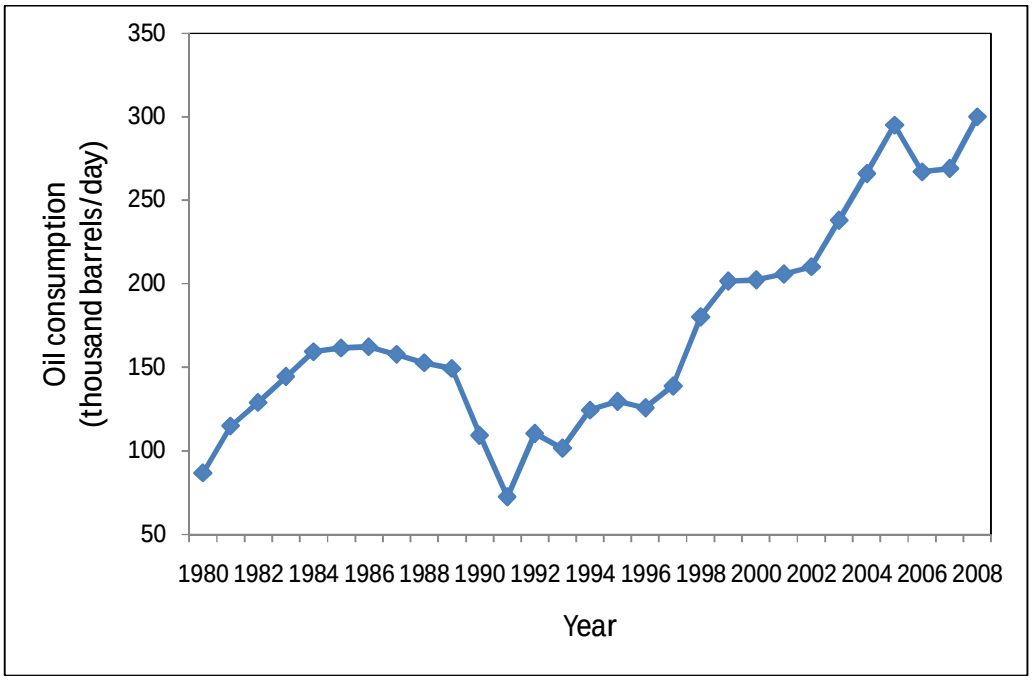

Figure 2.5 Oil Consumption in Kuwait for the period 1980-2008 (BP, 2009)

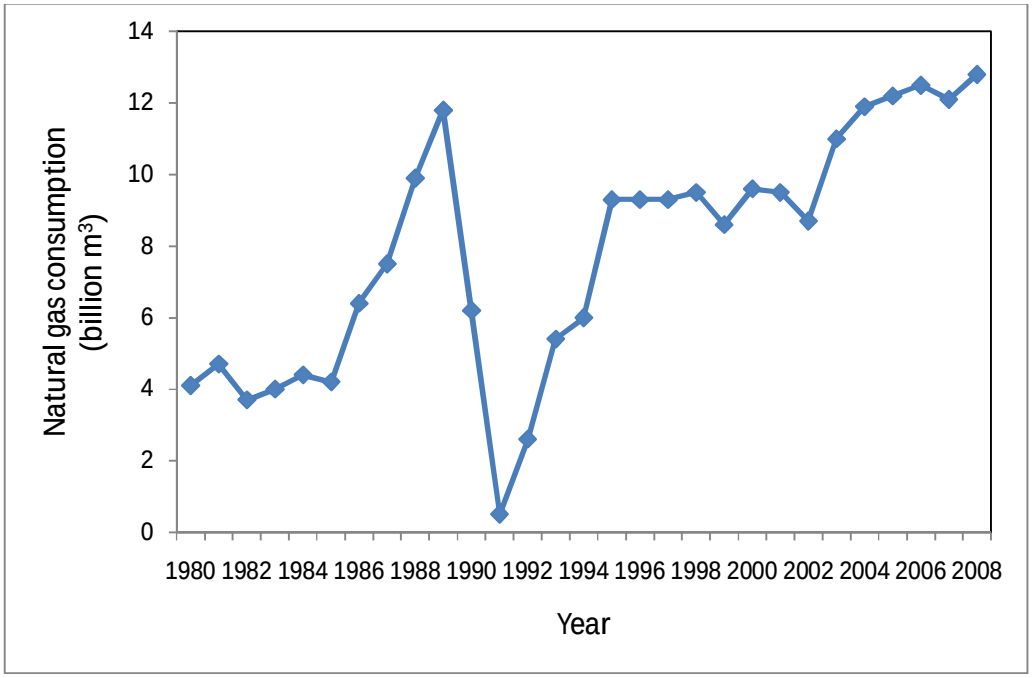

Figure 2.6 Natural gas consumption in Kuwait for the period 1980-2008 (BP,2009)

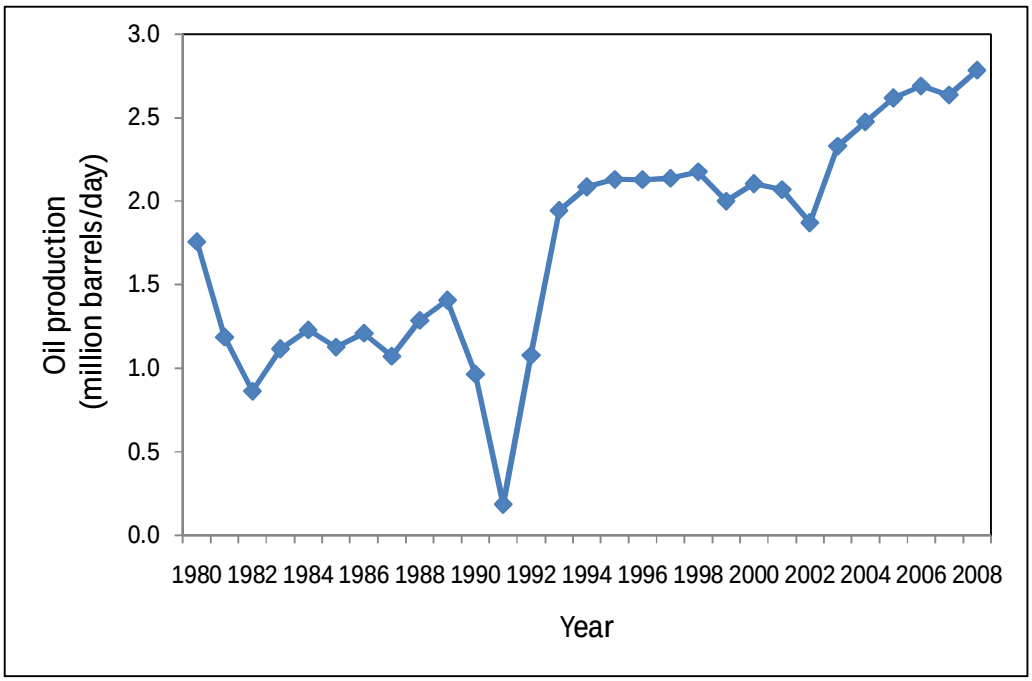

Figure 2.7 Oil production for the period 1980-2008 (BP, 2009)

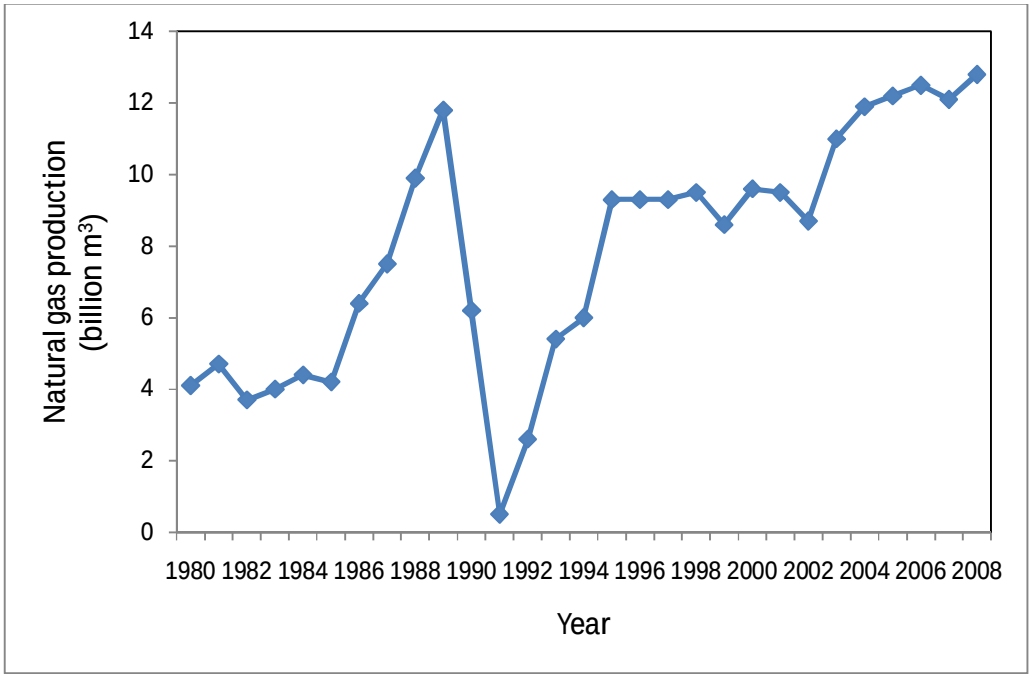

Figure 2.8 Natural gas production for the period 1980-2009 (BP, 2009)

2.6. Power Plants

Kuwait has six power stations: Shuwaikh, Doha East, Doha West, Subiya, Shuaiba South, and Az-Zour South. The total electrical generation capacity of these plants is about 10.48 GW. These power stations are powered by oil and natural gas. The consumption of the different fuels in power stations and the total fuel cost for the year 2007 are given in Table 2.1.

The plants simultaneously produce electricity and distilled water. Thus, the powerplants are equipped with steam turbines for the base load demand and the waste heat is used in multi-stage flash (MSF) desalination units to distillate seawater. All plants, therefore, are located near the sea shore to make use of it as a cooling medium for the powerplant condenser and a source for the desalination feedwater. Also, the plants include gas turbines that are only used for peak load demand, if necessary. The next sections will introduce the different power stations and their electricity and water production, and will also show the development in

demand for both. Table 2.2 shows the heat:power ratio when the plants are operating at full load and in cogeneration mode. The data is based on the acceptance test results at the time of commissioning of the plants.

The Shuwaikh powerplant used to produce both electricity and freshwater prior to August 1990. However, due to the large destruction of the plant during the Gulf War, it now produces electricity via gas turbines and modest amounts of distilled water from MSF units using steam directly from boilers. The installed gas turbine capacity at Shuwaikh plant is 208.2 MW (MEW, 2008a).

2.6.1. Electricity

Kuwait's electricity demand has been growing rapidly in recent years at a rate of around 6% annually, and is expected to continue increasing at the same rate in coming years, necessitating construction of new generating capacity. A 2,400 MW, $2.2 billion thermal plant at Al-Subiya came online in 2000, which relieved pressure on the system in the short-term. Over the next 7 years (2000-2007), the installed capacity was increased by 1.0 GW to keep up with the increasing demand and to avoid blackouts during the summer months (MEW, 2008a).

Table 2.1 Consumption of fuels and fuel cost in Kuwait's power stations for 2007 (MEW, 2008a)

Station	Fuel (PJ)					Fuel cost (million KD)*
	Natural gas	Gas oil	Crude oil	Heavy oil	Total	
Shuwaikh	16.04	0	0	0	16.04	6.5
Shuaiba South	37.28	0	0	0	37.28	13.1
Doha East	17.26	0	30.89	15.22	63.37	146.9
Doha West	7.76	0	0	11.76	124.59	316.3
Az-Zour South	46.97	22.39	48.27	74.41	192.04	468.0
Sabiya	13.16	0.24	16.67	80.82	110.89	278.3

*KD = Kuwaiti Dinar = US$ 3.5 (October 2009)

Table 2.2 Heat:power ration for the cogeneration plants in Kuwait

Power Plant	Power Output (MW)	Heat to Distiller (MW)	Heat:Power Ratio
Shuaiba	134	91.7	0.68
Doha East	150	93.16	0.62
Doha West	300	190.24	0.63
Az-Zour	300	196	0.65

Kuwait's Ministry of Electricity and Water (MEW), which is in charge of Kuwait's power sector, has plans to install new electric capacity at several sites to satisfy the increasing demand (MEW, 2008a):

- A 4.9 GW combined cycle powerplant at Azzour North site, which is expected to be constructed by 2014.
- A 0.56 GW capacity increase at Azzour South powerplant in combined cycle mode starting operation in 2010
- A 0.8 GW Shuaiba North powerplant
- A 2.0 GW combined cycle project at Sabiya powerplant, which is expected to start operating in 2010
- A 3 GW Al Kheran powerplant starting operation of some units by 2015

Also, to reduce excessive power demand and waste, Kuwait is considering trimming some of its power subsidies. Currently, Kuwaitis pay among the lowest prices for power in the world, and the MEW has urged them to use power more judiciously. Meanwhile, Kuwait continues to expand its national power grid.

2.6.2. Water

With the scarcity of freshwater resources, Kuwaitis relied on rain water and shallow wells for their potable water needs (i.e. 110 mm per year). But, due to the growth of population rain water became no longer sufficient to cater for the growing demand.

So, at the turn of the past century, Kuwaitis turned to "shaat al-Arab" near the Kuwaiti border in Iraq for freshwater, and it was brought by dhows. However, after the discovery of oil Kuwait could invest in modern freshwater production facilities. In the early days, the first desalination plant was built, and it was based on the submerged tube technique. When the flash method was introduced, Kuwait was the first to adopt it. Table 2.3 shows the development in freshwater production capacity since 1960.

As mentioned in the above section, one of the sources of potable water in Kuwait is the desalination of seawater by MSF distillation in cogeneration plants. However, there are other sources that contribute to the total freshwater production in the country, although with a smaller percentage share. The freshwater resources in Kuwait are:

- Groundwater
- Desalinated sea- and brackish groundwater
- Treated wastewater effluents

Table 2.3 Development of freshwater production capacity (MEW, 2008b)

Year	Capacity (million m^3)
1960	0.027
1970	0.122
1980	0.454
1990	1.145
2000	1.305
2007	1.905

2.6.2.1. Fresh Groundwater

As for fresh groundwater, limited quantities were discovered at both Al-Rawadatain and Um Al-Aish fields, with an estimated natural reserve of about 181 million m^3. Currently, water is pumped from the Al-Rawadatain field only at a rate between

4,546 and 9,000 m^3/day to a bottling plant to avoid exhaustion of the natural reserve. The fresh groundwater has a total dissolved solids (TDS) concentration of 600-1000 parts per million (ppm) (MEW, 2008b).

2.6.2.2. Seawater Desalination

At present desalination of seawater is achieved in four cogeneration plants and one desalination only plant using the MSF technology. The capacity of these units ranges between 23,000 and 57,000 m^3/day. However, the total capacity of the distillation units in the cogeneration powerplants as of 2007 is 1.9 million m^3/day including high temperature operation of distillers at Doha West and Az-Zour South stations (MEW, 2008b). Distilled water is mixed with brackish water in order to produce potable water which is suitable for human use.

To keep up with the growing demand for freshwater in the country, MEW is planning to install new desalination units in the near and far future. The water desalination projects are:

- Increase in capacity of Shuwaikh plant from 89,000 m^3/day to 93,000 m^3/day.
- Erection of a RO seawater desalination plant at Shuwaikh at a total capacity of about 230,000 m^3/day by 2010.
- Installation of 3 MSF units at Shuaiba North with a total capacity of 203,000 m^3/day by 2010.
- Erection of six distillation units of 77,000 m^3/day each at Az-zour North and total capacity of 464,000 m^3/day by 2011.
- Erection of another six distillation units at Az-zour North by 2012 with a total capacity of 464,000 m^3/day.

2.6.2.3. Brackish water Desalination

Brackish ground water exists in Kuwait with a total output of 0.55 million m^3 per day, with a TDS of 4000-9000 ppm. This brackish water is used for: blending with distilled water; irrigation and landscaping; household purposes; livestock watering and construction works. It is distributed via a separate network parallel to the freshwater network. There, however, plans to increase the production capacity by 0.4 million m^3 per day in the future.

Desalination of brackish water is accomplished using the reverse osmosis (RO) technique. In 1987, the 14 RO units were installed, each with a capacity of 1100 m^3/day. By the year 1993, the total production capacity of desalinated brackish water was around 37,600 m^3/day. Presently, brackish water production by RO desalination is around 28,413 m^3/day (Hamoda, 2001; and MEW, 2008b).

2.6.2.4. Wastewater Treatment

The wastewater treatment plants treating municipal wastewater collected from urban areas in Kuwait are listed in Table 2.4. The total flow of treated wastewater from these plants about 415,244 m^3/day in 2005.

The tertiary treated effluents are stored in reservoirs with a total capacity of 400,000 m^3. A total 330,000 m^3 of treated wastewater was used for irrigation in 2005, which is about 80% of total treated effluent produced. However, this percentage is lower during the winter season (Hamoda, 2001 and Hamoda et al., 2004).

2.7. Electricity and Water Production and Demand Patterns

Figures 2.9 and 2.10 show the development in installed electric generation capacity and electricity consumption for the years 1985-2007, respectively. The sharp

Table 2.4 Wastewater treatment plants in Kuwait

Location	**Um Al-Haiman**	**Rekka**	**Jahra**	**Sulaibiya**
Date of commission	2002	1981	1981	2004
District serviced	N.E.	Ahmadi and surrounding suburbs	Jahra and surrounding suburbs	Rekka effluent
Design flow (m^3/day)	27,000	120,000	70,000	375,000
Actual flow (m^3/day)*	11,000	135,000	65,000	340,000
Secondary treatment processes	Extended aeration	Extended aeration	Extended aeration	Extended aeration
Tertiary treatment processes	Granular media filtration, UV and chlorination	Granular media filtration and chlorination	Granular media filtration and chlorination	UF, RO and chlorination

* Actual flow is for the year 2005

increase in the installed capacity is due to the commissioning of two steam turbines at Al-Subiya power station.

It is also useful to determine if the demand profile is temperature dependant or not. It will be helpful achieving the most efficient and feasible future power generation system in the country. The monthly exported electrical energy and average dry bulb temperature (DBT) for the year 2001 are shown in figure 2.11. We can clearly see that the demand closely matches the outdoor temperature. As the temperature increases, the demand for electricity also increases. This phenomenon is due to the high demand for air-conditioning (A/C) during the summer months in Kuwait. Unfortunately, the exact figure of A/C share of the total demand is not available at the moment from MEW. Also, the electricity share of each sector (e.g. residential, commercial, industrial etc.) is not published in the electricity statistical book of MEW.

The installed capacity of the MSF desalination units had to be increased rapidly over the years in order to satisfy the increasing need for potable water in the country. Figures 2.12 and 2.13 show the development in the installed distillation capacity and freshwater consumption for the years 1992-2001. Consumption for the different sectors is also not available.

Figure 2.14 shows the monthly net water consumption and the DBT for 2001. Water consumption, we can safely say, also is temperature dependent similar to the electrical demand.

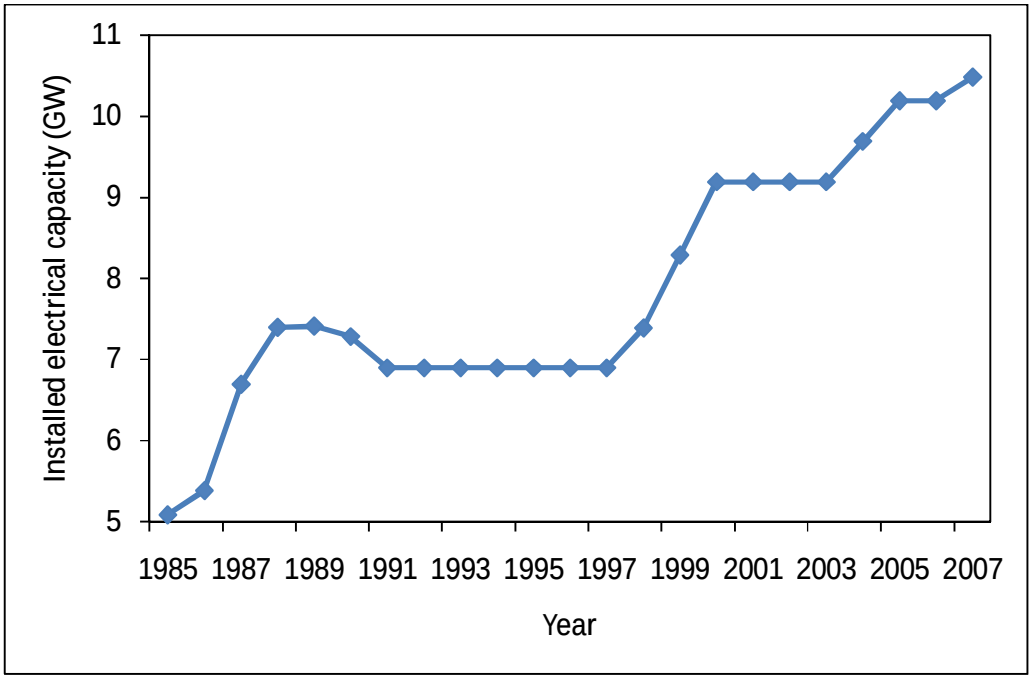

Figure 2.9 Development in electric generation capacity for the period 1985-2007 (MEW, 2008a)

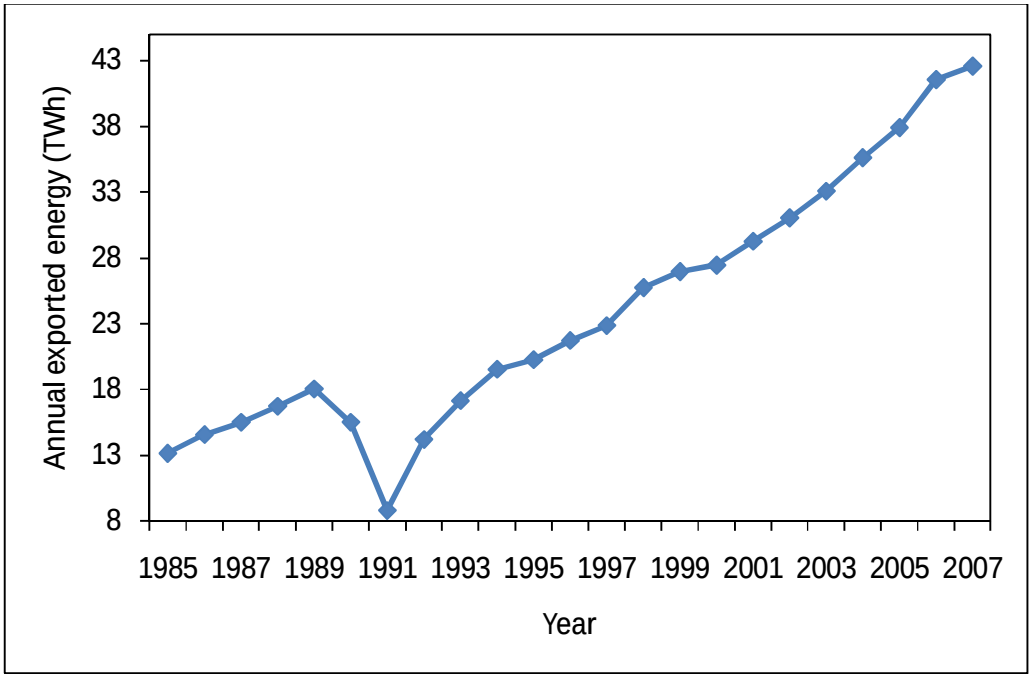

Figure 2.10 Annual exported energy for the period 1985-2007

(MEW, 2008a)

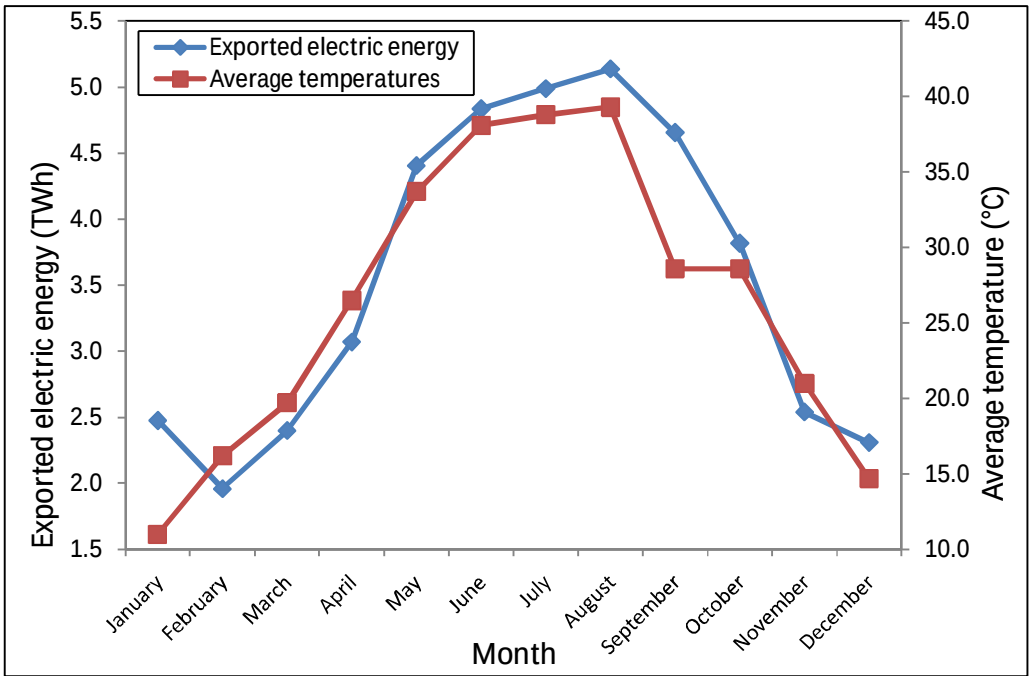

Figure 2.11 Monthly electrical demand and temperature profile for the year 2007

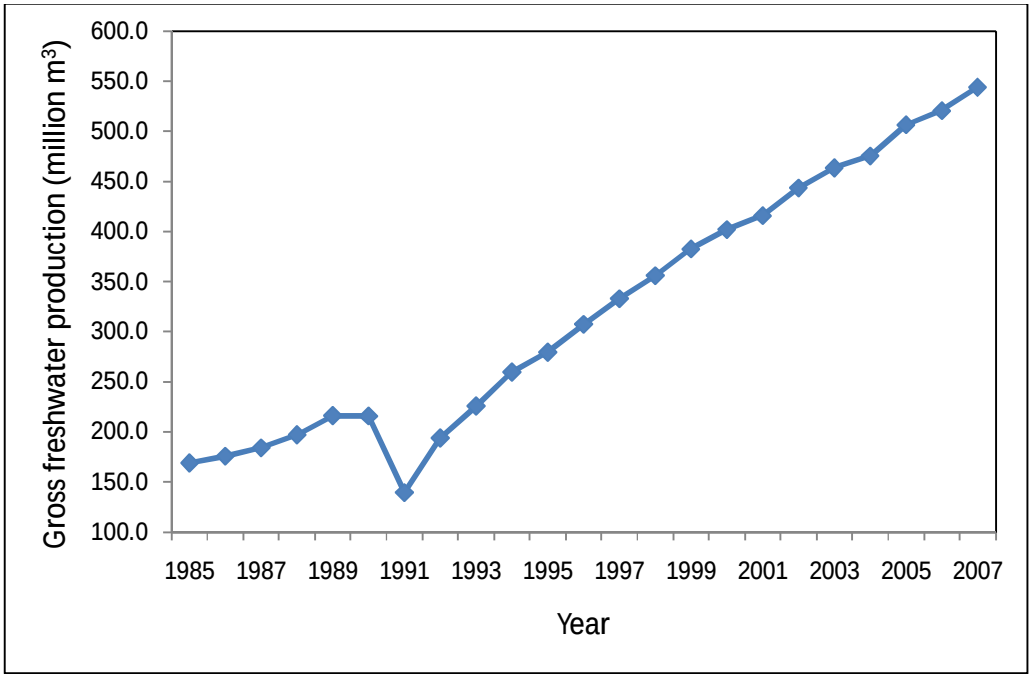

Figure 2.12 Development of freshwater production during 1985-2007 (MEW, 2008b)

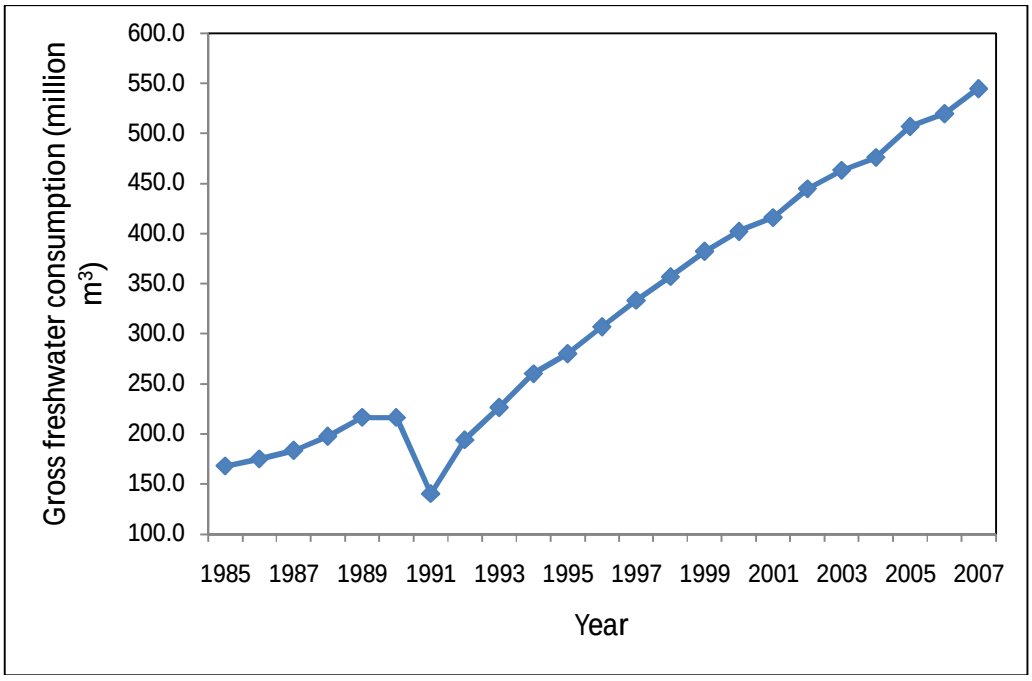

Figure 2.13 Freshwater consumption for the years 1985-2007 (MEW, 2008b)

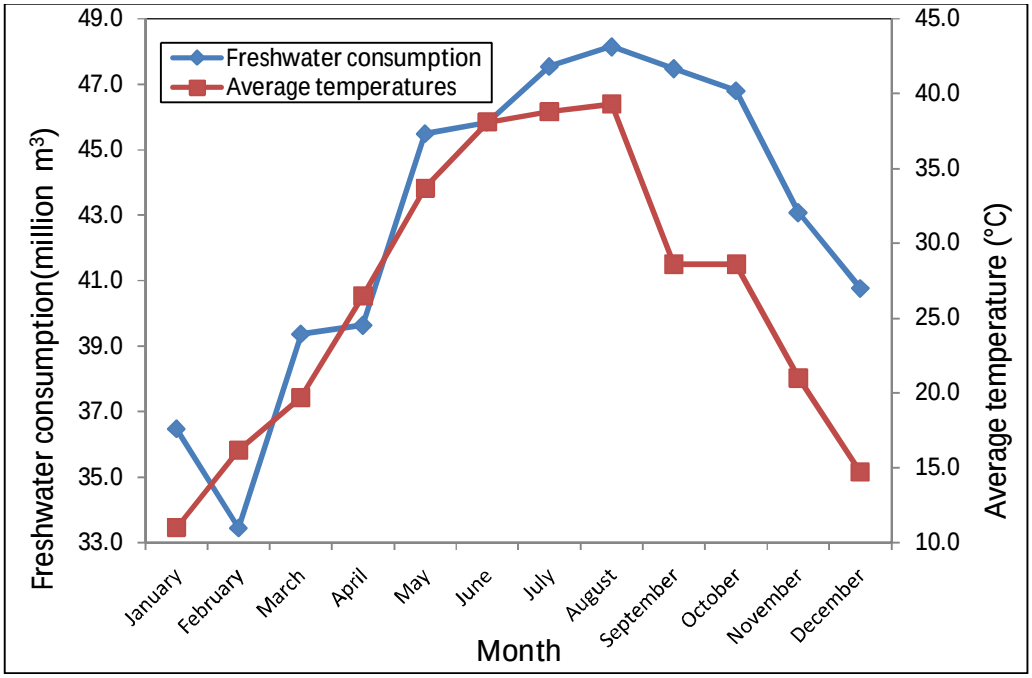

Figure 2.14 Monthly net water consumption and temperature profile for 2001

2.8. Conclusions

Kuwait is a hot country where summer lasts for seven months with average daily temperatures ranging from 42°C to 46°C. The harsh climate means that A/C systems are used all summer long in both residential and governmental buildings. This and the economic and population growth since the 1960s lead the government of Kuwait to invest heavily in large powerplants to satisfy the large demand for electricity. The dry climate and the scarcity of rain fall prompted the government to build cogeneration plants where freshwater can also be produced in the plant. The rapid increase in both demand and production capacity has been shown.

It was also shown that the powerplants burned fuel oil to produce electricity and water. The oil used in these plants is a commodity and the only source of income for Kuwait. Data obtained from MEW show that the total fuel cost in all powerplants is about 300 million Kuwaiti dinars in 2001, which is almost US $900 million.

The analysis of published electric data showed that the growth in electricity consumption will continue to increase at a rate of 7%-9% in coming years. This

means that the government needs to invest millions of oil revenues in the construction of new large-scale cogeneration powerplants. The large growth in consumption can be contributed mainly to the expansion in new residential areas and the large subsidies in electricity and water prices at 70% to 80%.

Demand for freshwater has been also rapidly increasing due to the same reasons mentioned above. The government has been planning to install more MSF capacity to satisfy the growing demand. Figures show that both electricity and water consumption profiles are related to the temperature profile. In other words, as temperatures increase, the consumption increases.

The current situation in Kuwait indicates that the status quo must be reviewed and changed to be able to produce electricity and water more efficiently. Efficient electricity and water production will lead to savings in the use of oil in powerplants, which can be exported to raise the country's revenues. One low-cost strategy is to alter or add to the current powerplant configuration using existing and commercially proven technologies.

Chapter 3

3. Steam Rankine Cycle

The Rankine cycle is still the most widely used cycle for electric power generation. The working fluid is usually steam with the source of heat provided by coal, oil, natural gas or nuclear fuels. To improve the efficiency and output of the Rankine cycle, variations to the basic components such as superheat, reheat and regeneration are added to the simple ideal cycle.

This chapter introduces the basic working concept of the Rankine cycle and possible variations. A mathematical model is also introduced for the simulation of the cycle, and then verified using data from the DW powerplant.

3.1. Simple cycle with superheat

Figure 3.1 shows the simple Rankine cycle with superheat. The use of superheat improves the Rankine cycle efficiency by allowing heat addition at an average temperature higher than using saturated steam only. Superheat also results in drier steam at turbine exhaust, which helps in reducing the damage to the turbine blades (El-Wakil, 1984).

Superheat is accomplished in a separate heat exchanger called a superheater located within the boiler. The combination of boiler and superheater is referred to as a steam generator (Kojima, 1998; and Moran & Shapiro, 2004). The superheat temperature (i.e. turbine inlet temperature) is limited due to the endurance of the blade material of the steam turbine. This temperature cannot be allowed to exceed a maximum of 560°C from an economic point of view (Badr et al., 1990; and Kojima, 1998).

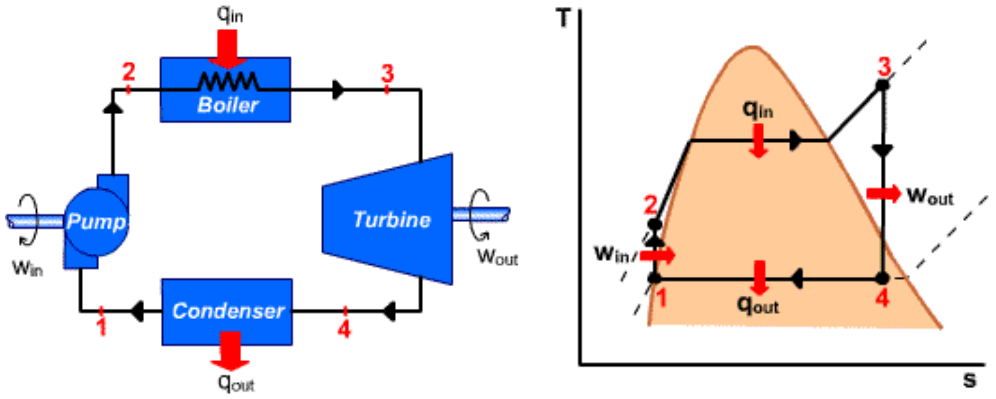

(a) Schematic diagram (b) T-s diagram

Figure 3.1 Simple Rankine cycle with superheat (University of Oklahoma, 2004)

Assuming a steady-flow of a unit mass flow and neglecting changes in kinetic and potential energies, the first-law analysis of the Rankine cycle gives:

Heat addition in the boiler	$q_{in} = q_{2-3} = h_3 - h_2$	(3.1)
Turbine work	$w_{out} = w_{3-4} = h_3 - h_4$	(3.2)
Heat rejection in the condenser	$q_{out} = q_{4-1} = h_1 - h_4$	(3.3)
Work of feed-water pump	$w_{in} = w_{1-2} = h_1 - h_2$	(3.4)

The compressed liquid water can be treated as an incompressible fluid. The work input to the feed-water pump can be estimated as:

$$w_{in} = h_1 - h_2 = -\int_1^2 v dp = v_1 (p_1 - p_2) \tag{3.5}$$

where

v is a specific volume of the compressed water

The thermal efficiency of the Rankine cycle can be expressed as:

$$h_{th} = \frac{w_{net}}{q_{in}} = \frac{w_{out} - |w_{in}|}{q_{in}} = \frac{(h_3 - h_4) - (h_2 - h_1)}{h_3 - h_2} = \frac{(h_3 - h_4) - v_1(p_2 - p_1)}{h_3 - h_2} \quad (3.6)$$

or

$$h_{th} = 1 - \frac{|q_{out}|}{q_{in}} = 1 - \frac{h_4 - h_1}{h_3 - h_2} \quad (3.7)$$

3.2. Steam Rankine-cycle with reheat

To further increase the cycle efficiency, steam reheat is added at the exit of the high-pressure turbine. In a reheat cycle (Figure 3.2), the fed steam is partially expanded in a high-pressure turbine doing some work, and then it is fed back to the boiler where it is reheated to about its original temperature. The reheated steam then continues expanding through the low-pressure turbine to the condenser pressure. In practice, the efficiency of the reheat cycle is better than the efficiency of the superheat-steam cycle due to the increase in the average temperature at which heat is added. Another benefit of reheat is drier steam at the turbine exhaust. However, reheat presents an increased capital outlay in terms of reheater pipework.

Modern fossil-fuelled powerplants employ superheat and at least one stage of reheat. Some employ two. However, employing more than two stages complicates the cycle and increases capital cost which is not justified by improvements in efficiency (El-Wakil, 1984).

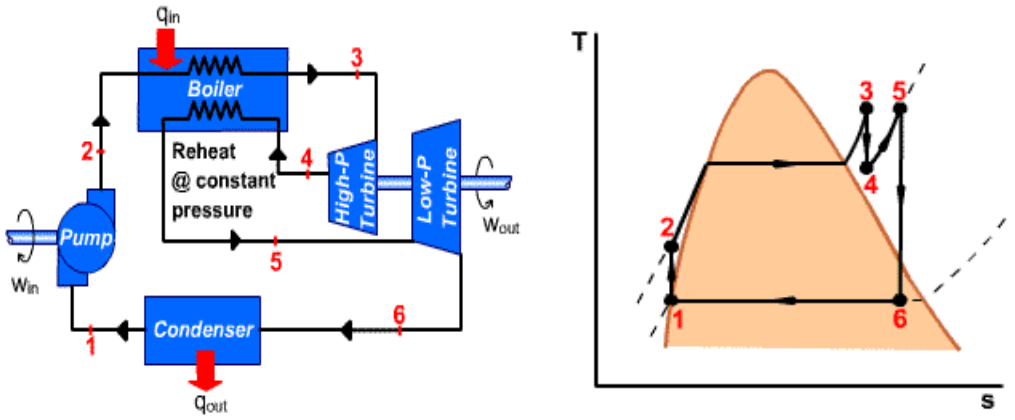

(a) Schematic diagram (b) T-s diagram

Figure 3.2 Reheat Rankine cycle (University of Oklahoma, 2004)

A disadvantage of the reheat cycle is that the same amount of flow is circulating through the entire system. The size of the low-pressure turbine stage is, therefore, considerably larger than that of the higher-pressure stage which results in disproportionate power output per unit cost (Badr et al., 1990).

Referring to Figure 3.2, the thermal efficiency of the Rankine cycle with single reheat can be expressed as:

$$h_{th} = \frac{w_{net}}{q_{in}} = \frac{w_{T-HP} + w_{T-LP} - |w_{in}|}{q_{in1} + q_{in2}} = \frac{(h_3 - h_4) + (h_5 - h_6) - (h_2 - h_1)}{(h_3 - h_2) + (h_5 - h_4)} \tag{3.8}$$

Or

$$h_{th} = 1 - \frac{|q_{out}|}{q_{in}} = 1 - \frac{|q_{out}|}{q_{in1} + q_{in2}} = 1 - \frac{h_6 - h_1}{(h_3 - h_2) + (h_5 - h_4)} \tag{3.9}$$

3.3. Regenerative steam Rankine-cycle

To further enhance the thermal efficiency of the simple Rankine cycle, regenerative feed-water heating is used. The initial heating of feed-water in a simple cycle constitutes a major irreversibility in the cycle because of the large thermal potential between combustion product and the liquid water in the boiler. Regeneration solves this irreversibility problem. In regeneration, steam is bled from the turbine at selected stages to heat the liquid water before it enters the boiler via heat exchangers called feed-water heaters. Modern large steam powerplants employ between five to eight feed-water heaters (El-Wakil, 1984).

There are three types of feed-water heaters that are commonly used in modern powerplants, namely, open type (i.e. direct contact), closed type with drains cascaded backward and closed type with drains pumped forward.

3.3.1. Open-type feed-water heater

Figure 3.3 shows a schematic diagram of the regenerative Rankine cycle with one open-type feed-water heater and the corresponding T-s diagram. In the open-type feed-water heater, the extracted steam is mixed directly with the incoming subcooled feed-water to produce saturated water at the extraction steam pressure. In practice, the liquid water is heated only to a temperature slightly lower than the saturation temperature to avoid cavitation in the boiler feed-water pump.

Open-type feed-water heaters also double as dearators because of the breakup of water in the mixing process liberates the noncondensible gases (e.g. air, O_2, H_2 and CO_2) that can be vented to the atmosphere (El-Wakil, 1984).

Referring to Figure 3.4(a), the mass and energy balance for the open-type heater can be expressed as:

Mass balance : $m_c = m_a + m_b$ (3.10)

Energy balance : $m_c h_c = m_a h_a + m_b h_b$ (3.11)

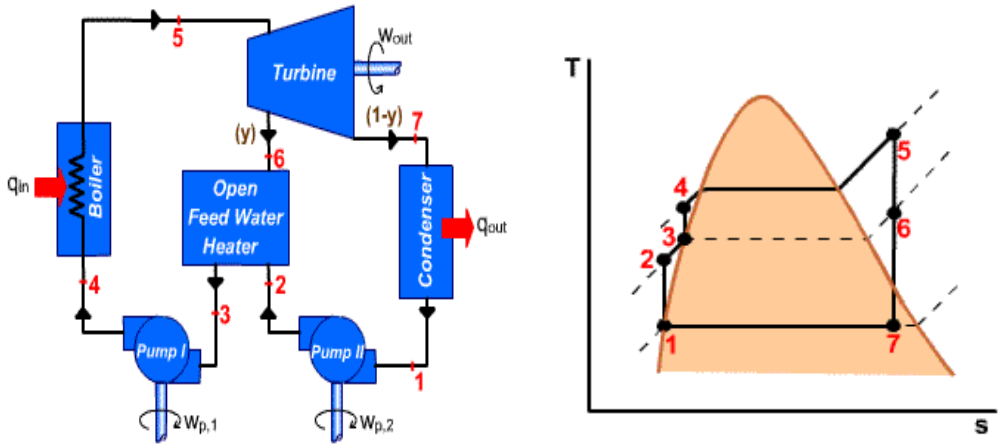

(a) Schematic diagram (b) T-s diagram

Figure 3.3 Regenerative Rankine cycle with an open-type feed-water heater (University of Oklahoma, 2004)

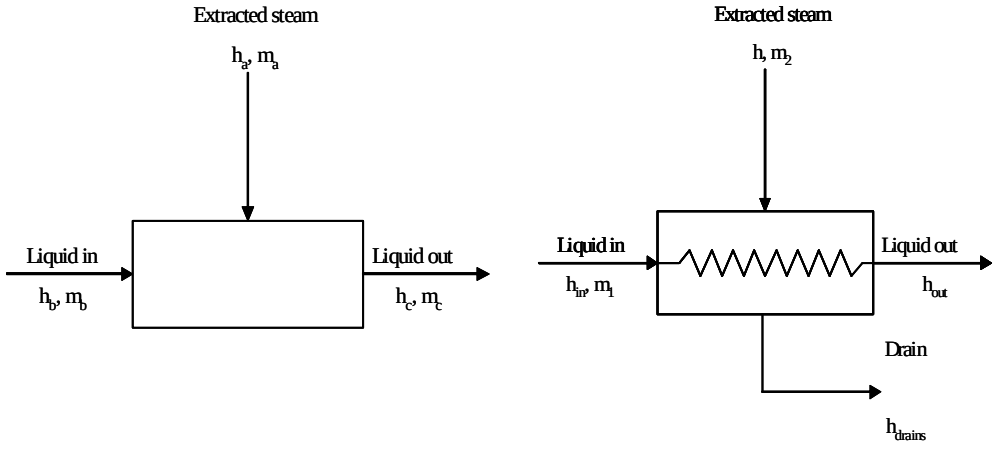

(a) Open type (b) Closed type

Figure 3.4 Mass and energy balance diagram for feed-water heaters

3.3.2. Closed-type feed-water heater with drains cascaded backward

Figure 3.5 shows a schematic diagram and the corresponding T-s diagram for a closed-type feed-water heater with drains cascaded backward. The closed-type heater is the simplest and most commonly used type in powerplants. It is a shell-and-tube heat exchanger. In both types of closed-type heaters, feed-water passes through the tubes and the bled steam, on the shell side, transfers its energy to the feedwater and condenses. In the case where the drains cascaded backward the condensed steam is throttled backward to the next lower-pressure feed-water heater with the condensate of the lowest pressure heater being fed back to the condenser. This type is also the most common type because no drain pumps are required, which means reduced running and maintenance costs. However, closed feedwater heaters are more complex because of the internal piping network, and therefore they require a higher capital investment. Heat transfer in closed feedwater heaters is less effective because the two streams do not directly mix (Cengel and Boles, 1994).

The temperature of the feed-water cannot reach that of the inlet steam. A terminal temperature difference (TTD) of between 4°C and 6°C (often in the order of 5°C) is practically maintained by the proper design of the heater (El-Wakil, 1984; and Badr et al., 1990). The TTD can be defined as the difference between the saturation temperature of bled steam and the exit water temperature:

$$TTD = T_{s,bled} - T_{w,exit} \tag{3.12}$$

From Figure 3.5, the energy balance for the closed-type feed-water heater can be expressed as:

$$y(h_5 - h_7) = (h_3 - h_2) \tag{3.13}$$

Referring to the notations used in Figure 3.4(b), the above equation can be written as follows:

$$m(h - h_{drain}) = (h_{out} - h_{in}) \tag{3.14}$$

3.3.3. Closed-type feed-water heater with drains pumped forward

This type of heaters avoids throttling but adds complexity to the cycle because of the use of drain pumps. The drains are pumped forward to the main feed-water line by the pumps. A certain degree of subcooling should be guaranteed for the trouble free operation of the drain pumps. For illustration of this cycle, we can refer to Figure 3.5. The only difference is that there will be a feed-water pump to pump the drains of this type of heater forward to the main feed-water line. The forward-type is commonly used as the lowest-pressure heater in an all-cascaded system, which prevents the throttling of the combined cascaded flows to the condenser pressure where energy will be lost to the environment.

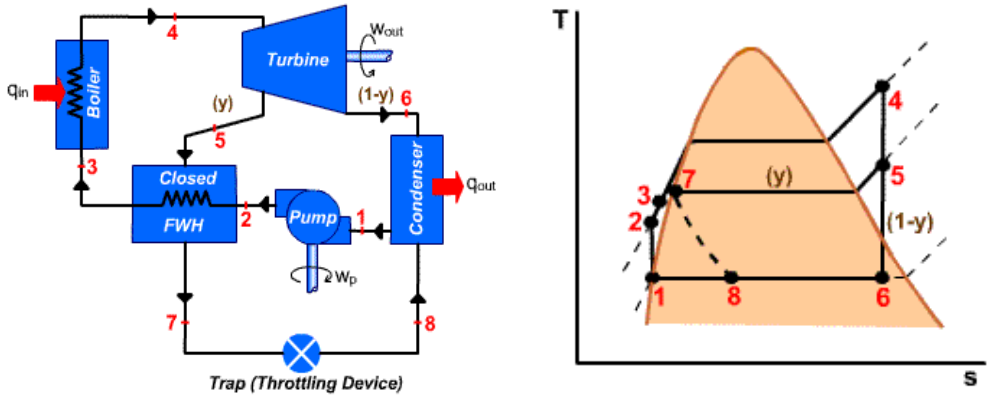

(a) Schematic diagram (b) T-s diagram

Figure 3.5 Regenerative Rankine cycle with one closed-type feed-water heater (Drains cascaded backward) (University of Oklahoma, 2004)

3.3.4. Selection of feed-water heaters

In general, the choice of feed-water heater type to be employed depends upon design optimisation, practical considerations, effectiveness and cost. But, there are features that are common for most steam powerplants. One open-type feed-water heater, which is also used as a dearator, is frequently employed in fossil-fuelled powerplants. The dearator is usually fed with steam at intermediate pressure (e.g. around 800 kPa in Kuwaiti powerplants). The closed-type with drains cascaded backward is the most common and it is usually used before and after the open-type heater. One closed-type feed-water heater with drains pumped forward is used as the lowest-pressure feed-water heater to pump all the accumulated drains back to the main feed-water line (El-Wakil, 1984; and Badr et al., 1990).

3.3.5. Assigning extraction-pressure levels

Optimum selection of the extraction-pressures from the turbine can be done by complete optimisation of the cycle. There is, however, a simple selection technique that is employed in practice, which helps in achieving maximum increase in efficiency. Equal temperature rises are to be achieved in the feed-water heaters, with an optimal temperature rise per heater, expressed as:

$$\Delta T_{opt} = \frac{(T_S)_B - (T_S)_C}{n+1} \tag{3.15}$$

where

$(T_S)_B$: the saturation temperature of the steam at the boiler pressure

$(T_S)_C$: the saturation temperature of the steam at the condenser pressure

3.3.6. Effects of Boiler and Condenser Pressure

Operating boiler pressure in modern powerplants can be as high as 30 MPa (Cengel and Boles, 1994). Increasing the boiler pressure and decreasing the condenser pressure, principally, improves the thermal efficiency of the simple Rankine cycle. However, the condenser pressure is less influential (Badr et al., 1990). Raising the boiler pressure increases the average temperature of heat addition. But, it will also increase the wetness of the steam at the turbine exhaust, which has a negative effect on the efficiency. Also, increasing the boiler pressure will increase the required pump work in order to pressurise the feed-water (Kojima, 1998).

Utilising the condenser pressure as a parameter to improve the efficiency of the cycle has limitations. Condenser pressure is a function of the temperature of available cooling medium for heat rejection. In practical cycles, the condenser pressure ranges from 3.5 MPa with wet cooling (i.e. cooling tower) to 12 MPa with dry cooling (i.e. air-cooled condenser) (Kojima, 1998). Other practical constraints against lowering condenser pressure are the increase in steam wetness in turbine exhaust and the increase in steam specific volume. Increased wetness tends to increase erosion of the turbine blades. An increase in specific volume implies higher volume flowrate through the condenser. The higher volume flowrate requires a larger pump and larger work input to the pump. Hence, this leads to loss of available energy produced in the powerplant (BEI, 1991).

3.4. Review of Process Modelling Methods

Modelling refers to formulating a set of equations that describe mathematically any industrial process under consideration. In the simulation phase, the formulated model is solved using a suitable solution procedure, by employing the values of input process parameters (i.e. independent variables). Typically, simulation is done using a computer. A process termed computer-aided simulation. The goals of modelling and simulation in the process industry include improving and optimising

designs, developing better insight into the working of the process and ultimately leading to the optimal operation and control of the process.

In plant simulation, the individual process units are represented separately, and they are coupled together by utilising the mathematical relationships among process variables. These relationships define the physical laws, material, energy and momentum balances, in the form of a set of generally nonlinear, algebraic and differential equations. The model should reflect all the important features of the process and it should not be too complex to become unmanageable for computation (Al-Shayji, 1998). The details of the mathematical model, also, depend upon the aim it has to serve, and at the same time the availability of the necessary information to support the model.

A simplified model is sufficient when the aim is preliminary checking of heat and material balances. However, a more rigorous model is required for in-depth studies (Husain et al., 1993).

There are two types of process models, namely:

- Steady-state models; and
- Dynamic models

Steady-state models are mainly used for design purposes as well as for parametric studies of existing plants to evaluate their performance and optimise operating conditions. On the other hand, dynamic models, which are time-dependent and contain differential equations, are used for start-up or shut-down conditions (i.e. unsteady-state operation) and for control purposes.

In the current work, steady-state modelling of the steam cycle and MSF processes is utilised since the purpose of the study is the analysis and performance maximising of existing dual-purpose plants currently operating in Kuwait.

3.5 Classification of solution methods

There are two basic approaches for solving the system of nonlinear equations with recycle loops, namely:

- Modular approach; and
- Equation-oriented or global approach

A third approach which is a hybrid of these two basic approaches and incorporating an iterative procedure may be used. The two basic solution methods are briefly described in this section.

A. Modular Approach

The modular approach involves grouping equations and constrains for each process unit into a separate computational module. Each module calculates values corresponding to the output streams for the given input parameters for that process unit.

There are two ways of solving the process unit equations under the modular approach, they are:

- Sequential method; and
- simultaneous modular method

The sequential method (i.e. stage-by-stage approach in MSF simulations) involves carrying out calculations from module to module, starting with the feed streams until products are obtained (Husain, 1986). Since the MSF system includes a recycle loop, partitioning and tearing of recycle streams is used to solve the system of equations. Partitioning involves breaking the system equations according to a solution strategy where each equation can be used to solve for a single variable sequentially. Whereas, tearing involves assigning values to the unknown variables at certain points. Then, an iterative procedure is used incorporating a suitable

convergence enhancement method to reduce the difference between the previous and current calculated values of the torn variables within a pre-assigned tolerance (Ramirez, 1997 and Husain et al., 1993).

The simultaneous modular method is similar to the sequential method in that the unit modules calculate outputs for given inputs and specified equipment parameter values. However, the main difference is that for each output value an additional module, which approximately relates each output value by a linear combination of all input values, has to be developed (Ramirez, 1997 and Husain, 1986).

The sequential method may be easy to use and seems more natural in solving the problem. However, it lacks convergence and stability. So, a combination of the sequential and simultaneous methods is used. In this combined method, the equations associated with a recycle loop are solved simultaneously. These nonlinear equations are suitably linearised. The work by Helal et al. (1986) uses the Tridiagonal matrix (TDM) method to achieve linearization for the MSF process. This method takes advantage of the special structure of the linearised model equations to decompose the large system of equations into a number of subsystems which are grouped according to the type of variables rather than the stage location.

B. Equation-Oriented Approach

In the equation-oriented or global approach, the mathematical model of the steady-state process is organised and handled as one large global set of equations representing the entire process, and then solved simultaneously. Because this approach analyzes all the equations representing the entire process, it takes full advantage of the specific features of the equations which are ignored in the modular approach (Husain, 1986). The advantages of the equation-oriented approach can be summarised as follows (Barton, 2000):

- It is much more efficient. No repeated passes through the flowsheet and nested convergence at unit operation level are needed as in the sequential modular approach.
- The artificial distinction between simulation and design specification set is removed. Hence, for design problems in particular, the equation-oriented approach is much more efficient.
- It is much easier to extend the model library and modify existing models.
- The computer code can be readily extended to other calculations such as dynamic simulation or flowsheet optimisation.
- Diagnosis of certain errors in problem formulation is much easier.

However, there are some disadvantages for the approach (Barton, 2000):

- The general purpose solvers based on the equation-oriented approach are not as robust and reliable as those for the sequential modular approach.
- This approach makes a large demand on computer resources, particularly machine memory.

3.6. Previous Rankine-cycle models

Chakraborty and Chakraborty (2002) developed a mathematical model for the simulation of power and process cycles. The model can be applied to both pure power cycles and to cogeneration plants. In their research, Chakraborty and Chakraborty (2002) used the equation-oriented solution method over the sequential method to solve the set of equations due to its flexibility and minimised requirements of computer speed and memory. Their model is based on the steady-state mass and energy balance laws for each component in the system (object-oriented modelling), after which the components are linked together by identifying the inlets and outlets and number them. Finally, the model is implemented using

C++ programming language because, as the authors claim, it is capable of supporting data structures and user-defined data.

The work of Lu et al. (1995) describes the powerplant dynamic and steady-state simulation toolbox called *Power Plant Analyser*. The toolbox is based on the object-oriented modelling method using C and C++ programming languages, and is connected with the Matlab graphical toolbox *Simulink* (i.e. uses icon based objects and components). Thermodynamic properties of steam and water are estimated using the 1967 IFC formulations, which the authors claim, are suitable for accurate digital calculations. Fruehauf and Hobgood (2002) also utilised Simulink to perform dynamic simulation of a steam based plant with cogeneration. The aim of their research was to test the control strategy of the plant and to develop initial tuning constants. From their point of view, Fruehauf and Hobgood (2002) state that Simulink has the advantage of dealing with explicit equations, is proven mathematically, and is a robust software.

Uche et al. (2003) also developed a software for the design and analysis of powerplants, but with the aim of filling the gap in the research and education sectors for a user-friendly object-oriented software. The software is a multi-platform, Java language oriented program compatible with windows, OS, Linux and Mac. The authors list the following functions of the software:

- Graphical design of plant layouts
- Calculation of mass and energy balances
- Thermo-economic analysis
- Parametric calculations

Uche et al. (2003), however, do not discuss the flexibility and accuracy of the developed program in their published work. The paper discusses only a case study showing the different features of the software.

The work of Badr et al. (1990) and Habib et al. (1995 & 1999) analysed the Rankine cycle more extensively. In their research, Badr et al. (1990) developed a program in Basic programming language to simulate and analyse the performance of the Rankine-cycle powerplants. It also estimates the thermodynamic properties of steam and water. The aim of their research is to utilise the developed program for predicting the optimal design and operating conditions of a proposed Rankine-cycle system for different applications. In their work, Badr et al. (1990) first validated the formulation used to estimate the thermodynamic properties, after which they concluded that the formulations are accurate enough to be used for engineering applications. The developed thermodynamic formulations were used in their model to model and predict the performance of the different types of the Rankine cycle.

On the other hand, the main aim of the work by Habib et al. (1995 & 1999) is to optimise the reheat pressures in Rankine-cycle based thermal powerplants. To achieve that, they use first-law and exergy analyses. Although the procedure is in general form, it is applied specifically for a thermal powerplant having two reheat pressure levels and two open-type feedwater heaters. Results of the model developed by Habib et al. (1995 & 1999) are not compared to other actual or simulation data to show how accurate the procedure is. They also do not provide details of the formulations used to estimate the thermodynamic properties of water and steam.

Some researchers utilise commercially available modelling softwares to analyse the performance of steam powerplants. In their work, Kamal and Sims (1995) used the softwares *Steampro* and *Gatecycle* for different powerplant configurations to determine heat rates and energy requirements. The authors, however, do not include an assessment of the softwares they used in their research.

3.7. Summary of modelling methods

Literature concerning the analysis of powerplants shows that researchers use mainly two methods to model and simulate the system. They commonly develop their own

formulations and programs or they use commercially-available simulation softwares to study powerplants. It can be concluded also that the programming languages used are diverse, and this means that the simulation of powerplants is flexible.

This review shows that the literature available in the subject of modelling and simulation of steam powerplants does not contain abundant research that is both thorough and extensive. Most researchers tend to concentrate on describing the aims of their work and publishing the results of case studies. The main aim of this current research is to model and analyse the performance Rankine-cycle based steam powerplants. Hence, the work of Badr et al. (1990) is the most suitable guide for this research because it includes validated formulations for the properties of steam and water and it studies the different configurations of the steam Rankine-cycle in a most logical and thorough way.

3.8. Thermodynamic properties of steam and water

In order to model and analyse the Rankine cycle employed in modern steam powerplants, steam properties at each specified state point are required. As summarised previously, the formulations for estimating water and steam properties in this report are based on procedures reported by (Badr et al., 1990).

Estimation of water and steam properties and Rankine-cycle calculations are carried out using MATLAB version 6.5. The equation-oriented approach is utilised for the process modelling. However, the subroutines for each unit operation are solved sequentially. Each unit operation is represented by a subroutine that calculates outputs associated with given inputs and parameters.

3.8.1. Superheated steam region

Correlations for estimation of specific enthalpy, specific entropy and specific volume as functions of temperature and Pressure were presented

by Schnackel (1958).

$$h = F + 101.31358\left\{F_0 \frac{p}{101325.0} + \frac{B_0}{2}\left(\frac{p}{101325.0T}\right)^2\right\} \times\left\{-B_6 + B_0\left(B_2 - B_3 + B_0 B_7\left[\frac{p}{101325.0T}\right]^2\right)\right\} \quad (3.16)$$

$$s = 1472.2626\ln T - 461.4874\ln p + 0.7557174T + 3830.4065 - \frac{47845.076}{T} - 101.31344b \quad (3.17)$$

$$v = 1.000035\times 10^{-3}\left(\frac{46153943T}{p} + B\right) \quad (3.18)$$

Where

$$\left.\begin{aligned} B &= B_0\left\{1 + \frac{B_0 p}{101325.0T^2}\left[B_2 - B_3 + \left(\frac{B_0 p}{101325.0T}\right)^2 (B_4 - B_5)\right]\right\} \\ B_0 &= 1.89 - B_1 \\ B_1 &= \frac{2641.62}{T} 10^{80870/T^2} \\ B_2 &= 82.546 \\ B_3 &= \frac{162460.0}{T} \\ B_4 &= 0.21828T \\ B_5 &\frac{126970}{T} \\ B_6 &= B_0 B_3 - 2F_0(B_2 - B_3) \end{aligned}\right\} \quad (3.19a)$$

$$
\left.
\begin{aligned}
B_7 &= -B_0 B_5 + 2F_0 (B_4 - B_5) \\
F_0 &= 1.89 - B_1 \left(\frac{372420}{T^2} + 2 \right) \\
F &= 1804036.3 + 1472.265T + 0.37789824T^2 + 47845.137 \ln T \\
b &= \frac{1}{T} \left[(B_0 - F_0) \frac{p}{101325.0} + \frac{B_0}{2} \left(\frac{p}{101325.0T} \right)^2 \right] \\
&\times \left[\left(B_6 + \frac{1}{2} \left(\frac{B_0 p}{101325.0T} \right)^2 \times \{ B_0 (B_4 - B_5) - 2B_7 \} \right) \right]
\end{aligned}
\right\} \qquad (3.19b)
$$

For steam powerplant applications, however, properties as functions of p, h or p, s are usually required. In MATLAB, the function, *fzero*, can be used with the above equations to find the unknown temperature which in turn can be utilised with the known pressure to find the thermodynamic properties of interest. The function *fzero*, simply, finds the root of a given equation. It is a simple practical alternative to various iteration techniques that are used for the calculation of thermodynamic properties.

3.8.2. Saturated steam line

Up to a maximum temperature of 441K, the saturation pressure can be estimated as a function of temperature by using Antonie's vapour-pressure correlation

$$
\ln p_S = 23.196452 - \frac{3816.44}{T - 46.13} \qquad (3.20)
$$

For $441\text{K} \le T \ge 647.3\text{K}$, the Harlacher and Braun vapour-pressure correlation

$$
\ln p_S = 60.228852 - \frac{6869.5}{T} - 5.115 \ln T + 7.875 \times 10^{-3} \frac{p_S}{T^2} \qquad (3.21)
$$

When using Equation (3.21), the saturation pressure can be estimated by using a suitable iteration procedure. However, MATLAB's *fzero* function is a simpler way of calculating the saturation pressure from a given saturation temperature.

Estimation of the saturation temperature as a function of the pressure, instead, is done by using the backward equation developed by the International Association for the properties of Water and Steam (IAPWS) (Wagner et al., 2000), which is valid for the pressure range that the equation covers is 611.213 Pa$\leq p \geq$ 22.064 MPa.

$$\frac{T_s}{T^*} = \frac{n_{10} + D - \left[(n_{10} + D)^2 - 4(n_9 + n_{10} D)\right]^{0.5}}{2} \tag{3.22}$$

where

$$\left.\begin{aligned} T^* &= 1K \\ D &= \frac{2G}{-F - \left(F^2 - 4EG\right)^{0.5}} \\ E &= b'^2 + n_3 b' + n_6 \\ F' &= n_1 b'^2 + n_4 b' + n_7 \\ G &= n_2 b'^2 + n_5 b' + n_8 \\ b' &= \left(\frac{p_s}{p^*}\right)^{0.25} \\ p^* &= 1MPa \end{aligned}\right\} \tag{3.23}$$

The coefficients n_i of Equation 3.22 are listed in Table 3.1.

Specific enthalpy, specific entropy and specific volume for saturated steam can be estimated from Equations (3.16), (3.17) and (3.18) as functions of the temperature and the corresponding saturation pressure.

Table 3.1 Coefficients of Equation (3.22)

i	n_i
1	$0.116\,705\,214\,527\,67 \times 10^{4}$
2	$-0.724\,213\,167\,032\,06 \times 10^{6}$
3	$-0.170\,738\,469\,400\,92 \times 10^{2}$
4	$0.120\,208\,247\,024\,70 \times 10^{5}$
5	$-0.323\,255\,503\,223\,33 \times 10^{7}$
6	$0.149\,151\,086\,135\,30 \times 10^{2}$
7	$-0.482\,326\,573\,615\,91 \times 10^{4}$
8	$0.405\,113\,405\,420\,57 \times 10^{6}$
9	$-0.238\,555\,575\,678\,49$
10	$0.650\,175\,348\,447\,98 \times 10^{3}$

3.8.3. Saturated water line

The specific enthalpy of the saturated liquid water can be calculated as a difference between the specific enthalpy of saturated steam and the latent heat of vaporisation at the same temperature. The latent heat can be estimated as:

For $450\text{K} \leq T \geq 647.3\text{K}$

$$\Delta h_{lat} = 2115173.3\left(1-\frac{T}{647.3}\right)^{0.354} + 1125343.9\left(1-\frac{T}{647.3}\right)^{0.456} \tag{3.24}$$

For $373.15\text{K} \leq T \geq 450\text{K}$

$$\Delta h_{lat} = 6051.1583\left(\frac{c + c^{0.35298}}{1 + c^{0.13856}}\right)T \tag{3.25}$$

where

$$c = 1.3615467\left(\frac{647.3 - T}{T}\right) \tag{3.26}$$

For T < 373.15K, the specific enthalpy of saturated water can be estimated as

$$h_l = 4186.8(T - 273.15) \tag{3.27}$$

The specific entropy of saturated liquid water can be estimated in a similar way to that applied in evaluating its enthalpy

$$\Delta s_{lat} = \frac{\Delta h_{lat}}{T} \tag{3.28}$$

If the normal-boiling point is adopted as the reference state, the equations for estimating the required specific volume take the form

$$v_l = 3.104304 \times 10^{-3} V(1 - 0.344\Gamma) \tag{3.29}$$

where

For T≤518K

$$V = 0.33593 - 5.2453267 \times 10^{-4} T + 3.6263003 \times 10^{-6} T^2 - 7.4667901 \times 10^{-9} T^3 + 6.346708 \times 10^{-12} T^4 \tag{3.30}$$

For 518K < T < 647.3K

$$V = 1 + 0.5645828\left(1 - \frac{T}{647.3}\right)^{0.5} \ln\left(1 - \frac{T}{647.3}\right) - 0.50879\left(1 - \frac{T}{647.3}\right) - 0.91534\left(1 - \frac{T}{647.3}\right)^2 \tag{3.31}$$

$$\Gamma = 0.29607 - 1.3973428 \times 10^{-4} T - 1.1556161 \times 10^{-7} T^2 \tag{3.32}$$

3.8.4. Compressed water region

The specific enthalpy of compressed liquid water can be assumed to be equal to that of saturated water at the same temperature with a satisfactory degree of accuracy if the difference between the actual and the saturation pressures is quite small (El-Wakil, 1984).

The specific entropy of compressed liquid water can be estimated by considering it as an incompressed fluid (El-Wakil, 1984).

$$s = s_l + 4186.8 \ln \frac{T}{T_S} \tag{3.33}$$

where

s_1 : specific entropy of the saturated liquid water at the same temperature.

T_S : saturation temperature of the saturated liquid water at the same pressure.

The specific volume of the compressed liquid water can be estimated as a function of the specific volume of the saturated water at the same temperature

$$v = \frac{v_1}{\left[1 + 9.347651 \times 10^{-8} N\left(p - p_S\right)\right]^{1/9}} \tag{3.34}$$

where

v_1 : specific volume of saturated liquid water at the same pressure

$$N = 0.69384 \exp\{6.9547 - 0.1178515T + 4.5658052 \times 10^{-4} T^2 - 7.50449588 \times 10^{-7} T^3 + 4.7142686 \times 10^{-10} T^4 \} \tag{3.35}$$

3.8.5. Accuracy of the estimated properties

To assess the accuracy of the values of properties of water and steam estimated by employing the developed code, the results are compared with published steam tables by Keenan et al. (1969) and ChemicaLogic Corporation (2003). The steam tables produced by ChemicaLogic Corporation are based on the IAPWS-95 formulation. The method used for estimating the accuracy of the evaluated property (τ) is the percentage difference, which is defined as

$$\%Difference = \left(\frac{t_{estimated} - t_{published}}{t_{published}} \right) \times 100 \tag{3.36}$$

Tables 3.2, 3.3 and 3.4 list the predicted accuracies of the calculated properties of superheated steam, saturated steam and saturated water, respectively. The results show that the maximum difference is 7.24% for the specific volume of saturated water. Otherwise, most of the data range is below 5%. This means that the formulations used in this research to estimate the thermodynamic values of steam and water are acceptable and accurate for the analysis of the steam Rankine-cycle.

Table 3.2 Ranges of percentage differences for the properties of superheated steam (p=0.1MPa to 28.0MPa, T=100°C to 900°C)

Property	% difference (Keenan et al., 1969)	% difference (ChemicaLogic Corp., 2003)
h	0.01 – 3.48	0.04 – 3.39
s	0.00 – 2.83	0.00 – 0.25
v	0.00 – 5.73	0.00 – 1.12

Table 3.3 Ranges of percentage differences for the properties of saturated steam (T=29°C to 175°C)

Property	% difference (Keenan et al., 1969)	% difference (ChemicaLogic Corp., 2003)
h_g	0.01 – 0.31	0.04 – 2.87
s_g	0.00 – 0.06	0.00 – 0.05
v_g	0.00 – 0.05	0.00 – 0.02

Table 3.4 Ranges of percentage differences for the properties of saturated water (T=29°C to 175°C)

Property	% difference (Keenan et al., 1969)	% difference (ChemicaLogic Corp., 2003)
h_f	0.02 – 2.28	0.01 – 7.18
s_f	0.17 – 0.67	0.14 – 0.69
v_f	0.20 – 4.86	0.19 – 7.24

3.8. Validation of Rankine-Cycle Mathematical Procedure

Figure. 3.6 shows a flow chart for the code developed to analyse a regenerative Rankine cycle with multiple feed-water heaters. To validate the computer code developed for the different types of Rankine cycles, a comparison with an actual powerplant is made. The selected plant for the comparison is a fossil-fuel fired powerplant in Kuwait. Figure 3.7 shows the heat balance diagram for the powerplant in power-only mode with a power output of 300MW per steam-turbine set (Darwish, 2001). However, it is normally a steam Rankine-cycle based dual-purpose (i.e. cogeneration) plant producing electricity and desalted water. Table 3.5 lists operating parameters of the powerplant.

In order to simplify the calculations performed via the developed code, certain assumptions are made that do not necessarily resemble the actual operation of the powerplant. Assumptions made are:

a. Each component is at steady state.
b. Except the turbines and the pumps, all other processes are internally reversible.
c. Kinetic and potential energy effects are negligible.
d. Pressure drop in pipes and joints is negligible.
e. Steam is bled only to the feed-water heaters.

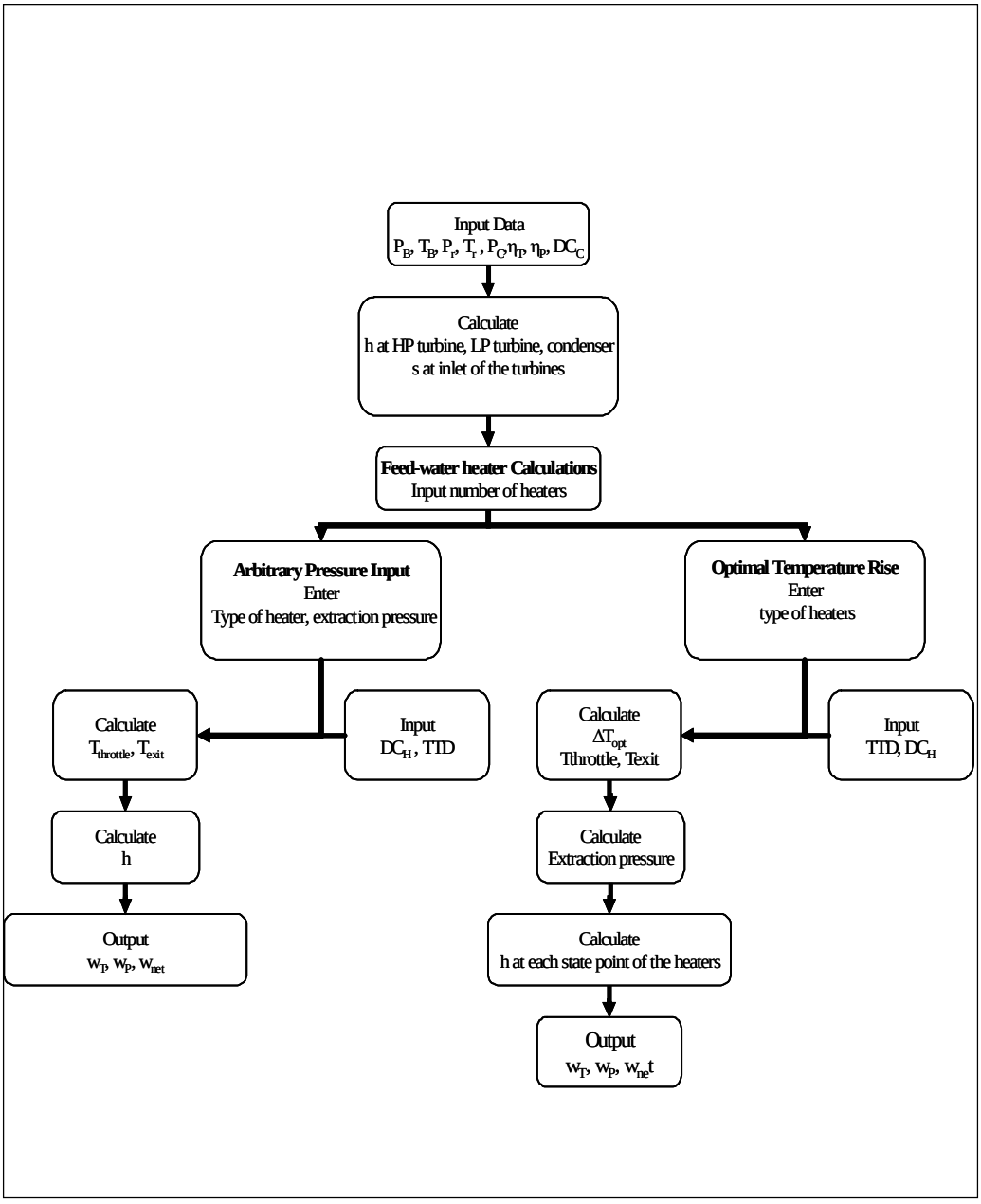

Figure 3.6 Flow chart for a computer program to estimate the performance of a regenerative Rankine cycle with multiple feed-water heaters.

From the available operating parameters, thermodynamics properties for the regenerative Rankine cycle are calculated for each state point. One method of evaluating the developed computer code is to compare the actual specific output in

Table 3.5 Operating parameters of a Kuwaiti regenerative powerplant

Parameter	Value
Output (MW)	300.00
No. of feed-water heaters	6
Boiler mass flow rate (kg/hr)	261.04
Turbine efficiency (%)	84.32
HP turbine inlet pressure (bar)	139.00
HP turbine inlet temperature (°C)	535.00
Reheat Pressure (bar)	36.70
Reheat Temperature (°C)	535.00
Condenser pressure (bar)	0.085

kJ/kg with the estimated one. Actual specific output can be estimate from

$$w_{actual} = \frac{output}{\dot{m}} = \frac{300 \times 10^3 (kW)}{261.04 (kg/s)} = 1149.25 kJ/kg \tag{3.37}$$

The estimated specific net-work is calculated from the difference between the work of the turbines (w_T) and the pumps (w_P), which is equal to $1153.30 kJ/kg$. Using Equation 3.36, the difference between actual and estimated values is 0.35%, which is very minor considering the assumptions listed above. However, the estimated output will change when the optimal temperature difference criterion is used to calculate the level of extraction pressure. The specific work output when using the estimated optimal extraction pressures is $1054.00 kJ/kg$, which is lower than the output when using actual extraction pressures for the powerplant. However, the thermal efficiency changes from 42% in the case of actual pressures, to 44% for optimal extraction-pressure input.

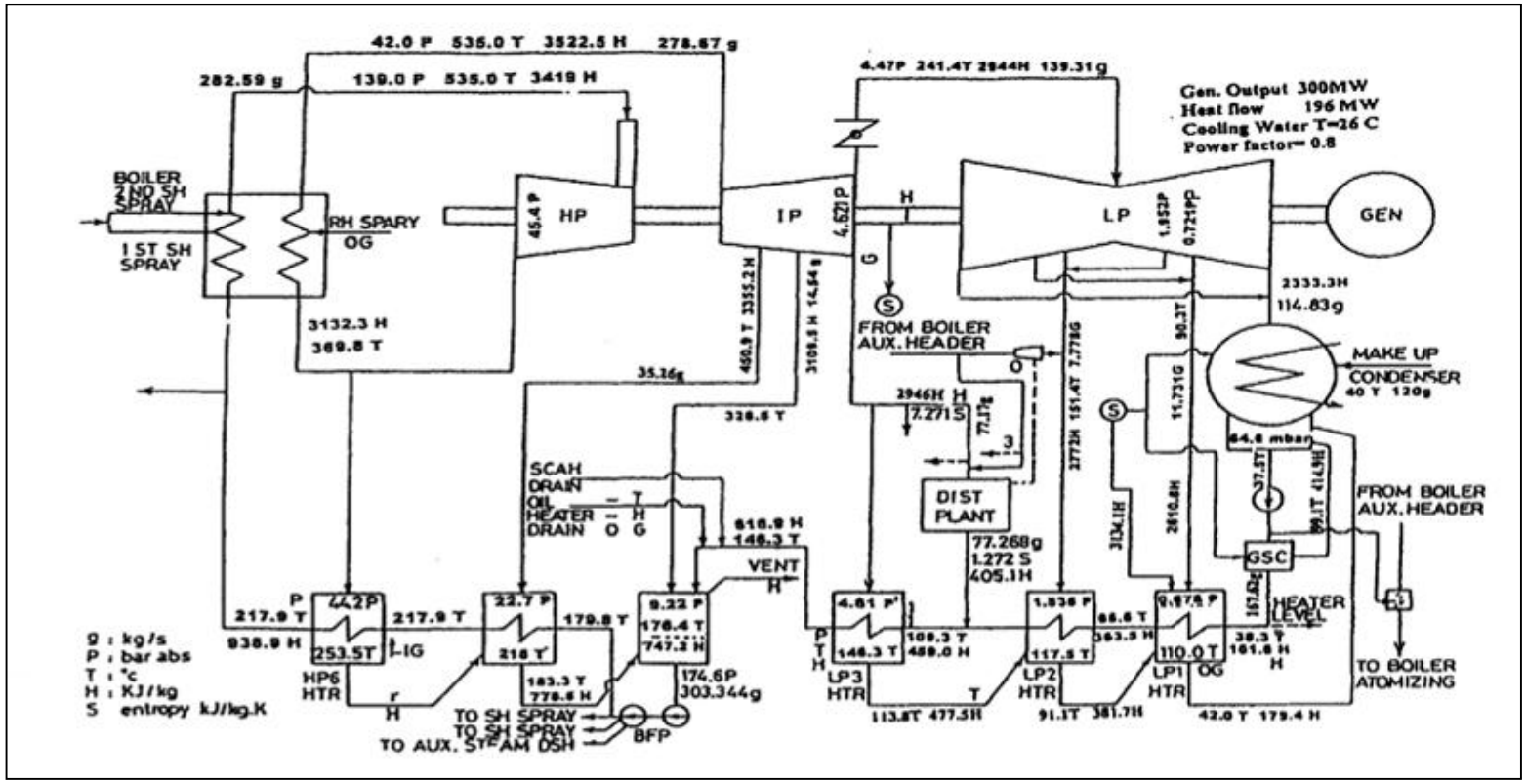

Figure 3.7 Heat balance diagram of steam powerplant in Kuwait operated in power-only mode

3.9. Conclusions

The steam Rankine cycle was studied, analysed and modelled in this chapter. The different types of the steam Rankine cycle were first discussed, however, the regenerative cycle with reheat is the one commonly employed in modern powerplants. Hence, the main aims of this chapter are to model and simulate this cycle. To successfully predict the performance of the steam cycle, a mathematical procedure for estimating the thermodynamic properties of steam and water was also developed and presented in this chapter.

The estimated values of the thermodynamic properties of steam and water were compared with other published data to validate the developed formulations. The comparison showed that the mathematical procedure is sufficiently accurate to be used in this research. The results of the model describing the regenerative Rankine cycle with reheat were compared with an existing steam powerplant currently operating in Kuwait using the heat balance diagram of the powerplant. Comparison of estimated and actual net power outputs of the plant resulted in a difference of 0.35%. This means that the developed model is accurate enough to be used in this research. The next step is to link the program developed in Matlab to the other programs simulating other processes and obtain performance results.

Chapter 4

4. Seawater Desalination Processes

Rapid progress and decreasing cost of desalination makes it the major contributor to freshwater supplies in the world today (Ettouney et al., 2002). There are many different desalting processes used around the world currently, but the most researched and practically-used technologies are distillation and membrane processes. Distillation (i.e. evaporation) processes include multi-stage flash (MSF), multiple-effect distillation (MED) and vapour compression (VC). Membrane technology includes reverse osmosis (RO) and electrodialysis (ED). Other processes include freezing, membrane distillation and solar humidification, but these are not yet successful commercially (Johansen et al., 1995; Buros, 2000; and Ettouney et al., 2002).

Evidence from different studies show that the most widely used large-scale seawater desalination techniques in the world in general and the Middle East specifically are MSF and RO (Al-Sahlawi, 1999; Cardona et al., 2002; and Ettouney et al., 2002). According to the International Desalination Association (IDA) inventory of the main desalination technologies used in the world in 1998, MSF and RO make up 86% of the installed desalination capacity (Buros, 2000). 44.1% of total MSF and RO world-wide capacity is installed by the Member states of the GCC (DESWARE, 2003). Figures 4.1 and 4.2 show the dominance of MSF and RO over the other desalination processes. In Kuwait, MSF continues to be the only technology used for seawater desalination since it was first introduced in 1956 (El-Saie, 1993), and the Kuwaiti Government has no plans to abandon this technology in the foreseeable future. However, RO desalination process may be introduced may be introduced in the future (MEW, 2002b).

In recent years MED and VC desalination processes have been developing and are becoming more commercially popular, but only for small and medium capacities

(Rautenbach, 1993; Wade, 1993; and Buros, 2000). Since Kuwait depends on desalination for most of its freshwater needs, large capacity desalination units are needed to satisfy the growing demand. As far as ED process is concerned, it is normally used for desalination of brackish water (Johansen et al., 1995; and Buros, 2000).

The above literature review shows that MSF and RO the most used, commercially-successful and technically-proven large-scale desalination systems. Hence, these two systems are analysed in this research and incorporated with the mathematical models to find the most suitable configuration for a hybrid powerplant.

The chapter includes a detailed description and analysis of multistage flash desalination (MSF) and reverse osmosis (RO) desalination technologies. Section 4.1 presents the basic description of the MSF system and the steady-state mathematical model describing the MSF process developed for this study. It will also cover the different solution methodologies of the steady-state MSF model used by different researchers. Then, the most suitable solution method for this study will be presented.

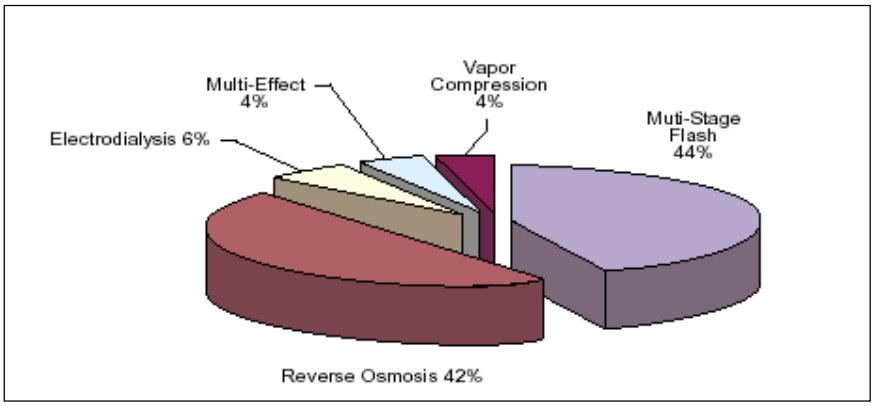

Figure 4.1 Desalination capacity by process as percentage of total world-wide capacity in 1998 (Buros, 2000)

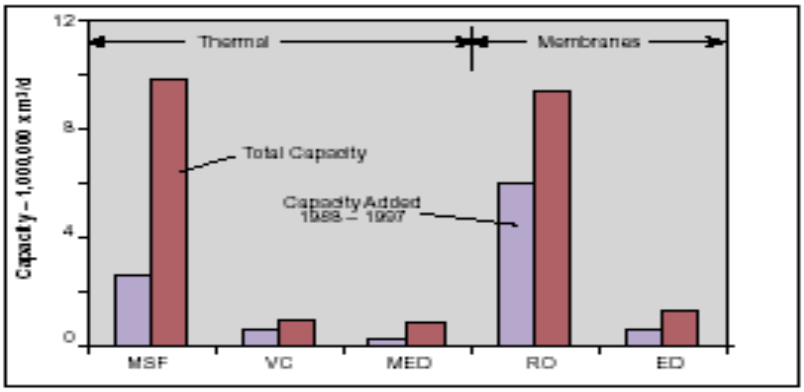

Figure 4.2 Installed capacity in the 10-year period 1987 to 1997 (Buros, 2000)

Section 4.2 introduces the RO process and its components. The section also includes details of the energy requirements of the RO desalination plant that are published in literature. Finally, the energy consumption of the RO system per unit product is estimated from a pilot RO plant operating in Kuwait.

4.1. Multistage Flash Desalination

Multistage stage flash (MSF) desalination is the only method used in Kuwait to process seawater into potable water for everyday use. It is installed within the powerplants to make use of the steam raised for the steam turbines, where the combination of the two systems is called a cogeneration or dual-purpose plant. To be able to study and analyse the operation of the MSF plant, a mathematical model must be used.

4.1.1. Process Description

The basic idea of the MSF distillation process is to evaporate seawater and then condense it to produce salt-free (distilled) water. Seawater is fed to a flash chamber (i.e. evaporator) with a pressure lower than the saturation pressure, which causes the

flashing process. The steam then condenses when it passes through the condenser tubes to a saturation temperature at the chamber pressure.

Figure 4.3 illustrates the MSF desalination plant. The MSF plant is divided into three sections: heat input (i.e. brine heater), heat recovery and heat rejection. Each of the heat recovery and rejection sections contains flashing chambers or stages. The number of flashing stages in the heat rejection section is commonly limited to three. On the other hand, the number of flashing stages in the heat recovery section varies between 21 and 40. In addition, the plant contains pumping units, venting system and cooling water control loop. These different plant sections involve six main streams: intake seawater, rejected cooling seawater, distillate product, rejected brine (i.e. blowdown), brine recycle and heating steam.

Seawater is introduced into the inside of the preheater (i.e. condenser) tubes of the last flashing stage in the heat rejection section. Similarly, the brine recycle stream is introduced into the inside of the preheater tubes of the last flashing stage in the heat recovery section. The flashing brine flows counter to the brine recycle from the first to the last flashing stage.

The saturated heating steam with a temperature range of 97-117ºC drives the flashing process. The heating steam flows on the outside of the brine heater tubes and the brine stream flows on the inside of the tubes. As the heating steam condenses, the brine stream gains the latent heat of condensation and its temperature reaches the desired top brine temperature (TBT).

The hot brine enters the first flashing stage, where a small amount of product vapour is formed. The flashing process reduces the temperature of the unevaporated brine. The temperature reduction across the flashing stages is associated with a drop in the stage pressure, where the highest stage pressure is found in the first stage after the brine heater and the lowest pressure is that of the last stage. A vacuum is applied to the flash chambers by steam ejectors to generate the progressively reducing pressure

through the evaporators. Also, the minimum pressure and temperature in the last stage are fixed by vapour volume and heat rejection considerations. The pressure drop across the stages allows for brine flow without the use of interstage pumping units.

In each stage (Figure 4.4), the flashed off vapour flows through the demister, which removes entrained droplets of unevaporated brine. The vapour then condenses on the outside surface of the preheater/condenser tubes. The condensed vapour collects over the distillate trays across the flashing stages to form the final product water, which is approximately at 40ºC. The condensation process releases the vapour latent heat, which is used to preheat the brine recycle stream in the heat recovery section. The same process takes place in the preheater tubes in the heat rejection section. This results in an increase in the seawater temperature to a higher value, equal to the temperature of the flashing brine in the last stage of the heat rejection section. The intake seawater stream leaves the heat rejection section, where it splits into two streams. The first stream is the cooling seawater stream, which is rejected back to the sea, and the second is the feed seawater stream, which is mixed in the brine pool in the last flashing stage in the heat rejection section (Johansen et al., 1995; El-Dessouky et al., 1999; and Buros, 2000).

Additional units in the desalination plant include pre-treatment of the feed and intake seawater streams. Treatment of the intake seawater is limited to simple screening and filtration. On the other hand, treatment of the feed seawater is more extensive and includes deaeration and addition of antiscalant and foaming inhibitors (El-Dessouky et al., 1999). To reduce the chemical treatment cost, 75-80% of the brine is recirculated, and only the make-up seawater is chemically treated (Johansen et al., 1995). Other basic units in the system include pumping units for the feed seawater, brine recycle and brine blowdown.

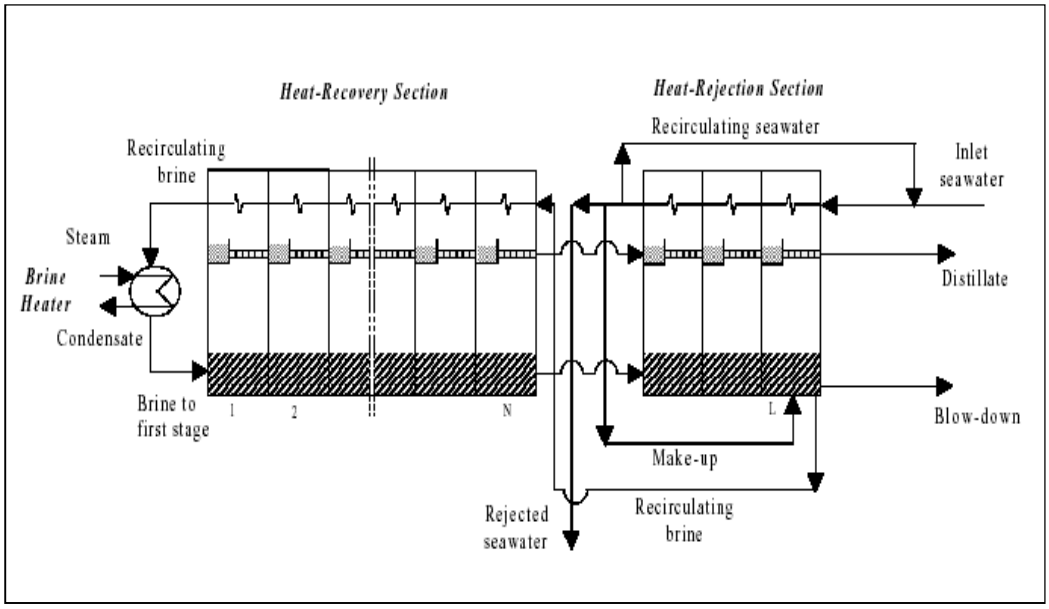

Figure 4.3 Schematic diagram of a MSF desalination plant (Al-Shayji, 1998)

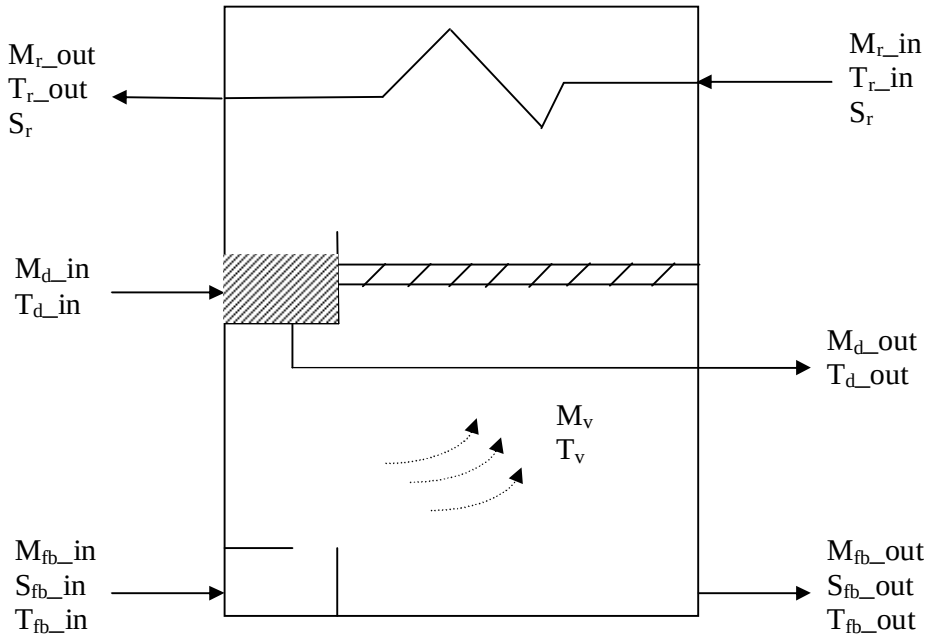

Figure 4.4 Schematic diagram of a single flashing stage

4.1.2. Review of previous modelling work

Because of its simplicity and robust nature, the stage-to-stage solution approach is the most widely method used by researchers to solve the steady-state MSF process equations in analysis and optimisation studies (Glueck and Bradshaw, 1970; Beamer and Wilde, 1971; Babrba *et al.*, 1973; and Montagna *et al.*, 1991).

The mathematical model presented by Glueck and Bradshaw (1970) is one of the first models specifically developed for MSF performance evaluation rather than design studies. They divide the single flashing stage into four compartments, namely, brine pool, vapour space, product tray (i.e. distillate) and tube bundle. Differential equations with supporting thermodynamic correlations are constructed to describe the behaviour of system variables in each section for all flashing stages. To obtain a steady-state model, zero values are assigned to all the derivatives.

The steady-state model obtained by Glueck and Bradshaw (1970) comprises eight nonlinear algebraic equations. The model is solved by a nested and iterative stage-by-stage method utilising the Newton-Raphson procedure to accelerate convergence. The model is described by the term “nested” due to two facts. One is because of countercurrent flow in the stages. The other is due to nonlinearities and dependence of physical properties on temperature, pressure and salinity.

The Newton-Raphson method was also used by Hayakawa et al. (1973) to obtain speedy and accurate solutions from a simulator which uses graphic representation to solve the large number of interrelated variables of MSF desalination process. Each stage is divided to 3 streams, namely, flashing brine, distillate and recycle streams. Solution of the model commences from the hot side of the plant. This model was developed to obtain the necessary information for determining the fouling factor as a design value and the most suitable partial load operation curves. However, the model can be adopted to study other parameters of the MSF process.

Barba et al. (1973), on the other hand, first solved a simplified steady-state model to establish the quantity of heat supplied to the brine heater and the cooling water temperature at the rejection section outlet as the initial guesses. A rigorous model was then initialised starting with the hot side. The rigorous model included two major loops. In an inner loop, the reject cooling water temperature was adjusted iteratively and computations were performed on the different rejection stages until the computed feed temperature matched its specified value. A guess for the heat input to the plant was made prior to the start of the inner loop and stage-by-stage calculations of the heat recovery section were performed. After completing inner-loop calculations, the outer loop is engaged by performing a check on the overall enthalpy (i.e. energy) balance for the whole plant. Computations were terminated if the overall enthalpy balance was satisfied. If not, the guess of the heat input to the plant was updated and calculations repeated. The model converged in two iterations with a running time of 25 seconds for every simulation.

In his work, Helal (1985) presented an extensive review of work carried out in the area of simulating the MSF desalination process and presented a unique method for solving the set of non-linear equations of the MSF system developed from reviewing past studies. In his literature review, Helal (1985) pointed out that some researchers developed approximate models assuming constant physical properties, heat transfer coefficient and temperature drop in all stages. These simplifying assumptions always result in a reduction in the number of equations to be solved. He concluded that these simple models are useful to initialise more rigorous calculations and for preliminary design evaluations.

Helal (1985) developed a Tridiagonal Matrix (TDM) algorithm. In the TDM method, iteration variables are updated simultaneously for each computational loop. The model equations were linearised to take advantage of the special structure of the equations to decompose the large system of equations into a number of subsystems which were grouped according to the type of variables rather than stage location. The direct substitution method was used to modify the flashing brine temperature for

the performance calculations. The simultaneous approach used in the algorithm minimises loop nesting. This solution approach presented by Helal (1985) can be categorised under the global approach (i.e. the simultaneous solution of the complete set of equations). The main features of the developed TDM algorithm are its high convergence stability, reliability and flexibility under different case scenarios.

The TDM algorithm was also used by Fathalah (1995) and Husain et al. (1993 & 1994) for the assessment of both dynamic and steady-state simulation of the MSF process. The algorithm by Husain et al. (1993 & 1994) represents a more realistic situation by feeding seawater directly to the last rejection stage. On the other hand, Helal (1985) assumed that a separate mixer for combining makeup and recycle streams is used.

In the TDM model by Fathalah (1995), calculations were initiated at the hot side of the plant for a given TBT and seawater temperatures, and it proceeded iteratively with calculations of flashing brine temperature rather than the brine recirculation temperature. To solve the governing equations, the Nachtsheim-Swigert iteration method was used. The author concludes that comparison of model output with actual data for a typical plant was satisfactory.

Husain et al. (1993 & 1994) also utilised the commercial package SPEEDUP to model stead-state operation of the MSF process. SPEEDUP is an equation oriented flowsheeting software which has the capability for both stead-state and dynamic simulations. The basic features of the software are (Husain et al., 1994):

- Starts with a user-defined or built-in global set of equations.
- Performs local linearization of the nonlinear equations by generating partial derivatives.
- Carries out symbolic manipulation by PASCAL routines and they then generate FORTRAN sub-program to calculate derivatives.
- Decomposes the global set of equations by re-ordering them to a block triangular form.

Results from both TDM formulations and SPEEDUP package show close agreement with actual MSF plant data.

SPEEDUP commercial package was also used by Al-Shayji (1998) to simulate both steady-state and dynamic situations of the MSF process. She concludes that results from the package show excellent agreement with actual plant data. The package is flexible at various levels of complexity but it is not suitable for day-to-day simulations of a desalination plant because input preparation for the package takes a large amount of time which may lead to convergence problems.

IPSEpro is another commercial simulation tool used utilised by Schausberger et al,. (2003) for the simulation of a cogeneration plant that includes the MSF desalination process. It is an equation-oriented simulation tool designed for power engineering applications. The package consists of the following two parts (Schausberger et al., 2003):

- Process simulation environment (PSE)
- Model development kit (MDK)

PSE is the flowsheeting tool, where the user defines the process graphically via model library icons. At the same time, PSE creates the underlying system of equations which are then solved by the simulation engine.

Schausberger et al. (2003) validated the model developed in IPSEpro using published data on MSF plant performance in literature, which showed good agreement.

Bourouis et al. (1995) utilised a global (i.e. equation-oriented) approach to simulate the MSF process. In this approach, the variables and equations were grouped into subvectors and subsystems, each of which is associated with a plant unit. To initialise the solution, the temperature of the brine leaving the brine heater and the

freshwater production flowrate were specified. To solve the linearised set of equations, they employed the Gaussian elimination method followed by an inverse substitution with a local search of the pivot. They reported that the advantages of the suggested approach are high speed convergence and ease of manipulation of specification equations.

El-Dessouky and Bingulac (1996) presented an algorithm for solving the steady-state model of the MSF process. The developed model can be used either for designing new plants or analysis and optimisation of existing plants. The steady-state model was solved using a one-dimensional fixed-point iteration and was implemented using the computer-aided design iterative package LAS. To solve the model, all equations were grouped according to stages and then the relations between variables in successive stages were established. Finally, equations describing a single stage were divided into the following three groups (i.e. subsets):

- Brine following through the brine pre-heater;
- Non-evaporating brine flowing through the flash chamber; and
- Mass of vapour formed.

Each group of these equations can be expressed as a single nonlinear equation with only one variable. The authors concluded that the main advantages of this method are:

- Less sensitivity to initial guesses;
- Less iterations to obtain the required solution;
- No need for calculating derivatives; and
- Flexibility in changing any design value.

Continuing their extensive research in modelling of desalination processes, Ettouney (2004) and Ettouney and El-Dessouky (1999) developed their own simulation package for thermal and membrane processes. The package, written in Visual Basic, comprises of a number of mathematical models developed previously. The

simulation package, which can model mechanical vapour compression (MVC), thermal vapour compression (TVC), absorption vapour compression (ABVC), adsorption vapour compression (ADVC) and MSF desalination process, includes the following features (Ettouney, 2004):

- Ability to design and perform cost estimate for conventional desalination processes.
- Ability to select and adjust the design and cost parameters used in the calculations.
- The codes check and limit the value of input parameters within practical ranges.
- Availability of help and tutorial files.

By the development of this simulation software, the authors seek ease of use, flexibility and accuracy of results.

Ali et al. (1999) solved both the steady-state and dynamic mathematical models describing the MSF process using the orthogonal collocation method. This method was utilised to obtain a reduced model for the MSF process. The states of the full-order model are approximated compactly by polynomials of an order equal to the number of chosen collocation points. By using the orthogonal collocation method, computational time was considerably reduced.

The orthogonal collocation method is a subset of the method of weighted residuals. This method is iterative in nature where a first guess at the solution is provided by the user. The solution is then imposed to satisfy the governing equations along with the boundary conditions. Residuals arise because the chosen solution does not satisfy either the equation or the boundary conditions. The basis for the method of weighted residuals is the intelligent selection of the *test* function that minimises the residual terms, which in turn leads to small error in the approximate solution (Stewart et al., 1985). The variations in the method are distinguished by this test

function. There are five widely used variations in engineering applications (Rice and Do, 1995):

- Collocation method;
- Subdomain method;
- Least square method;
- Moment method; and
- Galerkin method

The collocation method is widely because of several advantages:

- It is easy to use because its formulation is straight forward;
- Excellent accuracy when many collocation points are used; and
- Computation time is minimal

In the collocation method, the test function is the Dirac delta function at N *interior* points, called collocation points, within the domain of interest. If these interior collocation points are chosen as roots of an orthogonal jacobi polynomial, the method is called the orthogonal collocation method (Rice and DO, 1995).

4.1.3. Summary of previous MSF models

Published work on modelling and simulation of the nonlinear system of equations involved in the MSF process falls under the two basic methods. The methods are the modular approach and equation-oriented or global approach. Some models, however, use uses a hybrid or combination of the two methods.

Much of the early work on MSF modelling and simulation utilised the stage-by-stage modular approach due to its ease of use, in spite of its problems in convergence and lack of stability. Recently, workers have been interested in using the global approach due to the improvement in speed and capacity of computers.

From the review presented, a clear-cut answer cannot be given about which approach to choose over another since all published work on the subject claim accuracy and flexibility of their models. Also, the problem of saving running time and computer memory does not exist anymore because of the advancement of computers. Hence, the type and nature of assumptions made to formulate the equations which comprise the MSF process have more affect on accuracy of the model developed. Thus, the author of this work chooses to use the stage-by-stage sequential approach because it is simpler to formulate, check and change than having a large set of equations describing the entire MSF desalination plant.

4.1.4. Simplified MSF desalination Model

A simplified (i.e. linear) mathematical model for the MSF desalination system is a useful tool for quick design studies, evaluation of plant performance and developing an initial guess for rigorous mathematical models. The main advantage of the simplified model is that it does not require an iterative procedure and needs only minimal computation time. The linear model developed by (El-Dessouky and Ettouney, 2002) is used in this study.

The following assumptions are used to obtain the simplified MSF model (El-Dessouky and Ettouney, 2002):

- Constant and equal specific heat for all liquid streams.
- Equal temperature drop per stage for the flashing brine.
- Equal temperature drop per stage for the feed seawater.
- Average latent heat of vaporisation in each stage.
- Effect of temperature drop across the demister (i.e. mesh) within the stage is negligible.
- Temperature of feed seawater leaving heat rejection section is equal to the brine temperature in the last stage.

Other assumptions that are common in both simple and rigorous MSF mathematical models are:

- The distillate (i.e. product) leaving any stage is salt free. The salt concentration in the final product is only between 5 and 30 ppm compared with feed concentration of 45,000 ppm.
- Mass of flashed-off distillate as it enters the next stage is negligible.
- No mist entrainment in flashing brine.
- No heat losses to surroundings
- The heats of mixing for brine solutions are negligible.
- No subcooling of condensate in the brine heater (i.e. heat input section).
- Pressure drops and the consequent saturation temperature depression in the condenser can be neglected. This can be justified because the MSF plant operates at vacuum, which causes pressure recovery to momentum change and compensates the friction pressure loss (El-Dessouky et al., 1995).
- Effect of non-condensable gases on heat transfer coefficient and condensation temperature decrease is neglected due o the continuous withdrawal of these gases from the flashing chamber and brine heater.
- Vapour escaping to vents is small and not accounted for in the mass balances.

4.1.4.1. Temperature Profiles

A linear temperature profile is assumed for the flash chambers and the condensers. The temperature drop per stage, ΔT, is obtained from the top brine temperature (T_0) and temperature of brine leaving last flashing stage (T_n):

$$\Delta T = \left(T_O - T_n\right) \Big/ n \tag{4.1}$$

where n is the number of flashing stages

A general expression for the temperature of stage i is given:

$$T_i = T_O - i\Delta T \tag{4.2}$$

From an energy balance on stage i and the given expression for the temperature of stage i of the heat recovery section, a general equation is developed for the temperature of the recycled brine in the condenser tubes:

$$T_{ri} = T_n + (n - j)\Delta T - (i - 1)(\Delta T) \tag{4.3}$$

where j is the number of stages in the heat rejection section

Assuming that the difference between the temperatures of the flashing brine and the flashed-off steam in the stage has negligible effects on the energy balance and that the temperature profile is linear, the following equation can be written for the temperature drop in the heat rejection section:

$$\Delta T_{ji} = (T_n - T_{cw}) \Big/ j \tag{4.4}$$

where T_{cw} is the temperature of the seawater input to the condenser tubes of the rejection section

From the previous equation, the general equation for the cooling seawater temperature in the rejection section is:

$$T_{ji} = T_{cw} + (n - i + 1)(\Delta T_{ji}) \tag{4.5}$$

4.1.4.2. Stage Mass and Salt Balances

The following equation is obtained by applying the conservation of energy law for first flashing stage:

$$M_{v1} l_{avg} = M_r C_{P,avg} \Delta T \tag{4.6}$$

The amount of flashed-off vapour can be obtained by re-arranging the above equation:

$$M_{v1} = yM_r \tag{4.7a}$$

Where,

$$y = {C_{P,avg} \Delta T} \Big/ {l_{avg}} \tag{4.7b}$$

The vapour mass flowrate for the second stage is:

$$M_{v2} = y(M_r - M_{v1}) \tag{4.8}$$

By substituting the expression obtained for M_{v1}, the mass flowrate of the second stage vapour becomes:

$$M_{v2} = y(M_r - yM_r) \tag{4.9a}$$

and,

$$M_{v2} = M_r y(1-y) \tag{4.9b}$$

From the above, a general expression for the amount of vapour in each flashing stage is obtained:

$$M_{vi} = M_r y(1-y)^{i-1} \tag{4.10}$$

Assuming that all the flashed-off vapour in the stage condenses on the condenser tube, the total mass flowrate of distillate produced in all stages can be written as:

$$M_d = M_r\left[1-(1-y)^n\right] \tag{4.11}$$

This equation can be used to calculate the mass flowrate of the recycled brine since either the total mass of distillate or steam into brine heater is always specified in performance evaluation studies.

The mass flowrate of the flashing brine leaving stage i is given by the following general expression:

$$M_{fb} = M_r - \sum_{k=1}^{i} M_{d,k} \tag{4.12}$$

The salt concentration (S_r) of the recycled brine is obtained from the salt balance on the heat rejection section of the plant:

$$S_r M_r + S_{bd} M_{bd} = S_{sea} M_f + S_n\left(M_r - M_d\right) \tag{4.13}$$

Re-arranging the above equation for S_r

$$S_r = \frac{\left[S_{sea} M_f + S_n\left(M_r - M_d\right) - S_{bd} M_{bd}\right]}{M_r} \tag{4.14}$$

Let $S_{bd} = S_n$ and $M_f = M_{bd} + M_d$, the equation is further simplified:

$$S_r = \frac{\left[\left(S_{sea} - S_n\right) M_f + S_n M_r\right]}{M_r} \tag{4.15}$$

The salt concentration of the flashing brine in stage i is given by:

$$S_{fb} = \frac{\left(M_r - \sum_{k=1}^{i} M_{d,k} \right)}{M_{fb}} \tag{4.16}$$

To obtain the cooling seawater flowrate (M_{cw}), the overall energy balance around the MSF plant is used. Intake seawater temperature is the reference temperature in the balance:

$$M_s l_s = M_{cw} C_{P,avg} (T_n - T_{sea}) + M_{bd} C_{P,avg} (T_n - T_{sea}) + M_d C_{P,avg} (T_n - T_{sea}) \tag{4.17}$$

Re-arranging the above energy balance for M_{cw}, we get:

$$M_{cw} = \frac{\left[M_s l_s - M_f C_{P,avg} (T_n - T_{sea}) \right]}{C_{P,avg} (T_n - T_{sea})} \tag{4.18}$$

An energy balance is performed on the brine heater to obtain the mass flowrate of the steam used to heat the brine:

$$M_s l_s = M_r C_{P,avg} (T_O - T_{r1}) \tag{4.19}$$

The equation is re-arranged to calculate M_s:

$$M_s = \frac{M_r C_{P,avg} (T_O - T_{r1})}{l_s} \tag{4.20}$$

4.1.4.3. Physical and Thermodynamic Properties

Latent heat of evaporation (El-Dessouky and Ettouney, 2002)

The following correlation is used for calculating latent heat of evaporation (l) in kJ/kg. It is valid for $5 \le T \ge 200°C$:

$$l = 2501.897149 - 2.407064037T + 0.001192217T^2 - 1.5863\times10^{-5}T^3 \qquad (4.21)$$

Boiling point elevation (El-Dessouky and Ettouney, 2002)

The following correlation is valid for $10{,}000 \le S \ge 160{,}000 ppm$ and $10 \le T \ge 180°C$:

$$\left.\begin{aligned} &BPE = AS + BS^2 + CS^3 \\ &Where \\ &A = \left(8.325\times10^{-2} + 1.883\times10^{-4}T + 4.02\times10^{-6}T^2\right) \\ &B = \left(-7.625\times10^{-4} + 9.02\times10^{-5}T - 5.2\times10^{-7}T^2\right) \\ &C = \left(1.522\times10^{-4} - 3\times10^{-6}T - 3\times10^{-8}T^2\right) \end{aligned}\right\} \qquad (4.22)$$

Non-equilibrium allowance (El-dessouky *et al.*, 1995)

$$\left.\begin{aligned} &NEA_{10} = (0.9784)^{T_{FBi}} (15.7378)^{H} \left(1.3777^{\phi_b\times10^{-6}}\right) \\ &NEA = \left(\frac{NEA_{10}}{(0.5\Delta T + NEA_{10})}\right)^{0.3281L} (0.5\Delta T + NEA_{10}) \end{aligned}\right\} \qquad (4.23)$$

4.1.5. Reference MSF Desalination Plant

The Doha West MSF plant operating in Kuwait is used in this study to validate the developed simple MSF model, and to perform analysis of the MSF desalination

process in general. The plant (Figure 4.5), commissioned in 1983, uses a cross-tube type MSF evaporator with recirculating brine. The plant comprises 24 flash stages, 21 in the heat recovery section and 3 in the heat rejection section. There are a total of 16 multistage flash units within the plant, with their output ranging from 27,277 m^3/day (6.0 MG/D) to 32,732 m^3/day (7.2 MG/D) depending on the operation mode of the plant (i.e. low or high-temperature).

4.1.5.1. Validation of MSF model

Table 4.1 lists the DW operational parameters used as input to the simple MSF model. The operational parameters for the plant are for summer operation at 100% capacity and 32.32 °C seawater feed. The results of the model are compared to actual plant data and to output from the commercial software "DistX" by *Advanced Energy Systems Analysis* consultancy company.

Tables 4.2 to 4.4 list results of the simple model, actual data and output from the commercial software *DistX* for the flashing brine, distillate vapour and recycled brine streams. The conclusions from the results of the three streams are:

1) Flashing brine stream

The results show excellent agreement between flashing brine output parameters from the simple model on one hand and actual and *DistX* on the other. The mean error for temperatures, mass flowrate and salt content between model and actual values is 1.54, 0.21 and 0.20 percent, respectively.

2) Distillate vapour stream

Results of the model are given in Table 4.3. The model vapour temperatures are close to actual and *DistX* vapour temperatures. The mean percentage error between model and actual values is 1.9%.

O the other hand, the percentage error is larger for the mass flowrate of the vapour. The largest error of about 26% occurs at stage 22 where there is a large decrease in the actual mass flowrate of vapour.

3) Recycled brine stream

Just like the previous two streams, the temperatures of the model recycled brine are very close to actual and *DistX* values. The mean percentage error for temperatures between model and actual is about 1%.

Comparison of model and actual recycle brine mass flowrate gives a mean percentage error of 0.12%. However, a large error could occur if a thermodynamic property such the specific heat is not estimated accurately. This in turn will affect the values of flashing brine mass flowrate and distillate vapour mass flowrate.

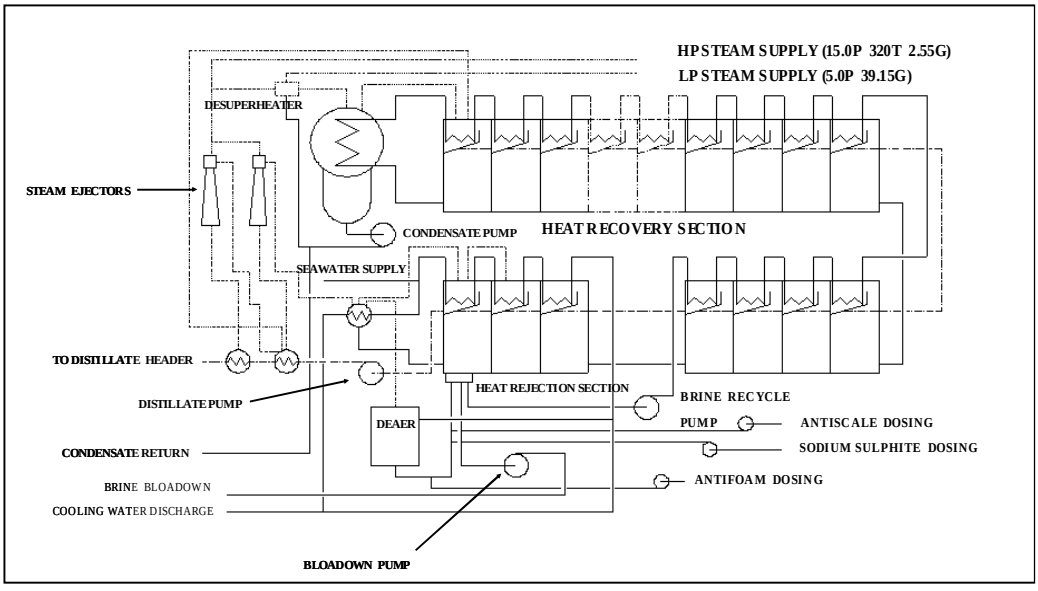

Figure 4.5 Simplified diagram of the Doha West cogeneration plant (desalination)

Table 4.1 Input parameters to the simple MSF model

Parameter	symbol	Unit	Value
Total distillate produced	M_d	kg/s	313.25
Seawater temperature	T_{sea}	°C	32.2
Seawater salinity	S_{sea}	ppm	45,000
Brine heater steam temperature	T_s	°C	100
Brine heater steam pressure	P_s	kPa	101
Last stage brine temperature	T_n	°C	40.5
Top brine temperature	T_O	°C	90.56
Stage width	W	m	17.66
Brine specific heat	C_P	kJ/kg.°C	3.84

Table 4.2 Model results for flashing brine variables

Stage	Flashing Brine								
	Temperature (°C)			Mass flowrate (kg/s)			Concentration (ppm)		
	Model	Actual	DistX	Model	Actual	DistX	Model	Actual	DistX
1	88.47	88.40	88.47	3959.68	3953.64	3936.02	67739	67751	67716
2	86.39	86.20	86.39	3946.15	3939.11	3922.07	67971	68000	67957
3	84.30	83.90	84.30	3932.67	3924.03	3908.22	68204	68262	68198
4	82.22	81.70	82.22	3919.24	3909.08	3894.45	68438	68523	68439
5	80.13	79.40	80.13	3905.85	3894.33	3880.78	68672	68783	68680
6	78.04	77.20	78.04	3892.51	3879.72	3867.19	68907	69041	68921
7	75.96	75.00	75.96	3879.21	3865.33	3853.69	69144	69299	69163
8	73.87	72.70	73.87	3865.96	3851.08	3840.28	69381	69555	69404
9	71.79	70.50	71.79	3852.76	3837.06	3826.95	69618	69809	69646
10	69.70	68.30	69.70	3839.59	3823.17	3813.71	69857	70063	69888
11	67.62	66.20	67.62	3826.48	3809.50	3800.55	70097	70314	70130
12	65.53	64.00	65.53	3813.41	3796.00	3787.48	70337	70564	70372
13	63.44	61.90	63.44	3800.38	3796.00	3774.48	70578	70811	70614
14	61.36	59.80	61.36	3787.40	3782.75	3761.57	70820	71056	70857
15	59.27	57.70	59.27	3774.46	3769.72	3748.74	71063	71298	71099
16	57.19	55.60	57.19	3761.57	3756.92	3735.98	71306	71536	71342
17	55.10	53.60	55.10	3748.72	3744.42	3723.31	71551	71770	71585
18	53.01	51.60	53.01	3735.92	3732.19	3710.71	71796	72001	71828
19	50.93	49.70	50.93	3723.15	3720.25	3698.19	72042	72226	72071
20	48.84	47.80	48.84	3710.44	3708.64	3685.75	72289	72446	72314
21	46.76	45.90	46.76	3697.76	3697.36	3673.38	72537	72661	72558
22	44.67	44.40	44.67	3685.13	3686.44	3661.09	72785	72847	72801
23	42.59	42.60	42.59	3672.54	3677.33	3648.88	73035	73051	73045
24	40.50	40.50	40.50	3660.00	3666.78	3636.73	73285	73285	73289

Table 4.3 Model results for distillate vapour variables

Distillate Vapour						
Stage	Temperature (°C)			Mass flowrate (kg/s)		
	Model	Actual	DistX	Model	Actual	DistX
1	87.26	87.20	86.91	13.57	14.69	14.01
2	85.17	85.00	84.84	13.53	14.53	13.94
3	83.08	82.80	82.76	13.48	15.08	13.86
4	81.00	80.50	80.69	13.43	14.94	13.76
5	78.91	78.20	78.62	13.39	14.75	13.68
6	76.83	76.00	76.55	13.34	14.61	13.59
7	74.74	73.80	74.48	13.30	14.39	13.50
8	72.66	71.50	72.41	13.25	14.25	13.41
9	70.57	69.30	70.34	13.21	14.03	13.33
10	68.48	67.10	68.26	13.16	13.89	13.24
11	66.40	65.00	66.19	13.12	13.67	13.16
12	64.31	62.80	64.12	13.07	13.50	13.08
13	62.23	60.60	62.05	13.03	13.25	12.99
14	60.14	58.50	59.98	12.98	13.03	12.91
15	58.05	56.30	57.91	12.94	12.81	12.83
16	55.97	54.20	55.84	12.89	12.50	12.75
17	53.88	52.20	53.77	12.85	12.22	12.68
18	51.80	50.10	51.70	12.81	11.94	12.60
19	49.71	48.40	49.63	12.76	11.61	12.52
20	47.63	46.10	47.56	12.72	11.28	12.44
21	45.54	44.20	45.50	12.67	10.69	12.37
22	43.45	42.60	43.43	12.63	9.33	12.29
23	41.37	40.70	41.36	12.59	10.56	12.22
24	39.28	38.60	39.29	12.54	11.69	12.14

Further analysis can be performed to check the accuracy of the developed model. One way is to calculate some overall performance parameters and compare them with actual values. Table 4.5 shows model and actual performance variables. It can be seen that the percentage error ranges between 0.21% and 7.95% for the different properties. These calculated errors are acceptable considering the assumptions made for the simple MSF model.

Table 4.4 Model results for recycled brine variables

Stage	Recycled Brine					
	Temperature (°C)			Mass flowrate (kg/s)		
	Model	Actual	DistX	Model	Actual	DistX
1	84.30	84.89	84.6	3973.25	3968.33	3950.02
2	82.22	82.70	82.5	3973.25	3968.33	3950.02
3	80.13	80.50	80.5	3973.25	3968.33	3950.02
4	78.05	78.30	78.4	3973.25	3968.33	3950.02
5	75.96	76.00	76.3	3973.25	3968.33	3950.02
6	73.87	73.70	74.2	3973.25	3968.33	3950.02
7	71.79	71.50	72.2	3973.25	3968.33	3950.02
8	69.70	69.30	70.1	3973.25	3968.33	3950.02
9	67.62	67.10	68.0	3973.25	3968.33	3950.02
10	65.53	64.80	66.0	3973.25	3968.33	3950.02
11	63.44	62.70	63.9	3973.25	3968.33	3950.02
12	61.36	60.50	61.8	3973.25	3968.33	3950.02
13	59.27	58.30	59.8	3973.25	3968.33	3950.02
14	57.19	56.20	57.7	3973.25	3968.33	3950.02
15	55.10	54.10	55.6	3973.25	3968.33	3950.02
16	53.02	52.00	53.5	3973.25	3968.33	3950.02
17	50.93	49.90	51.5	3973.25	3968.33	3950.02
18	48.84	47.90	49.4	3973.25	3968.33	3950.02
19	46.76	45.90	47.3	3973.25	3968.33	3950.02
20	44.67	44.00	45.3	3973.25	3968.33	3950.02
21	42.59	42.10	43.2	3973.25	3968.33	3950.02
22	40.50	40.23	40.2	3973.25	3968.33	3950.02
23	37.73	38.00	37.4	3973.25	3968.33	3950.02
24	34.97	35.30	34.6	3662.64	3968.33	3950.02

Table 4.5 Performance parameters of Doha West MSF desalination plant

Parameter	Model	Actual	% error
Performance ratio	7.64	8.00	4.65
Brine circulation ratio (recycle kg/kg product)	12.68	12.67	0.11
Gain ratio (capacity/steam input)	7.41	8.00	7.95
Heat input (kJ/kg product)	304.78	282.10	7.44
Steam input (kg/s)	42.27	39.16	7.36
Recycled brine (kg/s)	3973.25	3968.33	0.12
Cooling seawater (kg/s)	1949.76	1862.19	4.49
Brine blowdown (kg/s)	498.31	499.36	0.21
Total seawater feed (kg/s)	2995.49	2878.50	3.91

4.1.6. Analysis of Doha West MSF Plant

In this section, the energy consumption by the plant is calculated and analysis of variables affecting its performance is presented.

4.1.6.1. Energy Consumption

The MSF desalination plant consumes both thermal and mechanical energy. The three main contributors to energy consumption in the plant are:

- ***Brine heater in the form of low-pressure steam***

The steam extracted from the low-pressure turbine to brine heater is the energy source used to produce freshwater in the MSF desalination process. The heat input per kg product to the brine heater, at a value of 304.78 kJ/kg from Table 4.5 above, is calculated from:

$$q_{bh} = \dot{m}_s * \left(h_{superheat} - h_{sat,liquid}\right) / M_d \qquad (4.24)$$

- ***Water pumps***

The MSF plant usually comprises recirculation, cooling seawater, distillate, blowdown and condensate pumps. The pumping energy is estimated using the following equation:

$$W_{pump} = \dot{Q} * \Delta P / h_{pump} \qquad (4.25)$$

Table 4.6 shows the mechanical energy consumption of the different pumps. The total work is at a value of 2099.93 kW, which equals 6.70 kJ/kg product.

- ***Steam-jet ejectors in the form high-pressure steam***

The steam is extracted to the ejector at a pressure of 15 bar (or 1500 kPa) at saturation conditions. Thus, the specific heat input (i.e. heat input per kg product) to the ejector is calculated from:

$$q_e = \dot{m}_e l_e / M_d \tag{4.26}$$

From the above equation, the heat input to the ejector per kg product is 15.83 kJ/kg when l_e is at 1945.2 kJ/kg and $\dot{m}_e$ is at 2.55 kg/s.

4.1.6.2. Steam Extraction

The mass flowrate of the extracted steam into the brine heater is varied to study its effect on MSF plant distillate output. The results plotted in Figure 4.6 show that there is a positive linear relationship between steam input and distillate production. The same direct relation also exists between steam temperature and distillate production. However, the performance ratio, gain ratio and heat input to brine heater do not change with the change in steam mass flowrate because the ratio M_s/M_d stays constant when varying the steam mass flowrate.

Table 4.6 Power consumption by pumps in MSF desalination plant

Pump	Volumetric flowrate m^3/s	Head kPa	Energy consumption kW
Distillate	0.31	275.79	107.99
Recirculation	3.97	280.65	1393.87
Cooling seawater	2.18	150.99	412.18
Blowdown	0.50	137.89	85.89
Other*	N/E	N/E	100.00
Total			2099.93

*steam condensate, ejector condensate and chemical dosing taken as 5% of calculated pumping power (Darwish *et al.*, 1997)

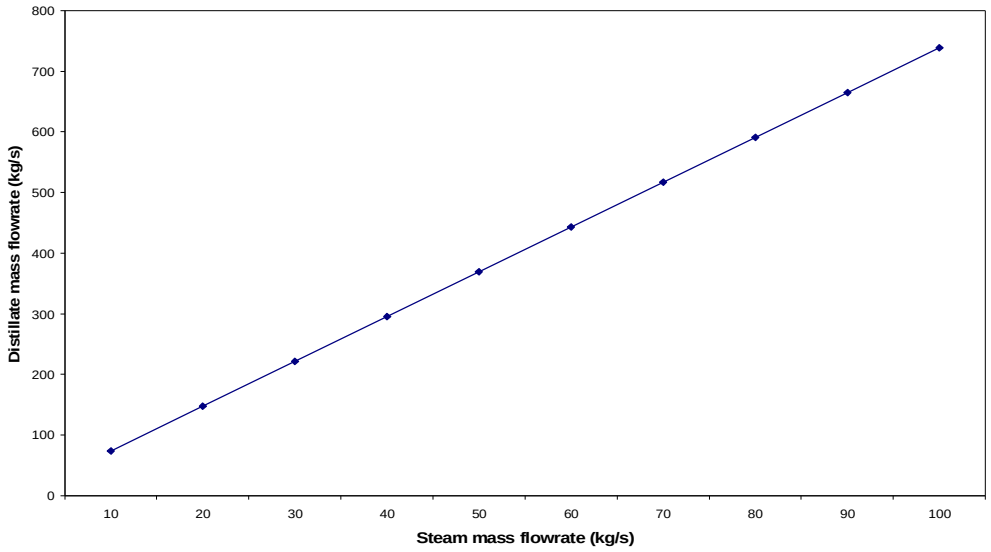

Figure 4.6 Diagram of distillate production vs. steam mass flowrate into brine heater

4.1.6.3. Number of Stages & Top Brine Temperature (TBT)

Figures 4.7 and 4.8 illustrate the effects of number of stages and TBT on the specific flowrate of cooling seawater and specific flowrate of recirculated brine, respectively. Figure 4.7 shows that the three lines represented data for different TBTs are almost superimposed. This means that the TBT has negligible effect on the specific cooling seawater flowrate (i.e. M_{cw}/M_d). The figure also shows that the ratio M_{cw}/M_d decreases with the increase of number of stages.

Figure 4.8, on the other hand, shows that the specific recirculated brine flowrate is independent of the number of stages. However, the figure shows that the ratio M_r/M_d decreases with increasing TBT. These results agree with findings by El-Dessouky et al. (1995).

The performance ratio (PR) is plotted against the TBT for different stage numbers in Figure 4.9. It is shown from the figure that the PR is independent of the TBT, and that it increases with increasing the number of the stages. This improvement in plant

PR may be due to the simultaneous increase of the distillate flowrate and decrease of steam flowrate. However, results published in El-Dessouky et al. (1995) show that there is a slight increase in PR as the TBT increases for a specified number of stages. This discrepancy may be attributed to the fact that a linear model is used in this study but El-Dessouky et al. (1995) used a nonlinear model for the MSF desalination plant.

In figure 4.10 the ratio M_r/M_d is plotted against the TBT at different stage numbers. It is shown that the plotted lines for the ratios at different stage numbers are drawn on top of each other. This means that the number of stages in a plant have negligible effect on the M_r/M_d. Furtehrmore, the figure shows that M_r/M_d is inversely proportional to the TBT. The decrease in this ratio also means that specific pumping energy will be decrease as well.

From the above analysis we can see that increasing certain parameters, such as steam temperature and flowrate, and number of stages, in MSF plant will result into increased distillate production and better plant performance. Nevertheless, there should be a compromise when choosing these parameters keeping in mind fixed and variable costs. For example, increasing the number of stages will increase the overall cost of the plant but variable (i.e. running) costs may decrease when increasing the number of stages. Also, increasing steam temperature means increasing the pressure of the steam, which means more expensive steam.

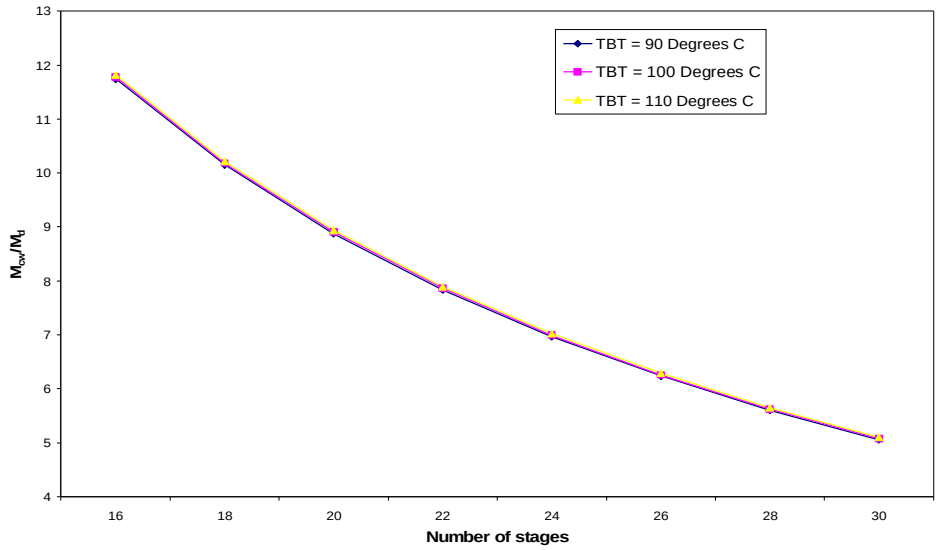

Figure 4.7 Effect of number of stages on specific cooling seawater flowrate at different TBTs

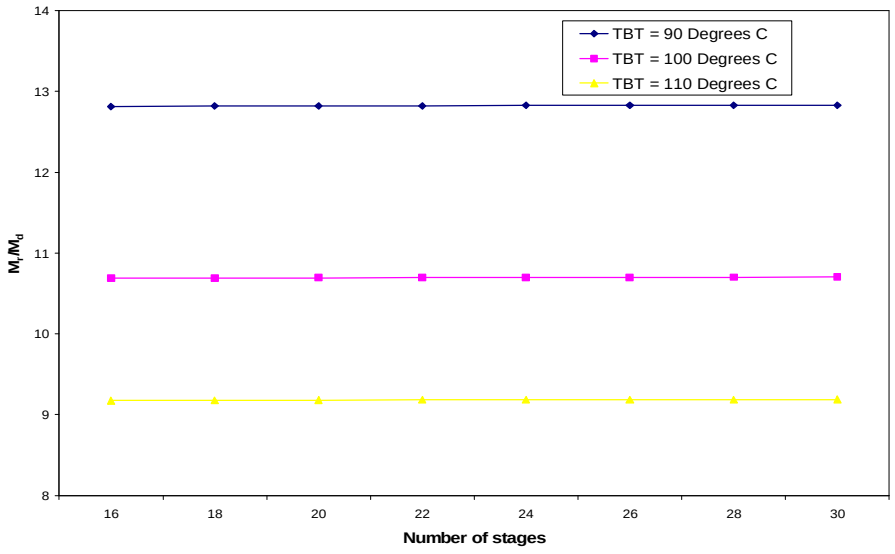

Figure 4.8 Effect of number of stages on specific recirculated brine flowrate at different TBTs

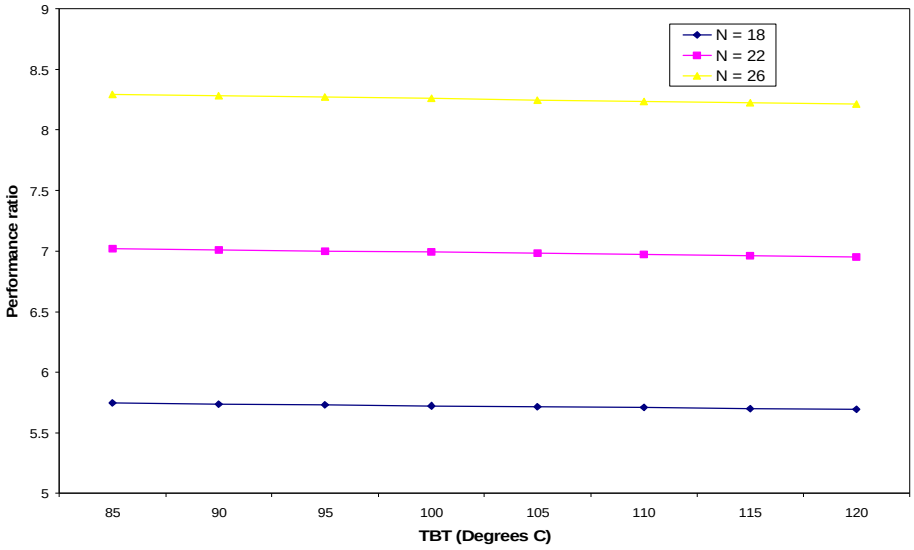

Figure 4.9 Effect of TBT on performance ratio at different number of stages

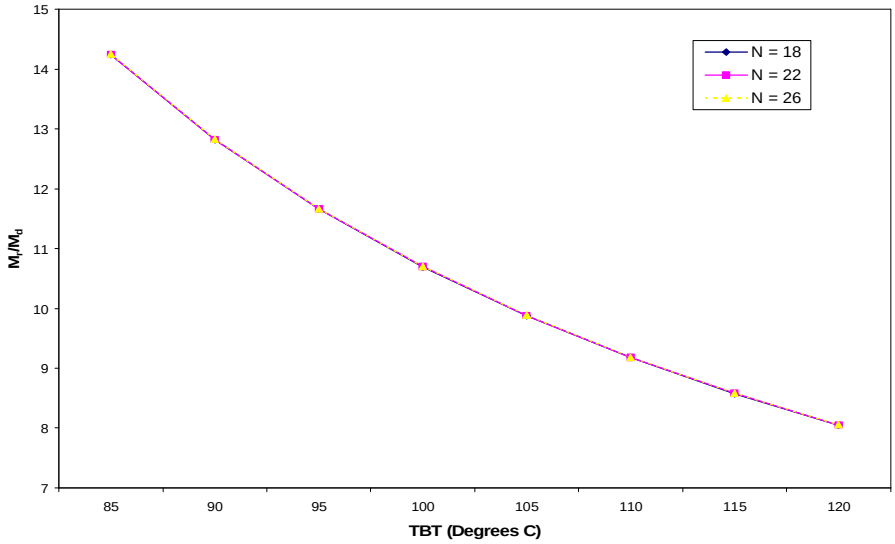

Figure 4.10 Effect of TBT on specific recirculated brine flowrate at different number of stages

4.2. Reverse Osmosis

The principle of osmosis is based on the fact that, if two solutions of different concentration are separated by a semi-permeable membrane, the solvent flows from the dilute solution to the more concentrated solution. The process continues until the osmotic pressure between the solutions is the same (i.e. reaching an equilibrium state) (Heitmann, 1990).

The principle of osmosis can be reversed by applying pressure to the more concentrated solution that exceeds the osmotic pressure. The solvent, in this case, will flow to the dilute solution. Using RO in desalination of seawater, there is no heating and the only energy required is electricity for pressurising the feed water. This pressure ranges from 54 to 80 bar for seawater desalination (Amjad, 1993; and Buros, 2000). Figure 4.11 shows the basic components of a RO plant.

According to Johansen et al. (1995) and Buros (2000), the successful commercialisation and implementation of RO started in the 1970s, but in the 1980s, RO became competitive with the classical distillation techniques (Van der Bruggen and Vandecasteele, 2002). Since then, capacities of RO units have increased

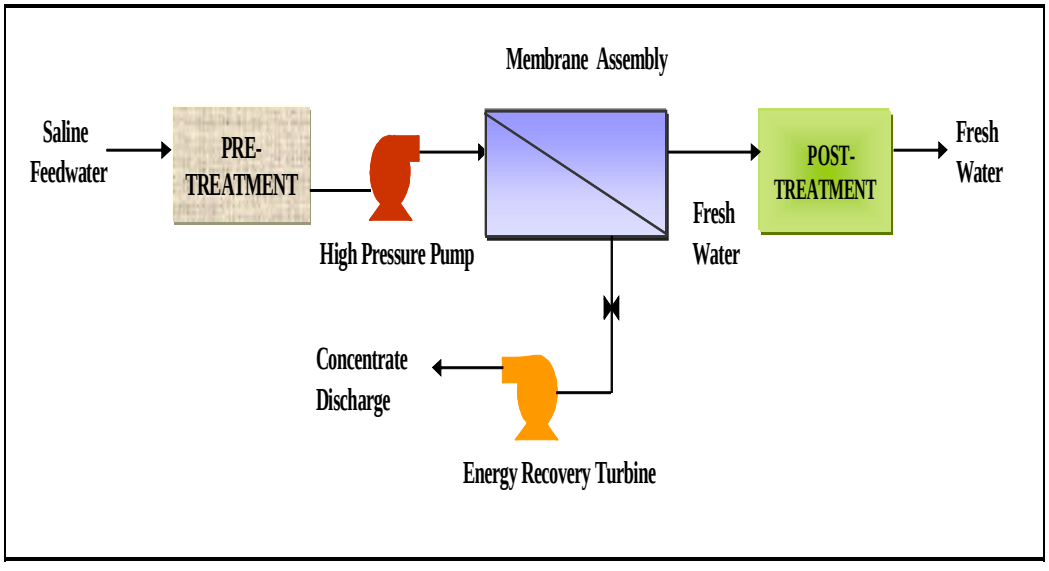

Figure 4.11 Basic components of a RO plant

dramatically to reach installation sizes of 45,000 m^3/day in Bahrain and 56,000 m^3/day in Jeddah, Saudi Arabia (Wade, 1993). According to Johansen (1995), a RO process occupying 1 m^3 of space can produce 100-500 m^3 of potable water per day. Buros (2000) reported that the world's largest RO plant in Yuma, USA produces 270,000 m^3/day of potable water from the Colorado River. In seawater RO plants, 20 to 70% of the feed is discharged to waste (Buros, 2000).

4.2.1. Seawater Intake

The location of the intake is of vital importance because of its influence on the pre-treatment efficiency, plant availability and operating cost (Chida, 1997). The location of the intake, however, is site-specific and can not be generalised.

According to Chida (1997), a minimum depth of 8 to 10 m is usually acceptable. Bell-mouth location of the intake pipe should be positioned to have a minimum clearance of 3 to 5 m from the bottom and 2 to 2.5 m clearance on all other sides to minimise contamination by planktonic, algae and other marine suspensions. Glueckstern (1999) reported that seawater obtained directly from surface water always requires comprehensive pre-treatment, such as media filtration and continuous or intermittent disinfection, prior to final filtration. Glueckstern (1999) also claims that economics of a medium-size seawater RO plant fed by high-quality water from beach wells is better than for a plant fed by an open surface intake.

4.2.2. System Configurations

RO configurations include single-stage, two-stages, and two-pass systems. Selection among these configurations depends on the desired quality of the product water. In this regard, the two-pass system gives the highest purity product. Therefore, it is suitable for preparation of make-up boiler water. The single-stage system gives the simplest layout of all configurations and its use is quite common in

various desalination applications. The two-stage system is frequently employed for brackish water use, where it is necessary to increase the overall recovery ratio. The recovery ratio (i.e. water conversion factor) is defined as the percentage of the feed water that is converted to permeate in a RO plant (Amjad, 1993).

4.2.3. Membranes

The membrane is the heart of the RO system. Therefore, careful consideration should be given to the selection of the membrane material and configuration based on water end-use requirements and feed water quality (Amjad, 1993). Membranes usually vary in their ability to pass freshwater and reject the passage of salts. No membrane is perfect in its ability to reject salts.

Membranes are thin-sheet like materials, which form a barrier in the feedwater path. RO membranes, while allowing water to pass through, retain 90-99% of all inorganic substances in a solution, 95-99% of the organic constituents and almost 100% of the most finely divided colloidal matter (i.e. bacteria, viruses, colodial silica) (Khan, 1986).

A membrane should have the following characteristics to function ideally (Amjad, 1993):

- High water-flux rates
- High salt rejection
- Tolerant to chlorine and other oxidants
- Resistant to biological attacks
- Resistant to fouling by colloidal and suspended material
- Inexpensive
- Easy to form into thin films or hollow fibres
- Tolerates high pressures
- Chemically stable
- Able to withstand high temperatures

4.2.4. Membrane Materials and Configurations

Over the years, there have been many developments in membrane materials and there are hundreds of membranes commercially available for saline water processing (Johansen et al., 1995). However, there are three commercially popular and well-developed membrane materials:

- Cellulose acetate
- Aromatic polyamide
- Thin film composites

RO membranes are divided into four basic configurations, namely (Byrne, 1995 and Amjad, 1993):

- ***Plate-and-frame*** – They are not common in RO applications because they require a large amount of high-pressure hardware to construct, which makes it expensive.

- ***Tubular*** – These systems have minimal membrane area compared to flow volume through the tubes which makes them expensive to purchase and operate.

- ***Hollow fiber*** – These types of membranes are widely used in seawater desalination applications due to their ability to produce a large amount of permeate from a single element. However, the elements are more prone to fouling because their design does not allow for turbulent or uniform flow across the fiber surface. It is also difficult to clean.
- ***Spiral wound*** – There is small potential for these membranes to experience fouling or scale formation due to the uniform flow velocities and turbulence across the membrane surface. They are also relatively inexpensive to manufacture.

4.2.5. Product-Water Quality

Ideally, the end-product from RO desalination units contains 5% to 10% of the original total dissolved solids (TDS). But, organics are almost completely removed. Also, a residual TDS between 400 and 1100 ppm is normally achieved in one-pass RO plants. Alternatively, a TDS down to 80 ppm can be achieved in two-pass RO plants (Johansen, 1994).

4.2.6. Energy Consumption

The main energy requirement for RO desalination plants is the electrical power applied to the electric motor-driven high pressure pumps. However, other load contributions come from the source water supply, pre-treatment system, second stage pump and the distribution pump (Khan, 1986). On the other hand, diesel or steam engine may be used to provide the mechanical power required.

In RO systems with energy recovery, the high-pressure brine exiting the final RO stage is fed into an energy recovery unit. These units may be hydroturbines directly coupled to the shaft of the high-pressure feed pump or Pelton wheels, which are usually connected to induction motor/generator sets (Amjad, 1993). Amjad (1993) and Al-Mutaz (1996) reported that energy recovery can reduce energy consumption in RO systems by 30 to 40%.

Darwish et al. (2002) reports the performance characteristics of the Jeddah-1 RO plant phase II. The plant consists of 10 units, each with a capacity of 5680 m^3/d (237 m^3/h). The feed salinity is about 43,300 ppm. However, the authors do not give a range for the feed seawater temperature. Table 4.7 shows the performance characteristics of the plant.

The table gives a figure of 3.84 kWh/m^3 for the energy consumption of the high pressure pump when energy recovery turbine is used. However, the author assumes 20% additional energy consumption by other pumps in the plant (e.g. seawater

supply, seawater boost, chemical dosing pumps). The specific energy consumption comes to a value of 5.09 kWh/m^3 when considering the additional energy consumed.

According to Abou Rayan and Khaled (2002) the energy consumption of the RO desalination plant located in Dahab City, Sinai, Egypt is 8.81 kWh/m^3. The plant comprises four units each with a 500 m^3/d (20.83 m^3/h) capacity. The salinity of the feed seawater is 44,000 ppm. Table 4.8 shows the energy consumption by the different pumps in the plant. The authors assumed a pump efficiency of 90%. Energy recovery is not utilised in this plant, which explains the relatively higher specific energy consumption by this RO plant.

Table 4.7 Specific energy consumption of the Jeddah-1 RO plant

Parameter	**Value**
Feed pressure (bar)	60
Feed flowrate (m^3/h)	677
Product flowrate (m^3/h)	237
Reject Pressure (bar)	56
Reject flowrate (m^3/h)	440
Feed pump efficiency (%)	76
Turbine efficiency (%)	84
Energy without energy recovery (kWh/m^3)	6.27
Recovered energy (kWh/m^3)	2.43
Net energy consumption (kWh/m^3)	3.84

Table 4.8 Energy consumption of a single unit in the Dahab RO desalination plant

Pump	**Power consumption (kW)**	**Specific energy consumption (kWh/m^3)**
Sea pump	14	0.66
Filter pump	18	0.86
Additive pumps	1	0.05
High pressure feed pump	231	11
Energy recovery turbine	79	3.76
Total	***188***	***8.81***

Avlonitis et al. (2003) summarise the performance of small and medium sized RO plants operating in Greece. Table 4.9 lists operation characteristics and energy

consumption of the different plants. The table shows that the range of energy consumption is between 3.02 kWh/m^3 and 9.38 kWh/m^3. On the other hand, DESWARE (2003) reported that the total energy consumption for seawater RO desalination is in the range 5 to 7 kWh/m^3. Also, Buros (2000) claimed that newly commissioned seawater RO plants with energy recovery can have energy consumption as low as 3 kWh/m^3.

4.2.7. Pilot Plant at Kuwait Institute for Scientific Research (KISR)

The pilot plant is located at the Desalination Research Plant (DRP) (Figure 4.12). System performance data available for the spiral wound membranes between the dates 14/08/1995 and 03/01/1996 are used to estimate the specific energy consumption of the high pressure feed pump (Table A-1, Appendex-1). The feed seawater is drawn from a beachwell intake system using submersible pump with a temperature range between 25°C and 26°C. The seawater salinity is around 41,000 ppm.

The RO plant with the spiral wound (SW) membranes is used as the reference plant in this research because it is recommended by KISR over the hollow fiber (HF) plant. According to Bou-Hamad et al. (1998), the spiral wound membranes had several advantages over the hollow fiber ones:

- SW membranes are less prone to fouling due to slime.
- Higher availability. The availability of SW was 99.61% compared to 93.16% for HF for a period of 12 months.
- Salt rejection for SW membrane remained at design value throughout the year of operation.
- SW-based RO plants can operate under low pressure.

Plant nominal capacity is 300 m^3/d (12.5 m^3/h), however, it varies between 10.70 and 12.86 m^3/h in the measured data used by the author. On the other hand, feed

Table 4.9 Energy consumption of RO plants operating on the Greek islands

Location	Capacity (m^3/h)	Feed pressure (bar)	Temperature (°C)	Energy recovery system	Specific energy consumption (kWh/m^3)
Oia	17	62	25-27	Pelton wheel	4.60
Oia	7.5	61	25-27	Turbo charger	4.65
Oia	12.5	59	25-27	Pelton wheel	5.28
Ios	21	67	25-27	Px-60	3.02
Ithaki	25	71	25-27	Pelton wheel	9.38
Syros	24	56	25-27	Pelton wheel	6.16
Mykonos	21	70	25-27	Pelton wheel	8.36

pressure and flowrate varied between 46 bar and 56 bar and 33.02 m^3/h and 36.72 m^3/h, respectively. In order to estimate the energy consumption at each measurement point without and with energy recovery turbines, Equations (4.27) and (4.28) were used, respectively.

$$E = \frac{P_{feed} \dot{Q}_{feed}}{\dot{Q}_{product} * 3600 * e_{pump}} \tag{4.27}$$

$$E_{net} = E - \frac{P_{reject} * \dot{Q}_{reject} * e_{turbine}}{\dot{Q}_{product} * 3600} \tag{4.28}$$

Pressures are in kPa and volumetric flowrates are in m^3/h. Pump efficiency is around 65% and efficiency of Pelton wheel turbine is at 80%.

An average figure is then calculated for the specific energy consumption from the estimated values of the energy consumption at each single measurement point. The calculated average specific energy consumption of the high pressure pump without the use of energy recovery is at a value of ***6.41 kWh/m^3***. As given by Darwish et al. (2002), 20% additional energy consumption by other pumps in the plant is added to the figure calculated for the high-pressure pump. The new value for total energy consumption in the plant is ***7.70 kWh/m^3***. On the other hand, the average total

consumption for the plant when the pelton wheel turbine is fully loaded is at a value of ***5.49 kWh/m^3*** (average value of 4.21 kWh/m^3 when considering high-pressure pump only).

The performance data provided by the KISR RO pilot plant and the estimated energy consumption will be used in this research for modelling and calculations which include RO desalination plants. The reason for this choice is because the research is concerned with powerplants in Kuwait and the experimental study is performed in Kuwait also. The estimated figure of 5.49 kWh/m^3 for the energy consumption in RO plants is acceptable when compared with the figures given in published literature.

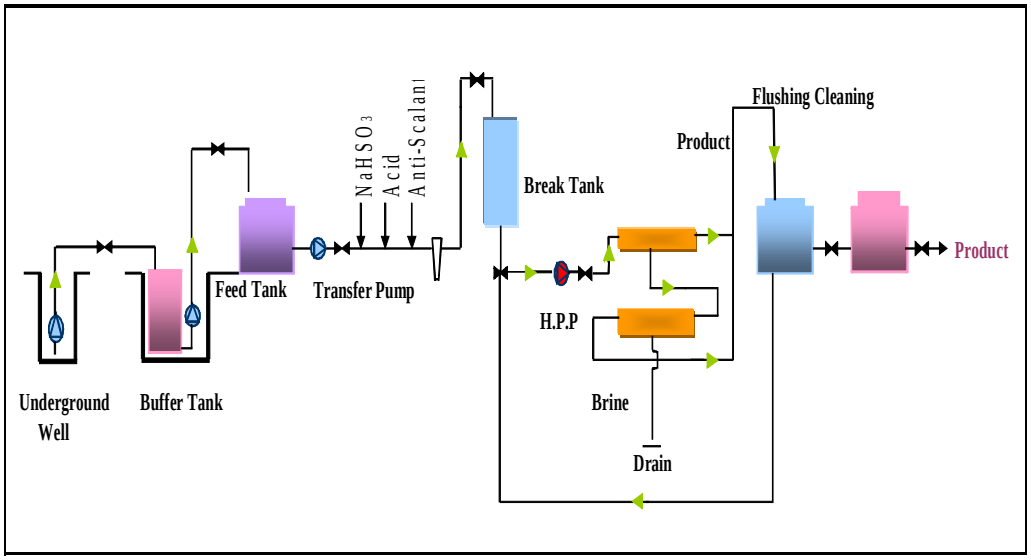

Figure 4.12 RO plant at KISR's Desalination Research Facility

4.3. Conclusions

MSF and RO remain the most widely used and commercially successful seawater desalination technologies in the world and Middle East. In Kuwait, MSF is the only

desalination technology utilised for seawater desalination. A mathematical model describing the MSF system has been developed to be able to correctly analyse the technology in general and MSF desalination plants in Kuwait specifically. A thorough literature review of previous modelling work was presented to be able to arrive at the method that best suits this research. It was concluded that the stage-by-stage sequential approach to be used for this work because it is simpler to formulate, check and change than having a large set of equations describing the entire MSF desalination plant.

A simplified and linear formulation of the MSF system was combined with the sequential approach which has the advantage of not requiring a rigorous iterative procedure, which in turn results in minimal computation time. The developed linear mathematical was applied to an existing desalination plant in Kuwait in order to validate it. Results of the analysis showed that the developed model in this work is generally accurate in predicting the performance of the MSF plant.

The second part of the chapter concentrated on RO desalination technology. RO desalination plants are becoming more popular in the Middle East and Arabian Gulf region due to its simplicity and low energy consumption. Modelling of the RO system was not attempted in this work, rather, the energy consumption of the RO desalination plant was estimated. Modelling of the RO system would not add any benefit to this research since it is a system which consumes electricity rather than thermal input such as steam. The available data from the RO pilot plant at the KISR facility in Kuwait were used to estimate the required energy of a typical spiral wound RO plant. The estimated figure of 5.49 kWh/m^3 is acceptable when compared with the figures given in published literature.

Chapter 5

5. Air-Conditioning Systems

The two air-conditioning (A/C) systems that are studied in this chapter are vapour-compression (VC) and absorption refrigeration (AR). Air-conditioning systems installed in Kuwait are based on the vapour-compression cycle. The VC-based A/C systems are not modelled in this work because their performance data and electricity consumptions are available from published research and annual statistics published by Kuwait's government. On the other hand, AR systems are modelled because they consume steam and that is not readily available for the conditions of Kuwait in general and DW powerplant specifically.

The first part of the chapter gives a basic background on VC systems and types of A/C units installed in Kuwait. Section 5.2.2 gives a detailed description of the AR single and double–effect cycles. The model describing the double-effect absorption cycle is given in section 5.2.3 with the supporting thermodynamic property equations.

5.1. Vapour-compression Refrigeration Cycle

In this section the ideal and actual VC cycles are discussed. The section also includes analysis of the types of A/C systems used in Kuwait and the performance of these A/C systems.

5.1.1. Ideal Cycle

The VC refrigeration cycle is the most widely used cycle for air-conditioning of homes and commercial buildings. Figure 5.1 shows the ideal VC cycle. In the ideal cycle, the refrigerant enters the compressor at point 1 as saturated vapour and is

compressed to condenser pressure. During the compression process the temperature of the refrigerant increases above the surrounding temperature. The refrigerant then enters the condenser at point 2 as superheated vapour and exists at point 3 as saturated liquid because of the heat rejection process to the surroundings. Saturated liquid refrigerant passes through an expansion tube and its temperature drops below the temperature of the cooled space. The cycle is completed when the refrigerant enters the evaporator at point 4 as saturated vapour-liquid mixture where it is completely evaporated and becomes saturated vapour.

5.1.2. Actual Cycle

In practice, the ideal VC cycle does not exist due to the irreversible nature of the throttling process, pressure losses in components and irreversibilities in the compression process.

To avoid damage to the compressor, complete evaporation of the vapour is ensured before the refrigerant leaves the evaporator by superheating it. On the other hand, the liquid in the condenser is sub-cooled to a temperature less than the saturation

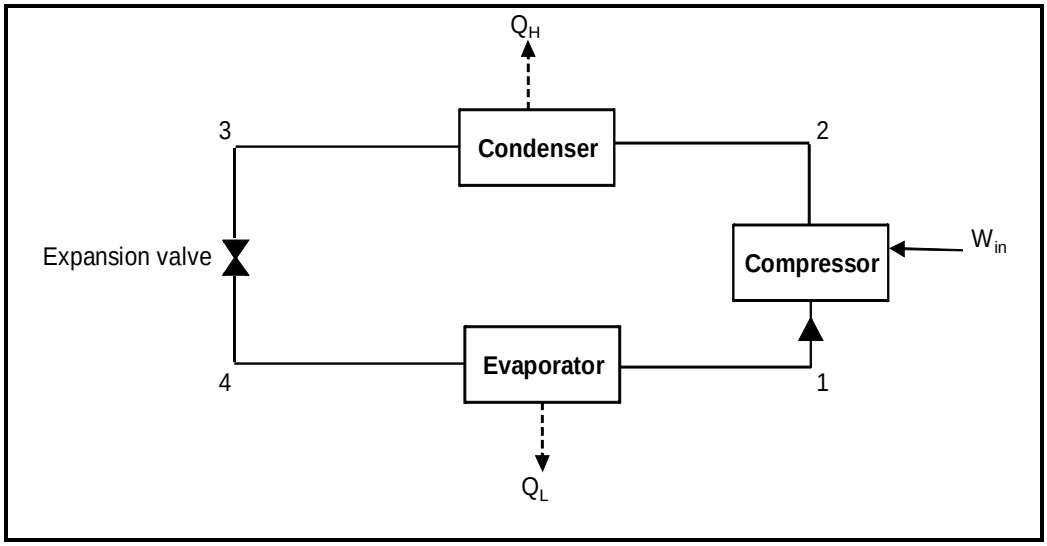

Figure 5.1 Schematic diagram of the ideal vapour-compression refrigeration cycle

temperature to avoid flashing of the liquid to gas before reaching the expansion valve. These two improvements to the basic cycle cause the dryness fraction reduction and an increased refrigeration effect.

5.1.3. Types of A/C systems in Kuwait

Research conducted by KISR categorised the available A/C system in Kuwait as follows (Maheshwari et al., 2000):

- Window and mini-split units
- Packaged and ducted-split units
- Chilled water systems

However, the most widely installed A/C systems in Kuwait are the packaged and ducted split units and chilled water systems (a.k.a. chillers). The packaged and split systems are generally installed at residential areas, while chillers are installed in governmental and commercial buildings.

5.1.4. Performance and Capacity of A/C systems in Kuwait

The performance of the three above mentioned A/C systems is studied to estimate an average coefficient of performance (COP) of these systems. The COP then can be used to calculate the monthly refrigeration load at the DW powerplant, where:

$$RF_{AC} = (Pr_{AC})(COP)$$

The average COP for the different systems is calculated based on Table B1 in Appendix B. Table 5.1 shows the steps required to estimate the average COP based on the available data from Kuwait, which is at a value of 2.01.

Table 5.1 Estimation of average COP for different types of A/C systems in Kuwait

Type	PR (kWe/kW_R)	COP (1/PR)	Market share (%)	Corrected COP
Packaged + ducted split	0.483	2.07	70	1.45
Air cooled	0.583	1.72	25	0.43
Water cooled	0.374	2.67	5	0.13

5.2. Absorption Refrigeration Systems

Absorption refrigeration systems (ARSs) are currently utilised in industrial applications such as the chemical and food industries and in domestic applications to provide cooling for houses and commercial buildings. ARSs use heat in the form of steam or hot water as the input to produce the cooling effect. This heat source is usually a waste or extra steam (or hot water) that does not cause a penalty. Absorption chillers can be of the direct-fired type but the economic and environmental penalties do not justify its use. In this research, a mathematical model depicting the operation of ARSs is developed and linked to the main powerplant model to be able to simulate and predict its viability for supplying chilled water in a conventional powerplant. The economic and environmental implications of linking ARSs to the powerplant are also analysed in the study.

This section starts with a discussion of the reasons for selecting the double-effect water- lithium bromide (LiBr) fluid-pair for modelling in this research.

5.2.1. Selection of Appropriate AR System

Basic AR cycles can be of the single or double-effect configurations. Single-effect absorption cycles have a lower efficiency than the double-effect cycles and usually are unable to effectively utilise high temperature heat sources. The double-effect cycle is more popular in A/C applications due to its improved efficiency and ability

to use higher temperature steam. Also, the double-effect chiller makes-up 70% of the AR market (Xu et al., 1996 and Arun et al., 2001). Hence, the double-effect cycle is modelled and analysed in this research.

The working fluid-pairs are the refrigerant and the absorbent solutions in the cycle. The most common refrigerant-absorbent mixtures are the water-LiBr and the ammonia-water mixtures. The latter fluid-pair is generally used for refrigeration purposes requiring sub-zero cooling. The water-LiBr mixture, on the other hand, is limited by the freezing point of water and therefore it is mostly used in A/C systems (Dincer and Dost, 1996; Sun, 1997). Since the H_2O-LiBr mixture is more commonly used in A/C applications, it is selected as the fluid-pair for this research too. Hence, the double-effect H_2O-LiBr AR chiller is selected for modelling and analysis in this research.

5.2.2. Description of AR System

5.2.2.1. Single-Effect AR Cycle

The basic single-effect AR cycle is shown in Figure 5.2. As shown in the figure, the cycle comprises four main components, namely, absorber, generator, condenser and evaporator. Contrary to VC refrigeration where there is one working fluid known as the refrigerant, the absorption cycle utilises two working fluids known as the refrigerant and the absorbent. These two fluids should have a strong chemical affinity to each other. As mentioned above, the H_2O-LiBr and ammonia- H_2O fluid pairs are the two most common working fluids in ARSs (Dincer and Dost, 1996). However, a large number of fluid-pair combinations are available either commercially or in test laboratories (Badr, 2001).

In Figure 5.2, the low pressure refrigerant vapour (water) at point 10 and the liquid carryover from the evaporator at point 11 enter the absorber and are absorbed by a strong absorbent solution (e.g. LiBr) at low temperature. When the solution contains

a small amount of refrigerant it is referred to as a strong solution, meaning that it has a strong ability to absorb more refrigerant. On the other hand, a weak solution is one which contains a large amount of refrigerant. When the absorber absorbs the refrigerant it releases heat which is commonly removed by cooling water. The weak solution leaving the absorber is pumped to the generator pressure and is preheated by strong solution leaving the generator. The preheated solution enters the generator at point 3. The heat added to the generator in shape of steam or hot water causes the refrigerant in the solution to evaporate, and then it passes to the condenser at point 7. The strong solution remaining in the generator is throttled back to the absorber via the heat exchanger at points 4, 5 & 6. On the other hand, the refrigerant vapour releases its latent heat in the condenser and is transformed into a high-pressure, low-temperature liquid. The liquid refrigerant is throttled as it is taken to the evaporator at point 9 where it extracts the heat (i.e. cooling load). The refrigerant is passed to the absorber again.

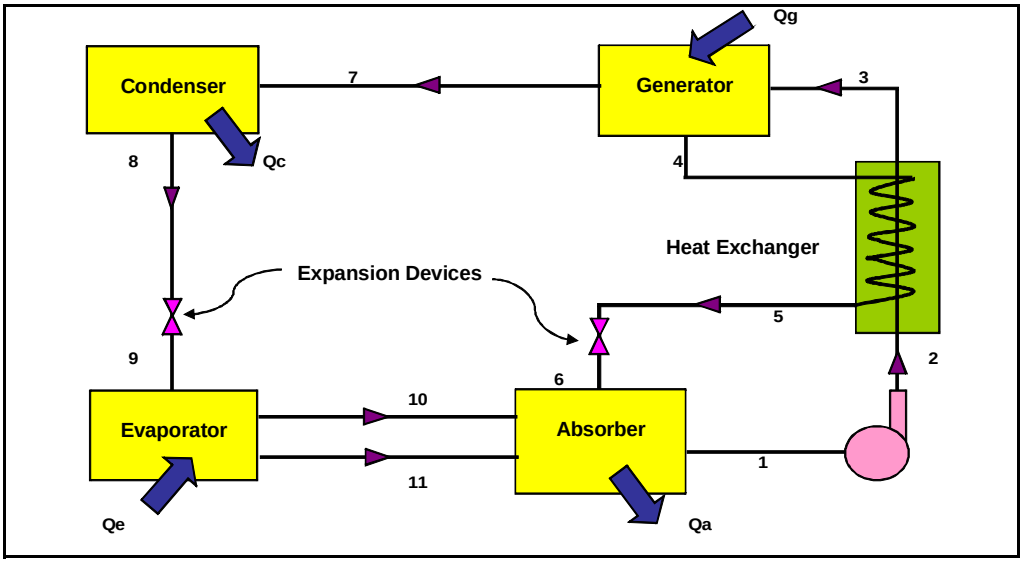

Figure 5.2 Single-effect AR cycle

5.2.2.2. Double-Effect AR Cycle

The double-effect cycle is similar to the single-effect but it includes a second generator and an extra heat exchanger. High-grade heat is added to the generator, which improves the performance of the cycle (Arun et al., 2001). The idea is to recycle the heat from the high-temperature generator to drive a lower-temperature generator, leading to a higher cooling capacity.

There are three main types of double-effect absorption cycles, namely, the series flow, parallel flow and reverse parallel flow cycles (ASHRAE, 1998). However, the series-flow double-effect cycle is described in detail here because it is the most common configuration in A/C applications, which meets the criteria for this research. There are other various configurations that are discussed by Sirkhin et al. (2001), but are not commercially available yet. Specifically, the H_2O- LiBr working pair used in the series-flow system is selected due to its established efficiency in A/C applications (Ziegler and Riesch, 1993).

Figure 5.3 shows the double-effect series-flow cycle. As with the single-effect cycle, the weak H_2O-LiBr solution is pumped from the absorber to generator **I** through both the low and high temperature heat exchangers. At the high pressure and high temperature generator (i.e. generator **I**) part of the refrigerant evaporates the remaining strong solution is passed to generator **II** through the high-temperature heat exchanger. At generator **II**, more refrigerant is evaporated from the solution by the high pressure steam from generator **I**. The LiBr solution passes through the low temperature heat exchanger back to the absorber (points 8, 9 & 10). The condensed steam at generator **II** is throttled (point 12) and is passed to the condenser (point 13). The refrigerant vapour generated at generator **II** is also passed to the condenser (point 14). The liquid refrigerant goes through an expansion device (point 15) and passes to the evaporator (point 16) as a low-pressure and low-temperature liquid water. The saturated liquid is evaporated again by the cooling load and is passed to the absorber.

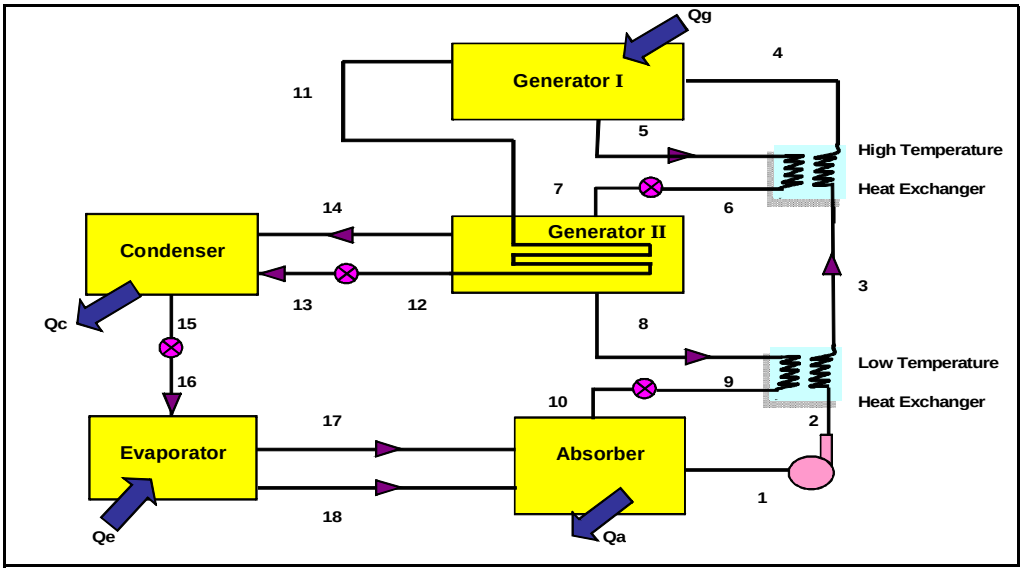

Figure 5.3 Double-effect AR cycle

5.2.3. Literature Review of AR System Models

This section includes a review of previous published work concerning the modelling of ARSs in general. The review is not limited to the double-effect H_2O-LiBr because the basic energy and mass balance equations are similar for most absorption cycles. Formulations and the solution method of the double-effect H_2O-LiBr are then presented.

Manohar et al. (2006) modelled the double-effect H_2O-LiBr cycle using the artificial neural network (ANN) technique. The purpose of the study was to evaluate the accuracy of the ANN technique in predicting the performance of the double-effect series-flow chiller. The designed model was trained with one year of experimental data. Results show that the predicted COP was within ±1.2% error of actual value. Manohar et al. (2006) concluded that the developed ANN algorithm can be used to predict the performance of the AR chiller quite accurately.

The models developed by Xu et al. (1996), Sun (1997) and Arun et al. (2001) to simulate and analyse the H_2O-LiBr double-effect cycle were based on energy and mass balances of the cycle and basic thermodynamic correlations estimating the temperatures, pressure and enthalpies of the refrigerant and solution. The research by Xu et al. (1996) was aimed at analysing the effect of design parameters such as solution circulation ratio, solution concentration, pressure in the generators and evaporator on the COP and heat transfer area of the double-effect series-flow cycle. On the other hand, Sun (1997) produced detailed thermodynamic design data and optimum design maps that, the author hoped, would be used as reference in designing and selecting new absorption refrigeration systems. The aim of the research by Arun et al. (2001) was to compare the performance of the parallel-flow absorption cycle with the series-flow.

Gordon and Choon Ng (1995) developed a general steady-state thermodynamic model for cooling systems and applied this model to ARSs. The main aim of their research was to utilise the developed model in capturing the irreversibilities in absorption chillers which, in turn, would be of diagnostic value and a useful tool in predicting chiller performance over a full range of operating conditions. The model showed good agreement with experimental and manufacturer catalogue data in terms of coefficient of performance (COP).

In a different approach to the above research, Fu et al. (2006) developed an object-oriented dynamic model aimed at providing building blocks and capability for designing ARSs based on different working fluids and cycle configurations. The model was tested by the authors through the construction of different absorption chiller models. Validations showed good agreement between model and experimental data. Other dynamic models are also presented in Anand et al. (1982), Butz & Stephan (1989) and Jeong et al. (1998).

A large percentage of research concerned with ARSs concentrates on modelling and simulation of the solar absorption cycle. These models can be found in Li and

Sumathy (2001), Florides et al. (2002), Joudi et al. (2003), Argiriou et al. (2005), Assilzadeh et al. (2005), and Casals (2006).

5.2.3.1. Summary

The review shows that the models describing the performance of the AR cycle are either steady-state or dynamic. Steady-state modelling is of importance to this research because it is sufficient for analysing the performance of the system and calculating energy input and output. Research also shows that the combination of energy and mass balance equations and thermodynamic properties of working fluids is the base for modelling and simulation of ARSs.

5.2.4. Modelling of AR Systems

The main objective of the ARS model is to:

- Estimate the number of absorption chillers required to satisfy the cooling capacity.
- Calculate the mass flowrate of steam input to the generator.
- Calculate the energy input to the generator.

To be able to complete the modelling of the AR cycle, the thermodynamic properties of pure water and solution must be calculated. The properties that are of importance to the modelling in this work are pressure, temperature, concentration and enthalpy.

5.2.4.1. Thermodynamic Properties

Solution Enthalpy

The enthalpy (h) in units of kJ/kg of the H_2O-LiBr solution is described as a function of solution temperature (°C) and concentration (%). The coefficients of the equation are listed in Table 5.2. (Patterson and Perez-Blanco,1988).

$$h(T,X)=\sum_{i=0}^{5}\sum_{j=0}^{2}a_{ij}X^{i}T^{j} \tag{5.1}$$

The working range of Equation 5.1 is:

$0 < T < 180°C$
$0 < X < 70\%$

Saturation Temperature of Water in Solution

The saturation temperature (T_{sat}) in °F of water in the H_2O-LiBr solution is given in terms of solution temperature (°F) and concentration (%). The coefficients of the equation are given in Table 5.3 as published by Patterson and Perez-Blanco (1988).

$$T_{sat}(T,X_a)=\sum_{i=0}^{5}\sum_{j=0}^{2}a_{ij}X_a{}^{i}T^{j} \tag{5.2}$$

Table 5.2 Coefficients of Equation 5.1(Patterson and Perez-Blanco,1988)

i	j	a_{ij}	i	j	a_{ij}	i	j	a_{ij}
0	0	1.134125E+00	0	1	4.124891E+00	0	2	5.743693E-04
1	0	-4.800450E-01	1	1	-7.64390E-02	1	2	5.870921E-05
2	0	-2.161438E-03	2	1	2.589577E-03	2	2	-7.375319E-06
3	0	2.336235E-04	3	1	-9.500522E-05	3	2	3.277592E-07
4	0	-1.188679E-05	4	1	1.708026E-06	4	2	-6.062304E-09
5	0	2.291532E-07	5	1	-1.102363E-08	5	2	3.901897E-11

Table 5.3 Coefficients of Equation 5.2 (Patterson and Perez-Blanco,1988)

i	j	a_{ij}	i	j	a_{ij}	i	j	a_{ij}
0	0	-1.313448E-01	0	1	9.967944E-01	0	2	1.978788E-05
1	0	1.820914E-01	1	1	1.778069E-03	1	2	-1.779481E-05
2	0	-5.177356E-02	2	1	-2.215597E-04	2	2	2.002427E-06
3	0	2.827426E-03	3	1	5.913618E-06	3	2	-7.667546E-08
4	0	-6.380541E-05	4	1	-7.308556E-08	4	2	1.201525E-09
5	0	4.340498E-07	5	1	2.788472E-10	5	2	-6.641716E-12

Mass Fraction of Solution

The solution concentration can be calculated by rearranging Equation 5.2 to appear in the form:

$$T_{sat} = A + BX + CX^2 + DX^3 + EX^4 + FX^5 \tag{5.3}$$

where,

$$A = -0.1313448 + 0.9967944T + 0.00001978788T^2$$
$$B = 0.1820914 + 0.001778069T - 0.0000177948T^2$$
$$C = -0.05177356 - 0.0002215597T + 0.000002002427T^2$$
$$D = 0.002827426 + 0.000005913618T - 0.00000007667546T^2$$
$$E = -0.00006380541 - 0.00000007308556T + 0.0000000012015225T^2$$
$$F = 0.0000004340498 + 0.0000000002788472T - 0.0000000000006641171T^2$$

The above equation is solved for the mass fraction (X) using Matlab's function *fzero* with the water saturation temperature ($Tsat$) and solution temperature (T) known.

Solution Density

The solution density (r) described by Equation 5.4 is estimated in terms of the solution temperature and concentration (Patterson and Perez-Blanco, 1988). The coefficients of Equation 5.4 are given in Table 5.4. The calculated solution density is used to estimate the power consumption of the solution pump.

$$r(T, X_a) = \sum_{i=0}^{4} \sum_{j=0}^{2} a_{ij} X_a{}^i T^j \tag{5.4}$$

Table 5.4 Coefficients of Equation 5.4 (Patterson and Perez-Blanco,1988)

i	j	a_{ij}	i	j	a_{ij}	i	j	a_{ij}
0	0	9.939006E-01	0	1	-5.631094E-04	0	2	1.392527E-06
1	0	1.046888E-02	1	1	1.633541E-05	1	2	-2.801009E-07
2	0	-1.667939E-04	2	1	-1.110273E-06	2	2	1.734979E-08
3	0	5.332835E-06	3	1	2.882292E-08	3	2	-4.232988E-10
4	0	-3.440005E-08	4	1	-2.523579E-10	4	2	3.503024E-12

The pump work can be calculated from:

$$W = \frac{m \times (P_2 - P_1)}{\rho \times \eta_{pump}} \tag{5.5}$$

However, it is assumed that the density does not change significantly from point 2 to point 1. Hence, the pump work is small enough and can be neglected in the calculations because the pump is compressing liquid which has very small values of specific volume in comparison to refrigerant vapour in VC cycles (Polyzakis, 2006).

Properties of pure water

The pressure of pure water is estimated using Equations. 3.20 and 3.21. While the saturation temperature as a function of known saturation pressure can be calculated from Equations. 3.22 and 3.23. The enthalpy of both superheated and saturated steam can be estimated from Equations. 3.16, 3.19a and 3.19b and the enthalpy of saturated liquid water is estimated using Equation 3.27.

5.2.4.2. Double-Effect Cycle Model

As discussed previously, the series-flow double-effect is the most common cycle used in A/C applications. The modelling of this cycle is done in Matlab by applying the energy and mass balance equations on the components of the cycle. The first step in the procedure is determining the inputs to the model. From the reviewed

literature (Sun, 1997 and Xu et. al., 1996) and manufacturers' catalogues, the inputs are selected to be:

- Absorber temperature (T_a)
- Condenser temperature (T_c)
- Evaporator temperature (T_e)
- Generator I temperature (T_{g1})
- Refrigeration capacity (Q_e)
- Heat exchanger effectiveness (ε)
- Liquid carryover (CO)
- Heat transfer potential (ΔT_{pot})

Liquid carryover occurs in the evaporator when a small amount of liquid refrigerant is not evaporated. The heat transfer potential is the temperature difference between Generator II and condenser I.

Assumptions

To be able to successfully model the cycle with a reasonable degree of accuracy the following assumptions has been made regarding the working fluids (ASHRAE, 2001 and Foy, 2001):

- Steady-state operation.
- Refrigerant is pure water.
- H_2O-LiBr solutions in generator I, generator II and absorber are in equilibrium (points 1, 5 & 7).
- The fluid in Generator I is saturated vapour, and it is fully condensed at the low-pressure generator II.
- Water refrigerant at the exit of the condenser and evaporator is saturated liquid (points 15 & 17).
- Liquid water carryover is saturated (point 18).

- No pressure changes in the pipes; pressure drop exists only in expansion valve and pump.
- Throttling process is isoenthalpic.
- Solution pump is 100% efficient.
- Negligible heat losses.

5.2.4.3. Modelling Procedure

The following procedure gives a detailed presentation of the double-effect cycle shown in Figure 5.3, which is influenced by the work of Foy (2001). The single-effect modelling procedure is given in Section B.2, Appendix B.

Step 1

To be able to proceed with the analysis of the cycle, the temperatures of generator II (T_{gII})and condenser (T_{cI}) must be known. So, as an initial step, T_{gII} is guessed at $^1/_2\,T_{gI}$. The condenser temperature is calculated from:

$$T_{cI} = T_{gII} + \Delta T_{pot} \tag{5.6}$$

Step 2

The input temperatures and the LiBr mass fractions are assigned to corresponding points in the cycle:

$$T_1 = T_a \qquad X_{11} = 0$$
$$T_2 = T_1 \qquad X_{12} = 0$$
$$T_5 = T_{gI} \qquad X_{13} = 0$$
$$T_8 = T_{gII} \qquad X_{14} = 0$$
$$T_{11} = T_{gI} \qquad X_{15} = 0$$
$$T_{12} = T_c \qquad X_{16} = 0$$

$$T_{14} = T_{gII} \qquad X_{17} = 0$$
$$T_{15} = T_{cII} \qquad X_{18} = 0$$
$$T_{17} = T_e$$
$$T_{18} = T_e$$

Since there is only state change across the evaporator from liquid to vapour:

$$T_{16} = T_e$$

Step 3

The pressure at the exit of generator II (P_{12}) can be calculated using Equation 3.20 from T_{12} and X_{12}, assuming:

$$T_{sat,12} = T_{12}$$

From the assumptions:

$$P_{sat,12} = P_{12}$$

Since it is assumed that there is no pressure drop in the pipes:

$$P_2 = P_{12} \qquad P_5 = P_{12}$$
$$P_3 = P_{12} \qquad P_6 = P_{12}$$
$$P_4 = P_{12} \qquad P_{11} = P_{12}$$

The procedure used to calculate P_{12} is followed to calculate the pressure at point 15 (P_{15}) where $P_{sat,15} = P_{15}$ and:

$$P_7 = P_{15} \qquad P_{13} = P_{15}$$
$$P_8 = P_{15} \qquad P_{14} = P_{15}$$
$$P_9 = P_{15}$$

The pressure at point 17 (P_{17}) is also calculated using the above procedure:

$$P_{16} = P_{17} \qquad P_{10} = P_{17}$$
$$P_{18} = P_{17} \qquad P_{1} = P_{17}$$

Step 4

The first step in calculating the concentration of LiBr at point 1 is to calculate the saturation temperature ($T_{sat,1}$) at the point. $T_{sat,1}$ is calculated using Equations 3.22 and 3.23 from the known T_1 and P_1.

The concentration of LiBr at point 1 (X_1) can now be calculated using Equation 5.3 with the known $T_{sat,1}$ and T_1 utilising the *fzero* command in Matlab's optimisation toolbox. Also:

$$X_2 = X_1$$
$$X_3 = X_1$$
$$X_4 = X_1$$

The concentrations of LiBr at points 5 and 8 (X_5 & X_8) are also calculated using the previous method, and:

$$X_6 = X_5$$
$$X_7 = X_5$$
$$X_9 = X_8$$
$$X_{10} = X_8$$

Step 5

The low-temperature heat exchanger temperatures T_3 and T_9 are calculated using the equation describing the effectiveness:

$$\varepsilon_{HX} = \frac{(T_8 - T_9)}{(T_8 - T_2)} = \frac{(T_3 - T_2)}{(T_8 - T_2)} \quad (5.7)$$

$$T_9 = T_8 + (T_8 - T_2)\varepsilon_{HX,low} \quad (5.8)$$

$$T_3 = T_2 + (T_8 - T_2)\varepsilon_{HX,low} \quad (5.9)$$

And for the high-temperature heat exchanger, T_4 and T_6 are calculated from:

$$\varepsilon_{HX} = \frac{(T_4 - T_3)}{(T_5 - T_3)} = \frac{(T_5 - T_6)}{(T_5 - T_3)} \quad (5.10)$$

$$T_4 = T_3 + (T_5 - T_3)\varepsilon_{HX,high} \quad (5.11)$$

$$T_6 = T_5 + (T_5 - T_3)\varepsilon_{HX,high} \quad (5.12)$$

The pressure at point 7 is assumed to be the saturation pressure (i.e. $P_{sat,7} = P_7$), from this the saturation temperature of water $T_{sat,7}$ can be calculated using Equations 3.22 and 3.23 as a function of $P_{sat,7}$. Now, the actual temperature of the solution at point 7 (T_7) using Equation 5.3 from the known $T_{sat,7}$ and X_7 through the use of the ***fzero*** command in Matlab, which eliminates the need for an iteration process.

The previous procedure for calculating T_7 is also used to calculate the temperatures at points 10 and 13 (T_{10} and T_{13}). By this, all the pressures, temperatures and LiBr mass fractions are now know and the next step is to calculate the enthalpies and the mass flowrates of fluids in the cycle

Step 6

I. Enthalpies

The enthalpies at points 1, 3, 4, 5, 6, 8 and 9 are calculated using Equation 5.1 from the known temperatures and LiBr concentrations at these points. Also:

$$h_2 = h_1$$
$$h_7 = h_6$$
$$h_{10} = h_9$$

The enthalpy of superheated water vapour at point 11 (h_{11}) is calculated from P_{11} and T_{11} using Equation 3.16. On the other hand, the enthalpies at points 12 and 14 (h_{12} and h_{14}) are calculated from the assumption that they are at saturation state using Equation 3.27.

It was assumed above that the refrigerant exiting the condenser is at saturation state, and $T_{sat,15} = T_{15}$. So, the enthalpy at point 15 can be calculated using Equation 3.27 from the known saturation temperature. The same procedure is used to calculate h_{17} and h_{18}.

Since there is no enthalpy change across the expansion device:

$$h_{13} = h_{12}$$
$$h_{16} = h_{15}$$

II. Mass flowrates

The mass flowrate at point 17 can be calculated using the mass and energy balance equations on the evaporator:

$$m_{16} = m_{17} + m_{18} \tag{5.13}$$

$$Q_e = m_{17}h_{17} + m_{18}h_{18} - m_{16}h_{16} \tag{5.14}$$

The mass flowrate of the liquid carryover from the evaporator (m_{18}) is calculated as a percentage of the vapour mass flowrate (m_{17}):

$$m_{18} = \frac{CO}{100} m_{17} \tag{5.15}$$

Rearranging the above equations to solve for m_{17}:

$$m_{17} = \frac{Q_e}{h_{17} + \left(\frac{CO}{100}\right) h_{18} - \left(1 + \frac{CO}{100}\right) h_{16}} \tag{5.16}$$

and,

$$m_{18} = \frac{CO}{100} m_{17} \tag{5.17}$$

$$m_{16} = m_{17} + m_{18} \tag{5.18}$$

$$m_{15} = m_{16}$$

To be able to calculate the mass flowrates of fluids through the absorber, an overall and LiBr mass balances are performed:

$$m_1 = m_{16} + m_{10} \tag{5.19}$$

$$m_1 X_1 = m_{10} X_{10} \tag{5.20}$$

The two equations above are used to solve for m_1:

$$m_1 = \frac{m_{16}}{\left(1 - \frac{X_1}{X_{10}}\right)} \tag{5.21}$$

also,

$$m_2 = m_1$$
$$m_3 = m_1$$
$$m_4 = m_1$$

A LiBr mass balance at generator I gives:

$$m_4 X_4 = m_5 X_5$$
$$\rightarrow m_5 = \frac{m_4 X_4}{X_5}$$

And,

$$m_6 = m_5$$
$$m_7 = m_5$$

A mass balance is applied on generator I:

$$m_{11} = m_4 - m_5 \tag{5.22}$$
$$m_{12} = m_{11}$$
$$m_{13} = m_{11}$$

The mass balance on the condenser gives:

$$m_{14} = m_{15} - m_{13} \tag{5.23}$$

With the mass flowrates and enthalpies known at all points on the cycle, an energy balance on generator II and condenser I is applied:

$$Q_{gII} = m_{14} h_{14} + m_8 h_8 - m_7 h_7 \tag{5.24}$$

$$Q_{cI} = m_{11}h_{11} - m_{12}h_{12} \quad (5.25)$$

At this point, the guessed temperature for generator II (T_{gII}) must be corrected because it affects the accuracy of the results. The assumptions listed for the model state that the heat rejected by condenser I is received by generator II, which is written as:

$$Q_{cI} = Q_{gII}$$

A *while loop* is added to the program to satisfy the above equilibrium condition, in which the convergence criterion is set at an error of less than 0.01. Once convergence is reached, the correct T_{gII} is stored and an energy balance on the other components is applied:

$$Q_{gI} = m_{11}h_{11} + m_5h_5 - m_4h_4 \quad (5.26)$$

$$Q_{cII} = m_{13}h_{13} + m_{14}h_{14} - m_{15}h_{15} \quad (5.27)$$

$$Q_a = m_{17}h_{17} + m_{18}h_{18} + m_{10}h_{10} - m_1h_1 \quad (5.28)$$

The COP is defined as:

$$COP = \frac{Q_e}{Q_{gI}} \quad (5.29)$$

5.2.4.4. Validation of AR model

The model was validated using results published by Foy (2001). The input variables for the model are listed in Table 5.5. The results of the model simulated in this research work are shown in Tables 5.6 and 5.7. A comparison between the

performance results from the developed Matlab model in Table 5.7 and Foy (2001) results in Table 5.9 shows that the percentage difference between the energy flows and COP is in the range 4.67% and 5.11%. This difference is acceptable if the difference in the modelling and simulation procedures and software interface are considered.

The author attempted to verify the results of the two models with examples given in ASHRAE (2001) but found that there are various errors in most physical properties and performance parameters. It may be due to the ambiguity of the input data given in the reference book.

Table 5.5 State points of double-effect model

Parameter	Unit	Value
Absorber temperature, T_a	°C	20
Temperature of refrigerant vapour to condenser, T_{c2}	°C	30
Evaporator temperature, T_e	°C	2.5
Primary generator temperature, T_{g1}	°C	120
Secondary generator temperature, T_{g2}	°C	$0.5*T_{g1}$
Refrigeration capacity, Q_e	kW	40
Heat exchanger effectiveness, ε	%	80
Heat transfer potential	°C	5
Liquid carryover	-	0

5.2.5. Reference AR Chiller

To have a powerplant that is as close to reality as possible and performance results that are reliable, an AR chiller that is commercially proven and available in the market is used. The Trane Horizon absorption chiller series is used as the system to be connected to the hybrid powerplant in this research. This particular company is used because of its sizable market share and availability of chiller performance data.

The chiller selected from their range of AR chiller is the ABTF-1150 model, 1165 Tons (Trane, 2005), and it was chosen because it had the highest COP and a relatively large refrigeration capacity of 4428 kW_R per chiller. The details of the

Trane AR chiller are given in Table 5.10 below. Other calculations concerning the steam flowrate, number of chillers required, fuel cost and CO_2 emissions are formulated and calculated in Chapters 6 and 7. The assumptions used in the developed Matlab program for an absorption double-effect cycle above are used to estimate the performance and steam consumption of this Trane chiller.

Table 5.6 state points of developed double-effect model

Point	Temperature °C	Pressure kPa	Concentration %	Enthalpy kJ/kg	Mass flowrate kg/s
1	20.00	0.71	47.91	37.76	0.072
2	20.00	50.53	47.91	37.76	0.072
3	65.28	50.53	47.91	137.84	0.072
4	109.06	50.53	47.91	236.20	0.072
5	120.00	50.53	54.20	259.13	0.064
6	76.22	50.53	54.20	167.75	0.064
7	61.29	4.22	54.20	167.75	0.064
8	76.60	4.22	61.44	191.92	0.057
9	31.32	4.22	61.44	107.18	0.057
10	43.79	0.71	61.44	107.18	0.057
11	120.00	50.53	0.00	2722.20	0.008
12	81.60	50.53	0.00	341.64	0.008
13	30.04	4.22	0.00	341.64	0.008
14	76.60	4.22	0.00	2644.70	0.008
15	30.00	4.22	0.00	125.60	0.016
16	2.50	0.71	0.00	125.60	0.016
17	2.50	0.71	0.00	2506.88	0.016
18	2.50	0.71	0.00	10.47	0.000

Table 5.7 Performance parameters of developed double-effect model

Q_e kW	Q_{g1} kW	Q_{g2} kW	Q_{c1} kW	Q_{c2} kW	Q_a kW	COP	CR
40.00	22.37	20.06	20.02	20.83	43.32	1.79	4.54

Table 5.8 Validated results published by Foy (2001)

Point	Temperature °C	Pressure kPa	Concentration %	Enthalpy kJ/kg	Mass flowrate kg/s
1	20.00	0.723	47.58	37.30	0.074
2	20.00	50.732	47.58	37.30	0.074
3	65.50	50.732	47.58	138.20	0.074
4	109.10	50.732	47.58	236.60	0.074
5	120.00	50.732	54.03	259.00	0.065
6	76.40	50.732	54.03	167.70	0.065
7	61.00	4.214	54.03	167.70	0.065
8	76.80	4.214	61.51	192.70	0.057
9	31.40	4.214	61.51	107.70	0.057
10	44.40	0.723	61.51	107.70	0.057
11	120.00	50.732	0.00	2721.80	0.009
12	81.80	50.732	0.00	342.80	0.009
13	30.10	4.214	0.00	342.80	0.009
14	76.80	4.214	0.00	2644.90	0.008
15	30.00	4.214	0.00	124.40	0.017
16	2.50	0.723	0.00	124.40	0.017
17	2.50	0.723	0.00	2505.70	0.017
18	2.50	0.723	0.00	9.60	0.000

Table 5.9 Validated performance parameters published by Foy (2001)

Q_e kW	Q_{g1} kW	Q_{g2} kW	Q_{c1} kW	Q_{c2} kW	Q_a kW	COP	CR
40.00	23.47	21.11	21.06	21.95	45.50	1.71	4.40

Table 5.10 Performance data of Trane ABTF-1150 AR chiller (Trane, 2005)

Parameter	Unit	Value
Absorber temperature, T_a	°C	35
Temperature of refrigerant vapour to condenser, T_{c2}	°C	38
Evaporator temperature, T_e	°C	6
Primary generator temperature, T_{g1}	°C	149
Secondary generator temperature, T_{g2}	°C	$0.5*T_{g1}$
Refrigeration capacity, Q_e	kW	4428
Heat exchanger effectiveness, ε	%	80
Heat transfer potential	°C	5
Liquid carryover	-	0

5.2.6. Conclusions

The chapter concentrated on two popular refrigeration cycles, the vapour-compression and the absorption refrigeration cycles. Section 5.1 described the electrically-driven VC A/C cycle and studied power consumption of the different types of A/C units used in Kuwait, and then the average power consumption was estimated.

The absorption refrigeration system was described in detail and discussed in Section 5.2. The two main types are the single- and double-effect systems. The double-effect cycle was selected for modelling and simulation in this research because of its higher COP and suitability for both residential and commercial sectors.

Chapter 6

6. Design and Modelling of Hybrid Configurations for the Doha West Powerplant in Kuwait

The Rankine steam cycle, MSF and RO desalination processes, and VC A/C and ARSs have been studied and analysed in Chapters 3, 4 and 5, respectively. Mathematical models for the steam-consuming processes were also developed to be able to simulate their performance under prevailing weather conditions in Kuwait and electric and water demand data. The models were validated using real data from existing processes and plants.

In this chapter, hybrid powerplant configurations are developed using the processes and technologies mentioned above that would satisfy the demand for electricity, freshwater and cooling required by the DW powerplant. Matlab programs developed for MSF desalination and AR chillers are integrated with the Rankine cycle program along with available data for VC A/C and RO desalination. The objective is to study the economic and environmental feasibility of turning this existing conventional (i.e. dual purpose) powerplant into a hybrid system.

Section 6.1 of this chapter discusses different hybrid powerplant configurations presented in literature, and introduces the configurations that are studied and analysed in this study. The assumption and constraints used to develop and simulate the hybrid configurations are discussed in Section 6.2. Section 6.3 contains the electricity and water consumption data that are used to simulate the DW monthly production profiles and the methodology used to estimate the base and A/C electric loads.

Sections 6.4 to 6.9 present the different powerplant configurations modelled and simulated in this research work and the corresponding mathematical correlations for

fuel cost and CO_2 emission estimation where applicable. The differences and modifications in equations for the various models are also discussed.

6.1. Hybrid Configurations

This section is divided into two parts. Section 6.1.1 presents a literature review of various hybrid powerplant configurations based on the steam cycle and various combinations of processes related to this research work, together with the anticipated benefits and negative impacts. Section 6.1.2 introduces the powerplant configurations that are selected for modelling and simulation in this research.

The main objective in selecting these different hybrid configurations is to reduce fuel cost and negative environmental impacts while satisfying demand for electricity, freshwater and cooling. One possibility is to reduce the demand for electricity during the summer by shifting the production of cooling from conventional A/C systems powered by electricity to cooling produced centrally using AR units that use steam as input, with MSF as the only desalination option. Another idea is to study the effect of using electricity for seawater desalination by utilising RO units instead of the steam-consuming MSF desalination process, while switching the cooling load to AR chillers.

6.1.1. Hybrid Plant Configurations in Literature

This literature review concentrates on powerplant configurations that incorporate technologies and processes of relevance to this research work.

6.1.1.1. Power-RO Systems

Single-purpose powerplants that generate power only and utilise the RO desalination process are becoming popular around the world, especially in the Gulf region. The low overall cost of RO desalination and its proven reliability are encouraging

governments to consider this option for new powerplants. The Yanbu Industrial City powerplant in the KSA is an example. The powerplant has a daily capacity of 50,400 m^3 of fresh-water production (Khawaji et al., 2007).

Other studies available on powerplants connected to only RO desalination units in the Gulf region are only theoretical analyses. Darwish et al. (2005) studied the performance of RO systems combined with gas turbines available at Kuwait's powerplants with very low utilisation period (See Figure 6.1). A more recent study by Darwish et al. (2009) considered RO desalination units in association with combined-cycle powerplants. These studies demonstrated the possibility of fuel savings and reductions in CO_2 emissions when using RO instead of other desalination processes. Methnani (2007) used the Desalination Economic Evaluation Program (DEEP) published by the International Atomic Energy Agency (AIEA) to compare the performance and fuel cost of a RO desalination unit operated in association with a combined-cycle powerplant with other desalination processes. When compared with the multiple-effect desalination (MED), Methnani (2007) concludes that RO desalination costs are significantly lower.

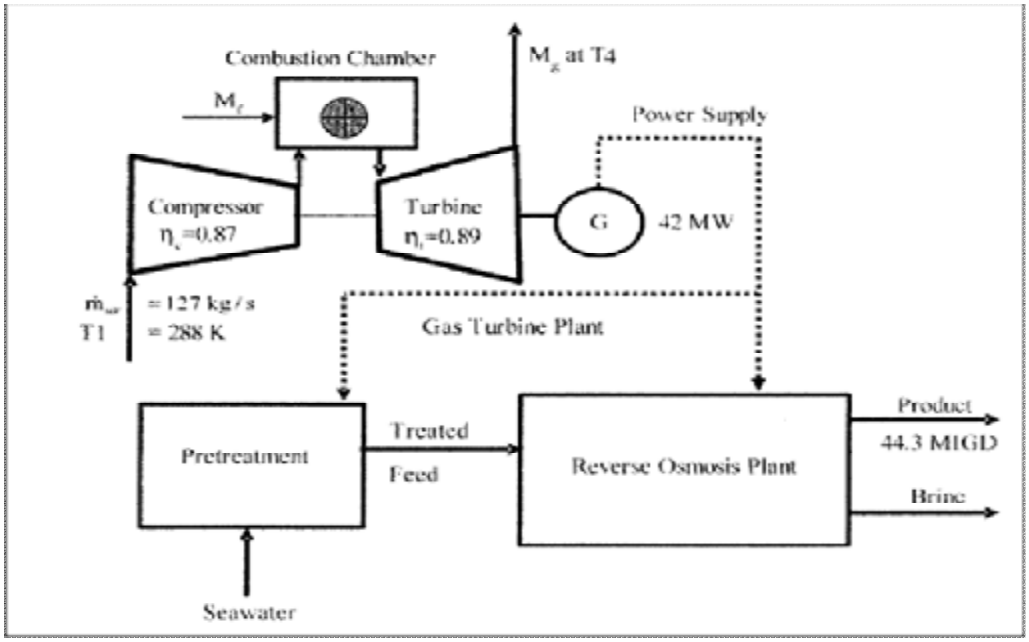

Figure 6.1 Gas turbine operating a RO desalination plant (Darwish et al., 2005)

Some of the recent studies on the feasibility of adding RO desalination at Kuwait's powerplants are Darwish and Darwish (2008), Darwish et al. (2008) and Darwish et al. (2007). The main conclusion from these studies is that applying RO desalination in Kuwait results in savings in fuel consumption at powerplants, reduced CO_2 emissions to the atmosphere and less water production cost.

6.1.1.2. Power Generation with MSF-RO Desalination

El-Sayed (2001) concluded that a cogeneration system with a variable-load can impose a fuel penalty on the system and raise the water production-cost considerably. This happens when there is a mismatch between the power and freshwater demands. The author suggested a modification to the system configuration to match power and water demands, if improvement to the efficiency of the system is desired. El-Sayed (2001) recommended a hybrid system in which another desalination technology is added, in this case vapour-compression, to avoid power-water mismatched demands by steadily producing water.

The work of Azoury (2001) focused on power and desalination in the Gulf region. The author argued that the low power-to-water ratio (PWR) for powerplants in the Gulf region is an indicator of water production priority over base load power generation. As plants are commonly designed according to summer peak conditions, this leads to low year-around operational thermal-efficiency. As a solution, Azoury (2001) recommended the use of RO desalination along with the existing MSF process in a hybridised thermal powerplant.

El-Sayed et al. (2000) and Agashichev and El-Nashar (2005) listed the following technical and economic benefits of hybridisation between MSF and RO systems:

- Higher product water recovery and less power consumption by RO.
- Maximum RO membrane permeability.
- Prolonged RO membrane life.
- Lower consumption of chemicals and RO membrane replacement rates.

- Greater flexibility in the cogeneration power/water systems (i.e. flexible range of power-to-water ratio).
- Possibility to use seasonal surplus of idle power.

El-Sayed et al. (2000) published results on the performance of two RO pilot plants, using two different membrane types, for an experimental MSF/RO hybrid set-up. The two RO plants have a nominal capacity of 300 m^3/day each. One plant is of the spiral-wound membrane type and the second uses the hollow-fiber membrane type. The two plants are fed by one common seawater header and utilise one common chemical dosing and cartridge filter system. When in hybrid mode, the feed is provided by a pre-treatment plant which is linked to the A-1 MSF unit of the Doha East powerplant in Kuwait. The pre-treatment plant receives the rejected seawater from the heat rejection section of the plant. Different performance parameters for both hybrid and single mode operation for the RO plant were published by El-Sayed et al. (2000).

The results showed that the specific electrical energy consumption under hybrid operation for the spiral-wound membrane is between 5 and 6 kWh/m^3, with the majority of the data being below 5.5 kWh/m^3 for the first 1000 hours of operation. On the other hand, the data for RO-only mode (i.e. using surface water as feed) showed that the specific energy consumption is between 6.5 and 7.0 kWh/m^3. The authors argued that the lower specific energy consumption for hybrid operation is due to the increase in product water recovery during this mode of operation. They also concluded that the electrical energy consumption under MSF/RO hybrid operation can be reduced by 15% to 25%.

In their theoretical study, Agashichev and El-Nashar (2005) presented a techno-economic evaluation and assessment of the sustainability for a “triple” hybrid system which consists of power generation via gas turbine (GT), MSF and RO desalination processes. In their proposed plant, the MSF and RO desalination

processes were completely separated and operated independently. What the authors meant by "hybrid scheme" here is that the plant produces freshwater simultaneously by utilising GT electricity to drive an RO unit, and thermal and some electrical energy for the MSF plant.

The following load-dependent indicators were calculated for the evaluation of the techno-economic performance of the hybrid plant proposed:

- Water cost.
- Electricity generation cost.
- Cost of low-grade heat.
- Specific CO_2 emissions.
- Cost of CO_2 due to imposed carbon tax.

In the analysis of the hybrid plant, the GT load was varied to study its effects on the above mentioned indicators. The authors argued that the drop in the operating load leads to a non-linear increase in specific fuel consumption. The cost of generated electricity increases too. It was also concluded that MSF desalination is more sensitive to variation in GT load than the RO system. When the GT load was dropped from 100% to 20%, the specific water production cost increased from US$ 0.93 to US$ 1.27 for MSF and from US$ 0.68 to US$ 0.87 for RO. Finally, specific CO_2 emissions were found to increase with the decrease in GT load. For a load drop from 100% to 20%, the specific CO_2 emissions increased from 9.29 to 18.03 $kgCO_2/m^3$ for MSF and from 2.77 to 4.91 $kgCO_2/m^3$ for RO. It is worth mentioning that the above results give a clear indication that RO desalination costs less to produce freshwater and contribute less CO_2 emissions to the environment than MSF desalination.

In a recent study by Al-Katheeri and Agaschichev (2008), a hybrid powerplant with the same components as the system suggested by Agashichev and El-Nashar (2005) was analysed but with a proposed aquifer storage and recovery (ASR) that adds flexibility and optimises water production. The advantages of this hybrid

configuration, the authors concluded are increased range of PWR, ability to use surplus power for water production by RO, efficient fuel utilisation and the creation of strategic water reserve.

Other studies that analysed and listed the advantages of power and MSF-RO hybrid plants include Cali et al. (2008), Sanz et al. (2007), Hamed (2005), Marcovecchio et al. (2005), Awerbuch (1997) and Al-sofi et al. (1992). The authors argued that the implementation of the hybrid power-MSF-RO concept could increase plant water production, reduces energy requirements, reduces capital cost through the use of a common seawater intake and adds flexibility to the system when there is a mismatch between water and electricity demands.

6.1.1.3. Power-AR Plants

In a study published by Al-Hawaj and Al-Mutairi (2007), a combined cycle powerplant was suggested with AR chillers included in the plant to replace the cooling load satisfied by the VC A/C system in Kuwait. The authors assumed that the chiller is a single-effect water-LiBr absorption unit powered by steam extracted at an intimidate pressure from the steam turbine. Results of the study showed that there are significant savings in power when this configuration is used.

Rosen et al. (1994) studied the advantages of implementing district cooling in Ontario, Canada using AR chillers that are supplied with heat cogenerated from a hydro-electric plant. The results were compared with a base-case year using energy quantities and environmental emissions. When the suggested configuration replaced 40% of the cooling requirement, savings of 30 PJ of total energy for the province were claimed to be achievable. The reduction in CO_2 emissions were around 758 metric ktonnes per year.

Studies on the subject of cogeneration plants and ARSs include Emho (2002), Xu et al. (2000), Tang and Rosen (1999), Rosen and Le (1996) and Tomimori et al. (1990).

6.1.1.4. Hybrid power--RO-AR Plants

Darwish (2002) proposed a district cooling system for a university campus in Kuwait based on AR chillers fed by steam from two existing steam turbines at the nearby Doha East powerplant. The freshwater demand would be satisfied by RO desalination units instead of the existing MSF unit, and the available extraction steam for the MSF would be used to feed the AR chillers. Advantages of such a configuration, he concluded, are the slowing down of the demand for extra powerplant capacity additions, lower energy consumption and shaving of peak power.

6.1.1.5. Summary

The literature review of different configurations involving the processes studied in this research shows that there is potential for energy savings and improvement in efficiency. Some of the advantages listed in these published studies are increasing utilisation factor of equipment at existing powerplants, solving the problem of power-water production mismatch and greater flexibility in the operation of the powerplant.

The configurations presented above will be the bases of the hybrid plant designs for this research work with other configurations added to ensure that the study covers all possible powerplant designs. For example, the hybrid power-MSF-AR and power-MSF-RO-AR configurations will be analysed also.

6.1.2. Suggested Hybrid Configurations

The conventional powerplant configuration (i.e. power-freshwater cogeneration) is first modelled and analysed in this work to be used as a base to compare other configurations with. Another configuration, which is not hybrid, is the power-RO configuration that uses electricity only to satisfy the various demands at the DW powerplant. This configuration is useful in determining the ability of RO desalination to satisfy the demand for freshwater and its effect on the number of turbines in operation. It is also used to compare the fuel efficiencies of both the MSF and RO desalination processes. The hybrid configurations that are modelled, simulated and analysed in this research work are:

i. Power-MSF-RO
ii. Power-MSF-AR
iii. Power-RO-AR
iv. Power-MSF-RO-AR

These hybrid powerplant configurations are discussed in detail in the following sections.

6.2. Assumptions and Constraints

The DW powerplant comprises 8 steam turbines and 16 MSF desalination units (every 2 MSF units operate on steam extracted from one turbine). Table 6.1 shows the operating parameters of the powerplant. The main objective of the hybrid powerplant configurations is to try to run the minimum number of steam turbines at full capacity, and operate MSF units and AR chillers on as much extracted steam as possible. Only in the case where extracted steam does not satisfy the demand of all processes, stand-by (or off-line) boilers already existing at DW will be brought online to make-up for the shortage.

The rationale behind using the stand-by boilers at the power station is that because there are 8 turbine sets each fed by a boiler. Results of the conventional (i.e. power-freshwater cogeneration) powerplant configuration (see Appendix C) show that not all 8 turbines are needed to satisfy the demand for electricity. Therefore, there are always available auxiliary, stand-by boilers to be used to provide the MSF units with the steam necessary to meet the demand on freshwater production.

Table 6.1 Operating parameters of DW cogeneration plant

Parameter	**Value**
Output (MW)	300.00
No. of feed-water heaters	6
Boiler steam mass flow rate (kg/s)	277
Turbine efficiency (%)	84
HP turbine inlet pressure (bar)	140.00
HP turbine inlet temperature (°C)	535.00
Reheat Pressure (bar)	36.80
Reheat Temperature (°C)	535.00
Condenser pressure (bar)	0.085

The amount of extra steam needed to be generated by the stand-by boilers is estimated in the Matlab program by subtracting the maximum value of steam that can be raised in the main boilers from the total amount of steam needed or operating the MSF units to meet the required demand for freshwater and when adding AR units to the plant. As both AR chillers and MSF units receive steam from the same stand-by boilers, steam pressure for AR chillers needs to be reduced steam via a pressure reduction station.

The constraints and assumptions of the hybrid configuration models are as follows:

- Turbines work at nominal (i.e. full) capacity of 300 MW.
- Maximum capacity of each main or auxiliary boiler is 277 kg/s.
- Steam is extracted from turbine for both MSF and AR units.
- Steam flowrates above the maximum capacity of 277 kg/s are generated in auxiliary boilers to satisfy MSF and AR demands.
- Steam raised in the auxiliary boilers is designated as Z in the program.

- Modifications are concerned with processes within the powerplant. Any additions or modifications required outside the powerplant (e.g. steam or chilled water distribution) are not considered.
- Price of oil is US$43.77/barrel.
- Price of natural gas is US$8.72/MMBtu.

These assumptions are incorporated into the developed model. The program is executed for all months of the year, except for the hybrid configurations that involve replacing VC A/C load with AR chillers, the program is run for the months March to November. Freshwater demand is always satisfied all year round regardless of the hybrid scenario being analysed.

6.3. Electricity Generation and Water Production Data

Electricity and water production data published by MEW for Kuwait's powerplants are used in the modelling and analysis of hybrid powerplant configurations. The available data are for 2001 since they were the latest available at the start of this research.

6.3.1. Electricity Production

The sets of data that were available from MEW are for the total electricity demand (in MW) for the entire of Kuwait from all power stations . The half-hourly profile was used to produce an electricity generation profile for each day of the month. These different data profiles will help in determining the electric base load and A/C load. Since this data could not be obtained for DW, which is the reference power station for this study, the percentage share of DW to total national annual electricity production in 2001 was estimated. Compared with a total electricity production of 34.299 TWh in 2001, DW production was 9.647 TWh (see Table 6.2), resulting in a percentage share ($\%_{DW}$) of DW of around 28%.

Some researchers have estimated the base load at the national level or for a power station to be the lowest production during the year. However, this assumption may not be entirely correct because the lowest generation might be due to unusual events such as holidays where a large number of the population has travelled abroad.

Table 6.2 National and DW electric generation in 2001 (MEW, 2002a)

Month	National electric generation GWh	DW electric generation GWh
January	1869	586
February	1619	536
March	1881	610
April	2526	775
May	3335	886
June	3797	961
July	4119	1095
August	4346	1135
September	3791	920
October	3094	867
November	2055	683
December	1866	592
Annual Total (TWh)	***34.3***	***9.6***

In this work, the months of December, January, February and half of March are assumed to be winter months where there is no A/C demand. The average hourly generation was estimated for each day during this period. At the national level, this resulted in a daily base load of ***59.313 GWh***. The daily A/C load is calculated for the rest of the months of the year as the difference between the total daily load and the estimated average value for the daily base load.

The above estimated base load value is the total national figure for all power stations. Hence, multiplying the national base load of 59.313 GWh by the estimated $\%_{DW}$ of 28%, the DW base load comes to a value of ***16.7 GWh/day***. The daily estimates of base load and electricity generation are multiplied by the days of the month to obtain monthly profiles. It would be more beneficial to have daily profiles of electricity generation and their economic and environmental effects, but the lack of consistent and reliable daily data has restricted the study to monthly-based profiles.

In this research the year is divided into two seasons, summer and winter seasons. The summer season is from April to November during which A/C systems are used in Kuwait round the clock. The winter months, on the other hand, are from December to February. The month of March is usually considered a spring month during which A/C systems are used in the second half of it when temperatures reach 25° C and above. Hence, the A/C load for March is assumed to be for 15 days but in the Matlab program are spread over the whole month for the sake of simplifying the output.

6.3.2. Water Production

The monthly water production data for 2001 are published by MEW (2002b). Table 6.3 shows the monthly water production at DW. The monthly water production is presented in million m^3. The freshwater produced in DW comes from seawater desalination from existing MSF desalination units at the plant.

Table 6.3 Monthly water production in 2001 at DW (MEW,2002b)

Month	**Monthly water production million m^3**
January	9.947
February	8.885
March	10.974
April	12.205
May	13.263
June	13.238
July	13.501
August	13.662
September	12.771
October	12.085
November	11.894
December	11.653

6.4. Conventional DW Configuration

The performance of the DW powerplant (Figure 6.1) must be assessed before hybrid plant configurations are developed and analysed. A simplified flow diagram is shown in Figure 6.2. The fuel consumption and CO_2 emissions of the conventional plant are estimated to use them as a bench-mark to compare the performance of hybrid powerplants against, after which the most efficient configuration for Kuwait can be suggested. The mathematical models for the steam Rankine cycle and the MSF desalination process developed and presented in Chapters 3 and 4 are linked together and run simultaneously to simulate the DW cogeneration plant.

6.4.1. Steam mass flowrate calculations

The main objective of the linear model describing the MSF is to calculate the mass flowrate of the steam to be bled from the turbine or fed from an auxiliary boiler to the brine heater. The calculated steam mass flowrate is then used as an input to the main program simulating the cogeneration plant.

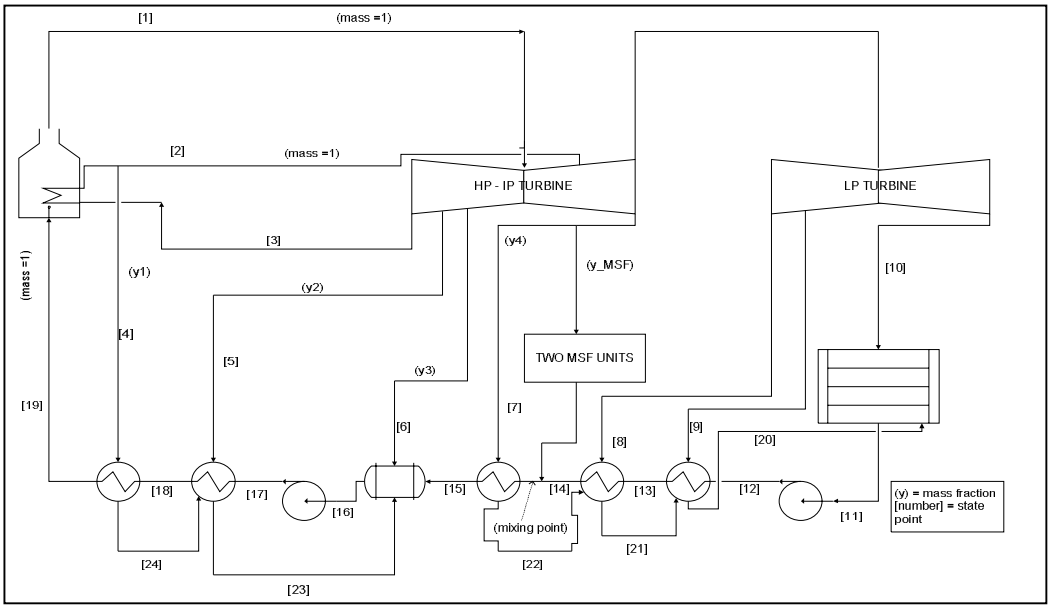

Figure 6.2 Schematic diagram of the DW conventional powerplant

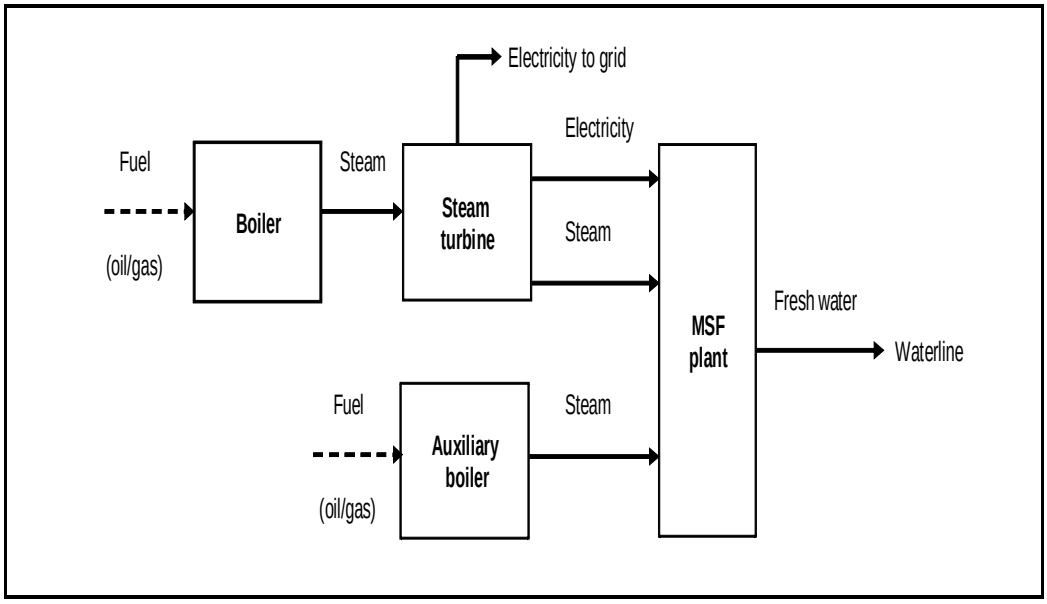

Figure 6.3 Simplified flow diagram of DW conventional powerplant

The objective of the program describing the power cycle, on the other hand, is to calculate the amount of steam input from the boiler to the steam turbine. So, the new additions to the Rankine cycle mathematical model are:

- Calculation of the number of MSF units to be operated at DW.
- Calculation of the number of steam turbines to be operated at DW taking into account the base load, A/C load and internal electricity consumption.
- Estimation of oil and natural gas consumed by DW and the corresponding cost.
- Estimation of carbon dioxide (CO_2) emissions.

The Rankine cycle model calculates all temperatures, pressures and enthalpies required for performance estimation of the cycle. In Figure 6.1, the enthalpies are numbered according the state point numbering between brackets from h_1 to h_{24} (kJ/kg). The MSF model is now executed to determine the mass flow rate of the steam ($m_{s,MSF}$) to be extracted from the turbine at point [7] on the diagram. Also, the enthalpy of the steam in and out of the MSF units is calculated from the known

thermodynamic properties from the Rankine cycle program. The mass fractions at points [4], [5] and [6] are calculated since all variables are known.

$$y_1 = \frac{(h_{19}-h_{18})}{(h_4-h_{24})} \tag{6.1}$$

$$y_2 = \frac{y_1(h_{23}-h_{24})+(h_{18}-h_{17})}{(h_5-h_{23})} \tag{6.2}$$

$$y_3 = \frac{(h_{16}-h_{15})-y_1(h_{23}-h_{24})-y_2(h_{23}-h_{15})}{(h_6-h_{15})} \tag{6.3}$$

Since the mass flowrate of steam ($m_{s,boiler}$) raised in boilers is unknown and should be estimated using the developed code, the mass fractions, turbine work and power can only be calculated by solving the following equations simultaneously using the Matlab function *fsolve*. A flow chart of the modelling procedure is presented in Figure 6.3.

$$h_{mixing} = \frac{(y_{MSF}\times h_{MSF,liquid})+h_{14}(1-y_1-y_2-y_3-y_{MSF})}{(1-y_1-y_2-y_3)} \tag{6.4}$$

and

$y_{MSF} = {}^{m_{S,MSF}}/_{m_{S,boiler}}$, which is the mass fraction of steam into MSF units.

$$y_4 = \frac{(1-y_1-y_2-y_3)\times(h_{15}-h_{mixing})}{(h_7-h_{22})} \tag{6.5}$$

$$y_5 = \frac{y_4(h_{21}-h_{22})+(1-y_1-y_2-y_3-y_{MSF})\times(h_{14}-h_{13})}{(h_8-h_{21})} \quad (6.6)$$

$$y_6 = \frac{(y_4+y_5)\times(h_{20}-h_{21})+(1-y_1-y_2-y_3-y_{MSF})\times(h_{13}-h_{12})}{(h_9-h_{20})} \quad (6.7)$$

The equation for turbine work output is,

$$\begin{aligned} W_T = {} & (h_1 - h_2) + (1 - y_1)(h_3 - h_5) + (1 - y_1 - y_2)(h_5 - h_6) \\ & +(1 - y_1 - y_2 - y_3)(h_6 - h_7) \\ & +(1 - y_1 - y_2 - y_3 - y_4 - y_{MSF})(h_7 - h_8) \\ & +(1 - y_1 - y_2 - y_3 - y_4 - y_5 - y_{MSF})(h_8 - h_9) \\ & +(1 - y_1 - y_2 - y_3 - y_4 - y_5 - y_6 - y_{MSF})(h_9 - h_{10}) \end{aligned} \quad (6.8)$$

The power output per turbine is calculated from the following equation

$$Output = m_{S,boiler} \times W_T \text{ in kW} \quad (6.9)$$

6.4.2. MSF Desalination Analysis

The DW powerplant comprises 16 MSF units, 4 of which have a maximum capacity of 27,277 m^3/day each, and 12 units with a maximum capacity of 32,732 m^3/day each. It is assumed in this work that the 4 units with the lower

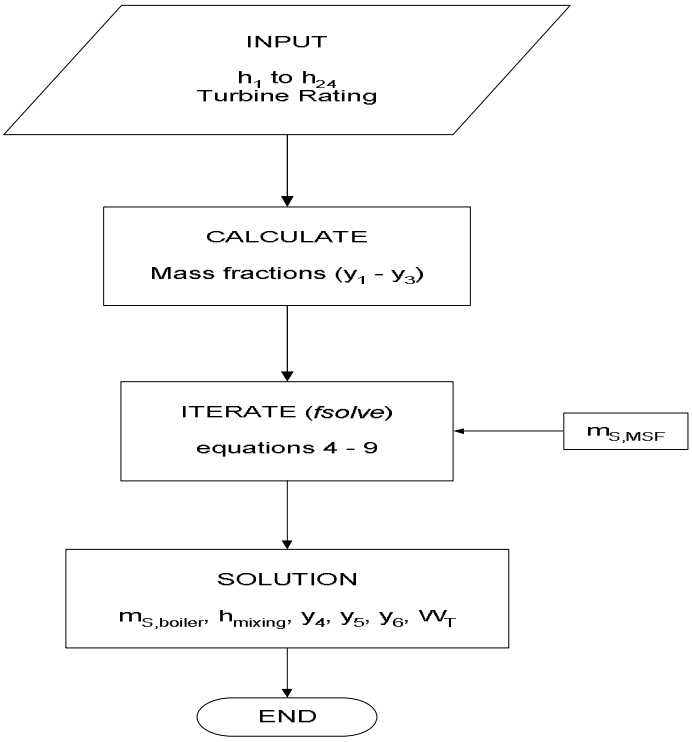

Figure 6.4 Flowchart of procedure to determine mass flowrate of steam raised in boiler

capacity are in constant operation and that they are always operated by steam extracted from the turbines in operation.

The following correlation is used to estimate the number of high capacity units that will be needed to satisfy the demand along with the 4 low capacity units:

$$N_{MSF,H} = \frac{WW_{demand} - \left(N_{MSF,L} \times Ca_{MSF,L} \times days\right)}{Ca_{MSF,H} \times days} \tag{6.10}$$

The total number of MSF units that need to be operated to satisfy freshwater demand is:

$$N_{MSF} = N_{MSF,L} + N_{MSF,H} \tag{6.11}$$

The next step is to estimate the number of MSF units that will be fed by steam extraction from the turbine. Each turbine set feeds steam to two MSF units. However, there is usually a mismatch between electricity and water demands, hence auxiliary boilers must come on-line to provide the required steam for the MSF units not connected to a turbine. So, the amounts of oil and natural gas consumed by the auxiliary boilers are calculated to be added later to those consumed by the main boilers of the powerplant.

- **Heavy oil consumption**

The monthly consumption of heavy fuel oil from the ***low*** capacity MSF units is:

$$m_{oil,MSF,L} = \left[\frac{m_{MSF,L} \times Q_{bh,L} \times N_{MSF,L}}{h_{boiler} \times CV_{oil}} \right] \times 3600 \times 24 \times days \tag{6.12}$$

The monthly consumption of oil from the ***high*** capacity MSF units is:

$$m_{oil,MSF,H} = \left[\left(\frac{m_{MSF,H} \times Q_{bh,H}}{h_{boiler} \times CV_{oil}} \right) \cdot \left(N_{MSF} - NT^2 \right) \right] \times 3600 \times 24 \times days \tag{6.13}$$

The total monthly consumption of heavy oil by auxiliary boiler feeding MSF units not covered by steam extraction is:

$$m_{oil,MSF} = m_{oil,MSF,L} + m_{oil,MSF,H} \tag{6.14}$$

The extra fuel energy ($E_{oil,MSF}$ MJ/month) consumed by the auxiliary boilers to run the MSF units is calculated using the following equation:

$$E_{oil,MSF} = CV_{oil} \times m_{oil,MSF} \tag{6.15}$$

- **Natural gas consumption**

The volume of natural gas consumed for the low capacity MSF units is:

$$V_{gas,MSF,L} = \left[\frac{m_{MSF,L} \times Q_{bh,L} \times N_{MSF,L}}{h_{boiler} \times CV_{gas}} \right] \times 3600 \times 24 \times days \qquad (6.16)$$

The volume of natural gas consumed for high capacity MSF units is:

$$V_{gas,MSF,H} = \left[\left(\frac{m_{MSF,H} \times Q_{bh,H}}{h_{boiler} \times CV_{gas}} \right) \cdot \left(N_{MSF} - NT^2 \right) \right] \times 3600 \times 24 \times days \qquad (6.17)$$

6.4.3. Total Powerplant Fuel Cost

The data concerning heavy oil and natural gas consumption at DW published in MEW (2002a) are used to determine the quantity of each fuel used at the plant in percentage terms. The analysis shows that heavy oil consumption at DW is 90% of the total and natural gas is 10%. Hence, when calculating the consumption of each fuel, the corresponding percentage values are considered when executing the program. The formulas used to estimate the cost of oil and natural gas at the powerplant are presented below.

- **Cost of oil**

To estimate the amount of oil consumed at the plant in terms of barrels, first the monthly mass flowrate of fuel consumed in main boilers to run the steam turbines is calculated:

$$m_{oil,power} = \left[\frac{m_{steam} Q_{boiler} NT}{h_{boiler} CV_{oil}}\right] \times 3600 \times 24 \times days \tag{6.18}$$

This equation is used to calculate the heavy oil energy in MJ per month consumed in the plant:

$$E_{oil,total} = \left(CV_{oil} \times m_{oil,power} \times 10^{-3} \times a_{oil}\right) + \left(E_{oil,MSF} \times a_{oil}\right) \tag{6.19}$$

The oil energy estimated is converted to barrels per month using,

$$NB_{oil} = E_{oil,total} \times k \tag{6.20}$$

and the cost of the oil in million $US consumed at the station is estimated from,

$$C_{oil} = NB_{oil} \times C_{barrel} \tag{6.21}$$

- **Cost of natural gas**

The monthly amount of natural gas in m^3 consumed at DW is calculated from:

$$V_{gas,total} = \left[\left(\left[\frac{m_{steam} Q_{boiler} NT}{h_{boiler} CV_{gas}}\right] \times a_{gas} \times 3600 \times 24 \times days\right) + \left(V_{gas,MSF} \times a_{gas}\right)\right] \tag{6.22}$$

$$E_{gas,total} = V_{gas,total} \times CV_{gas} \times w \tag{6.23}$$

The cost of the natural gas consumed at the station can now be estimated from:

$$C_{gas,total} = E_{gas,total} \times C_{gas} \times 10^{-6} \quad (6.24)$$

6.4.4. Carbon Dioxide Emissions

The published report by EPA (2005) is used in this research. It is useful in that the information required to calculate CO_2 emissions is simple yet comprehensive. Table 6.4 lists the values of the parameters required to estimate CO_2 emissions caused by combustion of heavy oil and natural gas at DW.

The correlation used to estimate CO_2 emission for various types of fuels is:

$$R_{CO_2} = CV \times CC \times F \times \left(44/12\right) \quad (6.25)$$

To estimate the monthly CO_2 emissions the amount calculated above is multiplied by the corresponding calculated amounts of oil (NB_{oil}) or natural gas ($V_{gas,total}$).

6.5. Power-RO Plant Configuration

The suggested configuration is for a single-purpose powerplant producing electricity only to satisfy the electric load (i.e. plant internal, basic and A/C loads) and supply electricity to RO desalination units that are used to meet freshwater demand (see Figure 6.4). MSF desalination is not utilised in this part of the modelling. The Matlab code developed for a Rankine cycle producing electricity only is utilised to analyse the performance of the powerplant.

The same monthly electricity and water demand profiles are used for this powerplant configuration as for the cogeneration plant. There are two parameters that have to be specified to complete the model for the power-RO plant. They are the capacity of the RO plant and the electricity consumption per unit of water produced.

Table 6.4 Heat contents and carbon content coefficients (EPA, 2005)

Fuel Type	Heat Content	Carbon Content Coefficients (kg carbon/kJ)	Fraction Oxidised
Solid Fuels	**MJ/kg**		
Anthracite coal	26.25	2.68E-05	0.99
Bituminous coal	27.78	2.42E-05	0.99
Sub-bituminous coal	19.93	2.51E-05	0.99
Lignite	14.97	2.49E-05	0.99
Coke	28.84	2.94E-05	0.99
Unspecified	29.08	2.40E-05	0.99
Gas Fuels	**MJ/m^3**		
Natural gas	38.30	1.37E-05	0.995
Liquid Fuels	**MJ/kg**		
Crude oil	40.52	1.92E-05	0.99
Nat gas liquids & LRGs	26.13	1.61E-05	0.995
Motor gasoline	36.40	1.83E-05	0.99
Aviation gasoline	35.28	1.79E-05	0.99
Kerosene	39.62	1.87E-05	0.99
Jet fuel	39.62	1.83E-05	0.99
Distillate fuel	40.73	1.89E-05	0.99
Residual oil	43.95	2.04E-05	0.99
Naptha for petrofeed	36.68	1.72E-05	0.99
Petroleum coke	42.06	2.64E-05	0.99
Other oil for petrofeed	40.73	1.89E-05	0.99
Soecial napthas	36.68	1.88E-05	0.99
Lubricants	42.41	1.92E-05	0.99
Waxes	38.71	1.88E-05	0.99
Asphalt/road oil	46.39	1.95E-05	0.99
Still gas	41.92	1.66E-05	0.99
Misc. products	40.52	1.92E-05	0.99

Note: For fuels with annually variable heat contents and carbon content coefficient, 2003 U.S. average values are presented. All factors are presented in higher heating values.

The selected capacity of the RO plant should be within the range of commercially available RO capacities. The recently commissioned Fujairah hybrid plant in the UAE includes a RO plant with a capacity of 170,475 m^3/day. But it is established that RO plants are available at capacities as high as 320,000 m^3/day (Veolia Water, 2005). To take advantage of the concept of "economies of scale", the current set-up of the MSF plant at DW will not be implemented for the suggested RO plant. In other words, it is best in terms of economics and efficiency to install fewer number of RO units with higher capacities than the current MSF units.

To be able to satisfy the highest distilled water demand during 2001 of 441,258 m^3/day and have spare capacity, the RO plant selected here will include 5 RO units of 110,000 m^3/day.

6.5.1. RO Energy Consumption

The specific energy consumption by RO units at DW estimated in *Chapter 4* is 5.49 kWh/m^3. Knowing the capacity of each RO unit and the energy consumption, the total monthly electricity consumed by RO can now be calculated.

- Number of required RO units

$$N_{RO} = \frac{W_{demand}}{Ca_{RO} \times days} \tag{6.26}$$

- Monthly electricity consumed by RO

$$E_{RO,total} = E_{RO,unit} \times Ca_{RO} \times N_{RO} \times days \tag{6.27}$$

Equations (6.21), (6.24), and (6.25) are used to estimate cost of oil, cost of gas, and the CO_2 emissions, respectively at the power-RO plant.

6.6. Power-MSF-RO Plant Configuration

The first hybrid configuration that can be suggested for the DW powerplant comprises of the conventional dual-purpose set-up with a RO seawater desalination system added to it. A flow diagram of the suggested configuration is shown in Figure 6.5. The feasibility of utilizing both the MSF and RO desalination technologies at the plant is studied and analysed. The capacity of RO desalination is

increased from 5% to 95% and MSF desalination is decreased by the same percentage. This research does not suggest any physical connection between RO and MSF technology by sharing the same water intake or using the discharge of one technology as feed to another. The suggested configuration assumes that these desalination processes work independently to satisfy freshwater demand of DW powerplant.

The rationale behind this configuration is to study the ability to use excess electricity generated by the steam turbines during low A/C load periods. In other words, the

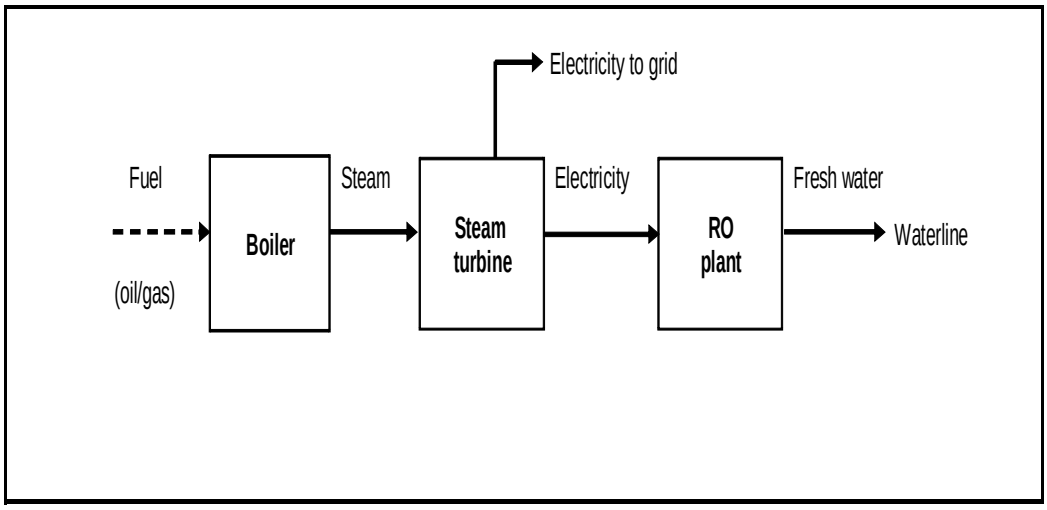

Figure 6.5 Simplified flow diagram of power-RO powerplant configuration

configuration helps in matching steam and electricity generation with demand. Utilising the RO desalination technology in the winter time when A/C load is zero helps make use of available electricity and avoids the use of auxiliary boilers to feed MSF units with steam. The constraints and assumptions listed previously apply for this configuration. Also, the input parameters and mathematical correlations used for the conventional and power-RO configurations (see Sections 6.4 and 6.5) are not changed for this configuration.

6.7. Power-MSF-AR Plant Configuration

The mathematical model of the power-MSF-AR hybrid configuration is a development of the model used to evaluate the performance of the DW cogeneration plant discussed in Section 6.4. This section describes the work undertaken to model a conventional plant that includes AR chillers. See Figures 6.6 and 6.7 for details.

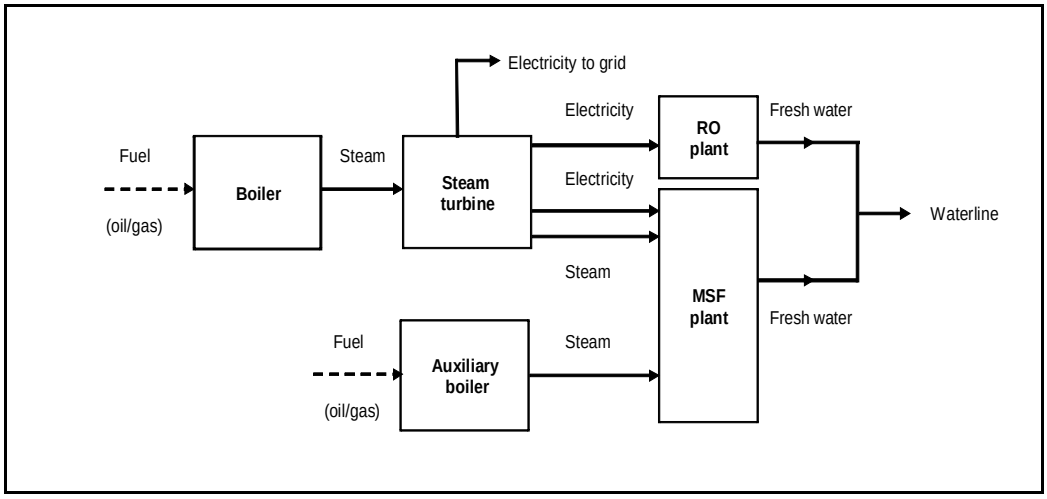

Figure 6.6 Simplified flow diagram of power-MSF-RO hybrid powerplant configuration

6.7.1. AR Energy Consumption

The model developed in *Chapter 5* to simulate the double-effect H_2O-LiBr chiller is utilised to estimate the energy (Q_{AR}) required to operate it, which is then fed to the main Rankine-cycle model. The first step in linking AR chillers to the conventional plant is to calculate the number of AR units that would replace the A/C load satisfied by VC units. The number of AR units at DW can be estimated from:

$$Unit_{AR} = \frac{(Pr_{AC})(COP)}{Ca_{AR,unit}} \quad (6.28)$$

The above equation estimates the total number of AR chillers that may be fed by the 8 turbine-sets at DW. The mass flowrate of steam required to operate one AR chiller is estimated from the following equation:

$$m_{AR,unit} = \frac{Q_{AR}}{(h_{AR,steam} - h_{AR,liquid})} \quad (6.29)$$

The mass flowrate of steam required to run *N* number of AR units for a ***single*** turbine-set can be calculated from:

$$m_{AR,total} = \frac{(Unit_{AR})(m_{AR,unit})}{NT} \quad (6.30)$$

6.7.2. Steam mass flowrate

The addition of AR to the conventional-plant model means that Equations (6.3) to (6.8) will have to be modified to account for the extracted steam ($m_{steam,AR}$) from the turbines. It must be noted that not all the required steam for AR will come from the turbines, but part of it must be raised in auxiliary boilers as will be detailed below. The modified equations are:

$$y_3 = \frac{(1-y_1-y_2)(h_{mixing,AR})+(y_1+y_2)(h_{23})-h_{16}}{(h_{16}-h_{mixing,AR})} \quad (6.31)$$

$$h_{mixing,AR} = \frac{(h_{AR,liquid})(y_{AR})+(1-y_1-y_2-y_3-y_{AR})(h_{15})}{(1-y_1-y_2-y_3)} \quad (6.32)$$

$$h_{mixing,MSF} = \frac{(y_{MSF})(h_{MSF,liquid})+h_{14}(1-y_1-y_2-y_3-y_{AR}-y_{MSF})}{(1-y_1-y_2-y_3-y_{AR})} \quad (6.33)$$

$$y_4 = \frac{(1-y_1-y_2-y_3-y_{AR})(h_{15}-h_{mixing,MSF})}{(h_7-h_{22})} \quad (6.34)$$

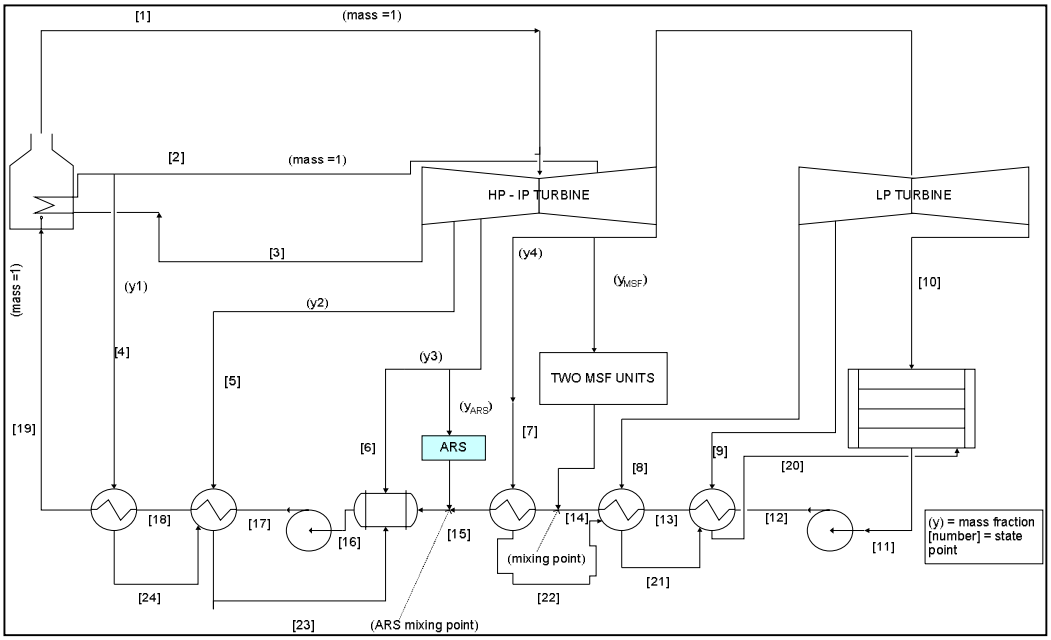

Figure 6.7 Schematic diagram of cogeneration powerplant wit AR steam extraction

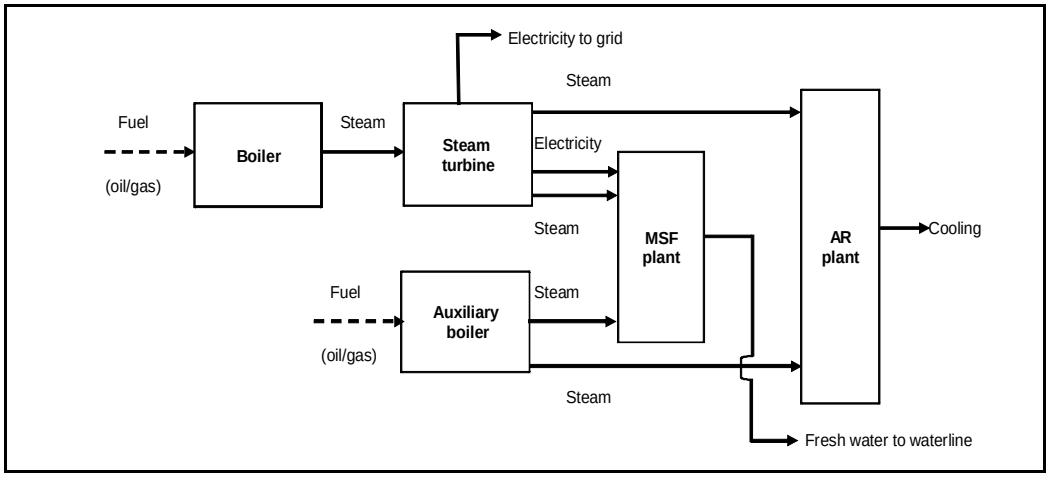

Figure 6.8 Simplified flow diagram of power-MSF-AR hybrid powerplant configuration

$$y_5 = \frac{y_4(h_{21}-h_{22})+(1-y_1-y_2-y_3-y_{AR}-y_{MSF})(h_{14})-h_{13}}{(h_8-h_{21})} \tag{6.35}$$

$$y_6 = \frac{(y_4-y_5)(h_{20}-h_{21})+(1-y_1-y_2-y_3-y_{AR}-y_{MSF})(h_{13}-h_{12})}{(h_9-h_{20})} \tag{6.36}$$

$$\begin{aligned} W_T = {} & (h_1-h_2)+(1-y_1)(h_3-h_5)+(1-y_1-y_2)(h_5-h_6) \\ & +(1-y_1-y_2-y_3-y_{AR})(h_6-h_7) \\ & +(1-y_1-y_2-y_3-y_4-y_{AR}-y_{MSF})(h_7-h_8) \\ & +(1-y_1-y_2-y_3-y_4-y_5-y_{AR}-y_{MSF})(h_8-h_9) \\ & +(1-y_1-y_2-y_3-y_4-y_5-y_6-y_{AR}-y_{MSF})(h_9-h_{10}) \end{aligned} \tag{6.37}$$

Where the unknowns to be solved-for in the program are (Figure 6.8):

- $m_{steam.boiler}$
- $h_{mixing,MSF}$
- y_3

- y_4
- y_5
- y_6
- W_T

6.7.3. Fuel Cost & CO_2 Emissions

Equations (6.12) to (6.16) are also modified to account for AR steam extraction and used in this section to estimate the cost of fuel and CO_2 emissions of the power-MSF-AR configuration. Since the objective is to analyse the viability of replacing VC A/C with AR chillers, the replacement takes place gradually based on percentage decrease of VC load and increase in AR load at increments of 10% until reaching 100% AR load. Details are given in Table 6.5.

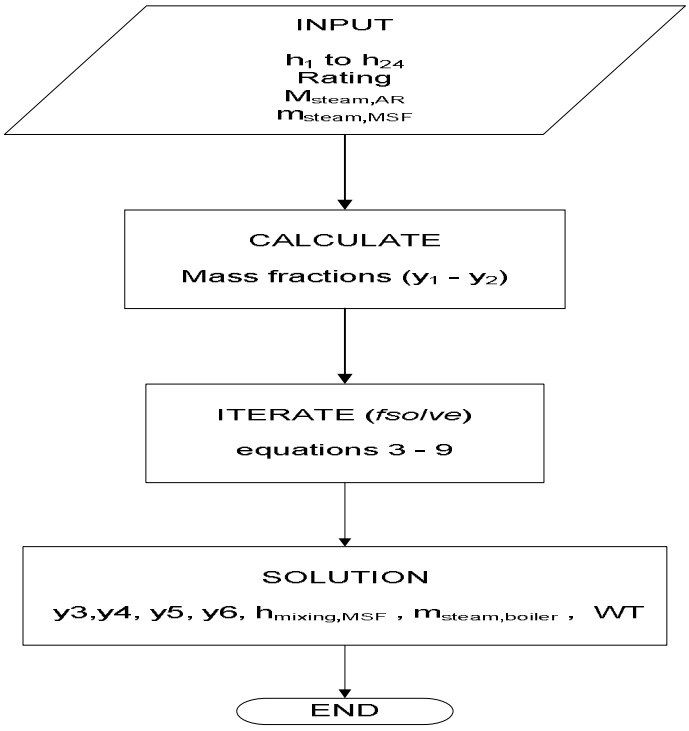

Figure 6.9 Flowchart of procedure to determine turbine output in a cogeneration + AR plant

Table 6.5 AR load variation in a conventional plant

AR load	Electric power consumed by A/C (MW)							
%	April	May	June	July	August	September	October	November
100	430	785	869	960	1026	917	554	275
90	387	706	782	864	387	387	499	248
80	344	628	695	768	821	734	443	220
70	301	549	608	672	718	642	388	193
60	258	471	521	576	616	550	332	165
50	215	392	435	480	513	458	277	138
40	172	314	348	384	411	367	222	110
30	129	235	261	288	308	275	166	83
20	86	157	174	192	205	183	111	55
10	43	78	87	96	103	92	55	28

For this configuration, there are three different processes that will consume either oil or natural gas. Fuel is supplied to boilers for steam turbines, MSF desalination units and AR units. The mass flowrate of oil consumed for MSF units is estimated using Equations (6.12), (6.13) and (6.14), and for steam turbines using Equation (6.18). The amount of oil consumed to raise steam in auxiliary boilers for part of AR demand is estimated using:

$$m_{oil,AR} = \left[\frac{(Z)(Q_{AR})(NT)}{(\eta_{boiler})(CV_{oil})}\right] \times 3600 \times 24 \times days \tag{6.38}$$

The energy consumption of AR auxiliary boiler is:

$$E_{oil,AR} = \left(CV_{oil} \times m_{oil,AR} \times \alpha_{oil} \times 10^{-3}\right) \tag{6.39}$$

Hence, an additional term is added to Equation (6.20) to account for $E_{oil,AR}$:

$$E_{oil.total} = \left(CV_{oil} \times m_{oil,power} \times NT \times \alpha_{oi} \times 10^{-3}\right) + \left(E_{oil,MSF} \times \alpha_{oil}\right) + \left(E_{oil.AR} \times \alpha_{oil}\right) \quad (6.40)$$

To calculate the oil consumption for the power-MSF-AR configuration in barrels the total cost Equations (6.20) and (6.21) are used.

The monthly consumption of natural gas due to the addition of AR chillers to the plant is:

$$V_{gas,AR} = \left[\frac{(Z)(Q_{AR})(NT)(\alpha_{gas})}{(\eta_{boiler})(CV_{gas})}\right] \times 3600 \times 24 \times days \quad (6.41)$$

The total monthly natural gas consumption for the *power-MSF-AR* configuration becomes:

$$V_{gas,total} = \left[\left[\frac{(Z)(Q_{AR})(NT)(\alpha_{gas})}{(\eta_{boiler})(CV_{gas})}\right] \times 3600 \times 24 \times days\right] + \left(V_{gas,MSF} \times \alpha_{gas}\right) + \left(V_{gas,AR} \times \alpha_{gas}\right) \quad (6.42)$$

The total natural gas energy for the power-MSF-AR configuration is calculated using Equation (6.23) and the cost by applying Equation (6.24).

Carbon dioxide emissions for the configuration are estimated using the same procedure discussed in the conventional plant section without any modifications to Equation (6.25).

6.8. Power-RO-AR Hybrid Plant Configuration

Figure 6.9 shows the flow diagram of power-RO-AR configuration. In this hybrid configuration, AR chillers are added to the electricity producing only powerplant with RO units as the seawater desalination system. The power-RO model discussed in Section 6.5 is modified to account for the steam that will be extracted for AR chillers. The same modelling procedure discussed in Section 6.7 is used. Equations (6.28) to (6.37) are added to the power-RO-AR model, with only the term y_{MSF} taken out since there is no MSF desalination. The fuel cost and CO_2 emissions of this hybrid configuration are estimated using Equations (6.38) to (6.42). Equations (6.40) and (6.42) without the MSF term become:

$$E_{oil.total} = \left(CV_{oil} \times m_{oil,power} \times NT \times \alpha_{oil} \times 10^{-3}\right) + \left(E_{oil.AR} \times \alpha_{oil}\right) \quad (6.43)$$

$$V_{gas,total} = \left[\left[\frac{(Z)(Q_{AR})(NT)(\alpha_{gas})}{(\eta_{boiler})(CV_{gas})}\right] \times 3600 \times 24 \times days\right] + \left(V_{gas,AR} \times \alpha_{gas}\right) \quad (6.44)$$

The aim of developing the hybrid power-RO-AR configuration is to study the effect on the fuel consumption of turning a power-only plant to a cogeneration plant a desalination process other than MSF. For the power-RO-AR hybrid configuration, only the performance during the summer months and March is studied since there is no A/C load in the winter and adding AR chillers would not make any difference.

6.9. Power-MSF-RO-AR Hybrid Plant Configuration

The power-MSF-RO-AR hybrid configuration comprises of all possible combinations of suggested systems (see Figure 6.10). The MSF and RO systems are utilised for seawater desalination, and VC and AR A/C to satisfy the cooling load. The power-MSF-AR mathematical model is modified to include RO desalination equations (Equations (6.26) and (6.27)). The RO load is varied, as in the power-

MSF-RO configuration, from 5% to 95% for every percentage AR load. The mathematical correlations and procedure used for previous hybrid configurations are also used to model the power-MSF-RO-AR configuration and estimate fuel cost and CO_2 emissions.

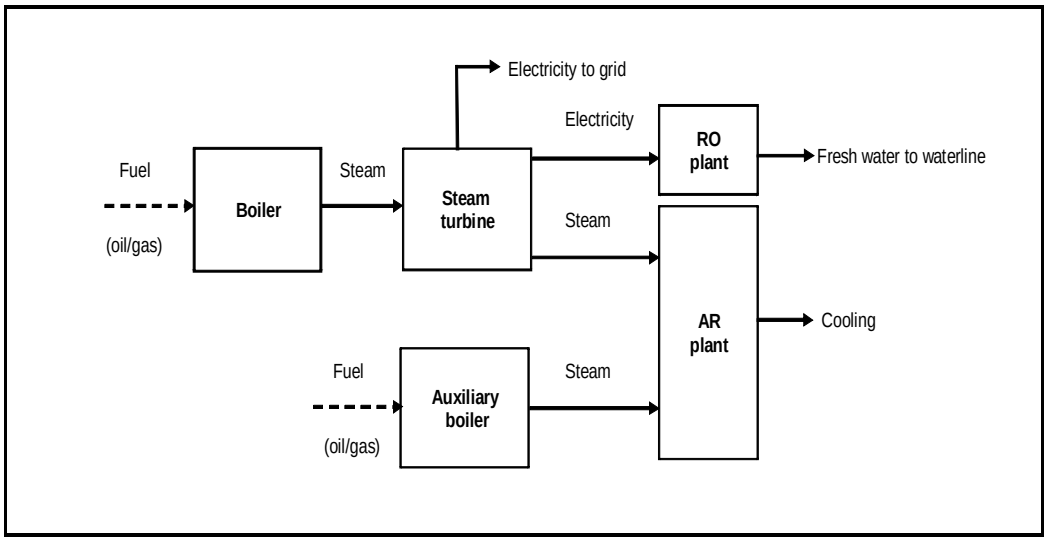

Figure 6.10 Simplified flow diagram of power-RO-AR hybrid powerplant configuration

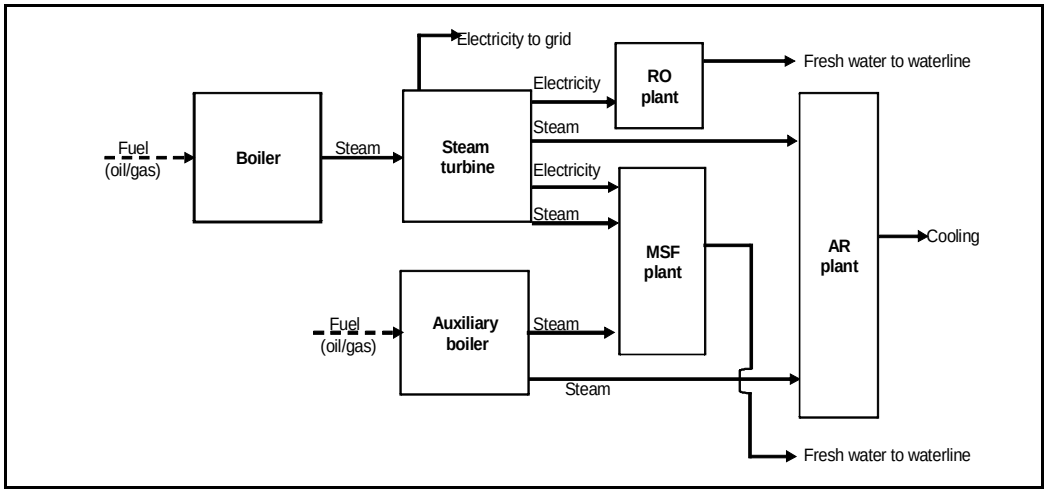

Figure 6.11 Simplified flow diagram of power-MSF-RO-AR hybrid powerplant configuration

Chapter 7

7. Performance Evaluation of Hybrid Configurations

The hybrid configurations suggested for the DW powerplant were discussed in Chapter 6 and the corresponding mathematical correlations were presented. The performance results of the suggested hybrid configurations are presented and analysed in this chapter. Specifically, the total fuel cost, which includes heavy oil and natural gas consumed at DW, is used in this work as an indicator of the efficiency of each powerplant configuration analysed. Based on the results, an operation strategy for winter and summer seasons is recommended.

The mathematical modelling of the hybrid configurations also includes the CO_2 emissions caused by burning the fuels inside the powerplant, but these results are not discussed here and instead they are presented in tabulated form in Appendix C. The reason for not including them in this chapter is that they follow the same pattern as the fuel cost graphs, and both quantities are dependent on the amount of fuel burned in the boilers. Also, cost as an indicator is easily understood by readers of all levels and backgrounds, and can be related to the number of barrels of oil saved which is important for an oil producing country like Kuwait.

The fuel cost for the DW conventional powerplant is presented and discussed in Section 7.1. In Section 7.2, the results of the power-RO configuration are presented and compared with the fuel cost of the conventional DW powerplant. The fuel cost of the hybrid configurations power-MSF-RO, power-MSF-AR, power-RO-AR and power-MSF-RO-AR are presented and discussed in Sections 7.3, 7.4, 7.5, and 7.6, respectively. Finally, the optimum configuration is selected for each month of the year in Section 7.7 using the fuel cost results presented in previous sections and an operation strategy is recommended for winter and summer months. The total annual

fuel cost is also presented with the corresponding savings in the quantities of fuels used at the powerplant.

7.1. Doha West Cogeneration Plant

The published data on electricity and water consumption and the developed mathematical model for a cogeneration plant are used to simulate the performance of the DW. It must be emphasised here that the objective of the exercise is not to exactly simulate the current situation at DW but to improve on some operation practises where applicable with the constraint of satisfying the demand at all times. Table C-1 in appendix-C shows the results of the simulation.

Figure 7.1 below shows the actual electricity consumption published by MEW (2002a) and the electricity generated using the developed model. It is clear from the figure that the electricity generated satisfies the demand despite the fact that the number of estimated turbines in operation being less than the actual published number. The discrepancy in the number of turbines can be attributed to two major reasons. The first is the assumption in this research that the turbines work only at fully capacity, which is not the practice in the existing powerplant. Turbines in an electric powerplant can vary in capacity to match the corresponding demand for electricity. Also, the DW plant is connected to the grid, which means that the plant can bring turbines on-line to make-up for a shortage of electricity supply from other power stations. In the model, DW is isolated from the influence of other stations for the purpose of simplifying the modelling procedure.

Figure 7.2, on the other hand, shows the monthly desalinated water consumption and production. It can be seen that the water production estimated using the mathematical model satisfies the consumption (i.e. demand) for the year 2001. Only in the month of July there is no spare capacity where the production and demand are equal.

The total monthly fuel cost for DW, which includes heavy oil and natural gas, is shown in Figure 7.3. The figure shows a general increasing trend as the temperature increases during the summer months. The highest cost is in August at the peak of summer, and then the cost starts to drop as temperatures start to decrease during the autumn and winter months. Figure 7.4, which shows the CO_2 emissions for the plant, also follows the same general trend. The main reason for the increase in electricity consumption during the summer and the corresponding increase in fuel cost is due to the A/C load.

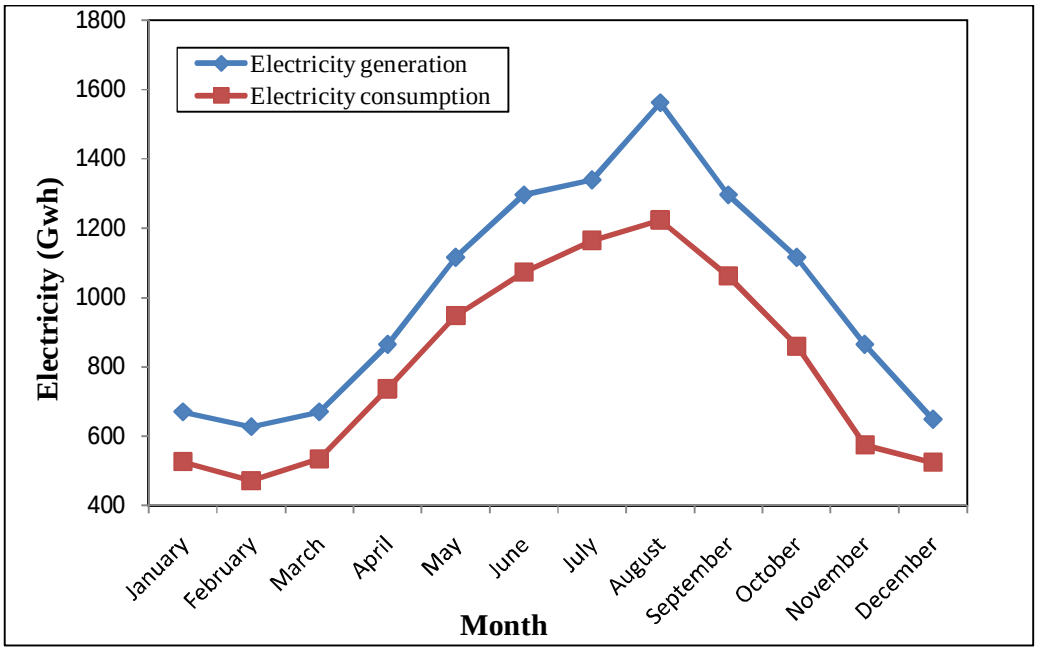

Figure 7.1 Comparison of actual and generated electricity at DW for 2001

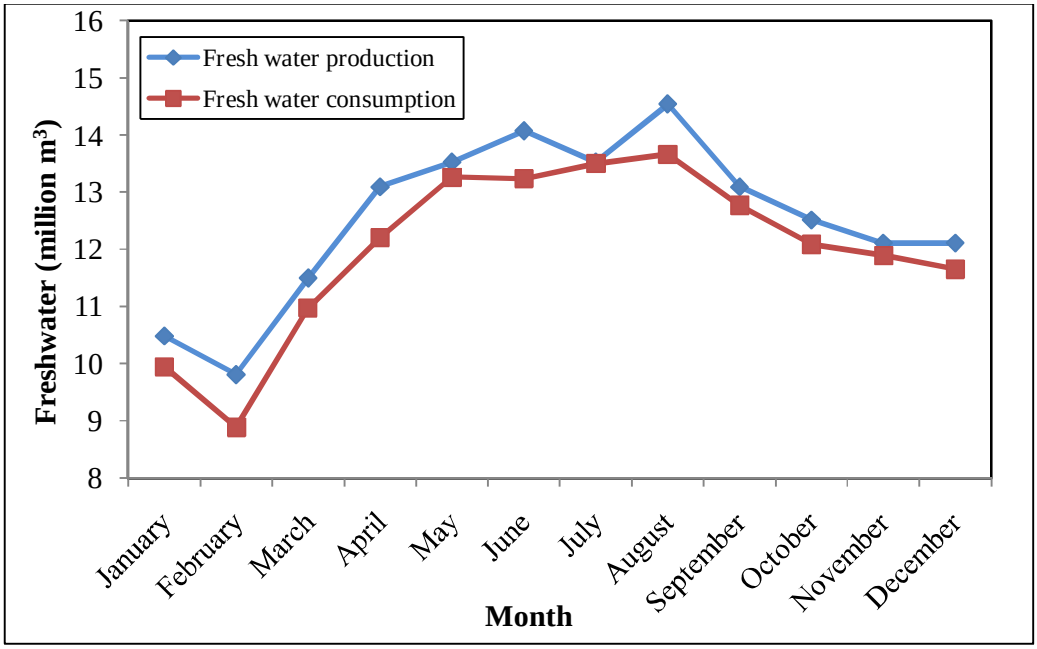

Figure 7.2 Comparison of desalinated water demand and production at DW for 2001

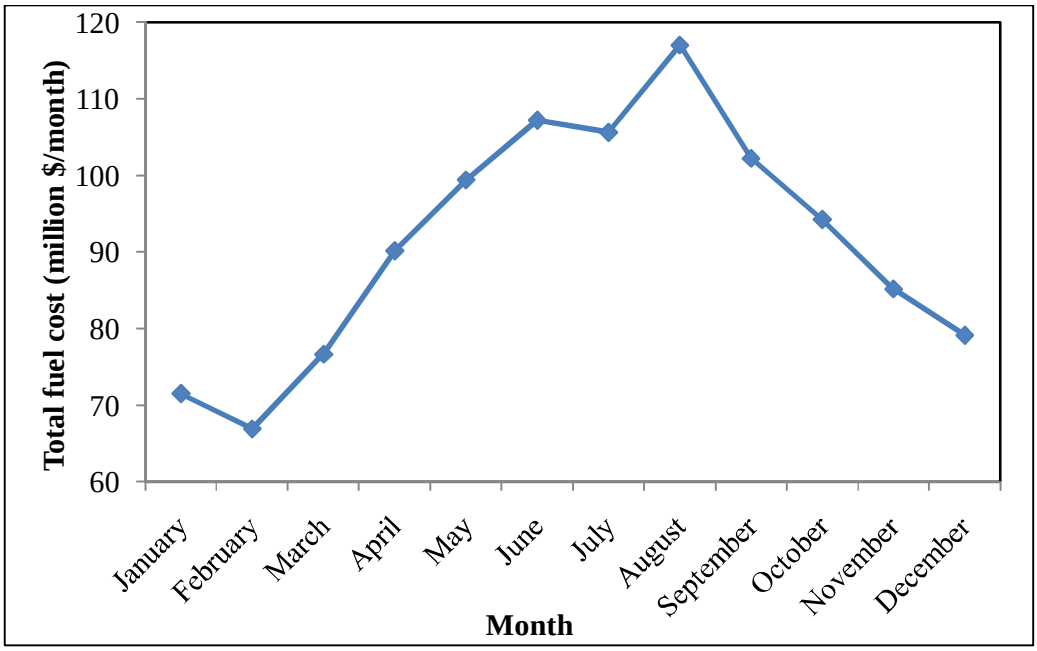

Figure 7.3 Total fuel cost at DW cogeneration plant for 2001

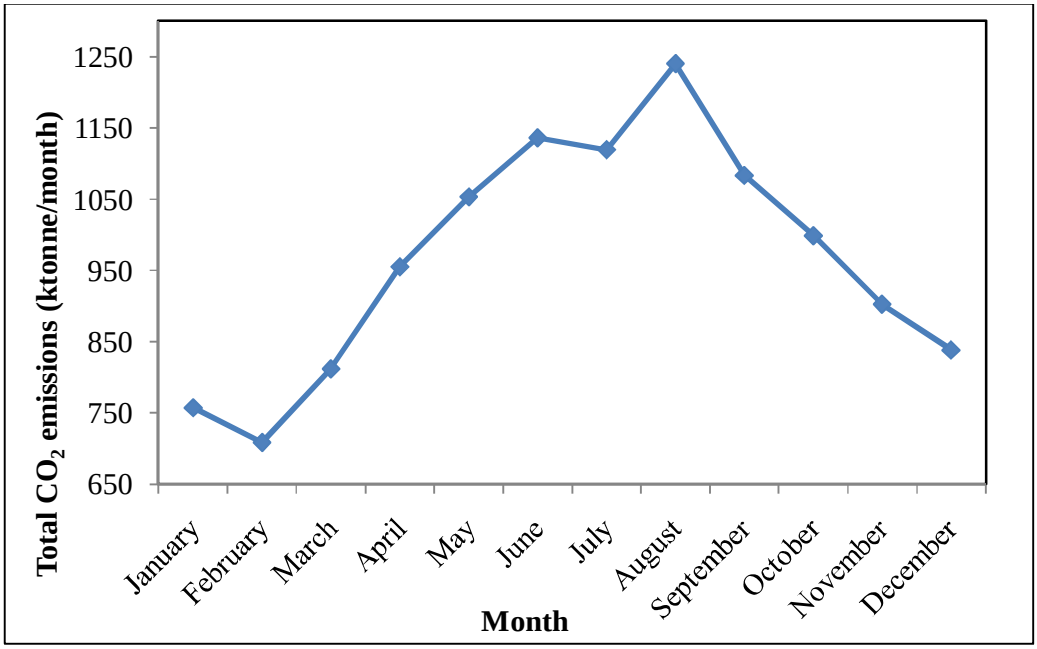

Figure 7.4 CO_2 emissions from DW cogeneration plant for 2001

7.2. Power-RO Plant Configuration

The results of the power-RO plant simulations are presented in Table C-2 in Appendix-C. Figure 7.5 shows the distilled water demand and the water produced by the RO plant. It can be seen that the selected capacity satisfies the demand for all months of the year. However, the water production in June and August is significantly higher than the demand during these months. This can be decreased, in theory, by reducing the seawater intake into the 5^{th} RO unit, which in turn would reduce the full capacity of 110,000 m^3/day.

Figures 7.6 and 7.7 show the total fuel cost and the CO_2 emissions for the power-RO plant compared with the conventional plant, respectively. The figures show that these parameters are lower for the power-RO plant except for the month of July. This could be attributed to the fact that the number of turbines operated by the

power-RO plant (7 turbines) is higher than those for the conventional plant (6 turbines) during the month of July.

It can be seen from figures that the power-RO plant is more fuel efficient than the cogeneration powerplant, contrary to the common believe that cogeneration plants are always more efficient. However, the main reason for the higher rate of fuel consumption by the conventional (i.e. cogeneration) powerplant is the extra amount of steam supplied by auxiliary boilers to operate the MSF units when there is a mismatch between electric and freshwater demands.

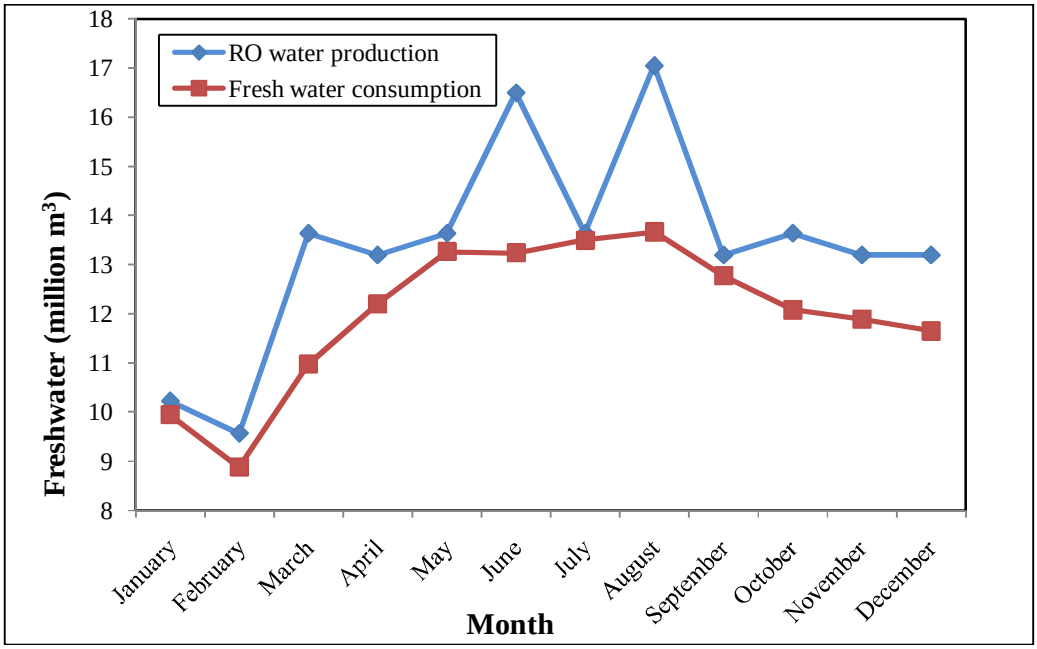

Figure 7.5 Comparison between freshwater demand and production by RO desalination

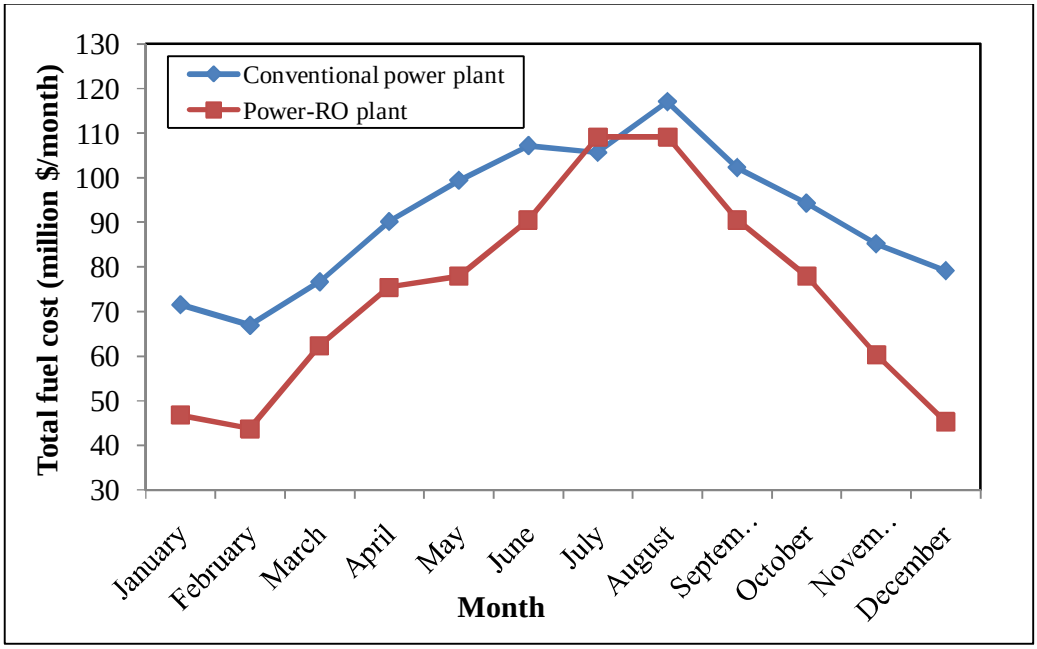

Figure 7.6 Fuel cost comparison between conventional DW and power-RO plants

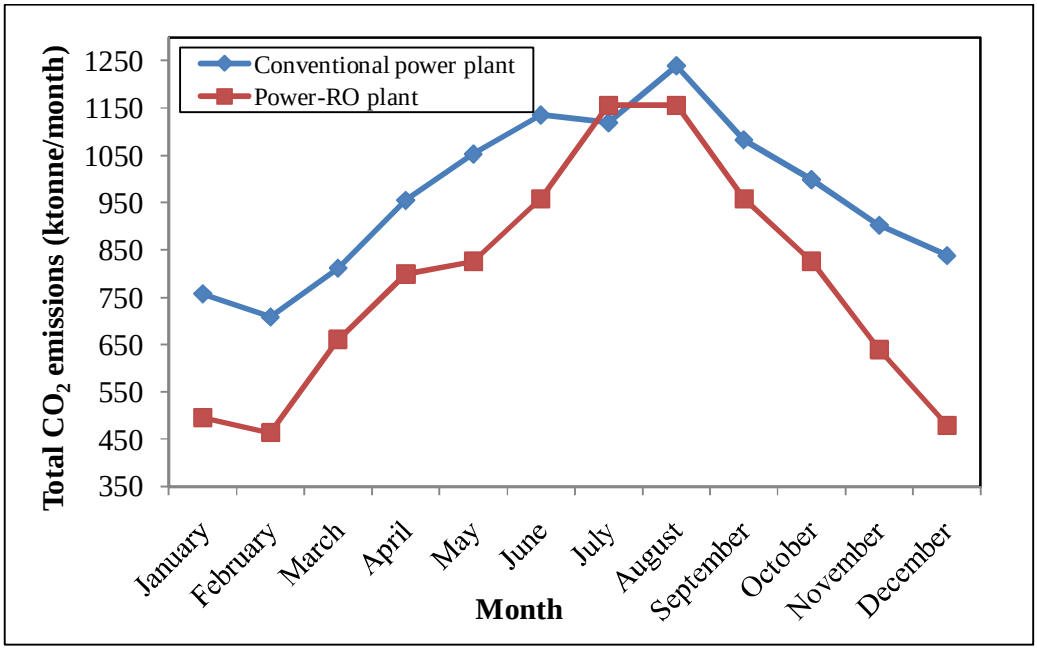

Figure 7.7 CO_2 emissions from conventional and power-RO plant

7.3. Power-MSF-RO Plant configuration

The fuel cost for the hybrid power-MSF-RO configuration is shown in Figures 7.8, 7.9 and 7.10 for the summer months, and Figure 7.11 for the winter months. March is included with the summer months because of, as explained in Chapter 6, A/C power consumption during the second half of it. Detailed results of the power-MSF-RO configuration are given in tabulated form in Appendix C.

7.3.1. Summer Results

The fuel cost in the figures ranges from approximately $50 million and $116 million at RO loads from 5% to 95%. The mildest summer months can be seen to be March, April and November where the cost is lower than the other months. The sharp increase in the cost for April at 85% RO load is due to the increased number of turbines to satisfy the electricity demand of the RO units, whereas the number of turbines during March and May remains constant. The decreasing trend for the mild summer months is a result of replacing MSF units operated by steam from auxiliary boilers with RO units running on available electricity in the powerplant. Furthermore, the constant cost in November starting at 40% RO load is due to the fact the there is no further benefit in reducing the number of MSF units in operation since they are operated on steam extracted from turbines. It must be mentioned here that the extracted steam to MSF units does not affect the output capacity of the turbines because the boilers are designed to feed a fully-loaded turbine and 2 MSF units.

Figure 7.9 shows the fuel cost for the hottest summer months of June, July and August. There are no savings in fuel cost in August, as depicted by the flat line, because there are 7 turbines in operation during the month due to the high A/C load. These 7 turbines cover the 14 MSF units in operation with extracted steam. Hence, there are no auxiliary boilers operating in August. The July profile overlaps with fuel cost in August at 80% RO load due to the increase of turbines from 6 to 7.

There is also a decreasing trend for June despite the number of turbines remaining constant. The reduction in cost is attributed to the reduction in steam from extra boilers to MSF units, which are replaced by RO units. The fuel cost results for September and October in Figure 7.10 follow the same pattern as the June results.

7.3.2. Winter Results

Figure 7.11 shows the fuel cost for the months of January, February and December. As for the results of the summer months, the RO load increases from 5% to 95% to replace MSF desalination units. The figure shows that the lowest fuel cost of the year is in February. It is the lowest month not only because there is no A/C load but also in February National and Independence days are celebrated, during which citizens usually travel abroad to spend their holidays. The figure also shows that the fuel cost stays constant at 45% RO load and above, and decreasing the number of MSF units has no benefit.

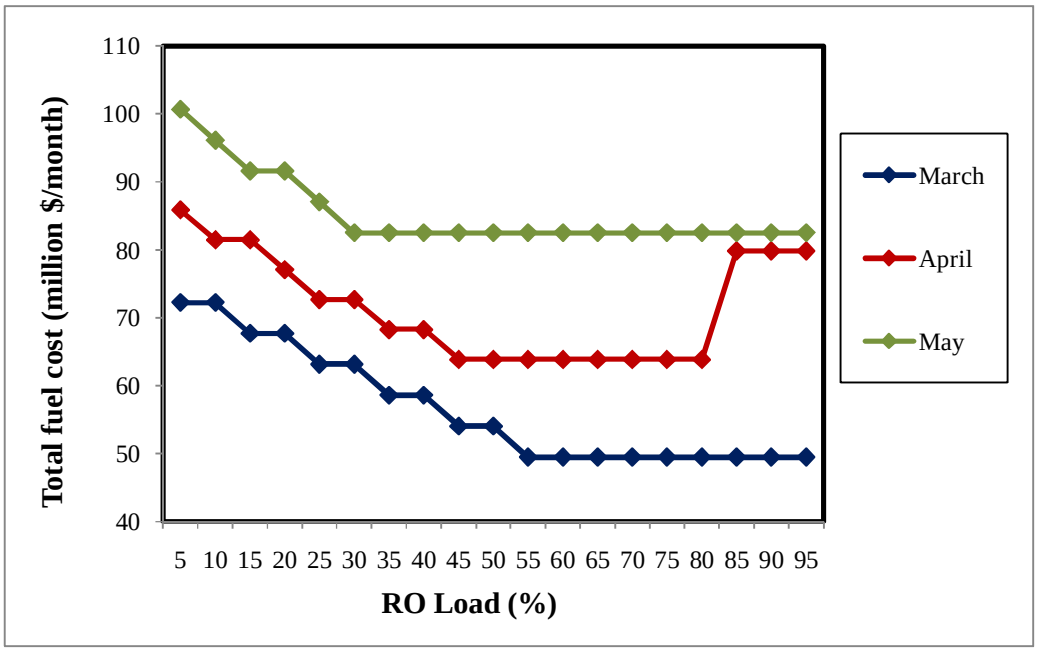

Figure 7.8 Fuel cost of power-MSF-RO configuration for March, April and May

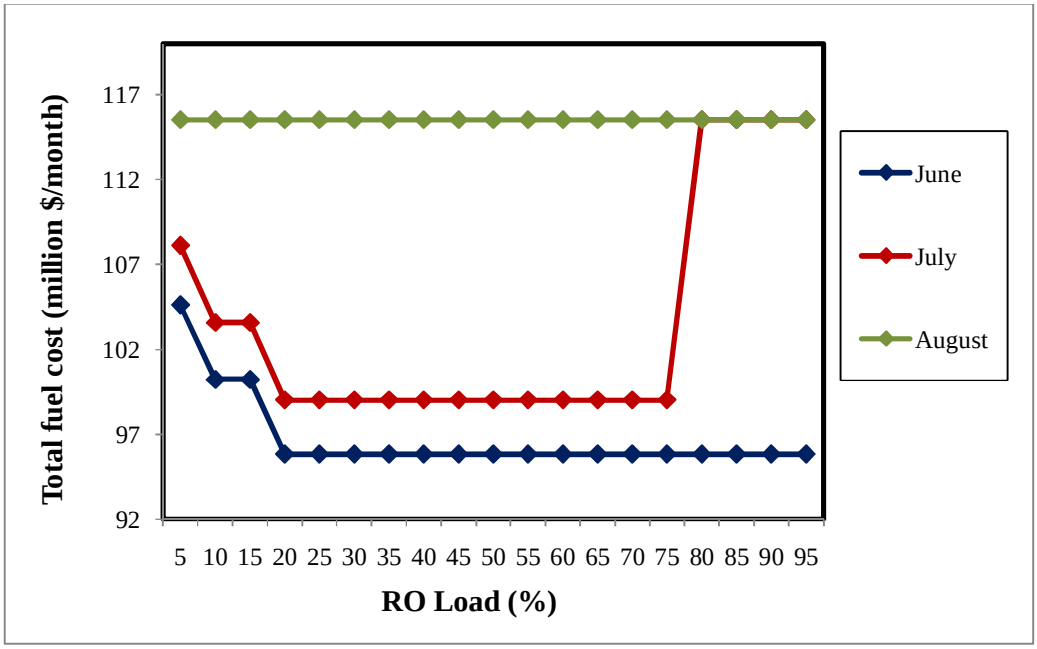

Figure 7.9 Fuel cost of power-MSF-RO configuration for June, July and August

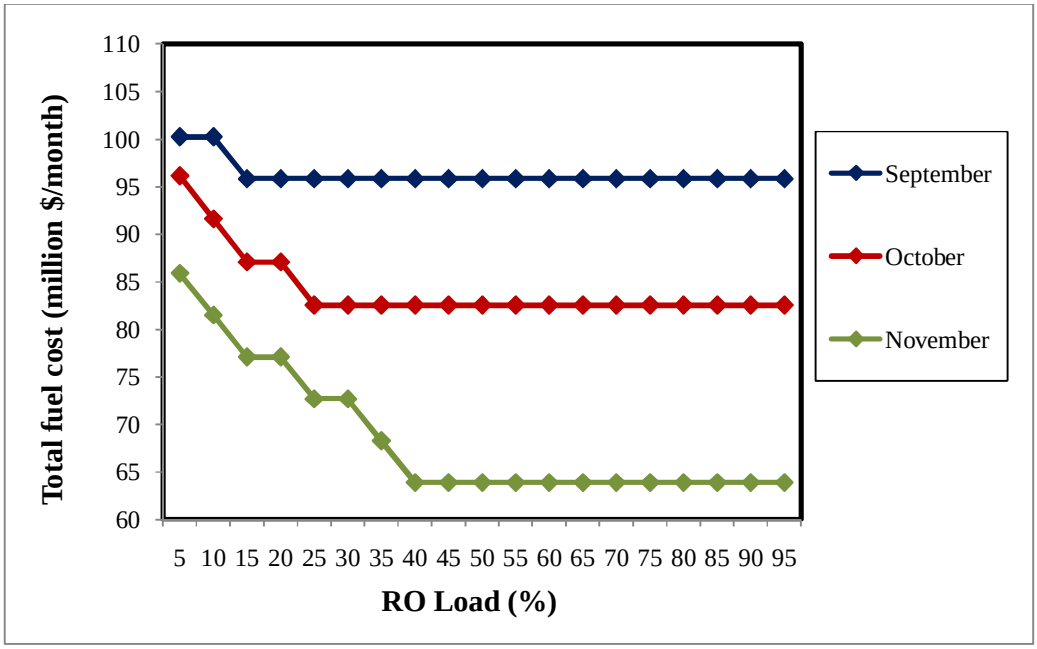

Figure 7.10 Fuel cost of power-MSF-RO configuration for September, October and November

It can also be seen that fuel cost in December starts higher than that of January, but it goes below at 60% RO load. The main reason for this is that in December the hybrid plant starts with a higher number of MSF units, which means more steam from auxiliary boilers. But, when the MSF units are 6 for both months (i.e. no auxiliary boilers needed), the fuel cost in December falls below that of January.

In general, the winter results for the power-MSF-RO configuration show that the RO desalination process can replace a large percentage MSF desalination load without the need to bring any extra turbines in operation above the base load number of 3 turbines. This means that the steam generated at the boilers can be reduced too since there is no steam extraction from the turbines to MSF units, hence, a reduction in fuel cost.

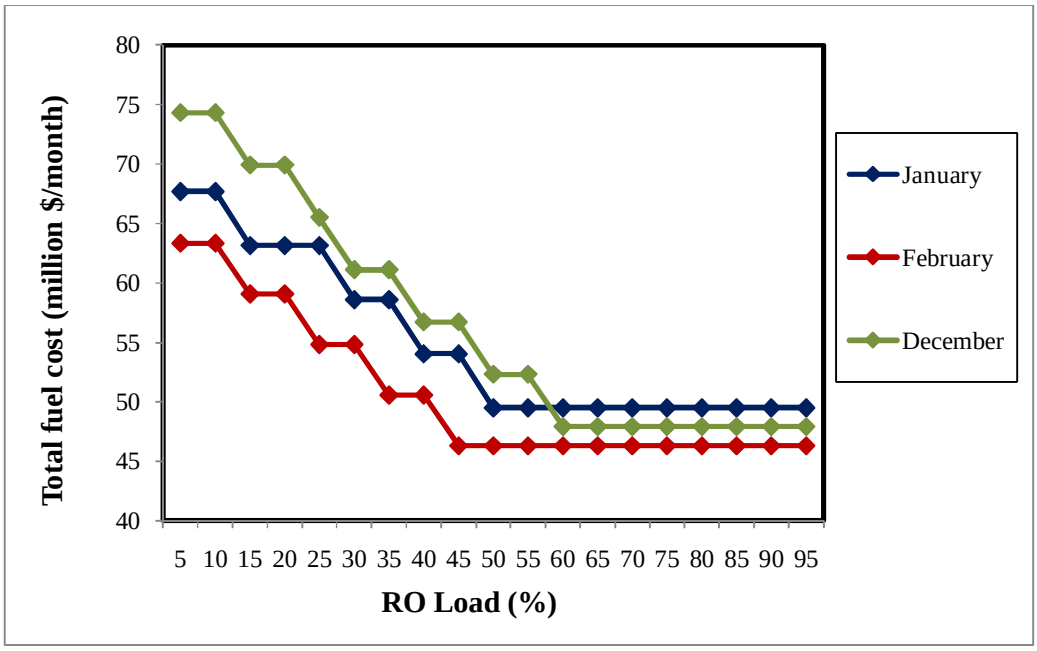

Figure 7.11 Fuel cost of power-MSF-RO configuration for winter months

7.3.3. Further Analysis

The optimum results of the power-MSF-RO configuration for the months March to November are presented in Table 7.1. The table shows that during the hottest month of the year, August, the RO load is the lowest compared to other summer months. This is due to the fact that in the peak of summer produced electricity is consumed mainly by VC-based A/C systems. On the other hand, the optimum results in the mildest summer months of March, April and November, the RO load is at 55%, 45% and 40%, respectively. This means that there is excess electricity produced by turbines running at full load (i.e. 300 MW) that can be utilised for RO instead of producing more steam to operate MSF units.

7.4. Power-MSF-AR Plant Configuration

The tabulated results of the power-MSF-AR hybrid configuration are presented in Appendix C. In this section the fuel cost results are presents in Figures 7.12, 7.13 and 7.14. The graphs show the fuel cost in $ million plotted against the AR load in percent. The 0% represents the plant in the conventional cogeneration mode. The results for January, February and December are not included since there is no A/C load during these months.

Table 7.1 Optimum Operation parameters of power-MSF-RO configuration From March to November

Month	RO load %	N_T	N_{MSF}	N_{RO}	C_{Fuel} million $	Q_{CO2} ktonne
March	55	3	6	2	50	524
April	45	4	8	2	64	677
May	30	5	10	2	83	874
June	20	6	12	1	96	1015
July	20	6	12	1	99	1049
August	5	7	14	1	116	1224
September	15	6	12	1	96	1015
October	25	5	10	1	83	874
November	40	4	8	2	64	677

The total fuel cost for March, April and May is shown in Figure 7.12. These months are mild summer months. The general trend of the results shows that the fuel cost increases when AR is added to the configuration while the number of turbines in operation remains constant. This is because there are now two processes in operation that require steam as input, MSF desalination and AR. On the other hand, there is a drop in fuel consumption when the number of turbines decreases. The main reason for the decrease in the number of turbines is that the electric load of the VC A/C is switched to thermal load in the shape of steam to satisfy the desalination and AR demands. In fact, when the number of turbines is 5 and less, there is no benefit to switch to the power-MSF-AR hybrid configuration.

The results show that there are small savings in fuel cost in the months of June, September, October and November, as shown in Figures 7.13 and 7.14. In June, the fuel cost at 20% AR load is less than that of the original cogeneration plant. However, this is the only AR load that shows savings over the cost of 0% AR load.

In October, however, the hybrid configuration is more fuel efficient than the cogeneration plant at 20% and 30% AR loads. The best performance for the hybrid configuration is in November, where the fuel cost and emissions are less than those for cogeneration at AR loads from 30% to 70%. For the hot summer months of July and August, there are no savings in fuel consumption since the A/C load is high and the use of AR chillers requires large quantities of steam from stand-by boilers which reverses any benefits obtained from reducing the number of turbines in operation.

The optimum operating conditions for the power-MSF-AR hybrid configuration are given in Table 7.2. The table shows the lowest cost values for the months that showed fuel savings over the conventional powerplant fuel cost.

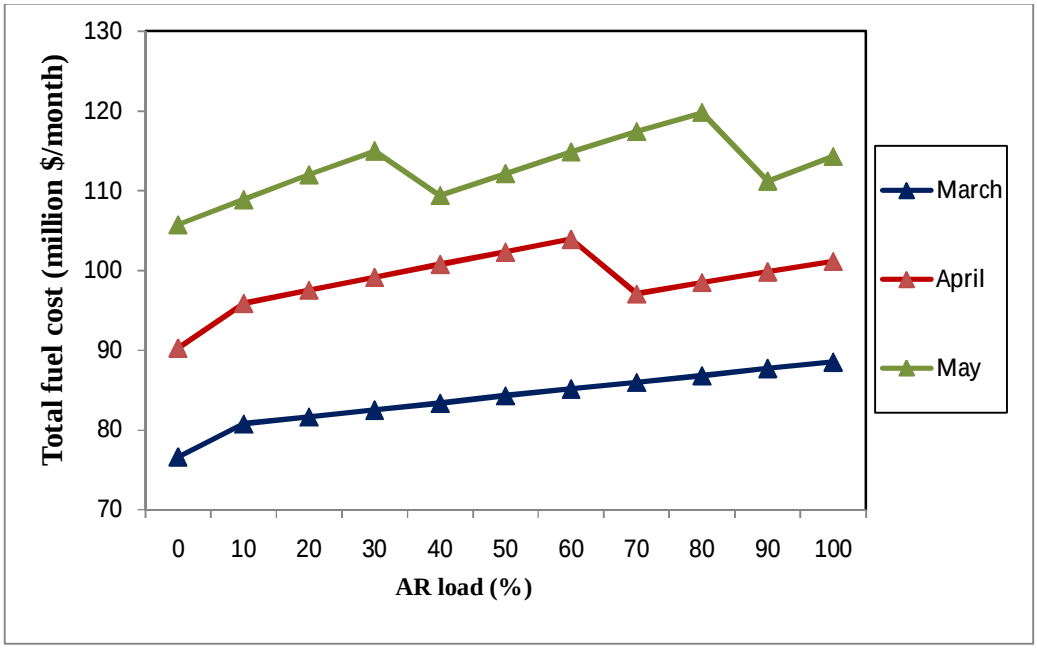

Figure 7.12 Fuel cost of power-MSF-AR configuration for March, April and May

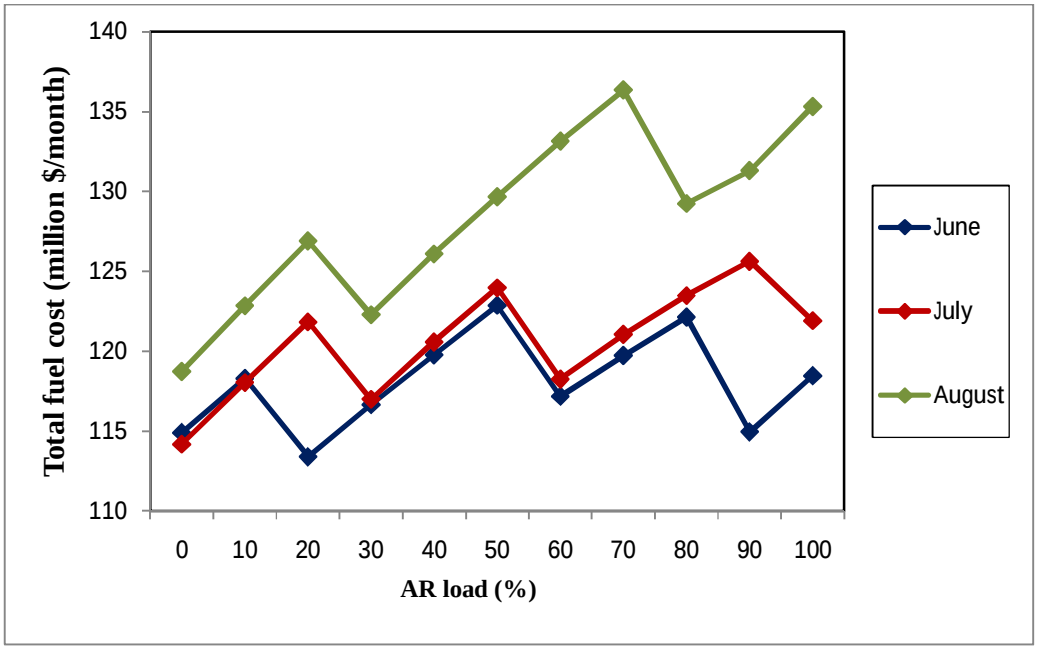

Figure 7.13 Fuel cost of power-MSF-AR configuration for June, July and August

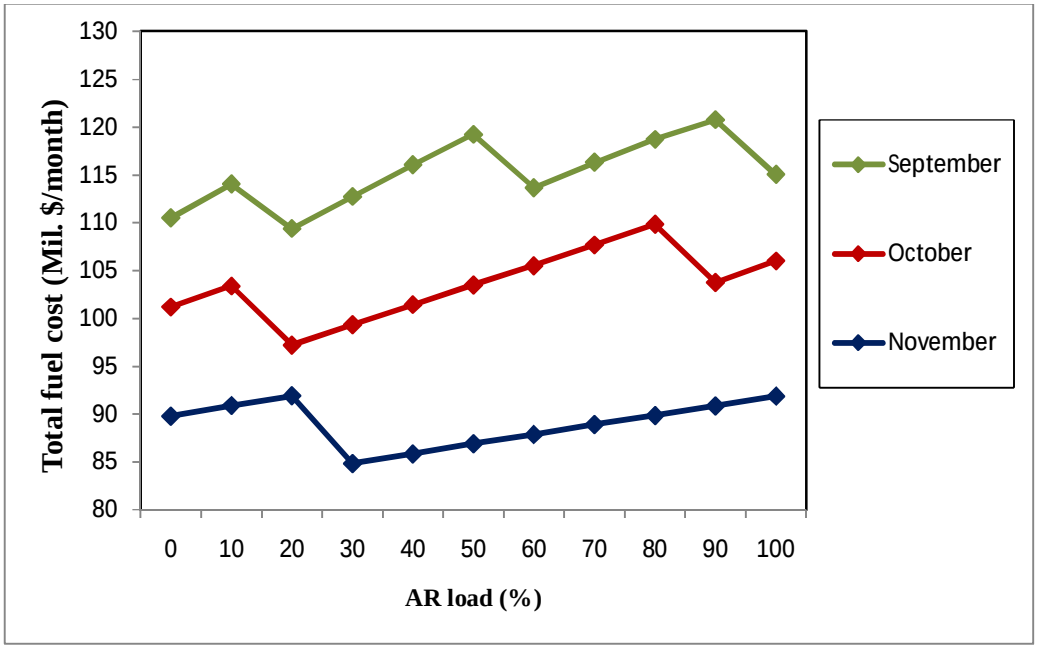

Figure 7.14 Fuel cost of power-MSF-AR configuration for September, October and November

Table 7.2 Optimum operation parameters of power-MSF-AR configuration

Month	AR load %	N_T	N_{AR}	N_{RO}	$m_{s,boiler}$ tonne/s	$m_{s,aux}$ kg/s	$m_{s,AR}$ kg/s	C_{Fuel} Million $	Q_{CO2} ktonne
June	20	5	79	15	1.39	189	110	113	1215
September	20	5	84	14	1.39	195	116	109	1170
October	20	4	51	13	1.11	134	71	97	1044
November	30	3	38	13	0.83	100	53	85	918

7.5. Power-RO-AR Plant Configuration

The total fuel cost for the power-RO-AR hybrid configuration is presented in Figures 7.15, 7.16 and 7.17. As in the previous section, the summer months are divided into three periods with the fuel cost plotted against the AR load. Other plant details and CO_2 emissions are given in Appendix C.

The total fuel cost for March, April and May are shown in Figure 7.15. The graph shows no general trend for these three months. Instead, the cost in May shows a general increasing trend, except at 50% AR load when the number of turbines in operations drops from 5 to 4. So this can be said to be the optimum operating point for the power-RO-AR configuration for May. On the other hand, the cost in April is lower for all AR loads than the cost for a power-RO plant. The cost decreases sharply for 100% AR load because the number of turbines changes from 4 to 3. During March, there are significant savings at 60% AR load when the number of turbines decreases from 4 to 3.

Figure 7.16 shows the total fuel cost for June, July and August, and Figure 7.17 shows the cost for September, October and November. The general trend in these figures is that there is a sharp drop in fuel consumption when a turbine is put out of operation then an increase when the number of turbines remains constant. The other trend that can be noticed is that the peaks and troughs increase in numbers during the hottest months of the year (i.e. June, July, August and September). The cost remains approximately constant in November because the number of turbines remains 4 for AR loads from 0% to 90%. The sharp decrease in November, like April, is due to the decrease in the number of turbines to 3. This means that the steam needed to satisfy the total A/C load by AR chillers is less than the steam needed to run the fourth turbine.

It can be said, as a general remark, that there is no optimum AR percentage loading that can be generalised for all months under investigation, since it can be seen from the figures that the absolute minimum is changing for different months.

Table 7.3 includes the optimum operation parameters that result in minimum fuel cost and CO_2 emissions. The table basically gives the most efficient combination for the hybrid power-RO-AR configuration. The number of RO desalination units is relatively small because of the large specific output capacity of the units assumed. On the contrary, the number of required AR chillers needed to satisfy the cooling

load is large because the specific capacity of available chillers on the market is small, about 4.43 MW for the units used in this research. It can also be seen that the amount of steam raised in auxiliary boilers is small compared with that of the power-MSF-AR configuration.

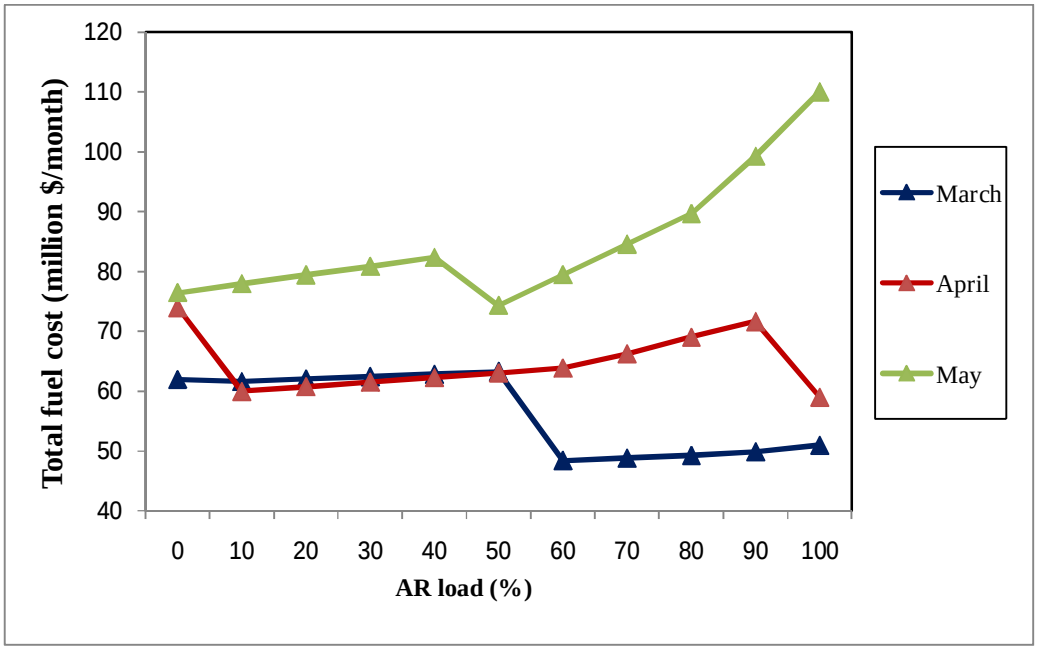

Figure 7.15 Fuel cost of power-RO-AR configuration for March, April and May

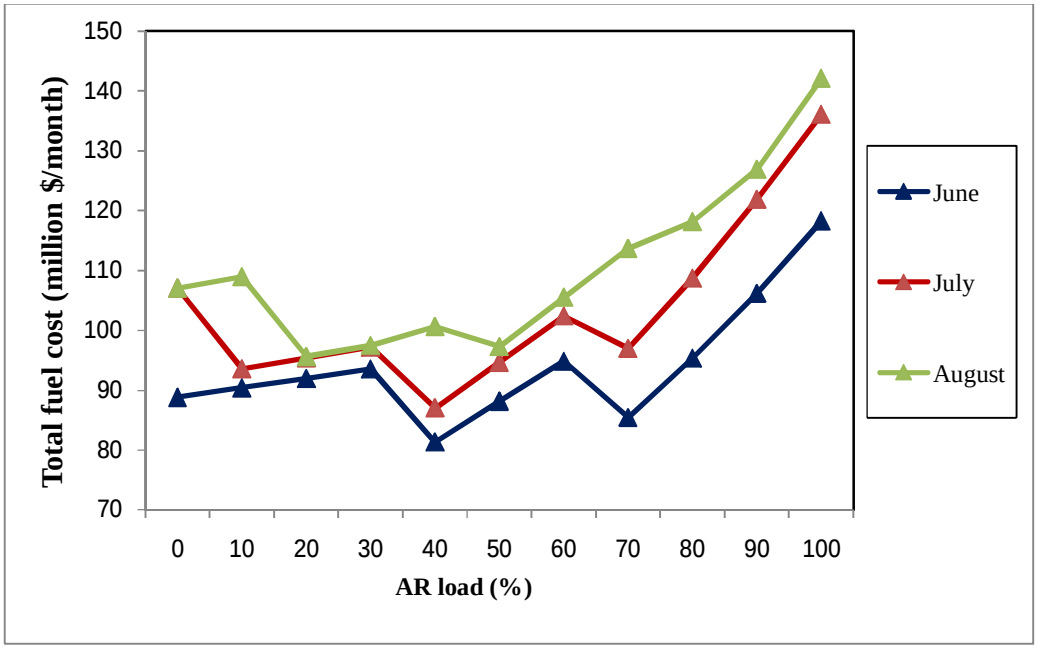

Figure 7.16 Fuel cost of power-RO-AR configuration for June, July and August

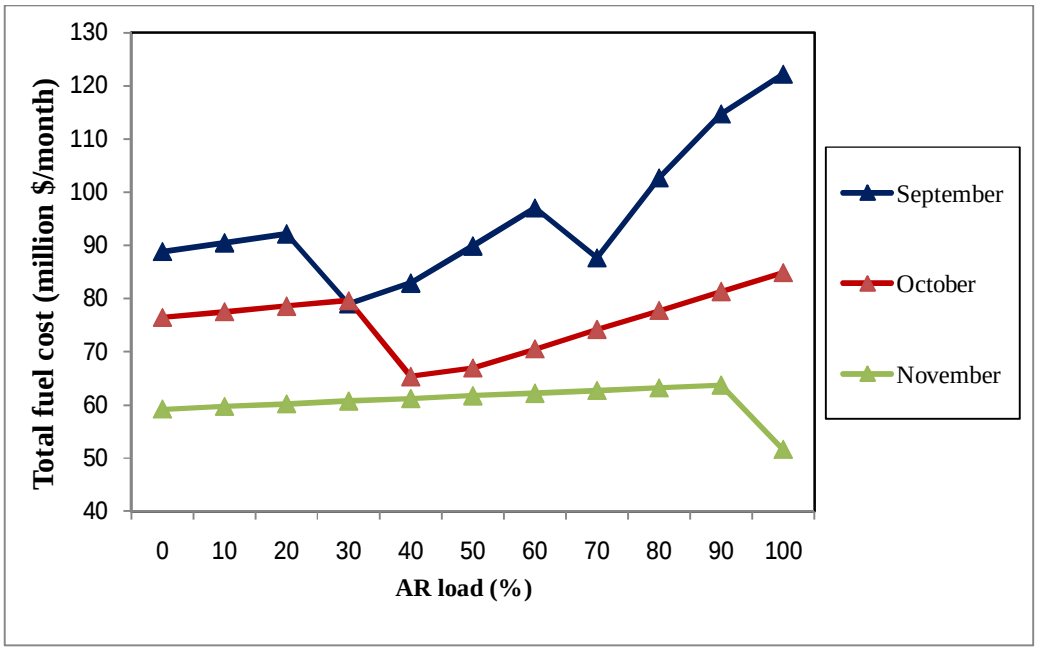

Figure 7.17 Fuel cost of power-RO-AR configuration for September, October and November

Table 7.3 Optimum Operation parameters of power-RO-AR configuration

Month	AR load %	N_T	N_{AR}	N_{RO}	$m_{s,boiler}$ tonne/s	$m_{s,aux}$ kg/s	$m_{s,AR}$ kg/s	C_{Fuel} million $	Q_{CO2} ktonne
March	60	3	62	3	0.81	0	86	48	513
April	100	3	196	4	0.83	73	272	59	630
May	50	4	178	4	1.11	40	247	74	791
June	40	5	158	5	1.39	6	219	81	862
July	40	5	175	4	1.39	17	243	87	924
August	20	6	94	5	1.60	0	130	96	1013
September	30	5	125	4	1.37	0	173	79	837
October	40	4	101	4	1.09	0	140	65	692
November	100	3	125	4	0.83	24	173	52	548

7.6. Power-MSF-RO-AR Plant Configuration

The power-MSF-RO-AR Matlab program is run for the months March to November. During the winter months of January, February and December the powerplant will switch to the power-MSF-RO configuration (Section 7.3) since the assumption that there is no A/C load during these months.

To be able to study the performance at all possible combinations, the AR load is varied from 10% to 100% and the RO load is varied from 5% to 95% at each AR load. The results shown in Figures 7.18, 7.19 and 7.20 are for the lowest fuel cost for summer months for a specific RO load at AR loads from 10% to 100%. For more details, see power-MSF-RO-AR results in Appendix C, Section C.6.

Figure 7.18 shows the optimum fuel cost at AR loads ranging from 10% to 100% for March, April and May. The optimum values in March show a gradual increase and are always occurring at RO loads of 50%. The large decrease in cost at 100% AR load for April is due to the change in the number of turbines from 4 to 3, at which the A/C load is satisfied by only AR units.

During the month of May, there are two decreasing trends because the number of turbines drops from 5 to 4 at 40% AR load and from 4 to 3 at 100% AR load. As in April, the absolute minimum fuel consumption is at 100% load which coincides with 60% RO load and 3 turbines in operation

The fuel cost results for June, July and August are shown in Figure 7.19. The graphs show that the profile increases and decreases several times due to the change in the number of turbines at different AR loadings. During the months of July and August, there are more peaks and valleys than the previous months and this is mainly due to the change in the number of turbines 3 times, from 6 to 3. This means that this suggested hybrid configuration allows for extra turbines available for future increase in electricity demand in Kuwait.

Figure 7.20 shows the optimum fuel cost profiles for September, October and November. In September, the optimum cost is at 60% AR and 45% RO loads, and 4 turbines. In October the absolute minimum cost is reached at 100% AR load at which there are only 3 turbines in operation with a RO load of 60%. It can be noticed from Table C.110 in Appendix C that there are 3 turbines working at 90% AR load as well, but the difference is in the extra MSF unit that operates on steam from the auxiliary boiler.

Finally, during November the minimum cost of fuel is at 70% AR load. At that point there are 3 turbines working at a RO load of 60%. Tables C.118 to C.121 in Appendix C show that the number of turbines, MSF and RO units are equal for AR loads from 70% to 100%. Here, what makes the difference is the AR load itself, which requires more steam from auxiliary boilers as it increases.

In general, the results show that the optimum cost always occurs when there are no auxiliary boilers feeding steam to MSF units, which clearly indicates that the integration of RO with MSF is more efficient. Also, these optimum results occur at

different RO loads, indicating that there is a different optimum MSF-RO combination for each month.

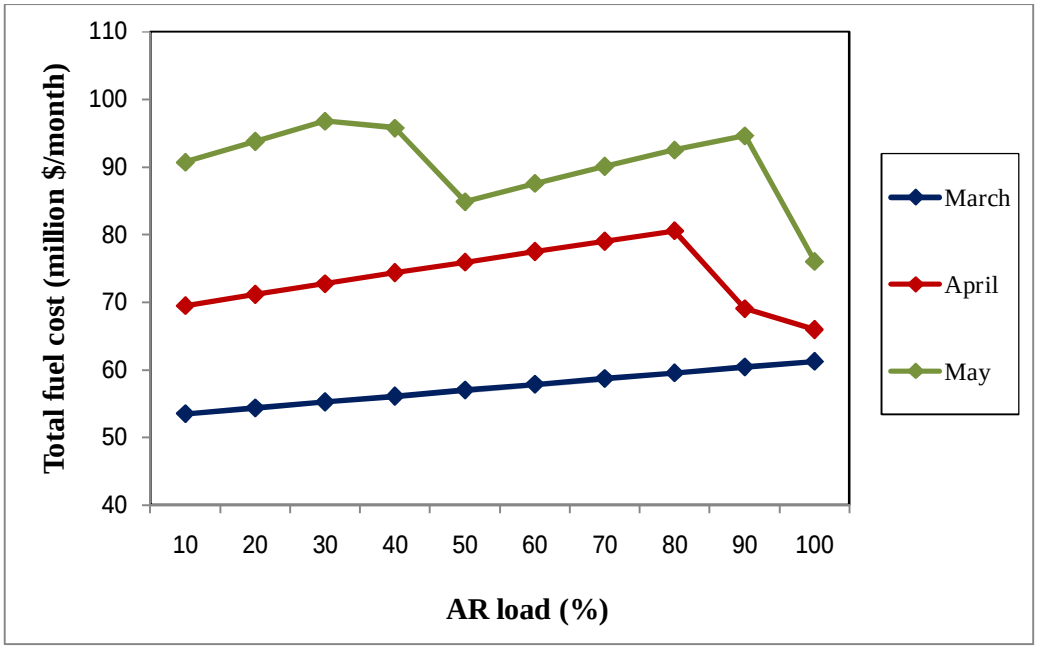

Figure 7.18 Optimum fuel cost of power-MSF-RO-AR hybrid configuration for March, April and May

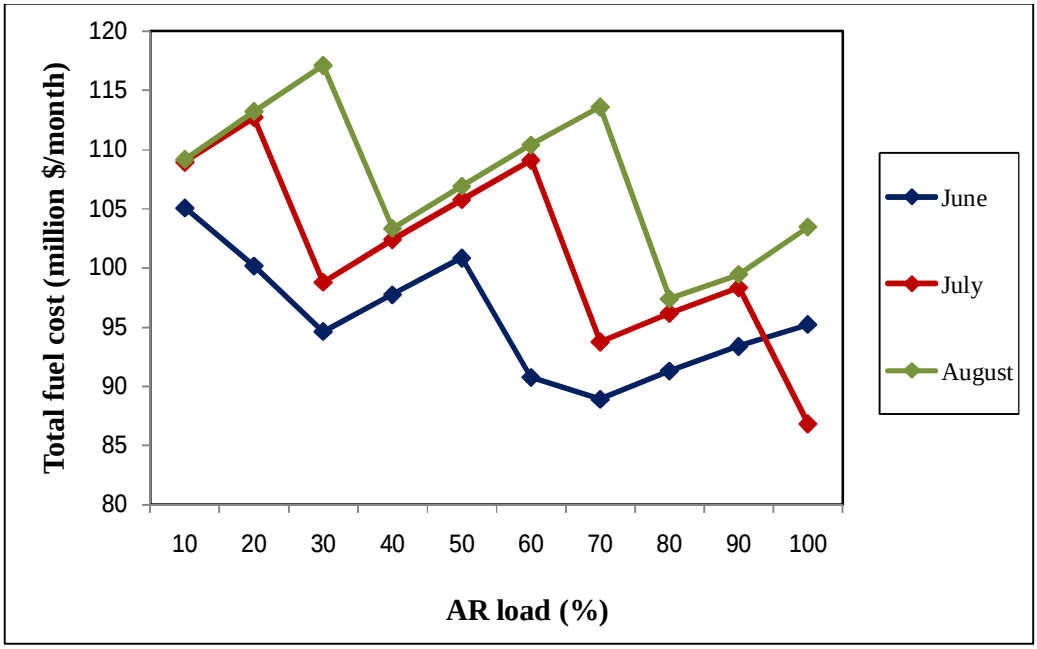

Figure 7.19 Optimum fuel cost of power-MSF-RO-AR hybrid configuration for June, July and August

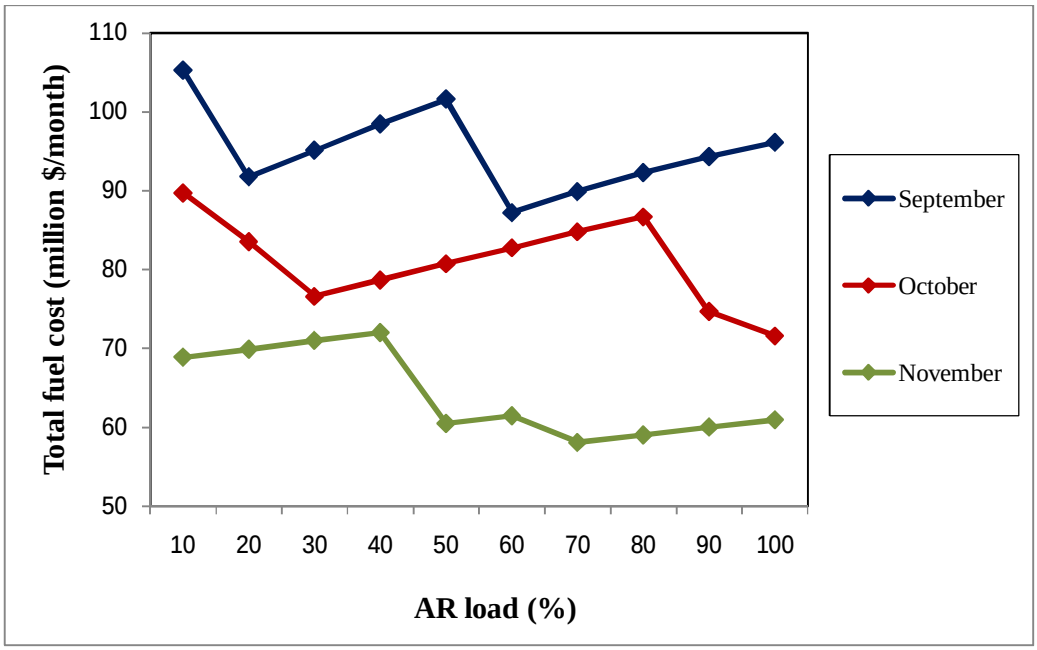

Figure 7.20 Optimum fuel cost of power-MSF-RO-AR hybrid configuration for September, October and November

7.7. Selection of Optimum Hybrid Configuration and Operation Strategy

The results of the suggested hybrid configurations have been presented and discussed in previous sections. The total fuel cost, which includes the cost of oil and natural gas, was used as an indicator of the fuel efficiency of the different plant configurations. The aim of this research work, as stated previously, is to recommend an optimum hybrid powerplant configuration and operation strategy that will satisfy the demand for electricity, freshwater and cooling. The objective is discussed in this section using the total fuel cost results.

Table 7.4 summarises the total fuel cost for the developed hybrid configurations and compares it with the fuel cost of the DW conventional powerplant. It must be emphasised that the fuel cost results for the hybrid powerplants are the lowest costs obtained from the different system combinations. In Table 7.4 the lowest value for each month is in bold.

The fuel cost during the winter months of January, February and December is estimated for only the conventional, power-RO and power-MSF-RO configurations. The results show that the most efficient powerplant configuration for winter, when there is no A/C load, is the power-RO configuration. The superiority of the power-RO configuration over the other 2 is due to the low energy consumption of the RO desalination process per unit output compared with the existing MSF desalination. The lack of A/C load during winter means that only 3 turbines are needed to satisfy demand during winter.

The results in Table 7.4 show that the power-RO-AR hybrid configuration results in the most viable for Kuwait. The power-RO-AR hybrid configuration has the lowest total fuel cost except for July, during which its fuel cost is equal to that of the power-MSF-RO-AR configuration. There are two possible justifications for the efficient performance of the power-RO-AR configuration over others. The first reason is the lower steam consumption per unit output of AR chillers compared to

MSF desalination units. This leads to lower fuel cost when there is a need for auxiliary boilers. The second reason is the lower number of turbines as a result of switching the desalination load from electrical to thermal, and the full use of available electricity by RO desalination units when the turbines are operating at full capacity of 300 MW per turbine.

Table 7.5 gives the recommended hybrid powerplant configuration for each month of the year and the corresponding operation strategy. The power-RO-AR hybrid mode is selected for 9 months (i.e. all summer months) of the year. However, the AR chiller load and the number of turbines vary for different months. In July, however, the power-MSF-RO-AR configuration is not recommended along with the power-RO-AR powerplant because it requires the installation of 436 AR units which is more than double the number of units for the power-RO-AR configuration of 175. During the winter months, on the other hand, the power-RO operation strategy is selected because of its superior performance compared with other hybrid configurations. The lack of A/C load during winter time helps fully use the electricity generated by the 3 on-line turbines.

The fuel cost savings when switching to the suggested hybrid powerplant configurations are given in Table 7.6. The savings are estimated by subtracting the fuel cost of the hybrid configurations from the fuel cost of the conventional DW powerplant. The total fuel cost savings for the whole year is about $363 million, which is divided as $328 million for heavy oil and $35 million for natural gas. This amounts to savings of about ***8 million barrels*** of oil and ***114 million m^3*** of natural gas per year.

Table 7.4 Summary of total fuel cost for conventional plant & hybrid configurations ($ millions)

Month	conventional	P-RO	P-MSF-RO	P-MSF-AR	P-RO-AR	P-MSF-RO-AR
January	72	***47***	50	N/A	N/A	N/A
February	67	***44***	46	N/A	N/A	N/A
March	77	62	50	81	***48***	54
April	90	74	64	96	***59***	66
May	106	76	83	109	***74***	76
June	115	89	96	113	***81***	89
July	114	107	99	118	***87***	***87***
August	119	107	116	122	***96***	97
September	111	89	96	109	***79***	87
October	101	76	83	97	***65***	72
November	90	59	64	85	***52***	58
December	79	***45***	48	N/A	N/A	N/A

Table 7.5 Operation parameters & strategy of recommended optimum hybrid configurations

Month	Configuration	AR load %	RO load %	NT	RO units	AR units	Fuel cost million $	CO_2 ktonne
January	P-RO	0	100	3	4	0	47	495
February	P-RO	0	100	3	4	0	44	463
March	P-RO-AR	60	100	3	4	62	48	513
April	P-RO-AR	100	100	3	4	196	59	630
May	P-RO-AR	50	100	4	4	178	74	791
June	P-RO-AR	40	100	5	4	158	81	826
July	P-RO-AR	40	100	5	4	175	87	924
August	P-RO-AR	20	100	6	4	94	96	1013
September	P-RO-AR	30	100	5	4	125	79	837
October	P-RO-AR	40	100	4	4	101	65	692
November	P-RO-AR	100	100	3	4	125	52	548
December	P-RO	0	100	3	4	0	45	479

Table 7.6 Monthly fuel cost savings for suggested plant configurations in million $

Month	Configuration	Fuel cost savings
January	P-RO	25
February	P-RO	23
March	P-RO-AR	29
April	P-RO-AR	31
May	P-RO-AR	32
June	P-RO-AR	34
July	P-RO-AR	27
August	P-RO-AR	23
September	P-RO-AR	32
October	P-RO-AR	36
November	P-RO-AR	38
December	P-RO	34
Total		***363***

7.8. Economic Analysis of New Systems

In order to justify the investment in the new processes and integrate them to existing cogeneration powerplants in Kuwait, the cost of these systems is estimated in this section. The cost analysis will help in knowing the payback period and whether the savings in fuel cost cover the investment cost. The costs of the RO desalination plant and AR chillers are calculated and analysed in this section.

7.8.1. RO Desalination Costs

The cost of the RO plant in this work is based on the cost of the RO pilot plant at KISR discussed in Chapter 4. The reason for choosing to base the economic evaluation on this RO plant is because the electric consumption of RO plants in this research is based on that plant and for the extensive experience at KISR in RO research for over 15 years. The different costs published in Ebrahim et al. (1999)

using data collected from KISR's RO pilot plant are based on the following assumptions:

- Single-stage RO system using beachwell intake.
- Plant capacity of 27,300 m^3/day.
- Spiral-wound memberanes
- Continuous plant operation.
- 90% plant availability.
- Electricity prices at US$0.062 per kWh.

Table 7.7 Lists the capital and operating cost components used in the study by Ebrahim et al. (1999). The cost break-down for the RO plant is given in Table 7.8 in Kuwaiti Dinars (KD) as it was published by Ebrahim et al. (1999). The capital cost is divided into two categories, building and construction (A) and RO unit cost (B). Category A is applied once only. However, the RO unit category (B) is multiplied by the RO plant capacity, then by the number of RO units to be installed at the site. The capacity of the RO plant, as stated previously, is 110,000 m^3/d.

The total cost of A in Table 7.8 is:

$$C_{build,total} = \left(C_{build,unit}\right) \times \left(Capacity_{RO}\right) \quad (7.1)$$
$$= (127) \times (110{,}000) = \$13.97\ million$$

The total cost of a single RO system investment is:

$$C_{ROplant} = \left(C_{RO,unit}\right) \times \left(Capacity_{RO}\right) \quad (7.2)$$
$$= (693.31) \times (110{,}000) = \$76.26\ million$$

The cost of purchasing 5 RO desalination units is $\$381.3\ million$

Therefore, the total capital cost of site preparation and installation of 5 RO units desalination with a capacity of 110,000 m^3/d each is:

$$\$13.97\ million + \$381.3\ million = \mathbf{\$395.27\ million}$$

For the operating cost, on the other hand, the "Energy" category in Table 7.8 is not considered in the calculations since the electricity consumption of the hybrid plants is considered in Section 7.7. Hence, the cost of RO units operating in Kuwait is US$0.127 per m^3.

The annual total operating cost is:

$$C_{op} = (0.127) \times (110{,}000) \times (5) = \mathbf{\$69,850}$$

Table 7.7 Capital and operating cost components for a seawater RO plant

Capital cost components	Operating cost components
- Site development, buildings and offices	- Energy
- Power supply, instruments and control	- Chemicals
- Pipelines and transfer pumps	- Filter cartridges
- Seawater intake structure	- Other consumables
- Pretreatment system	- Labour
- RO unit and membranes	- Maintenance
- Brine discharge facilities	
- Product water treatment and storage	

Table 7.8 Cost of a single RO desalination plant in Kuwait

Items	Cost (KD per m^3/d)	Cost (US$ per m^3/d)
Capital cost:		
A. Building, Furnishings, A/C	37.074	127.00
B. RO unit (membranes & machinery)	202.425	693.31
Operating cost:		
Labour	0.017	0.058
Chemicals	0.011	0.038
Energy	0.095	0.325
Spare parts & maintenance	0.009	0.031
Total operating cost	***0.132***	***0.452***

1 KD = US$ 3.425

7.8.2. AR Chillers Costs

The total capital cost of an AR plant comprises the following main costs:

- Cost of AR chiller unit
- Cost of pumps
- Cost of cooling tower
- Operation & maintenance costs

The cost of the AR chiller plants published in specialised literature is used since it is not available in Kuwait for the lack of AR chiller manufacturers and distributors. The cost data presented by Tri-State, the Generation and Transmission Association Incorporation, are given in Table 7.9. The table shows the total installation cost of a steam-fired double-effect AR chiller (including pumps and cooling tower & piping) for different refrigeration capacities and annual maintenance cost for each of these capacities. The chiller size of interest for this research is of the 1000 RT capacity. It can be seen that it has the lowest installation and maintenance costs of 605 $/RT and 22.6 $/RT, respectively. Capacities of the chiller are at Air-conditioning and Refrigeration Institute (ARI) standard conditions.

The cost data presented in Table 7.9 can be verified by comparing it with other published cost data for AR chillers. Table 7.10 shows the cost chillers from data gathered in 2006 by the U.S. Department of Energy (DOE). The data in the table are for a direct-fired double-effect AR chiller. It can be seen from Table 7.10 that the installation and maintenance costs are comparable with those listed in Table 7.9 for the 1000 RT double-effect chiller. Therefore, the above mentioned costs in Table 7.9 are used for the economic analysis in this research work.

The capital and maintenance cost calculations of the AR chiller plant should be based on the maximum number of AR chillers estimated for the hybrid plant configuration. Results in Table 7.5 show that the AR chiller load is at 100% during

April and July. However, the power-MSF-RO-AR configuration is not selected because it requires a large number of AR chillers compared with the power-RO-AR configuration for the same month, which is not feasible from an economic point of view. Therefore, the 196 chillers (N_{AR}) in April are selected as the maximum number to be installed for the new hybrid configuration. The refrigeration capacity of the reference AR chiller, as mentioned in Chapter 5, is 1165 tons. The capital cost calculations of the AR plant is:

$$C_{AR,capital} = (Capacity_{AR}) \times \left(C_{capital,unit}\right) \times (N_{AR}) \quad (7.3)$$
$$= (1165) \times (605) \times (196) = \$\mathbf{138.15}\ \boldsymbol{million}$$

The annual maintenance cost of the AR plant is:

$$C_{AR,mant} = (Capacity_{AR}) \times \left(C_{mant,unit}\right) \times (N_{AR}) \quad (7.4)$$
$$= (1165) \times (22.6) \times (196) = \$\mathbf{5.16}\ \boldsymbol{million}$$

Table 7.9 Cost of steam-fired- double-effect absorption chillers (Tri-State, 2009)

Chiller capacity RT	Installation cost $/RT	Maintenance cost $/RT
200	957	38.6
300	847	33.6
400	777	28.7
500	722	25.4
600	691	25.4
700	666	24.3
800	642	23.7
900	623	23.2
1000	605	22.6

Table 7.10 Cost of direct-fired double-effect absorption chillers cost (DOE, 2009)

Chiller capacity RT	Installation cost $/RT	Maintenance cost $/RT
300	625	
500	625	18-31
1000	625	

7.8.3. Payback Period

To prove that the recommended hybrid powerplant configuration is economically viable, the payback period is estimated using the capital costs of additional processes to be installed at DW powerplant. The payback period is defined as the length of time needed before the initial investment is recouped. This method is sufficient for this research work since the aim is to study the viability of one recommended scenario. Other more complex financing methods can be used when multiple project alternatives need to be compared. The following correlation is used to calculate the payback period for installing RO desalination units and AR chillers at the DW powerplant (DEED, 1999):

$$\sum_{t=1}^{y} \frac{(FS - C_{mant})}{(1+d)^t} \geq C_{capital} \tag{7.5}$$

The following assumptions have been made to complete the calculations:

- Maximum 5 year study period for investment payback
- The same annual operating costs for every year
- The same fuel savings every year
- Energy cost is not included
- 5.75% discount rate (d) (CBK, 2008)

Results of the payback period calculations are shown in Table 7.11. The net savings is the parameter used to determine the payback period of the investment, which is the difference between the cumulative savings and the capital investment. The results show that the invested capital in RO desalination and AR chiller plants is recouped in the second year of commissioning. This is a very good return period for such an investment and emphasises the benefit of hybridising existing cogeneration powerplants in Kuwait.

Table 7.11 Payback period and costs of new processes in million $

Year	Annual O&M costs	Fuel savings	Cumulative savings	Capital cost	Net savings
1	5.23	363	339	533	-194
2	5.23	363	660	533	127
3	5.23	363	963	533	430
4	5.23	363	1250	533	717
5	5.23	363	1520	533	988

7.9. Conclusions

The results of the mathematical models developed in Chapter 6 for the hybrid powerplant configurations were presented in this chapter. Specifically, the total fuel cost was presented as the performance indicator for the different configurations and the selection of an appropriate operation strategy. First the results of the DW conventional plant, which was modelled also, were presented and used as a bench mark to compare the performance of other models against. The input data for the models were for the year 2001. The DW powerplant was studied as a single-purpose (single output) plant with the power-RO configuration. The power-RO configuration showed significant savings in fuel cost over the conventional DW plant.

The analysis and comparison of all developed powerplant configurations showed that the most fuel efficient operation strategy is the power-RO-AR hybrid mode for all summer months. During winter, it was recommended to operate the powerplant in power-RO single-output mode. The total yearly fuel cost savings for the new developed configurations are approximately $363 million, with 90% of the cost attributed to heavy oil. The savings in oil are about 8 million barrels, and 114 million m^3 of natural gas per year. The payback period for the installation of RO desalination and AR chiller systems at the DW powerplant is only one year. The capital and annual operating costs were considered in the calculations excluding the energy costs since they have been calculated separately.

Chapter 8

8. Conclusions and Recommendations for Future Work

8.1. Conclusions

Kuwait has been investing heavily in the commissioning of capital-intensive cogeneration powerplants to keep-up with the growing demand for electricity and freshwater during the past 30 years, which has been averaging around 7% each annually. However, the available electric capacity could not cope with the ever increasing demand and the country experienced power shortages in 2006 in most residential areas (Sebzali, 2007). It was shown that the continuous building of new cogeneration plants and increase in consumption is due to rapid population increase, urbanisation and development of new cities, generous electricity and water subsidies and most importantly A/C consumption during 7–9 months of the year. These powerplants are burning oil and natural gas to produce the required power and freshwater. Kuwait's reserves of oil and natural gas, which represent the main source of the national revenue, are limited. Therefore, it is in Kuwait's interest to find a solution or a strategy to conserve its oil resources and to slow down the rate of commissioning of new expensive cogeneration powerplants. Another added benefit is the reduction in CO_2 emissions to the environment.

The concept of hybrid powerplants has been the topic of various recent research papers written by experts and organisations interested in the power sector in the Gulf region. The basic idea of a hybrid powerplant is to integrate several processes that utilise thermal energy or electricity within the powerplant to satisfy the demands for electricity, water and in some cases cooling or heating simultaneously (See Section 6.1). One of the scenarios is to incorporate efficient processes to existing cogeneration plants to improve its flexibility and efficiency in satisfying the demand

for electricity and water. The most popular and efficient seawater desalination process is the RO system, which is being installed at many powerplants around the region (See Section 5.2). Another suggested configuration is to use the steam extracted from the steam turbines at powerplants to operate AR chillers to satisfy the cooling demand instead of VC A/C systems, and use excess electricity to run the efficient RO desalination. Hence, these different systems were investigated and studied in this thesis. In addition, the heat-based process such as the steam Rankine cycle, MSF desalination and ARSs were modelled and simulated to estimate the amount of steam required for each of them.

The steam Rankine cycle was modelled, simulated and analysed in Chapter 3. The mathematical model is based on the regenerative cycle with reheat, which is the working cycle of steam powerplants in Kuwait. First the thermodynamic properties of steam and water were estimated using correlations published in literature and then verified. The comparison between properties estimated using the developed code and those published in literature (See Section 3.5) showed that the modelled thermodynamic properties are accurate within ± 5%.

A steam powerplant operating in Kuwait was simulated to analyse its performance (Section 3.6). The accuracy of the model was estimated using actual data from that reference powerplant without steam extraction to multi-stage flash (MSF) desalination units. The percentage difference between the actual data and model outputs were around 0.35%, which is fairly accurate considering the number of assumptions made in modelling the powerplant.

The MSF is the only seawater desalination process used in Kuwait to produce freshwater and it is the most popular desalination process around the world. To complete the analysis of Kuwait cogeneration (i.e. dual-purpose) powerplants, the MSF was modelled and simulated (Chapter 4). A simplified MSF mathematical model was utilised as an acceptable compromise between computing time and accuracy. The model was validated using actual data from the DW MSF plant in

Kuwait and output from a commercial software for the same desalination plant. A comparison between actual performance parameters and those from the model developed in this study showed that the percentage difference was between 0.21% and 7.95%. These values are deemed acceptable for this research work. Furthermore, the energy consumption of the DW MSF plant, as a reference plant, was estimated to be used as an input to the main program simulating the DW cogeneration plant and the developed hybrid configurations.

The seawater reverse osmosis (RO) desalination process has gained popularity in the past few years because of its efficiency compared to the energy-intensive MSF process. The RO process uses electrical input to drive the high pressure pumps as its source of energy to produce freshwater (Section 4.2). The electric energy consumption of a reference RO pilot plant at Kuwait Institute for Scientific Research (KISR) was estimated at 5.49 kWh/m^3. This value is comparable with published energy consumption figures for seawater RO plants in literature.

During the seven to nine hot summer months, residential, commercial and governmental buildings in Kuwait use the vapour compression (VC) cycle-based A/C systems to keep thermal comfort within these buildings. The so called package and split-units are mostly used in villas and apartment buildings, while large capacity chilled-water systems are used in commercial and governmental buildings. An average coefficient of performance (COP) of about 2.01 was estimated for these different A/C systems using available published data. This value was used to calculate the monthly A/C load at DW powerplant. It was assumed that there is no A/C cooling load during the months of January, February and December.

Absorption refrigeration systems (ARSs) are gaining popularity, as a replacement for VC A/C systems, in district cooling schemes where there is an available source of steam or hot water as an input to produce the required cooling. The double-effect water-LiBr AR chiller was selected for modelling and simulation due to its improved efficiency, ability to utilise higher temperature steam, popularity in A/C

applications (see Section 5.2). The developed model is based on steady-state energy and mass balance equations combined with formulations of thermodynamic properties of the working fluid-pair. The main objective of the model was to estimate the energy input in the form of steam to the AR chillers. The model was fairly accurate when compared with a similar published model for a double-effect chiller. Finally, to simulate a real AR plant, the Trane Horizon AR chiller series was selected as a reference model, and then simulated to estimate the steam required per AR chiller to produce the cooling effect.

With the thermal processes involved (i.e. steam Rankine cycle, MSF desalination and ARSs) modelled, and the electric energy consumption of VC A/C systems and RO desalination estimated, hybrid powerplant configurations can be developed and analysed by integrating the Matlab programs.. The basic configuration used as the basis of any hybrid configuration is the Rankine-cycle based DW cogeneration powerplant currently operating in Kuwait. One configuration that is not under the "hybrid" category is the single-purpose power-RO plant, which generates electricity only to satisfy the demand for power and freshwater via the electrically-driven RO desalination system. The hybrid powerplant configurations selected for analysis in this research include (Section 6.1):

a. Power-MSF-RO
b. Power-MSF-AR
c. Power-RO-AR
d. Power-MSF-RO-AR

The rationale behind selecting these hybrid configurations is to include all possible electrical and thermal combinations to satisfy the demand for electricity, freshwater and cooling, and study their monthly effects on fuel consumption and CO_2 emissions. Configurations b, c and d are applied for summer months only since there is no cooling load during the winter months, which means AR chillers will not be needed.

Each developed configuration was simulated for every month of the year to satisfy the various demands, assumptions and constraints (Sections 6.2 & 6.3). For the different hybrid configurations, the RO load was varied from 5% to 95% and AR chiller load from 10% to 100% and the powerplants were simulated at these different combination. Performance comparisons for the different simulated hybrid configurations were based primarily on total fuel cost, which comprises of the cost of heavy oil and natural gas consumed at the powerplant. It was decided by the author that fuel cost is a more significant factor in the final selection of the optimum hybrid configuration for Kuwait than CO_2 emissions because cost as an indicator is easily understood by readers of all levels and backgrounds, and can be related to the number of barrels of oil saved which is important for an oil producing country like Kuwait.

The following powerplant configurations were simulated to estimate the fuel cost during the winter months of January, February and December:

- Cogeneration
- Power-RO
- Power-MSF-RO

The results of winter simulations show that the power-RO operation strategy is the most efficient with the minimum fuel cost (Table 7.4). During these months, the powerplant requires only 3 turbines to satisfy the demand for both electricity and freshwater, in spite of operating the electrically-driven RO desalination process. The power-MSF-RO configuration comes second. This means that the current operation strategy of cogeneration powerplants in Kuwait is inefficient and it is costing the country millions of Dollars in oil revenues.

On the other hand, the power-RO-AR hybrid operation strategy is the most efficient during all summer months from March to November. During July, however,

simulations of the power-RO-AR and power-MSF-RO-AR hybrid configurations result in equal fuel cost. However, the power-MSF-RO-AR configuration is not recommended because it requires more than double the number of AR units required for power-RO-AR configuration. There are two possible justifications for the efficient performance of the power-RO-AR configuration over others. The first reason is the lower steam consumption per unit output of AR chillers compared to MSF desalination units. This leads to lower fuel cost when there is a need for auxiliary boilers. The second reason is the lower number of turbines as a result of switching the A/C load from electrical to thermal, and the full use of available electricity by RO desalination units when the turbines are operating at full capacity of 300 MW per turbine.

The fuel cost savings resulting from switching to the power-RO configuration during winter and power-RO-AR configuration during summer are estimated by subtracting the fuel cost of the new configuration from the fuel cost of the conventional DW powerplant. The total fuel cost savings for the whole year is about $363 million, which is divided as $328 million for heavy oil and $35 million for natural gas. This amounts to savings of about 8 million barrels of oil and 114 million m^3 of natural gas per year.

The cost analysis of adding RO desalination and AR systems to the powerplant show that the total capital cost is around $533 million and the annual operating and maintenance cost for both processes is $5.23 million. The calculated payback period of invested capital in the new processes is only one year, where the net savings in the second year of operation is around $127 million. This shows that the hybridisation of existing cogeneration powerplants in Kuwait is economically viable and logical.

However, the research did not study the cost of chilled-water distribution and district cooling scheme for the recommended powerplant configurations. The high cost of commissioning a new district cooling scheme due to piping and infrastructure work

would increase the total cost of powerplant configurations that include AR systems as a cooling production option. Therefore, the inclusion of district cooling cost to the economic analysis of adding new systems might have lead to a different result in regard to the recommended operation strategy for the summer season, and that conventional powerplants might be a preferred option from an economic point of view.

8.2. Recommendations for Future Work

The research work presented in this thesis can be improved further by focusing on other efficient technologies and processes, and improving the details and analysis of plant demand profiles. Hence, future work can include the following:

- Implementation of hybrid powerplant configurations that include RO desalination and AR systems.
- Studying and analysing the technical and economic feasibility of chilled-water distribution network to the powerplant configurations that comprise AR systems.
- The analysis and optimisation of daily and hourly operation of the powerplant. One example is the production of freshwater by RO desalination during non-peak hours during the summer months when A/C load is at a minimum.
- Consideration of operating the stand-by (back-up) gas turbines installed at Kuwait's powerplants in a combined cycle with high temperature steam generators (HTSG) and steam turbines.
- Modelling and simulation of RO desalination to be able to study the effects of performance improvements on its energy consumption.
- Analysis of the effects of integration of MSF and RO desalination by using the cooling seawater reject leaving heat-rejection section of MSF as feed to RO desalination.
- Including other desalination technologies that are gaining ground commercially such as low temperature multi-effect boiling (LT-MEB) and mechanical vapour compression (MVC).

- Investigating the possibility of adding water storage systems such as water towers or aquifers.
- Studying the effects of implementing hybrid power generation on the release of other gases to the atmosphere such as Nitrogen oxides (NOx) and Sulphur dioxide (SO_2).

References

Abou Rayan, M. and Khaled, I. (2002). Seawater desalination by reverse osmosis (case study). *Desalination*, 153, 245-251.

Agaschichev, S.P. and El-Nashar, A.M. (2005). Systemic approach for techno-economic evaluation of triple hybrid (RO, MSF and power generation) scheme including accounting of CO_2 emission. *Energy*, 30, 1283-1303.

Al-Fuzai, M. (2007). No electricity in oil-rich Kuwait. *Kuwait Times*, May 23rd, 2007.

Al-Hawaj, O.M. and Al-Mutairi, H. (2007). A combined power cycle with absorption air conditioning. *Energy*, 32, 971-982.

Ali, E., Alhumaizi, K. and Ajbar, A. (1999). Model reduction and robust control of multi-stage flash (MSF) desalination plants. *Desalination*, 121( ), 65-85.

Al-Katheeri, E. And Agaschichev, S.P. (2008). Feasibility of the concept of hybridization of existing co-generative plant with reserve osmosis and aquifer storage. *Desalination*, 222, 87-95.

Al-Mutaz, I. S. (1996). A comparative study of RO and MSF desalination plants. *Desalination*, 106(1-3), 99-106.

Al-Sahlawi, M. A. (1999). Seawater desalination in Saudi Arabia: economic review and demand projections. *Desalination*, 123, 143-147.

Al-Shayji, Khawla. (1998). *Modelling, simulation and optimization of large-scale commercial desalination plants*. PhD Thesis. Virginia Polytechnic Institute and State University, Blacksburg, Virginia, USA.

Al-Sofi, M.AK., Hassan, A.M. and El-Sayed, E.F. (1992). Integrated and non-integrated power/MSF/SWRO plants. *Desalination & Water Reuse*, 2.

Amjad, Z. (1993). *Reverse Osmosis: membrane technology, water chemistry, and industrial applications.* Van Nostrand Reinhold, New York, USA.

Anand, D. K., Allen, R. W. And Kumar, B. (1982). Transient simulation of absorption machines. *Journal of Solar Energy Engineering*, 104(8), 197-203.

Argiriou, A. A., Balaras, C. A., Koontoyiannidis, S. And Michel, E. (2005). Numerical simulation and performance assessment of a low capacity solar assisted absorption heat pump coupled with sub-floor system. *Solar Energy*, 79(3), 290-301.

Arun, M.B., Maiya, M.P. and Murthy, S.S. (2001). Performance comparison of couble-effect parallel-flow and series flow water-lithium bromide absorption systems. *Applied Thermal Engineering*, 21, 1273-1279.

ASHRAE. (2001). *ASHRAE handbook – Fundumentals*, Chapter 1, Atlanta, GA, USA.

ASHRAE. (1998). *ASHRAE handbook – refrigeration (SI edition)*, Chapter 41, Atlanta, GA, USA.

Assilzadeh, F., Kalogirou, S. A., Ali, Y and Sopian, K. (2005). Simulation and optimization of a LiBr solar absorption cooling system with evacuated tube collectors. *Renewable Energy*, 30(8), 1143-1159.

Avlonitis, S.A., Kouroumbas, N. and Vlachakis, N. (2003). Energy consumption and membrane replacement cost for seawater RO desalination plants. *Desalination*, 157, 151-158.

Awerbuch, L. (1997). Power-desalination and the importance of hybrid ideas. *International Desalination Association World Congress*, Madrid, Spain.

Badr, O. (2001). *Refrigeration & air conditioning lecture notes*. Applied Energy MSc Course, School of Engineering, Cranfield University, UK.

Badr, O., Probert, D. and O'Callaghan, P. (1990). Rankine cycles for steam power-plants. *Applied Energy*, 36(3), 191-231.

Barba, D., Liuzzo, G. and Tagliaferri, G. (1973). Mathematical model for multiflash desalting plant control. *4th international symposium on fresh water from the sea*, Heidelberg, September 9-14 1973, Vol. 1, 153-168.

Barton, P. I. (2000). *The equation oriented strategy for process flowsheeting*. http://yoric.mit.edu/abacuss2/Lecture1.pdf. (accessed 6th January 2005).

Beamer and Wilde. (1971). The simulation and optimization of a single effect multi-stage flash desalination plant. *Desalination*, 9(3), 259-275.

BEI (British Electricity International). (1991). *Modern power station practice*, 3rd ed. Pergamon Press, UK.

Bogle, I.D.L. and Pantelides, C.C. (1988). Sparse nonlinear systems in chemical process simulation. *In : Simulation and optimisation of large systems, The Institute of Mathematics and its applications conference serie*s, 245-261. Oxford, England.

Bou-Hamad, S., Abdel-Jawad, M., Al-Tabtabaei, M. and Al-Shammari, S. (1998). Comparative performance analysis of two seawater reverse osmosis plants: twin hollow fiber and spiral wound membranes. *Desalination*, 120(1-2), 95-106.

Bourouis, M., Azzaro-Pantal, C., Floquet, P., Pibouleau, P., Duverneuil, P. and Domenech, S. (1995). Steady-state simulation of a multi-stage flash distillation process (MSF) using an equation-oriented approach. *International Desalination Association (IDA) world congress on desalination and water sciences*, Abu Dhabi, UAE, November 18-24 1995, volume IV, 167-184.

BP (British Petroleum). (2009). *BP statistical review of world energy*. (WWW document). http://www.bp.com. (accessed 28 October 2009).

Buros O. K.. (2000). *The ABCs of desalting*. International Desalination Association (IDA) publication. http://www.idadesal.org. (accessed March 2003).

Butz, D. and Stephan, K. (1989). Dynamic behaviour of an absorption heat pump. *International Journal of Refrigeration*, 12(4), 204-212.

Cali, G., Fois, E., Lallai, G. And Mura, G. (2008). Optimal design of a hybrid RO/MSF desalination system in a non-OPEC country. *Desalination*, 228, 114-127.

Cardona, E., Culotta, S. and Piacentino, A. (2003). Energy saving with MSF-RO series desalination plants. *Desalination*, 153(1-3), 167-171.

Casals, X. G. (2006). Solar absorption cooling in Spain: prspective and outcomes from the simulation of recent installations. *Renewable Energy*, 31(9), 1371-1389.

Central Bank of Kuwait (CBK). (2008). *Key economic and monetary indicators*. www.cbk.gov.kw. Accessed January 2009.

Cengel, Y. A. and Boles, M. A. (1994).*Thermodynamics: an engineering approach*, 2nd ed. McGraw-Hill Inc., USA.

Chakraborty, N and Chakraborty, S. (2002). A generalized object-oriented computational method for simulation of power and process cycles. *Journal of power and energy*, 216(A), 155-159.

ChemicaLogic Corporation. (2003). *Thermodynamic and transport propeties of water and steam*. http://www.chemicalogic.com.

Chida, K. (1997). Reverse osmosis plants operation and maintenance experience in the Middle Eastern region. *Desalination*, 110(1-2), 59-64.

Darwish, M.A. (2002). Substitution of MSF desalting plants with absorption water chillers: new district air conditioning in Arabian Gulf countries. *ASHRAE Transactions*, 108, 369-375.

Darwish, M. A. and Abdel-Jawad, M. (1989). Technical aspects of reducing desalting water cost by distillation methods. *Desalination*, 76(1), 305-322.

Darwish, M. A., Abdel-Jawad, M. and Aly, G. S. (1989). Technical and economical comparison between large capacity multi stage flash and reverse osmosis desalting plants. *Desalination*, 72(3), 367-379.

Darwish, M.A., Al-Fahed, S. And Chakroun, W. (2005). A reverse osmosis desalting plant operated by gas turbines. *Desalination*, 173, 13-24.

Darwish, M.A., Al-Najem, N.M. and Lior, N. (2009). Towards sustainable seawater desalting desalting in the Gulf area. *Desaliantion*, 235, 58-87.

Darwish, M.A., AlOtaibi, S. and AlFahad, S. (2008). On the reduction of desalting energy and its cost in Kuwait. *Desalination*, 220, 483-495.

Darwish, M.A., Al-Otaibi, S. and Al Shayji, K. (2007). Suggested modifications of power-desalting plants in Kuwait. *Desalination*, 216, 222-231.

Darwish, M.A., Al Asfour, N. and Al-Najem, N. (2002). Energy consumption in equivalent work by different desalting methods: case study for Kuwait. *Desalination*, 152(1-3), 81-92.

Darwish, M.A. and Darwish, A.M. (2008). Energy and water in Kuwait: A sustainability viewpoint, part II. *Desalination*, 230, 140-152.

DEED (Alaska Department of Education & Early Development). (1999). Life *cycle cost analysis handbook*. 1st edition.

DESWARE, Encyclopedia of Desalination and Water Resources. (2003). *Global production of desalinated water*. http://www.desware.net/desware/desa3.asp. (accessed 16th April 2003).

Dincer, I. and Dost, S. (1996). Energy analysis of an ammonia-water absorption refrigeration system. *Energy Sources*, 18(6), 727-733.

DOE (U.S. Department of Energy). *Distribution energy program, electricity delivery & energy reliability*. http://www.eere.energy.gov/de/equipment_costs.html. (accessed January, 2009).

Ebrahim, S. and Abdel-Jawad, M. (1994). Economics of seawater desalination by reverse osmosis. *Desalination*, 99(1), 39-55.

Ebrahim, S., Abdel-Jawad, M. and El-Sayed, E. (1999). Parametric cost assessment for reverse osmosis technology in Kuwait. *IDA world congress on desalination and water sciences*, San Diego, USA, 1999, volume II, 151-164.

EIA (U.S. Energy Information Administration). (2003). *Country analysis brief on Kuwait*. http://www.eia.doe.gov/emeu/cabs/kuwait.html. (accessed 5 June 2003).

EIA (U.S. Energy Information Administration). (2009). *Country analysis brief on Kuwait*. http://www.eia.doe.gov/emeu/cabs/kuwait/Profile.html. (accessed 28 October 2009).

El-Dessouky, H.T. and Ettouney, H.M. (2002). *Fundamentals of salt water desalination*, Elsevier Science B.V., Amsterdam, The Netherlands.

El-Dessouky, H. T., Ettouney, H. M. and Al-Roumi, Y. (1999). Multi-stage flash desalination: present and future outlook. *Chemical Engineering Journal*, 73(2), 173-190.

El-Dessouky, H. and Bingulac, S. (1996). Solving equations simulating the steady-state behaviour of the multi-stage flash desalination process. *Desalination*, 107( ), 171-193.

El-Dessouky, H.T., Shaban, H.I. and Al-Ramadan, H. (1995). Steady-state analysis of multi-stage flash desalination process. *Desalination*, 103(3), 271-287.

El-Saie, A. M. H., (1993). The MSF desalination process and its prospects for the future. *Desalination*,93(1-3), 43-56.

El-Sayed, Y.M. (2001). Designing desalination systems for higher productivity. *Desalination*, 134, 129-158.

El-Sayed, E., Abdel-Jawad, M., Ebrahim, S. and Al-Saffar, A. (2000). Performance evaluation of two RO membrane configurations in a MSF/RO hybrid system. *Desalination*, 128, 231-245.

El-Wakil, M.M. (1984). *Powerplant technology*, McGraw-Hill, New York, USA.

Emho, L. (2002). District energy efficiency improvement with absorption cooling: the Hungarian experience. *ASHRAE Transactions*, 108(2), 589-594.

Ettouney, H. (2004). Visual basic computer package for thermal and membrane desalination processes. *Desalination*, 165, 393-408.

Ettouney, H. and El-Dessouky, H. (1999). A simulator for thermal desalination processes. *Desalination*, 125, 277-291.

Ettouney, H. M., El-Dessouky, H. T., Faibish, R. S. and Gowin, P. J. (2002). Evaluating the economics of desalination. *Chemical Engineering Progress*, 98(12), 32-40.

EPA, American Environmental Protection Agency. (2005). *The U.S greenhouse gas inventory*. http://www.epa.gov/globalwarming/publications/emmisions.

Euromonitor International. (2003). *Statistics for various countries in the world* (WWW document). http://www.euromonitor.com. (accessed May 2003).

Fathalah, A. (1995). MSF- A mathematical model. *IDA world congress on desalination and water sciences*, Abu Dhabi, UAE, November 18-24 1995, volume IV, 203-226.

Florides, G. A., Kalogirou, S. A., Tassou, S. A. And Wrobel, L. C. (2002). Modelling, simulation and warming impact assessment of a domestic-size absorption solar cooling system. *Applied Thermal Engineering*, 22(12), 1313-1325.

Foy, Evan. (2001). *Development of software for modelling lithium bromide-water absorption refrigeration systems*. MSc thesis. Cranfield University, Cranfield, UK.

Fruehauf, S. F. and Hobgood, J. V. (2002). Dynamic simulation of a steam generation process with co-generation. ISA training and publication services,USA, Vol. 423, 205-218.

Fu, D. G., Poncia, G. And Lu, Z. (2006). Implementation of an object-oriented dynamic modelling library for absorption refrigeration systems. *Applied Thermal Engineering*, 26, 217-225.

Glueckstern, P. (1999). Design and operation of medium- and small-size desalination plants in remote areas. *Desalination*, 122(2-3), 123-140.

Glueck, A. R. and Bradshaw, R. W. (1970). A mathematical model for a multistage flash distillation plant. *3rd international symposium on fresh water from the sea*, Dubrovnik, 95-108.

Gordon, J. M. and Choon Ng, K. (1995). A general thermodynamic model for absorption chillers: theory and experimental. *Heat Recovery systems & CHP*, 15(1), 73-83.

Habib, M. A., Said, S. A. M. and Al-Zaharna, I. (1995). Optimization of reheat pressures in thermal power plants. *Energy*, 20(6), 555-565.

Habib, M. A., Said, S. A. M. and Al-Zaharna, I. (1999). Thermodynamic optimization of reheat regenerative thermal-power plants. *Applied Energy*, 63, 17-34.

Hamoda, M. F., (2001). Desalination and water management in Kuwait. *Desalination*, 138(1-3), 385-393.

Hamoda, M.F., Al-Ghusain, I. and Al-Mutairi, N.Z. (2004). Sand filtration of wastewater for tertiary treatment and water reuse. *Desalination*, 164, 203-211.

Hayakawa, K., Satori, H. and Konishi, K. (1973). Process simulation on multi-stage flash distillation plant. *4th international symposium on fresh water from the sea*, Heidelberg, September 9-14 1973, Vol. 1, 303-312.

Heitmann, H.-G. (1990). *Saline water processing*. VCH Publishers, New York, USA.

Helal, A. M. (1985). *Mathematical modelling and simulation of multistage flash (MSF) desalination plants*. Ph.D Thesis. University of Leeds, Leeds.

Husain, Asghar. (1986). *Chemical process simulation*, Wiley Eastern Limited, India.

Husain, A., Hassan, A., Al-Gobaisi, D., Al-Radif, A., Woldai, A. and Sommariva, C. (1993). Modelling, simulation, optimization and control of multistage flashing (MSF) desalination plants part I: Modelling and simulation. *Desalination*, 92(1-3), 21-41.

Husain, A., Woldai, A., Al-Radif, A., Kesou, A., Borsani, R., Sultan, H. and Deshpandey, P. B. (1994). Modelling and simulation of a multistage flash (MSF) desalination plant. *Desalination*, 97(1-3), 555-586.

International Monetary Fund (IMF). (2009). *International financial statistics yearbook*. Washington D.C.

Jeong, S., Kang, B.H. and Karng, S. W. (1998). Dynamic simulation of an absorption heat pump for recovering low grade waste heat. *Applied Thermal Engineering*, 18(1-2), 1-12.

Johansen, J. (1994). *Optimal design of a CHP/desalination plant*. MSc thesis, Cranfield University, UK.

Johansen, J., Babus'Haq, R. F. and Probert S. D. (1995). An integrated CHP and desalination plant. *Applied Energy*, 53(1-2), 157-178.

Joudi, K. A. And Abdul-Ghafour, Q. J. (2003). Development of design charts for solar cooling systems. Part I: computer simulation for a solar cooling system and development of solar cooling charts. *Energy conversion and management*, 44(2), 313-339.

Kamal, I. and Sims, V. (1995). Thermal cycle and financial modelling for the optimization of dual purpose power-cum-desalination plants. *International Desalination Association*, vol. III, 427-442.

Keenan, J. H., Keyes, F. G., Hill, P. G. And Moore, J. G. (1969). *Steam tables, thermodynamic properties of steam including vapor, liquid and solid phases*. John Wiley & Sons, Inc., New York.

Khan, A. H. (1986). *Desalination processes and multistage flash distillation practice.* Elsevier, New York, USA.

Khawaji, A.D., Kutubkhanah, I.K. and Wie, J-M. (2007). A 13.3 MGD seawater RO desalination plant for Yanbu Industrial City. *Desalination*, 203, 176-188.

KIBS (Kuwait Institute of Banking studies). (2009). *Finance and economy related data on Kuwait and GCC* (WWW document). http://www.kibs.edu.kw. (accessed 27 October 2009).

Kojima, Y. (1998). *Power plants for independent power producers: technical, economic and environmental assessment.* MSc Thesis. Cranfield University, Cranfield, England.

Kuwait Information Office. (2009). *Population profile for Kuwait* (WWW document). http://www.e.gov.kw. (accessed 26 October 2009).

Li, Z. F. and Sumathy, K. (2001). Simulation of a solar absorption air conditioning system. *Energy Conversion and Management*, 42(3), 313-327.

Library of Congress. (2003). *Profile on the state of Kuwait* (WWW document). http://lcweb2.loc.gov. (accessed 5th June 2003).

Lu, S., Swidenbank, E. and Hogg, B. (1995). Power plant analyser – an applied matlab toolbox. *IEE conference on applied control techniques using Matlab*, 26 January 1995, pp. 1-4.

Maheshwari, G.P., Hussain, H.J. and Suri, R.K. 2000. *Advancement of energy conservation standards and practical measures for their implementation in Kuwait.* DOE-1/Element 2/Subelement 2.2.4. KISR, Kuwait.

Marcovecchio, M.G., Mussati, S.F., Aquirre P.A., Nicholas, J. And Scenna. (2005). Optimization of hybrid desalination processes including multi stage flash and reverse osmosis systems. *Desalination*, 182, 111-122.

Methnani, M. (2007). Influence of fuel costs on seawater desalination options. *Desalination*, 205, 332-339.

MEW (The Kuwaiti Ministry of Electricity and Water). (2008a). *Electrical energy statistical year book.* Publication of Ministry of Electricity and Water, Kuwait.

MEW. (2008b). *Water statistical year book.* Publication of Ministry of electricity and Water, Kuwait.

MEW. (2002a). *Electrical energy statistical year book.* Publication of Ministry of Electricity and Water, Kuwait.

MEW. (2002b). *Water statistical year book*. Publication of Ministry of electricity and Water, Kuwait.

Montagna, J. M., Scenna, N. J. and Melli, T. (1991). Some theoretical aspects in simulation of multiple stage desalination systems. *12th international symposium on desalination and water re-use*, 437-448.

Moran, M.J. and Shapiro, H.N. (2004). *Fundamentals of engineering thermodynamics*, 5th ed. John Wiley & Sons, USA.

Patterson, M.R. and Perez-Blanco, H. (1988). Numerical fits of the properties of lithium-bromide water solutions. *ASHRAE Transactions*, 94(2), 2059-2077.

Poluzakis, A.L. (2006). *Technoeconomic evaluation of trigeneration plant: gas turbines performance, absorption cooling and district heating*, Cranfield University, Cranfield, England.

Ramirez, W. F. (1997). *Computational methods for process simulation*, 2nd ed. Butterworth-Heinemann, Oxford.

Rautenback, R. (1993). Progress in distillation. *Desalination*, 93(1-3), 1-3.

Rice, Richard and Do, Doung. (1995). *Applied mathematics and modelling for chemical engineers*. John Wiley & Sons, USA.

Rosen, M.A., Dimitriu, J. And Le, M. (1994). Opportunities for utility-based district cooling in Ontario using absorption chillers. *Thermodynamics and Design, Analysis and improvement of Energy Systems*, ASME, 33, 323-329.

Rosen, M.A. and Le, M.N. (1996). Efficiency analysis of a process design integrating cogeneration and district energy. *ASME-AES*, 36, 473-480.

Sanz, M.A., Bonnelye, V. And Cremer, G. (2007). Fujairah reverse osmosis plant: 2 years of operation. *Desalination*, 203, 91-99.

Schausberger, P., Rheina-Wolbeck, G., Friedl, A., Harasek, M. and Perz, E.W. (2003). Enhancement of an object-oriented powerplant simulator by seawater desalination topics. *Desalination*, 156, 355-360.

Schnakel, H.C. (1958). Formulations for the thermodynamic properties of steam and water. *Transactions of ASME*, 80, 959-966.

Sebzali, M. (2007). *Assessment of cool thermal storage strategies in Kuwait*, Cranfield University, Cranfield, England.

Srikhirin, P., Aphornratana, S. and Chungpaibulpatana, S. (2001). A review of absorption refrigeration technologies. *Renewable and Sustainable Energy Reviews*, 5, 343-372.

Stewart, W., Levien, K. and Morari, M. (1985). Simulation of fractionation by orthogonal collocation. *Chemical engineering and science*, 40(3), 409-421.

Sun, Da-Wen. (1997). Thermodynamic design data and optimum design maps for absorption refrigeration systems. *Applied Thermal engineering*, 17(3), 211-221.

Tang, R. And Rosen, M.A. (1999). Integrated systems for cogeneration and absorption chilling: comparison for varying chiller cops. *ASME-AES*, 39, 661-669.

Tomimori, K., Sakai, M. and Kawasaki, S. (1990). World-class district heating and cooling plant for new Shinjuku area. *Hitachi Review*, 39(3), 129-134.

Trane. (2005). *Trane Horizon Absorption series performance data*. http://www.trane.com. (accessed 2007).

Tri-State. (2009). *Comparison of chiller installation and operating & maintenance costs*. http://tristate.apogee.net/cool. (accessed January, 2009).

Uche, J.,serra, L., Herrero, L., Valero, A., Turegano, J. and Torres, C. (2003). Software for the analysis of water and energy systems. *Desalination*, 156, 367-378.

University of Oklahoma. (2004). *On-line lectures on Rankine cycles*. http://coecs.ou.edu/Feng.Chyuan.Lai/thermoweb. (accessed 20th June 2004).

Van der Bruggen, B. and Vandecasteele, C. (2002). Distillation vs. membrane filtration: overview of process evolutions in seawater desalination. *Desalination*, 143(3), 207-218.

Veolia Water. (2005). *Veolia water reverse osmosis desalination projects*. http://www.veoliawater.com.

Wade, N. M. (1993). Technical and economic evaluation of distillation and reverse osmosis desalination processes. *Desalination*, 93(1-3), 343-363

Wagner, W. *et al*. (2000). The IAPWS industrial formulation 1997 for the thermodynamic properties of water and steam. *Transactions of ASME*, 122, 150-182.

World Fact Book. (2009). *Facts on the State of Kuwait*. (WWW document). https://www.cia.gov/library/publications/the-world-factbook/geos/ku.html. (accessed 26 October 2009).

Xu, G. P., Dai, Y. Q., Tou, K. W. and Tso, C. P. (1996). Theoretical analysis and optimization of a double-effect series-flow-type absorption chiller. *Applied Thermal Engineering*, 16(12), 975-987.

Xu, F., Goswami, D.Y. and Bhagwat, S.S. (2000). A combined power/cooing cycle. *Energy*, 25, 233-246.

Ziegler, F. and Riesch, P. (1993). Absorption cycles. A review with regard to energetic efficincy. *Heat Recovery Systems & CHP*, 13(2), 147-159.

Appendix A

A. MSF Desalination Rigorous Model

A.1. MSF Rigorous Mathematical Model

First the basic mass, salt and energy balance equations for the stages of both recovery and rejection sections are developed with their supporting thermodynamic equations. Then the procedure used to solve the system of nonlinear equations is presented with a brief description of the underlying MATLAB algorithm for solving these equations.

A.1.1. Assumptions

The following assumptions are necessary to develop a mathematical model for a MSF desalination plant which best represents actual plant performance:

- The distillate (i.e. product) leaving any stage is salt free. The salt concentration in the final product is only between 5 and 30 ppm compared with feed concentration of 45,000 ppm.
- Mass of flashed-off distillate as it enters the next stage is negligible.
- No mist entrainment in flashing brine.
- No heat losses to surroundings
- The heats of mixing for brine solutions are negligible.
- No subcooling of condensate in the brine heater (i.e. heat input section).
- Pressure drops and the consequent saturation temperature depression in the condenser can be neglected. This can be justified because the MSF plant operates at vacuum, which causes pressure recovery to momentum change and compensates the friction pressure loss (El-Dessouky *et al.*, 1995).

- Effect of non-condensable gases on heat transfer coefficient and condensation temperature decrease is neglected due o the continuous withdrawal of these gases from the flashing chamber and brine heater.
- Vapour escaping to vents is small and not accounted for in the mass balances.

A.1.2. Brine Heater

Most of the heat required to run the MSF system is thermal energy in the form of low pressure steam fed to the brine heater. The low pressure steam is usually bled from the steam turbine in dual-purpose power plants.

- *Energy balance equation*

$$M_s L_s = M_r C_{P,BH} \left(T_0 - T_{ri}\right)$$

- *Heat transfer equation*

$$M_r C_{P,BH} \left(T_0 - T_{ri}\right) = U_{BH} A_{BH} \left(\frac{T_0 - T_{ri}}{\ln\left({T_s - T_{ri}} \big/ {T_s - T_0} \right)} \right)$$

A.1.3. Stage Model

From a heat and mass balance on an MSF plant with brine recicrculation, six equations can be developed for each stage of the heat recovery or rejection sections. The following equations represent stage number i in the recovery section at steady state:

- *Mass balance*

$$M_{FBi-1} + M_{Di-1} = M_{FBi} + M_{Di}$$

- *Salt balance*

$$M_{FBi-1}S_{FBi-1} = M_{FBi}S_{FBi}$$

- *Energy balance on flashing brine*

$$M_{FBi-1}C_{P,FBi-1}T_{FBi-1} = M_{Vi}L_{Vi} + M_{FBi}C_{P,FBi}T_{FBi}$$

where,

Cp_{FBi} is calculated at S_{FBi} and T_{FBi}; and

L_{Vi} is calculated at T_{Di}

- *Heat transfer equation*

$$M_r C_{P,r}\left(T_{ri-1} - T_{ri}\right) = UA_{HR}\left(\frac{T_{ri-1} - T_{ri}}{\ln\left(T_{vi-1} - T_{ri} \big/ T_{vi-1} - T_{ri-1}\right)}\right)$$

The above equation is rearranged to a simpler form:

$$\left(\frac{T_{ri-1} - T_{ri}}{\ln\left(T_{vi-1} - T_{ri} \big/ T_{vi-1} - T_{ri-1}\right)}\right) = EXP\left(\frac{UA_{HR}}{M_r C_{P,r}}\right)$$

where,

$T_{Vi} = T_{Di} + \Delta T_{mesh}$;

$C_{P,r}$ is calculated at S_r and $\frac{T_{ri-1} + T_{ri}}{2}$;and

U is calculated at T_{Di}

- *Temperature losses in brine pool*

$$T_{FBi} = T_{Di} + BPE + NEA + \Delta T_{mesh}$$

- *Stage overall energy balance*

$$M_{FBi-1}C_{P,FBi-1}T_{FBi-1} + M_{Di-1}C_{P,Di-1}T_{Di-1} = M_{FBi}C_{P,FBi}T_{FBi} + M_{Di}C_{P,Di}T_{Di} + M_r C_{P,r}\left(T_{ri} - T_{ri+1}\right)$$

The mass and salt balance equations are altered for the first stage of the heat recovery section. They can be written as follows:

- *First stage mass balance*

$$M_r = M_{FBi} + M_{Di}$$

- *First stage salt balance*

$$M_r S_r = M_{FBi} S_{FBi}$$

The above equations also apply for the heat rejection section, but there a few changes in notations where applicable. The subscript "HR" will be changed to "HJ" denoting the *heat rejection* section. Also, M_r will be replaced by M_{total}, which comprises the two streams, feed seawater (M_F) and cooling seawater (M_{CW}). The mass balance, salt balance and overall energy balance equations for the last stage can be written as follows:

- *Last stage mass balance*

$$M_{FBi-1}M_{Di-1}M_F = M_r + M_{BD} + M_{FBn} + M_{Dn}$$

Where the subscript *n* denotes the number of the last stage

- *Last stage salt balance*

$$M_{FBi-1}S_{FBi-1} + M_F S_F = S_n\left(M_r + M_{FBn} + M_{BD}\right)$$

- *Last stage overall energy balance*

$$M_{FBi-1}C_{P,FBi-1}T_{FBi-1} + M_{Di-1}C_{P,Di-1}T_{Di-1} + M_F Cp_F T_F = M_{FBn}C_{P,FBn}T_{FBn} + M_{Dn}C_{P,Dn}T_{Dn}$$
$$+ M_{BD}C_{P,BD}T_{FBn} + M_r C_{P,r}T_{FBn} + M_{total}C_{P,total}\left(T_{rn} - T_{sea}\right)$$

A.1.4. Splitters

- *Blow-down splitter*

$M_{BD} = M_{FBn} - M_r$

Equalities

$S_{BD} = S_r = S_{FBn}$

$T_{BD} = T_r = T_{FBn}$

- *Reject seawater splitter*

$M_{CW} = M_{total} - M_F$

Equalities

$S_{CW} = S_F = S_{sea}$

$T_{CW} = T_F = T_{NR+1}$

Where,

NR is the number of the recovery stages

A.1.5. Physical and Thermodynamic Properties

- *Seawater density* (El-Dessouky and Ettouney, 2002)

The following correlation is valid for $0 \le S \ge 160{,}000\,ppm$ and $10 \le T \ge 180°C$. The seawater density (ρ) is in kg/m^3:

$$r = \left(A_1 F_1 + A_2 F_2 + A_3 F_3 + A_4 F_4\right) \times 10^3$$

Where ,

$$\begin{cases} B = \dfrac{\left(\left(2S/1000\right) - 150\right)}{150} \\ G_1 = 0.5 \\ G_2 = B \\ G_3 = 2B^2 - 1 \\ A_1 = 4.032219\ G_1 + 0.115313\ G_2 + 0.000326\ G_3 \\ A_2 = -0.108199\ G_1 + 0.001571\ G_2 - 0.000423\ G_3 \\ A_3 = -0.012247\ G_1 + 0.00174\ G_2 - 9 \times 10^{-6} G_3 \\ A_4 = 0.000692\ G_1 - 8.7 \times 10^{-5} G_2 - 5.3 \times 10^{-5} G_3 \\ A = \dfrac{\left(2T - 200\right)}{160} \\ F_1 = 0.5 \\ F_2 = A \\ F_3 = 2A^2 - 1 \\ F_4 = 4A^3 - 3A \end{cases}$$

- *Pure water specific heat* (Al-Shayji, 1998)

The following correlation is valid for $10 \le T \ge 150°C$:

$$C_{P,w} = 4.2 - 3.66271 \times 10^{-4} T + 3.638 \times 10^{-6} T^2 + 3.3 \times 10^{-8} T^3$$

- *Seawater specific heat* (Al-Shayji, 1998)

The specific heat capacity of seawater is obtained by multiplying the heat capacity of pure water by a factor which depends on brine concentration given in ppm. The heat capacity is in kJ/kg ℃:

$$C_{P,sea} = \left(1 - S \times 10^{-3}\left(0.01094428 - 20.628 \times 10^{-6} T\right)\right) Cp_w$$

- *Latent heat of evaporation* (El-Dessouky and Ettouney, 2002)

The following correlation is used for calculating latent heat of evaporation (L_v) in kJ/kg. It is valid for $5 \le T \ge 200°C$:

$$2501.897149 - 2.407064037T + 0.001192217T^2 - 1.5863 \times 10^{-5} T^3$$

- *Overall heat transfer coefficient* (El-Dessouky *et al.*, 1999)

The following correlation calculates the overall heat transfer coefficient (U) for the brine heat and for heat/condenser tubes in kW/m^2 °C. It is valid for $40 \le T \ge 120°C$ with a standard deviation of 1.76%:

$$U = 1.7194 + 0.003206 3T + 1.5971 \times 10^{-5} T^2 - 1.9918 \times 10^{-7} T^3$$

- *Boiling point elevation* (El-Dessouky and Ettouney, 2002)

The following correlation is valid for $10{,}000 \le S \ge 160{,}000 ppm$ and $10 \le T \ge 180°C$:

$$BPE = AS + BS^2 + CS^3$$

Where

$$A = \left(8.325 \times 10^{-2} + 1.883 \times 10^{-4} T + 4.02 \times 10^{-6} T^2\right)$$
$$B = \left(-7.625 \times 10^{-4} + 9.02 \times 10^{-5} T - 5.2 \times 10^{-7} T^2\right)$$
$$C = \left(1.522 \times 10^{-4} - 3 \times 10^{-6} T - 3 \times 10^{-8} T^2\right)$$

- *Non-equilibrium allowance* (El-dessouky *et al.*, 1995)

$$NEA_{10} = (0.9784)^{T_{FBi}} (15.7378)^{H} \left(1.3777^{V_b \times 10^{-6}}\right)$$

$$NEA = \left(\frac{NEA_{10}}{(0.5\Delta T + NEA_{10})}\right)^{0.3281L} (0.5\Delta T + NEA_{10})$$

Where,

NEA_{10} = non-equilibrium allowance for stage length of 3 meters

NEA = non-equilibrium allowance for any other stage length

H = height of the brine pool in meters. H is higher than the gate height (GH) by 0.1-0.2 m

V_b = flashing brine flowrate per chamber width (kg/m s)

L = chamber length in meters

ΔT = stage temperature drop in °C

- *Temperature loss across demister* (Al-shayji, 1998)

$$\Delta T_d = \exp\left[\left(1.885 - 0.02063 T_{Di}\right)/1.8\right]$$

Where,

T_{Di} = distillate temperature in stage i in °C

- *Gate height* (El-Dessouky *et al.*, 1999)

$$\frac{\left[\left(M_r - \sum_{j=1}^{i-1} M_{Dj}\right)\left(2 r_{FBi} \Delta P_i\right)^{-0.5}\right]}{C_d W}$$

Where,

ΔP_i = pressure difference between stages i and i+1

C_d = gate discharge coefficient, ranging from 0.4-0.6

W = stage width

A.1.6. Solution Procedure of nonlinear equations

A.1.6.1. Brine Heater

As presented above, there are two equations to describe the performance of the brine heater. The two unknown variables are the temperature of the recirculation brine going into the brine heater (T_{r1}) and the recirculation brine mass flowrate (M_r). After defining the input variables, the two equations are solved simultaneously using the

optimization toolbox command *fsolve*. Initial guesses are provided by using the simple MSF model.

A.1.6.2. Heat Recovery section

The flowchart below shows the algorithm used to solve the system of nonlinear equations. There are six equations and six unknowns to be solved in each flashing stage in the recovery section. The 6 unknown variables are:

- Distillate mass flowrate (M_d)
- Vapour temperature (T_v)
- Flashing brine temperature (T)
- Flashing brine mass flowrate (M_{fb})
- Flashing brine salt concentration (S_{fb})
- Recirculation (recycled) brine temperature (T_r)

Input variables for each flashing stage are:

- Recirculation brine temperature from previous stage ($T_{r,i-1}$)
- Recirculation brine mass flowrate (M_r) determined from brine heater model
- Recirculation brine salt concentration (S_r)
- Stage dimensions (width,length,heat transfer area,heigh of brine)
- Stage pressure (P_i)
- The 6 solved variables from previous stage

The *fsolve* command is included in a separate function file and initial guesses required to run it are provided from the simple MSF model. This solution method could be categorised as a hybrid of the modular sequential and global methods. It is modular because it is solving the model in a stage-by-stage model, and the global part involves solving a set of 6 nonlinear equations simultaneously. It is a simple

method in that it does not require mathematical manipulation of the equations to put them in terms of certain output parameters.

The results for the temperatures of the flashing brine, vapour and recirculation streams were close to actual plant data. However, the mass flowrate and salt concentration of the flashing brine stream were fluctuating. In an actual plant, the mass flowrate of the flashing brine should gradually decrease and the salt concentration should be increasing. Figures A2 and A3 show the model result for both parameters.

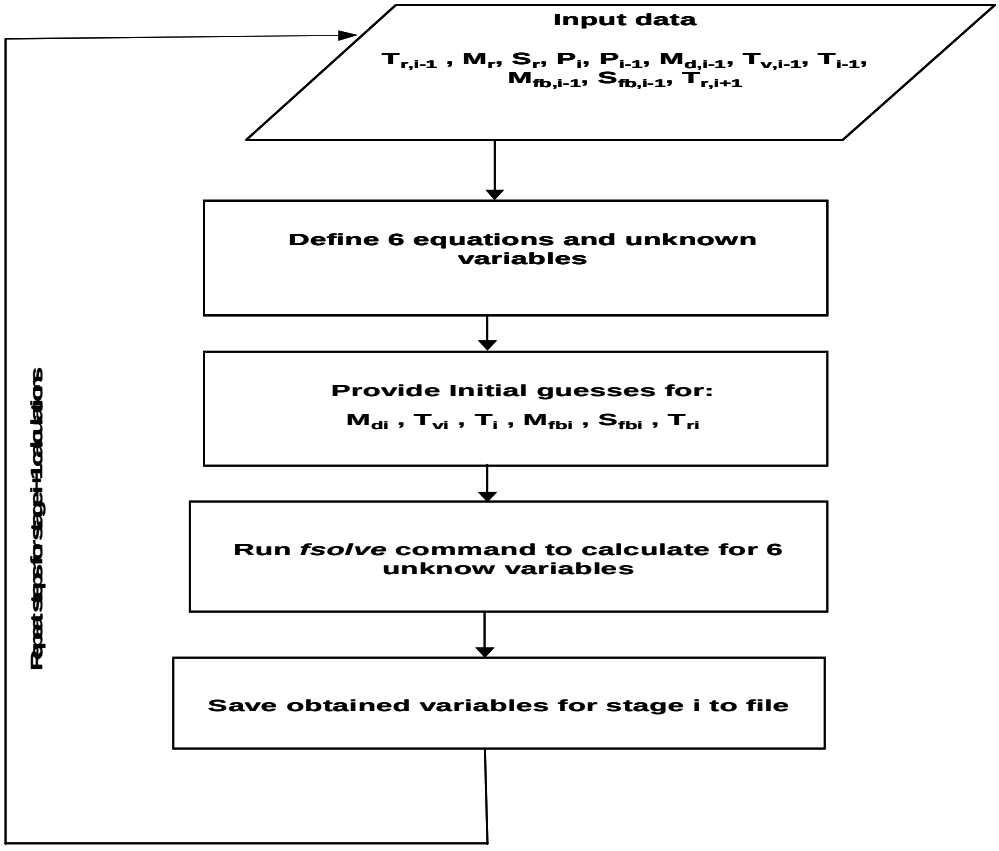

Figure A.1 Solution procedure of heat recovery section

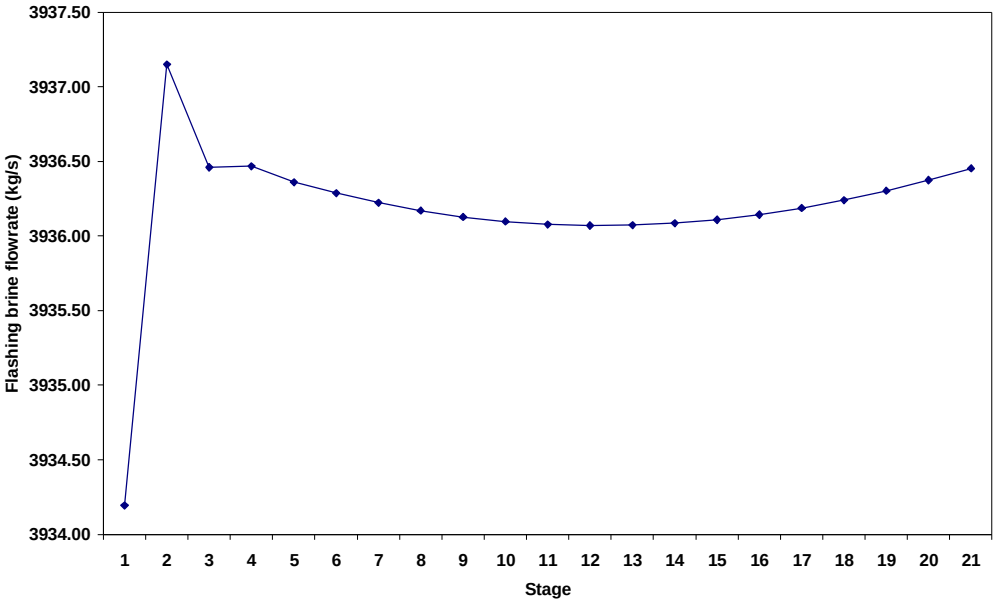

Figure A.2 Flashing brine mass flowrate for heat recovery stages

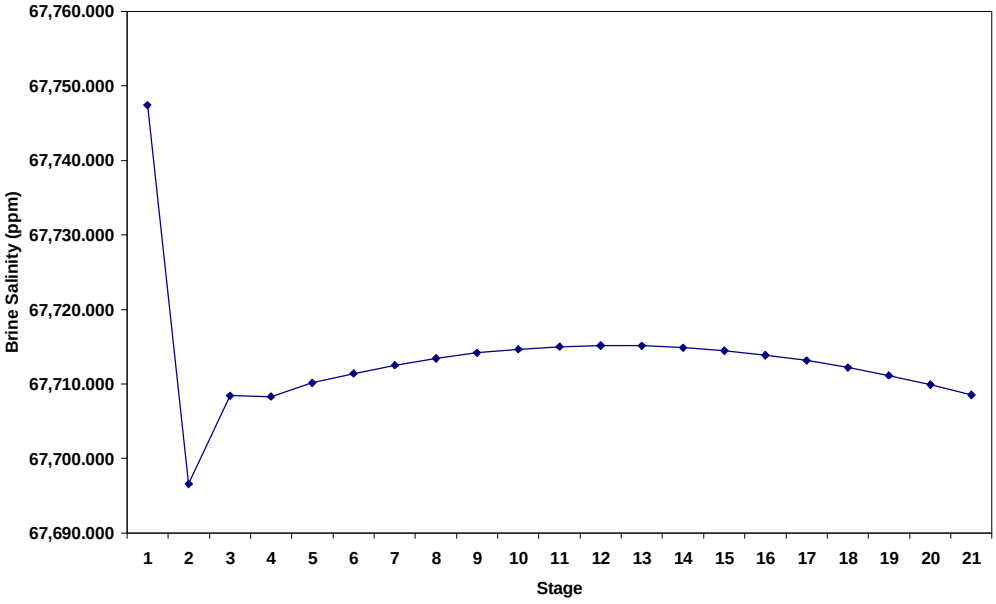

Figure A.3 Flashing brine salt concentration for heat recovery stages

A.1.6.3. Heat Rejection Section

A clear solution strategy for heat rejection section was *not* reached. More thought need to be put to determine what variables to be assumed known and what variables should be solved using the nonlinear model.

A.1.7. Solution Algorithm

MATLAB's *fsolve* function uses different built-in algorithms for solving a set of nonlinear equations, depending on what the user chooses the option to be. The algorithms are divided into two main categories: the large-scale and medium-scale algorithm. Since the number of unknown variables is relatively small in the developed MSF model presented here, the medium-scale algorithm is selected by the author to solve the MSF problem.

There are three methods that can be selected by the user to solve a set of nonlinear equations under the medium-scale algorithm. They are the Gauss-Newton, Trust-region dogleg and Levenberg-Marquardt methods. The trust-region dogleg method is utilised in this work because of its robustness, strong convergence properties. In other words, the trust-region method efficiently converges to the global minimum whereas the pure Newton method may cycle it and converge to a local minimum (Sadjadi and Ponnambalam, 1999). A description of the method is presented below.

A.1.7.1. Trust-region Dogleg Method

The basic idea of the trust-region method is to move from point x in $n$space to a point that results in a lower function value. This means that f is approximated with a simpler function q, which reasonably reflects the behaviour of function f in a neighbourhood N around the point x. The neighbourhood is called the *trust region*. A trial step s is computed by minimising over N. If $f(x+s) < f(x)$, the point is updated to be $x+s$. Otherwise, the current point remains unchanged and N is

shrunk, and the trial step computation is repeated (Mathworks, 2005 & Sadjadi and Ponnambalam, 1999). The trust region problem is mathematically presented as:

$$\min\left\{\frac{1}{2}s^T Hs + s^T g\right\} \text{ , subject to } \|Ds\| \le \Delta$$

where,

- H is the Hessian matrix
- g is the gradient of f at current point x
- D is a diagonal scaling matrix
- $\|.\|$ is the Euclidean norm
- Δ is a positive scalar

A.1.7.2. Nonlinear system of Equations

Solving a nonlinear system of equations $F(x)$ involves finding a solution that every equation in the nonlinear system is equal to zero. Meaning for n equations and n unknowns, $x \in K^n$ has to be found such that $F(x) = 0$ where

$$F(x) = \begin{bmatrix} F_1(x) \\ F_2(x) \\ \mathbb{M} \\ F_n(x) \end{bmatrix}$$

Using the trust-region strategy, a merit function is needed to decide if x_{k+1} is better or worse than x_k:

$$\min_d f(d) = \frac{1}{2}F(x_k + d)^T F(x_k + d)$$

where d is the search direction. From Newton's method, the search direction d_k can be solved such that:

$$J(x_k)d_k = -F(x_k)$$
$$x_{k+1} = x_k + d_k$$

where J is the n-by-n Jacobian matrix

But a minimum of $f(d)$ is not necessarily a root of $F(x)$. But the Newton step d_k is a root of

$$M(x_k + d) = F(x_k) + J(x_k)d$$

And d_k is also a minimum of $m(d)$ where

$$\min_d m(d) = \frac{1}{2}\|M(x_k + d)\|_2^2 = \frac{1}{2}\|F(x_k) + J(x_k)d\|$$
$$= \frac{1}{2}F(x_k)^T F(x_k) + d^T J(x_k)^T F(x_k)$$
$$+ \frac{1}{2}d^T \left(J(x_k)^T J(x_k)\right)d$$

Then $m(d)$ is a better choice of merit function than $f(d)$, and the trust-region subproblem can be formulated as follows:

$$\min_d \left[\frac{1}{2}F(x_k)^T F(x_k) + d^T J(x_k)^T F(x_k) + \frac{1}{2}d^T \left(J(x_k)^T J(x_k)\right)d\right]$$

subject to $\|D \cdot d\| \le \Delta$

A.2. Data from KISR's RO pilot plant

Table A.2.1 Performance data of KISR RO desalination pilot plant

P_{feed} kPa	Q_{feed} m^3/h	$Q_{product}$ m^3/h	P_{brine} kPa	Q_{brine} m^3/h	E_{total} kWh/m^3
4700	35.12	12.24	4700	22.88	4.96
4650	35.29	12.33	4650	22.96	4.90
4700	36.00	12.26	4700	23.74	5.05
4700	35.54	12.42	4700	23.12	4.95
4700	35.32	12.34	4700	22.98	4.95
4700	35.57	12.17	4700	23.40	5.04
4700	35.48	12.28	4700	23.20	4.99
4700	35.34	12.27	4700	23.07	4.98
4700	35.31	12.23	4700	23.08	4.99
4700	35.61	12.24	4700	23.37	5.02
4700	35.37	12.35	4700	23.02	4.96
4750	35.44	12.08	4750	23.36	5.11
4700	35.15	12.32	4700	22.83	4.94
4700	35.50	12.11	4700	23.39	5.05
4725	35.67	12.13	4725	23.54	5.09
4725	35.58	12.20	4725	23.38	5.05
4730	35.66	12.38	4730	23.28	5.01
4725	35.60	12.23	4725	23.37	5.05
4750	35.21	12.01	4750	23.20	5.10
4750	35.58	12.12	4750	23.46	5.11
4750	35.90	12.16	4750	23.74	5.13
4750	35.16	12.19	4750	22.97	5.04
4750	35.61	11.97	4750	23.64	5.16
4750	35.54	12.26	4750	23.28	5.06
4800	35.34	12.20	4800	23.14	5.11
4750	35.67	12.21	4750	23.46	5.09
4770	35.52	12.23	4770	23.29	5.09
4780	35.19	12.21	4780	22.98	5.07
4800	35.29	12.02	4800	23.27	5.16
4700	34.92	12.13	4700	22.79	4.98
4700	35.61	12.01	4700	23.60	5.09
4750	35.94	12.36	4750	23.58	5.07
4800	35.29	12.05	4800	23.24	5.15

Table A.1 Continued

P_{feed} kPa	Q_{feed} m^3/h	$Q_{product}$ m^3/h	P_{brine} kPa	Q_{brine} m^3/h	E_{total} kWh/m^3
4800	35.11	12.04	4800	23.07	5.13
4800	35.74	12.10	4800	23.64	5.19
4800	35.70	12.03	4800	23.67	5.21
4800	35.19	12.37	4800	22.82	5.03
4750	35.44	12.12	4750	23.32	5.09
4750	35.67	12.04	4750	23.63	5.14
4750	35.36	12.16	4750	23.20	5.07
4750	35.13	12.22	4750	22.91	5.02
4750	35.51	12.05	4750	23.46	5.12
4750	35.43	12.13	4750	23.30	5.09
4750	35.53	12.16	4750	23.37	5.09
4800	35.71	12.36	4800	23.35	5.10
4800	35.35	12.16	4800	23.19	5.12
4700	35.83	12.07	4700	23.76	5.10
4750	35.18	12.11	4750	23.07	5.07
4800	35.32	12.23	4800	23.09	5.10
4800	35.23	11.98	4800	23.25	5.17
4750	35.16	12.13	4750	23.03	5.06
4750	35.42	12.17	4750	23.25	5.07
4800	35.28	12.01	4800	23.27	5.16
4800	35.34	12.08	4800	23.26	5.15
4750	35.31	12.15	4750	23.16	5.07
4750	35.07	12.13	4750	22.94	5.05
4800	35.17	11.99	4800	23.18	5.16
4800	35.50	12.41	4800	23.09	5.06
4600	34.50	10.95	4600	23.55	5.23
4750	35.08	12.17	4750	22.91	5.03
4750	35.16	12.06	4750	23.10	5.08
4750	35.11	12.03	4750	23.08	5.08
4750	35.13	12.05	4750	23.08	5.08
4750	35.44	11.99	4750	23.45	5.14
4750	35.04	11.93	4750	23.11	5.11
4750	35.16	11.85	4750	23.31	5.15
4800	35.34	12.01	4800	23.33	5.17
4800	35.23	11.97	4800	23.26	5.17
4800	35.14	11.98	4800	23.16	5.16
4800	35.49	11.92	4800	23.57	5.22
4800	35.41	11.77	4800	23.64	5.26

Table A.1 Continued

P_{feed} kPa	Q_{feed} m^3/h	$Q_{product}$ m^3/h	P_{brine} kPa	Q_{brine} m^3/h	E_{total} kWh/m^3
4750	35.44	11.85	4750	23.59	5.18
4800	35.52	11.81	4800	23.71	5.26
4800	35.14	11.74	4800	23.40	5.24
4800	35.68	11.87	4800	23.81	5.26
4800	35.15	12.07	4800	23.08	5.13
4800	35.27	11.85	4800	23.42	5.22
4800	34.55	11.88	4800	22.67	5.12
4800	34.88	11.81	4800	23.07	5.19
4800	34.79	11.87	4800	22.92	5.15
4800	35.16	11.68	4800	23.48	5.27
4800	34.81	11.67	4800	23.14	5.23
4850	34.40	11.79	4850	22.61	5.19
4850	35.17	11.65	4850	23.52	5.33
4850	35.45	11.97	4850	23.48	5.25
4850	35.44	11.67	4850	23.77	5.36
4850	35.20	11.83	4850	23.37	5.27
4850	35.01	11.76	4850	23.25	5.27
4850	35.17	11.81	4850	23.36	5.27
4850	35.45	11.89	4850	23.56	5.28
4850	35.32	11.49	4850	23.83	5.41
4850	34.60	11.61	4850	22.99	5.28
4850	34.58	11.59	4850	22.99	5.28
4850	35.11	11.57	4850	23.54	5.35
4850	34.55	11.73	4850	22.82	5.23
4850	34.90	11.66	4850	23.24	5.30
4850	34.64	11.40	4850	23.24	5.36
4850	34.78	11.61	4850	23.17	5.30
4850	34.67	11.64	4850	23.03	5.28
4850	34.36	11.74	4850	22.62	5.20
4850	35.15	11.51	4850	23.64	5.38
4850	34.34	11.62	4850	22.72	5.24
4850	34.11	11.66	4850	22.45	5.20
4850	34.27	11.49	4850	22.78	5.28
4850	34.64	11.61	4850	23.03	5.28
4850	34.69	11.52	4850	23.17	5.32
4850	34.39	11.42	4850	22.97	5.32
4850	34.49	11.30	4850	23.19	5.38
4750	34.46	11.23	4750	23.23	5.29

Table A.1 Continued

P_{feed} kPa	Q_{feed} m^3/h	$Q_{product}$ m^3/h	P_{brine} kPa	Q_{brine} m^3/h	E_{total} kWh/m^3
4750	34.55	11.20	4750	23.35	5.31
4750	34.28	11.31	4750	22.97	5.24
4750	34.31	11.33	4750	22.98	5.24
4750	34.29	11.21	4750	23.08	5.28
4800	34.60	11.16	4800	23.44	5.39
4800	34.41	11.18	4800	23.23	5.36
4800	34.28	11.21	4800	23.07	5.33
4800	33.53	11.06	4800	22.47	5.30
4800	33.91	11.13	4800	22.78	5.32
4800	34.26	11.15	4800	23.11	5.35
4800	34.41	11.19	4800	23.22	5.36
4800	33.02	11.41	4800	21.61	5.10
4800	33.60	10.89	4800	22.71	5.37
4800	34.16	11.11	4800	23.05	5.36
4800	34.39	11.03	4800	23.36	5.42
4800	34.34	11.08	4800	23.26	5.39
4800	33.49	11.03	4800	22.46	5.30
4800	33.86	11.17	4800	22.69	5.29
4800	34.27	10.70	4800	23.57	5.53
4800	33.78	11.02	4800	22.76	5.34
4800	34.10	11.14	4800	22.96	5.34
4800	34.14	11.12	4800	23.02	5.35
4800	33.82	11.03	4800	22.79	5.34
4800	34.50	11.05	4800	23.45	5.42
4800	34.10	11.12	4800	22.98	5.34
4800	34.31	10.91	4800	23.40	5.45
4850	33.87	11.01	4850	22.86	5.41
4850	34.11	10.98	4850	23.13	5.46
4850	34.27	11.08	4850	23.19	5.44
4850	33.94	11.10	4850	22.84	5.39
4850	34.08	11.06	4850	23.02	5.42
4850	33.86	11.14	4850	22.72	5.36
4850	34.24	11.05	4850	23.19	5.45
4850	34.41	11.08	4850	23.33	5.45
4850	34.17	11.10	4850	23.07	5.42
4850	34.11	11.24	4850	22.87	5.35
4850	34.23	11.12	4850	23.11	5.42
4850	34.36	11.19	4850	23.17	5.41

Table A.1 Continued

P_{feed} kPa	Q_{feed} m^3/h	$Q_{product}$ m^3/h	P_{brine} kPa	Q_{brine} m^3/h	E_{total} kWh/m^3
4850	33.89	11.26	4850	22.63	5.32
4850	33.80	11.11	4850	22.69	5.37
4850	33.99	11.09	4850	22.90	5.40
4850	34.51	11.08	4850	23.43	5.47
4850	34.20	11.04	4850	23.16	5.44
4850	34.05	11.17	4850	22.88	5.37
4850	34.14	11.18	4850	22.96	5.38
4850	35.27	11.95	4850	23.32	5.24
4900	33.80	10.99	4900	22.81	5.47
4900	34.45	11.15	4900	23.30	5.49
4850	34.71	12.04	4850	22.67	5.14
4900	34.92	11.98	4900	22.94	5.24
4900	34.90	11.86	4900	23.04	5.28
4900	34.85	11.74	4900	23.11	5.32
4900	34.80	11.53	4900	23.27	5.39
4900	34.74	11.70	4900	23.04	5.32
4900	34.83	11.56	4900	23.27	5.38
4900	34.68	11.60	4900	23.08	5.35
4900	35.04	11.56	4900	23.48	5.41
4950	34.64	11.63	4950	23.01	5.38
4950	34.51	11.57	4950	22.94	5.39
4950	34.82	11.38	4950	23.44	5.50
4950	34.67	11.73	4950	22.94	5.35
4950	34.71	11.57	4950	23.14	5.42
4950	34.11	11.44	4950	22.67	5.39
4950	34.62	11.76	4950	22.86	5.33
4950	34.22	11.34	4950	22.88	5.44
4950	34.45	11.48	4950	22.97	5.42
4950	34.67	11.55	4950	23.12	5.42
4950	34.74	11.44	4950	23.30	5.47
4950	34.81	11.57	4950	23.24	5.43
4950	34.80	11.50	4950	23.30	5.45
4950	34.72	11.41	4950	23.31	5.48
4950	34.75	11.36	4950	23.39	5.50
5050	35.37	12.38	5050	22.99	5.31
5050	35.37	12.38	5050	22.99	5.31
5050	35.59	12.08	5050	23.51	5.45
5050	35.24	11.91	5050	23.33	5.46

Table A.1 Continued

P_{feed} kPa	Q_{feed} m^3/h	$Q_{product}$ m^3/h	P_{brine} kPa	Q_{brine} m^3/h	E_{total} kWh/m^3
5250	35.69	12.31	5250	23.38	5.59
5250	35.85	12.40	5250	23.45	5.58
5250	34.91	12.30	5250	22.61	5.50
5250	35.36	12.26	5250	23.10	5.57
5250	35.52	12.32	5250	23.20	5.57
5250	35.44	12.19	5250	23.25	5.60
5200	35.71	12.45	5200	23.26	5.49
5200	35.81	12.55	5200	23.26	5.47
5100	35.61	12.37	5100	23.24	5.40
5200	35.06	12.46	5200	22.60	5.41
5250	34.19	12.44	5250	21.75	5.36
5250	34.05	12.18	5250	21.87	5.43
5500	34.99	12.36	5500	22.63	5.75
5600	34.33	12.34	5600	21.99	5.77
5600	34.81	12.17	5600	22.64	5.90
5150	34.84	12.54	5150	22.30	5.30
5150	35.03	12.60	5150	22.43	5.31
5350	35.15	12.53	5350	22.62	5.55
5350	35.25	12.41	5350	22.84	5.60
5300	35.79	12.48	5300	23.31	5.59
5300	36.23	12.57	5300	23.66	5.62
5350	35.19	12.40	5350	22.79	5.60
5350	35.77	12.55	5350	23.22	5.62
5300	34.45	11.91	5300	22.54	5.63
5300	34.84	11.74	5300	23.10	5.75
5400	35.17	12.54	5400	22.63	5.60
5400	35.49	12.34	5400	23.15	5.71
5400	35.64	12.51	5400	23.13	5.67
5400	35.66	12.37	5400	23.29	5.72
5400	35.74	12.36	5400	23.38	5.74
5400	35.42	12.34	5400	23.08	5.70
5400	35.57	12.16	5400	23.41	5.79
5400	35.72	12.25	5400	23.47	5.78
5400	35.55	12.33	5400	23.22	5.72
5400	36.05	12.17	5400	23.88	5.85
5400	35.43	12.43	5400	23.00	5.67
5400	35.91	12.41	5400	23.50	5.74
5350	35.37	12.48	5350	22.89	5.60

Table A.1 Continued

P_{feed} kPa	Q_{feed} m^3/h	$Q_{product}$ m^3/h	P_{brine} kPa	Q_{brine} m^3/h	E_{total} kWh/m^3
5350	35.88	12.60	5350	23.28	5.62
5350	36.48	12.35	5350	24.13	5.78
5350	35.71	12.20	5350	23.51	5.74
5350	35.41	12.62	5350	22.79	5.55
5350	35.44	12.47	5350	22.97	5.61
5350	35.42	12.58	5350	22.84	5.57
5350	36.16	12.41	5350	23.75	5.72
5350	35.84	12.71	5350	23.13	5.57
5350	35.38	12.48	5350	22.90	5.60
5350	35.87	12.39	5350	23.48	5.69
5350	35.72	12.42	5350	23.30	5.66
5350	35.61	12.56	5350	23.05	5.60
5350	35.65	12.36	5350	23.29	5.67
5350	36.21	12.57	5350	23.64	5.67
5350	35.75	12.23	5350	23.52	5.73
5350	35.54	12.54	5350	23.00	5.60
5350	35.21	12.41	5350	22.80	5.60
5350	35.45	12.27	5350	23.18	5.68
5350	35.01	12.64	5350	22.37	5.50
5350	35.29	12.09	5350	23.20	5.73
5350	35.43	12.40	5350	23.03	5.63
5350	35.74	12.47	5350	23.27	5.64
5350	35.63	12.34	5350	23.29	5.68
5350	35.55	12.48	5350	23.07	5.62
5350	35.48	12.39	5350	23.09	5.64
5350	35.68	12.32	5350	23.36	5.69
5350	35.61	12.56	5350	23.05	5.60
5350	35.45	12.47	5350	22.98	5.61
5350	35.61	12.52	5350	23.09	5.61
5350	36.16	12.49	5350	23.67	5.69
5350	35.75	12.11	5350	23.64	5.78
5350	36.28	12.26	5350	24.02	5.79
5350	35.81	12.12	5350	23.69	5.78
5400	35.33	12.11	5400	23.22	5.78
5400	35.16	12.45	5400	22.71	5.63
5450	36.21	12.66	5450	23.55	5.74
5450	35.51	12.50	5450	23.01	5.71
5450	35.04	12.86	5450	22.18	5.53

Table A.1 Continued

P_{feed} kPa	Q_{feed} m^3/h	$Q_{product}$ m^3/h	P_{brine} kPa	Q_{brine} m^3/h	E_{total} kWh/m^3
5400	35.43	12.47	5400	22.96	5.66
5400	35.41	12.35	5400	23.06	5.70
5400	35.69	12.31	5400	23.38	5.75
5400	35.71	12.35	5400	23.36	5.74
5400	35.65	12.63	5400	23.02	5.63
5400	35.34	12.39	5400	22.95	5.68
5450	35.69	12.19	5450	23.50	5.85
5450	35.65	12.32	5450	23.33	5.79
5450	36.20	12.18	5450	24.02	5.92
5450	35.57	12.19	5450	23.38	5.83
5450	35.45	12.15	5450	23.30	5.83
5450	36.01	12.32	5450	23.69	5.84
5450	36.16	12.40	5450	23.76	5.83
5450	35.94	12.37	5450	23.57	5.81
5450	36.13	12.41	5450	23.72	5.82
5450	35.95	12.26	5450	23.69	5.86
5450	35.86	12.35	5450	23.51	5.81
5450	35.56	12.19	5450	23.37	5.83
5400	35.48	12.15	5400	23.33	5.78
5400	35.76	12.16	5400	23.60	5.81
5400	35.89	12.19	5400	23.70	5.82
5400	35.81	12.22	5400	23.59	5.80
5400	35.79	12.17	5400	23.62	5.81
5450	35.92	12.29	5450	23.63	5.84
5450	35.94	12.21	5450	23.73	5.87
5450	35.81	12.31	5450	23.50	5.82
5450	35.49	12.21	5450	23.28	5.81
5450	35.92	12.30	5450	23.62	5.84
5450	35.84	12.23	5450	23.61	5.85
5450	35.95	12.06	5450	23.89	5.93
5450	35.54	12.03	5450	23.51	5.89
5450	35.43	12.10	5450	23.33	5.85
5450	36.18	12.25	5450	23.93	5.89
5450	36.21	12.11	5450	24.10	5.95
5450	35.17	12.19	5450	22.98	5.78
5450	35.65	12.20	5450	23.45	5.84
5450	36.61	11.97	5450	24.64	6.06
5450	36.47	12.14	5450	24.33	5.97

Table A.1 Continued

P_{feed} kPa	Q_{feed} m^3/h	$Q_{product}$ m^3/h	P_{brine} kPa	Q_{brine} m^3/h	E_{total} kWh/m^3
5450	36.51	12.07	5450	24.44	6.00
5450	35.66	12.17	5450	23.49	5.85
5450	34.80	12.10	5450	22.70	5.77
5450	35.57	11.99	5450	23.58	5.91
5450	36.05	12.14	5450	23.91	5.91
5450	35.83	11.98	5450	23.85	5.95
5450	36.72	12.04	5450	24.68	6.04
5450	35.61	12.12	5450	23.49	5.86
5450	35.37	11.81	5450	23.56	5.95
5450	35.72	12.14	5450	23.58	5.87
5450	36.11	12.11	5450	24.00	5.93
5450	35.59	11.97	5450	23.62	5.92
5450	35.33	11.96	5450	23.37	5.89
5450	35.94	12.03	5450	23.91	5.94
5450	35.88	12.12	5450	23.76	5.90
5450	35.97	12.09	5450	23.88	5.92
5450	35.56	12.04	5450	23.52	5.89
5450	35.67	12.01	5450	23.66	5.91
5450	35.81	12.00	5450	23.81	5.94
5450	35.73	12.07	5450	23.66	5.90
5450	34.67	12.04	5450	22.63	5.77
5450	35.71	11.86	5450	23.85	5.98
5450	35.79	11.93	5450	23.86	5.96
5450	35.61	11.97	5450	23.64	5.92
5450	35.70	12.02	5450	23.68	5.91
5450	35.60	12.06	5450	23.54	5.89
5450	35.45	11.91	5450	23.54	5.93
5450	35.79	11.97	5450	23.82	5.95
5450	36.31	11.95	5450	24.36	6.02
5450	35.75	11.69	5450	24.06	6.05
5450	35.60	11.72	5450	23.88	6.02
5450	35.67	11.77	5450	23.90	6.01
5450	35.80	11.70	5450	24.10	6.06
5450	35.76	11.82	5450	23.94	6.00
5450	35.57	11.90	5450	23.67	5.95
5450	35.69	11.93	5450	23.76	5.95
5450	35.29	11.84	5450	23.45	5.93
5450	35.18	11.67	5450	23.51	5.99

Table A.1 Continued

P_{feed} kPa	Q_{feed} m^3/h	$Q_{product}$ m^3/h	P_{brine} kPa	Q_{brine} m^3/h	E_{total} kWh/m^3
5450	35.73	11.95	5450	23.78	5.95
5500	35.42	11.93	5500	23.49	5.97
5500	35.61	11.84	5500	23.77	6.03
5500	35.15	11.80	5500	23.35	5.98
5500	35.72	12.01	5500	23.71	5.98
5500	35.63	11.94	5500	23.69	5.99
5500	35.74	11.87	5500	23.87	6.03
5500	35.21	12.04	5500	23.17	5.90
5500	35.18	11.95	5500	23.23	5.93
5500	35.51	11.91	5500	23.60	5.99
5500	35.75	11.96	5500	23.79	6.00
5500	36.34	11.79	5500	24.55	6.15
5500	35.67	11.88	5500	23.79	6.02

A.3. References

Al-Shayji, Khawla. (1998). *Modelling, simulation and optimization of large-scale commercial desalination plants*. PhD Thesis. Virginia Polytechnic Institute and State University, Blacksburg, Virginia, USA.

El-Dessouky, H.T. and Ettouney, H.M. (2002). *Fundamentals of salt water desalination*, Elsevier Science B.V., Amsterdam, The Netherlands.

El-Dessouky, H.T., Ettouney, H.M. and Al-Roumi, Y. (1999). Multi-stage flash desalination:present and future outlook. *Chemical engineering Journal*, 73(), 173-190.

El-Dessouky, H.T., Shaban, H.I. and Al-Ramadan, H. (1995). Steady-state analysis of multi-stage flash desalination process. *Desalination*, 103(3), 271-287.

Mathworks Inc. (2005). *Documentation of the optimization toolbox*. http://www.mathworks.com/access/helpdesk/help/toolbox/optim/.

Sadjadi, S.J. and Ponnambalam, K. (1999). Advances in trust region algorithms for constrained optimization. *Applied Numerical mathematics*, 29, 423-443.

Appendix B

B. Air-Conditioning systems in Kuwait

B.1. Power Ratings of A/C systems in Kuwait

Table B.1 Power rating for different types of AC systems in Kuwait

System		Power rating (kW_e/RT)						Ratio
Type	**RT**	**PR_{CHIL}**	**PR_{CTF}**	**PR_{CW}**	**PR_{CHW}**	**PR_{AH}**	**PR_T**	**kW_e/kW_R**
Package & Ducted-split	0-15						1.700	0.483
Air-cooled	<100	1.600				0.380	2.050	0.583
	100-250							
	>100							
Water-cooled	<250	0.950	0.040	0.060	0.070	0.380	1.500	0.426
	250-500	0.750					1.300	0.370
	>500	0.700					1.250	0.355

B.2. Single-effect ARS Model

The modelling procedure starts with the single-effect cycle because of its simplicity and because it can be used as a base for modelling the double-effect cycle by applying certain modifications to the program.

The modelling of the cycle is done in Matlab by applying the energy and mass balance equation on the components of the cycle. The first step in the procedure is determining the inputs to the model. From the reviewed literature (Sun, 1997 and Xu et. al., 1996) and manufacturers' catalogues, the inputs are selected to be:

- Absorber temperature (Ta)
- Condenser temperature (T_c)
- Evaporator temperature (T_e)
- Generator temperature (T_g)
- Refrigeration capacity (Q_e)
- Heat exchanger effectiveness (ε)
- Liquid carryover

Liquid carryover occurs in the evaporator when a small amount of liquid refrigerant is not evaporated.

B.2.1. Assumptions

To be able to successfully model the cycle with a reasonable degree of accuracy the following assumptions has been made regarding the working fluids (ASHRAE, 2001 and Foy, 2001):

- Steady-state operation
- Refrigerant is pure water
- LiBr-H_2O solutions in generator and absorber are in equilibrium

- No pressure changes in the pipes; pressure drop exists only in expansion valve and pump
- States at points 1, 4, 6, 8, 11 are at saturated liquid phase
- State at point 10 is saturated vapour
- Throttling process is isoenthalpic
- Solution pump is 100% efficient
- Negligible heat losses

B.2.2. Modelling Procedure

The flow chart describing the single-effect modelling procedure is shown in Figure 5.3. The following procedure gives a detailed presentation of the flow chart.

Step 1

The first step after reading the known input is to assign the known input temperatures to the state points at the exit of the components. Hence:

$$T_1 = T_a$$
$$T_7 = T_g$$
$$T_4 = T_g$$
$$T_8 = T_c$$
$$T_{10} = T_e$$
$$T_{11} = T_e$$

And the mass fractions of LiBr at points 7 to 11 are:

$$X_7 = 0$$
$$X_8 = 0$$
$$X_9 = 0$$

$$X_{10} = 0$$

$$X_{11} = 0$$

Since there is only state change from liquid to vapour in the evaporator, then:

$$T_9 = T_{10}$$

Step 2

Since it is assumed that state points 8 and 10 are saturated vapour, the pressure can be calculated using Eqs 3.20 & 3.21 knowing T_8, $T_{10}$and:

$$P_8 = P_{sat,8}$$

$$P_{10} = P_{sat,10}$$

Since there is no pressure drop in the pure water refrigerant pipes, the following is true:

$$P_2 = P_8$$

$$P_3 = P_8$$

$$P_4 = P_8$$

$$P_5 = P_8$$

$$P_7 = P_8$$

$$P_9 = P_{10}$$

$$P_{11} = P_{10}$$

$$P_6 = P_{10}$$

$$P_1 = P_{10}$$

The enthalpies h_7, h_8 and h_{11} can be calculated now knowing T_7, P_7, T_8, T_{11} and P_{11} using Equations 3.16, 3.19a & 3.19b. Since the enthalpy across the expansion device does not change:

$$h_9 = h_8$$

The enthalpy at point 10,
h_{10}, can be calculated using Equation5.1 from T_{10} and X_{10}.

Step 3

To calculate the LiBr mass fraction in the solution at points 4 and 1, the saturation temperatures $T_{sat,4}$ and $T_{sat,1}$ are calculated first from P_4 and P_1 using Equations 3.22 and 3.23. Now X_4 and X_1 can be calculated from $T_{sat,4}$, T_4, $T_{sat,1}$ and T_1 using Equation 5.3. Also:

$$X_5 = X_4$$
$$X_6 = X_4$$
$$X_2 = X_1$$
$$X_3 = X_1$$

Step 4

It is assumed that there is no temperature rise in the solution leaving the pump, hence:

$$T_2 = T_1$$

Heat exchanger temperatures T_3 and T_5 are calculated using the equation describing the effectiveness:

$$\varepsilon_{HX} = \frac{(T_3 - T_2)}{(T_4 - T_2)} = \frac{(T_4 - T_5)}{(T_4 - T_2)}$$
$$T_3 = T_2 + (T_4 - T_2)\varepsilon_{HX}$$

$$T_5 = 4 + (T_4 - T_2)\varepsilon_{HX}$$

The pressure at point 6 is assumed to be the saturation pressure (i.e. $P_6 = P_{sat,6}$), from this the saturation temperature of water $T_{sat,6}$ can be calculated using Equations 3.22 and 3.23 as a function of $P_{sat,6}$. Now, the actual temperature of the solution at point 6 (T_6) using Equation 5.3 from the known $T_{sat,6}$ and X_6 through the use of the *fzero* command in Matlab, which eliminates the need for an iteration process.

The remaining enthalpies can be calculated now. Enthalpy at point 1 (h_1) is calculated using Equation 5.1 from the known T_1 and X_1. The same procedure is used to calculate h_3, h_4 and h_5. The enthalpy across the expansion device does not change, so:

$$h_6 = h_5$$

The enthalpy at point 2 (h_1) is calculated from the equation describing the isentropic pump work:

$$W = \frac{m_1(P_2 - P_1)}{\rho_1} = m_1(h_2 - h_1)$$

Rearranging the above equation leads to:

$$h_2 = \frac{(P_2 - P_1)}{\rho_1} + h_1$$

The solution density (ρ_1) is calculated using Equation 5.4.

By the completion of step 4, all the single-effect cycle temperatures, pressure, mass fractions and enthalpies are known. The next step is to calculate the mass flowrates of working fluids in the cycle and the energy inputs and outputs of the system.

Step 5

The first step in calculating the mass flowrates is to apply a mass and energy balances on the evaporator:

$$m_9 = m_{10} + m_{11}$$
$$Q_e = m_{10}h_{10} + m_{11}h_{11} - m_9h_9$$

The liquid carryover (*CO*) at point 11 is described as a percentage of the vapour mass flowrate (m_{10}):

$$m_{11} = \frac{CO}{100}m_{10}$$

The above equations are rearranged to solve for the mass flowrate at point 10:

$$m_{10} = \frac{Q_e}{h_{10} + \left(\frac{CO}{100}\right)h_{11} - \left(1 + \frac{CO}{100}\right)h_9}$$

Now,

$$m_9 = m_{10} + m_{11}$$
$$m_8 = m_9$$
$$m_7 = m_9$$

A mass balance on the absorber is applied to calculate the mass flowrate at point 1. The overall mass balance is:

$$m_1 = m_6 + m_9$$

The LiBr mass balance:

$$m_6 X_6 = m_1 X_1$$

The mass flowrate at point 1 is calculated from:

$$m_1 = \frac{m_9}{1 - \frac{X_1}{X_6}}$$

Also,

$$m_2 = m_1$$
$$m_3 = m_1$$

A mass balance on the generator results in:

$$m_4 = m_3 - m_7$$

Also,

$$m_5 = m_4$$
$$m_6 = m_4$$

Knowing the enthalpies and the mass flowrates of the different streams in the cycle, the different energy inputs and outputs can now be calculated:

Generator

$$Q_g = m_4 h_4 + m_7 h_7 - m_3 h_3$$

Condenser

$$Q_C = m_7 h_7 - m_8 h_8$$

Absorber

$$m_{10}h_{10} + m_{11}h_{11} + m_6h_6 - m_1h_1$$

Pump work

$$W = \frac{m_1(P_2 - P_1)}{\rho_1}$$

And the coefficient of performance can be calculated as:

$$COP = \frac{Q_e}{Q_g + W}$$

B.2.3. Validation of Single-Effect Model

Matlab programming software is used to apply the model presented here. The following are the known inputs:

Absorber temperature, T_a = 20°C
Condenser temperature, T_c = 20°C
Evaporator temperature, T_e = 2.5°C
Generator temperature, T_g = 70°C
Refrigeration capacity, Q_e = 40kW
Heat exchanger effectiveness, ε = 80%
Liquid carryover = 0

Table B.2 State points for the single-effect model

Point	Temperature °C	Pressure kPa	Concentration %	Enthalpy kJ/kg	Mass flowrate kg/s
1	20.0	0.71	47.91	37.8	0.083
2	20.0	2.31	47.91	37.8	0.083
3	52.0	2.31	47.91	108.3	0.083
4	60.0	2.31	59.26	150.6	0.067
5	28.0	2.31	59.26	88.6	0.067
6	39.4	0.71	59.26	88.6	0.067
7	60.0	2.31	0.00	2613.9	0.016
8	20.0	2.31	0.00	83.7	0.016
9	2.5	0.71	0.00	83.7	0.016
10	2.5	0.71	0.00	2506.9	0.016
11	2.5	0.71	0.00	10.5	0.000

Table B.3 Performance parameters of single-effect model

Q_e kW	Q_g kW	Q_c kW	Q_a kW	W_p kW	COP
40	42.82	40.37	42.82	0.092	0.93

Table B.4 Comparison of results

Variable	Model	Foy	sun (1997)
X_{ss} (%)	59.26	59.18	58.4
X_{ws} (%)	47.91	47.58	49.1
Q_e (kW)	40	40	40.38
Q_g (kW)	42.82	42.75	46.88
Q_a (kW)	42.82	42.73	45.08
Q_c (kW)	40.37	40.41	42.18
COP	0.93	0.934	0.86

Appendix C

C. Tabulated Results of Powerplant Configurations

C.1. Doha West Cogeneration power plant

Table C.1 Results of conventional plant simulation

Parameter	Unit	January	February	March	April	May	June	July	August	September	October	November	December
No. of turbines		3	3	3	4	5	6	6	7	6	5	4	3
No. of turbines(ACTUAL)		***5***	***6***	***6***	***6***	***6***	***7***	***7***	***7***	***7***	***7***	***6***	***7***
No. of MSF units		11	11	12	14	14	15	14	15	14	13	13	13
No. of MSF units(ACTUAL)		***11***	***12***	***13***	***15***	***16***	***16***	***16***	***15***	***16***	***14***	***15***	***16***
Electricity generated	*GWh/month*	670	626	670	864	1116	1296	1339	1562	1296	1116	864	648
Total steam input*	*kg/s*	830	830	830	1106	1383	1660	1660	1936	1660	1383	1106	830
Water produced	*Mil. m^3/month*	10	10	11	14	14	14	14	15	13	13	12	12
A/C demand	*GWh/month*	0	0	28	222	433	574	649	709	564	345	76.159	0
Internal electricity consm	*GWh/month*	58	54	67	77	85	90	104	100	88	83	71	66
Net electricity available	*GWh/month*	96	90	59	67	83	133	71	238	146	173	219	84
MSF oil energy	*TJ/month*	3031	2836	3738	3617	2325	1566	911	205	882	1618	2934	4301
MSF gas volume	*Mil. m^3/month*	79	74	98	94	61	41	24	5	23	42	77	112
Cost of oil	*Mil. $/month*	63	59	68	80	88	95	94	104	91	84	76	70
Cost of natural gas	*Mil. $/month*	8	8	9	10	11	12	12	13	12	11	10	9
Total fuel cost	*Mil. $/month*	72	67	77	90	99	107	106	117	102	94	85	79
CO_2 emissions from oil	*000 ton/month*	711	665	762	896	988	1065	1050	1163	1016	937	846	786
CO_2 emissions from gas	*000 ton/month*	47	44	50	59	65	71	69	77	67	62	56	52
Total CO_2 emissions	*000 ton/month*	758	709	812	955	1053	1136	1119.1	1240	1083	999	902	838

**** steam flow per turbine is 276.6 kg/s***

C.2. Power-RO Configuration

Table C.2 Results of power-RO plant simulation

Parameter	Unit	January	February	March	April	May	June	July	August	September	October	November	December
No. of turbines		3	3	4	5	5	6	7	7	6	5	4	3
No. of RO units		3	3	4	4	4	5	4	5	4	4	4	4
Electricity generated	*GWh/month*	670	626	893	1080	1116	1296	1562	1562	1296	1116	864	648
Water produced	*Mil. m^3/month*	10.2	9.6	13.6	13.2	13.6	16.5	13.6	17.1	13.2	13.6	13.2	13.2
Electricity consumed by RO	*GWh/month*	56	53	75	72	75	91	75	94	72	75	72	72
A/C demand	*GWh/month*	0	0	28	222	433	574	649	709	564	345	76	0
Internal electricity consm	*GWh/month*	58	54	67	77	85	90	104	100	88	83	71	66
Net electricity available	*GWh/month*	40	38	207	210	8	43	219	145	74	98	147	12
Cost of oil	*Mil. $/month*	41	39	55	67	69	80	97	97	80	69	53	40
Cost of natural gas	*Mil. $/month*	5	5	7	9	9	10	12	12	10	9	7	5
Total fuel cost	*Mil. $/month*	47	44	62	75	78	91	109	109	91	78	60	45
CO_2 emissions from oil	*000 ton/month*	465	435	620	749	774	899	1084	1084	899	774	600	450
CO_2 emissions from gas	*000 ton/month*	31	29	41	50	51	60	72	72	60	51	40	30
Total CO_2 emissions	*000 ton/month*	495	463	661	799	826	959	1156	1156	959	826	639	479

**** steam flow per turbine is 276.6 kg/s***

C.3. Power-MSF-RO Configuration

This section comprises of tabulated results of power-MSF-RO hybrid configuration for all months of the year.

Table C.3 January results of power-MSF-RO configuration

RO load %	MSF demand m^3	RO demand m^3	MSF units	RO units	NT	Fuel cost million $/month	CO_2 emissions ktonne/month
5	9.45E+06	4.97E+05	10	1	3	67.71	728.42
10	8.95E+06	9.95E+05	10	1	3	67.71	728.42
15	8.45E+06	1.49E+06	9	1	3	63.16	677.44
20	7.96E+06	1.99E+06	9	1	3	63.16	677.44
25	7.46E+06	2.49E+06	9	1	3	63.16	677.44
30	6.96E+06	2.98E+06	8	1	3	58.61	626.45
35	6.47E+06	3.48E+06	8	2	3	58.61	626.45
40	5.97E+06	3.98E+06	7	2	3	54.06	575.46
45	5.47E+06	4.48E+06	7	2	3	54.06	575.46
50	4.97E+06	4.97E+06	6	2	3	49.51	524.48
55	4.48E+06	5.47E+06	6	2	3	49.51	524.48
60	3.98E+06	5.97E+06	5	2	3	49.51	524.48
65	3.48E+06	6.47E+06	5	2	3	49.51	524.48
70	2.98E+06	6.96E+06	4	3	3	49.51	524.48
75	2.49E+06	7.46E+06	4	3	3	49.51	524.48
80	1.99E+06	7.96E+06	3	3	3	49.51	524.48
85	1.49E+06	8.45E+06	3	3	3	49.51	524.48
90	9.95E+05	8.95E+06	2	3	3	49.51	524.48
95	4.97E+05	9.45E+06	2	3	3	49.51	524.48

Table C.4 February results of power-MSF-RO configuration

RO load %	MSF demand m^3	RO demand m^3	MSF units	RO units	NT	Fuel cost million $/month	CO_2 emissions ktonne/month
5	8.44E+06	4.44E+05	10	1	3	63.34	681.43
10	8.00E+06	8.89E+05	10	1	3	63.34	681.43
15	7.55E+06	1.33E+06	9	1	3	59.08	633.73
20	7.11E+06	1.78E+06	9	1	3	59.08	633.73
25	6.66E+06	2.22E+06	8	1	3	54.83	586.03
30	6.22E+06	2.67E+06	8	1	3	54.83	586.03
35	5.78E+06	3.11E+06	7	1	3	50.57	538.34
40	5.33E+06	3.55E+06	7	2	3	50.57	538.34
45	4.89E+06	4.00E+06	6	2	3	46.32	490.64
50	4.44E+06	4.44E+06	6	2	3	46.32	490.64
55	4.00E+06	4.89E+06	5	2	3	46.32	490.64
60	3.55E+06	5.33E+06	5	2	3	46.32	490.64
65	3.11E+06	5.78E+06	4	2	3	46.32	490.64
70	2.67E+06	6.22E+06	4	2	3	46.32	490.64
75	2.22E+06	6.66E+06	4	3	3	46.32	490.64
80	1.78E+06	7.11E+06	3	3	3	46.32	490.64
85	1.33E+06	7.55E+06	3	3	3	46.32	490.64
90	8.89E+05	8.00E+06	2	3	3	46.32	490.64
95	4.44E+05	8.44E+06	2	3	3	46.32	490.64

Table C.5 March results of power-MSF-RO configuration

RO load %	MSF demand m^3	RO demand m^3	MSF units	RO units	NT	Fuel cost million $/month	CO_2 emissions ktonne/month
5	1.04E+07	5.49E+05	11	1	3	72.26	779.41
10	9.88E+06	1.10E+06	11	1	3	72.26	779.41
15	9.33E+06	1.65E+06	10	1	3	67.71	728.42
20	8.78E+06	2.19E+06	10	1	3	67.71	728.42
25	8.23E+06	2.74E+06	9	1	3	63.16	677.44
30	7.68E+06	3.29E+06	9	1	3	63.16	677.44
35	7.13E+06	3.84E+06	8	2	3	58.61	626.45
40	6.58E+06	4.39E+06	8	2	3	58.61	626.45
45	6.04E+06	4.94E+06	7	2	3	54.06	575.46
50	5.49E+06	5.49E+06	7	2	3	54.06	575.46
55	4.94E+06	6.04E+06	6	2	3	49.51	524.48
60	4.39E+06	6.58E+06	5	2	3	49.51	524.48
65	3.84E+06	7.13E+06	5	3	3	49.51	524.48
70	3.29E+06	7.68E+06	4	3	3	49.51	524.48
75	2.74E+06	8.23E+06	4	3	3	49.51	524.48
80	2.19E+06	8.78E+06	3	3	3	49.51	524.48
85	1.65E+06	9.33E+06	3	3	3	49.51	524.48
90	1.10E+06	9.88E+06	2	3	3	49.51	524.48
95	5.49E+05	1.04E+07	2	4	3	49.51	524.48

Table C.6 April results of power-MSF-RO configuration

RO load %	MSF demand m^3	RO demand m^3	MSF units	RO units	NT	Fuel cost million $/month	CO_2 emissions ktonne/month
5	1.16E+07	6.10E+05	13	1	4	85.90	923.45
10	1.10E+07	1.22E+06	12	1	4	81.50	874.11
15	1.04E+07	1.83E+06	12	1	4	81.50	874.11
20	9.76E+06	2.44E+06	11	1	4	77.09	824.77
25	9.15E+06	3.05E+06	10	1	4	72.69	775.43
30	8.54E+06	3.66E+06	10	2	4	72.69	775.43
35	7.93E+06	4.27E+06	9	2	4	68.29	726.09
40	7.32E+06	4.88E+06	9	2	4	68.29	726.09
45	6.71E+06	5.49E+06	8	2	4	63.89	676.75
50	6.10E+06	6.10E+06	7	2	4	63.89	676.75
55	5.49E+06	6.71E+06	7	3	4	63.89	676.75
60	4.88E+06	7.32E+06	6	3	4	63.89	676.75
65	4.27E+06	7.93E+06	6	3	4	63.89	676.75
70	3.66E+06	8.54E+06	5	3	4	63.89	676.75
75	3.05E+06	9.15E+06	4	3	4	63.89	676.75
80	2.44E+06	9.76E+06	4	3	4	63.89	676.75
85	1.83E+06	1.04E+07	3	4	5	79.86	845.93
90	1.22E+06	1.10E+07	2	4	5	79.86	845.93
95	6.10E+05	1.16E+07	2	4	5	79.86	845.93

Table C.7 May results of power-MSF-RO configuration

RO load %	MSF demand m^3	RO demand m^3	MSF units	RO units	NT	Fuel cost million $/month	CO_2 emissions ktonne/month
5	1.26E+07	6.63E+05	14	1	5	100.72	1078.07
10	1.19E+07	1.33E+06	13	1	5	96.17	1027.09
15	1.13E+07	1.99E+06	12	1	5	91.62	976.10
20	1.06E+07	2.65E+06	12	1	5	91.62	976.10
25	9.95E+06	3.32E+06	11	1	5	87.07	925.12
30	9.28E+06	3.98E+06	10	2	5	82.52	874.13
35	8.62E+06	4.64E+06	10	2	5	82.52	874.13
40	7.96E+06	5.31E+06	9	2	5	82.52	874.13
45	7.29E+06	5.97E+06	8	2	5	82.52	874.13
50	6.63E+06	6.63E+06	8	2	5	82.52	874.13
55	5.97E+06	7.29E+06	7	3	5	82.52	874.13
60	5.31E+06	7.96E+06	6	3	5	82.52	874.13
65	4.64E+06	8.62E+06	6	3	5	82.52	874.13
70	3.98E+06	9.28E+06	5	3	5	82.52	874.13
75	3.32E+06	9.95E+06	4	3	5	82.52	874.13
80	2.65E+06	1.06E+07	4	4	5	82.52	874.13
85	1.99E+06	1.13E+07	3	4	5	82.52	874.13
90	1.33E+06	1.19E+07	2	4	5	82.52	874.13
95	6.63E+05	1.26E+07	2	4	5	82.52	874.13

Table C.8 June results of power-MSF-RO configuration

RO load %	MSF demand m^3	RO demand m^3	MSF units	RO units	NT	Fuel cost million $/month	CO_2 emissions ktonne/month
5	1.26E+07	6.63E+05	14	1	6	104.64	1113.80
10	1.19E+07	1.33E+06	13	1	6	100.24	1064.46
15	1.13E+07	1.99E+06	13	1	6	100.24	1064.46
20	1.06E+07	2.65E+06	12	1	6	95.83	1015.12
25	9.95E+06	3.32E+06	11	2	6	95.83	1015.12
30	9.28E+06	3.98E+06	11	2	6	95.83	1015.12
35	8.62E+06	4.64E+06	10	2	6	95.83	1015.12
40	7.96E+06	5.31E+06	9	2	6	95.83	1015.12
45	7.29E+06	5.97E+06	9	2	6	95.83	1015.12
50	6.63E+06	6.63E+06	8	3	6	95.83	1015.12
55	5.97E+06	7.29E+06	7	3	6	95.83	1015.12
60	5.31E+06	7.96E+06	7	3	6	95.83	1015.12
65	4.64E+06	8.62E+06	6	3	6	95.83	1015.12
70	3.98E+06	9.28E+06	5	3	6	95.83	1015.12
75	3.32E+06	9.95E+06	5	4	6	95.83	1015.12
80	2.65E+06	1.06E+07	4	4	6	95.83	1015.12
85	1.99E+06	1.13E+07	3	4	6	95.83	1015.12
90	1.33E+06	1.19E+07	3	4	6	95.83	1015.12
95	6.63E+05	1.26E+07	2	4	6	95.83	1015.12

Table C.9 July results of power-MSF-RO configuration

RO load %	MSF demand m^3	RO demand m^3	MSF units	RO units	NT	Fuel cost million $/month	CO_2 emissions ktonne/month
5	1.28E+07	6.75E+05	14	1	6	108.13	1150.93
10	1.22E+07	1.35E+06	13	1	6	103.58	1099.94
15	1.15E+07	2.03E+06	13	1	6	103.58	1099.94
20	1.08E+07	2.70E+06	12	1	6	99.03	1048.96
25	1.01E+07	3.38E+06	11	1	6	99.03	1048.96
30	9.45E+06	4.05E+06	10	2	6	99.03	1048.96
35	8.78E+06	4.73E+06	10	2	6	99.03	1048.96
40	8.10E+06	5.40E+06	9	2	6	99.03	1048.96
45	7.43E+06	6.08E+06	9	2	6	99.03	1048.96
50	6.75E+06	6.75E+06	8	2	6	99.03	1048.96
55	6.08E+06	7.43E+06	7	3	6	99.03	1048.96
60	5.40E+06	8.10E+06	6	3	6	99.03	1048.96
65	4.73E+06	8.78E+06	6	3	6	99.03	1048.96
70	4.05E+06	9.45E+06	5	3	6	99.03	1048.96
75	3.38E+06	1.01E+07	4	3	6	99.03	1048.96
80	2.70E+06	1.08E+07	4	4	7	115.53	1223.78
85	2.03E+06	1.15E+07	3	4	7	115.53	1223.78
90	1.35E+06	1.22E+07	2	4	7	115.53	1223.78
95	6.75E+05	1.28E+07	2	4	7	115.53	1223.78

Table C.10 August results of power-MSF-RO configuration

RO load %	MSF demand m^3	RO demand m^3	MSF units	RO units	NT	Fuel cost million $/month	CO_2 emissions ktonne/month
5	1.30E+07	6.83E+05	14	1	7	115.53	1223.78
10	1.23E+07	1.37E+06	13	1	7	115.53	1223.78
15	1.16E+07	2.05E+06	13	1	7	115.53	1223.78
20	1.09E+07	2.73E+06	12	1	7	115.53	1223.78
25	1.02E+07	3.42E+06	11	2	7	115.53	1223.78
30	9.56E+06	4.10E+06	11	2	7	115.53	1223.78
35	8.88E+06	4.78E+06	10	2	7	115.53	1223.78
40	8.20E+06	5.46E+06	9	2	7	115.53	1223.78
45	7.51E+06	6.15E+06	9	2	7	115.53	1223.78
50	6.83E+06	6.83E+06	8	3	7	115.53	1223.78
55	6.15E+06	7.51E+06	8	3	7	115.53	1223.78
60	5.46E+06	8.20E+06	7	3	7	115.53	1223.78
65	4.78E+06	8.88E+06	6	3	7	115.53	1223.78
70	4.10E+06	9.56E+06	5	3	7	115.53	1223.78
75	3.42E+06	1.02E+07	5	3	7	115.53	1223.78
80	2.73E+06	1.09E+07	4	4	7	115.53	1223.78
85	2.05E+06	1.16E+07	0	4	7	115.53	1223.78
90	1.37E+06	1.23E+07	3	4	7	115.53	1223.78
95	6.83E+05	1.30E+07	2	4	7	115.53	1223.78

Table C.11 September results of power-MSF-RO configuration

RO load %	MSF demand m^3	RO demand m^3	MSF units	RO units	NT	Fuel cost million $/month	CO_2 emissions ktonne/month
5	1.21E+07	6.39E+05	13.00	1.00	6.00	100.24	1064.46
10	1.15E+07	1.28E+06	13.00	1.00	6.00	100.24	1064.46
15	1.09E+07	1.92E+06	12.00	1.00	6.00	95.83	1015.12
20	1.02E+07	2.55E+06	12.00	1.00	6.00	95.83	1015.12
25	9.58E+06	3.19E+06	11.00	1.00	6.00	95.83	1015.12
30	8.94E+06	3.83E+06	10.00	2.00	6.00	95.83	1015.12
35	8.30E+06	4.47E+06	10.00	2.00	6.00	95.83	1015.12
40	7.66E+06	5.11E+06	10.00	2.00	6.00	95.83	1015.12
45	7.02E+06	5.75E+06	8.00	2.00	6.00	95.83	1015.12
50	6.39E+06	6.39E+06	8.00	2.00	6.00	95.83	1015.12
55	5.75E+06	7.02E+06	7.00	3.00	6.00	95.83	1015.12
60	5.11E+06	7.66E+06	6.00	3.00	6.00	95.83	1015.12
65	4.47E+06	8.30E+06	6.00	3.00	6.00	95.83	1015.12
70	3.83E+06	8.94E+06	5.00	3.00	6.00	95.83	1015.12
75	3.19E+06	9.58E+06	4.00	3.00	6.00	95.83	1015.12
80	2.55E+06	1.02E+07	4.00	4.00	6.00	95.83	1015.12
85	1.92E+06	1.09E+07	3.00	4.00	6.00	95.83	1015.12
90	1.28E+06	1.15E+07	2.00	4.00	6.00	95.83	1015.12
95	6.39E+05	1.21E+07	2.00	4.00	6.00	95.83	1015.12

Table C.12 October results of power-MSF-RO configuration

RO load %	MSF demand m^3	RO demand m^3	MSF units	RO units	NT	Fuel cost million $/month	CO_2 emissions ktonne/month
5	1.15E+07	6.04E+05	13	1	5	96.17	1027.09
10	1.09E+07	1.21E+06	12	1	5	91.62	976.10
15	1.03E+07	1.81E+06	11	1	5	87.07	925.12
20	9.67E+06	2.42E+06	11	1	5	87.07	925.12
25	9.06E+06	3.02E+06	10	1	5	82.52	874.13
30	8.46E+06	3.63E+06	10	2	5	82.52	874.13
35	7.86E+06	4.23E+06	9	2	5	82.52	874.13
40	7.25E+06	4.83E+06	8	2	5	82.52	874.13
45	6.65E+06	5.44E+06	8	2	5	82.52	874.13
50	6.04E+06	6.04E+06	7	2	5	82.52	874.13
55	5.44E+06	6.65E+06	7	2	5	82.52	874.13
60	4.83E+06	7.25E+06	6	3	5	82.52	874.13
65	4.23E+06	7.86E+06	5	3	5	82.52	874.13
70	3.63E+06	8.46E+06	5	3	5	82.52	874.13
75	3.02E+06	9.06E+06	4	3	5	82.52	874.13
80	2.42E+06	9.67E+06	4	3	5	82.52	874.13
85	1.81E+06	1.03E+07	3	4	5	82.52	874.13
90	1.21E+06	1.09E+07	2	4	5	82.52	874.13
95	6.04E+05	1.15E+07	2	4	5	82.52	874.13

Table C.13 November results of power-MSF-RO configuration

RO load %	MSF demand m^3	RO demand m^3	MSF units	RO units	NT	Fuel cost million $/month	CO_2 emissions ktonne/month
5	1.13E+07	5.95E+05	13	1	4	85.90	923.45
10	1.07E+07	1.19E+06	12	1	4	81.50	874.11
15	1.01E+07	1.78E+06	11	1	4	77.09	824.77
20	9.52E+06	2.38E+06	11	1	4	77.09	824.77
25	8.92E+06	2.97E+06	10	1	4	72.69	775.43
30	8.33E+06	3.57E+06	10	2	4	72.69	775.43
35	7.73E+06	4.16E+06	9	2	4	68.29	726.09
40	7.14E+06	4.76E+06	8	2	4	63.89	676.75
45	6.54E+06	5.35E+06	8	2	4	63.89	676.75
50	5.95E+06	5.95E+06	7	2	4	63.89	676.75
55	5.35E+06	6.54E+06	7	2	4	63.89	676.75
60	4.76E+06	7.14E+06	6	3	4	63.89	676.75
65	4.16E+06	7.73E+06	5	3	4	63.89	676.75
70	3.57E+06	8.33E+06	5	3	4	63.89	676.75
75	2.97E+06	8.92E+06	4	3	4	63.89	676.75
80	2.38E+06	9.52E+06	4	3	4	63.89	676.75
85	1.78E+06	1.01E+07	3	4	4	63.89	676.75
90	1.19E+06	1.07E+07	2	4	4	63.89	676.75
95	5.95E+05	1.13E+07	2	4	4	63.89	676.75

Table C.14 December results of power-MSF-RO configuration

RO load %	MSF demand m^3	RO demand m^3	MSF units	RO units	NT	Fuel cost million $/month	CO_2 emissions ktonne/month
5	1.11E+07	5.83E+05	12	1	3	74.33	803.61
10	1.05E+07	1.17E+06	12	1	3	74.33	803.61
15	9.91E+06	1.75E+06	11	1	3	69.92	754.27
20	9.32E+06	2.33E+06	11	1	3	69.92	754.27
25	8.74E+06	2.91E+06	10	1	3	65.52	704.92
30	8.16E+06	3.50E+06	9	2	3	61.12	655.58
35	7.57E+06	4.08E+06	9	2	3	61.12	655.58
40	6.99E+06	4.66E+06	8	2	3	56.72	606.24
45	6.41E+06	5.24E+06	8	2	3	56.72	606.24
50	5.83E+06	5.83E+06	7	2	3	52.32	556.90
55	5.24E+06	6.41E+06	7	2	3	52.32	556.90
60	4.66E+06	6.99E+06	6	3	3	47.92	507.56
65	4.08E+06	7.57E+06	5	3	3	47.92	507.56
70	3.50E+06	8.16E+06	5	3	3	47.92	507.56
75	2.91E+06	8.74E+06	4	3	3	47.92	507.56
80	2.33E+06	9.32E+06	4	3	3	47.92	507.56
85	1.75E+06	9.91E+06	3	4	3	47.92	507.56
90	1.17E+06	1.05E+07	2	4	3	47.92	507.56
95	5.83E+05	1.11E+07	2	4	3	47.92	507.56

C.4. Power-MSF-AR Configuration

Table C.15 March results of power-MSF-AR configuration

AR load %	MSF units	AR units	NT	Fuel cost million $	CO_2 emissions ktonne
0	12.00	0	3	77	812
10	12.00	11	3	80.8	872.73
20	12.00	21	3	81.673	881.97
30	12.00	31	3	82.54	891.16
40	12.00	41	3	83.4	900.27
50	12.00	52	3	84.339	910.22
60	12.00	62	3	85.185	919.17
70	12.00	72	3	86.022	928.05
80	12.00	82	3	86.852	936.83
90	12.00	93	3	87.753	946.38
100	12.00	103	3	88.563	954.95

Table C.16 April results of power-MSF-AR configuration

AR load %	MSF units	AR units	NT	Fuel cost million $	CO_2 emissions ktonne
0	14.00	0	4	90.30	955
10	14.00	20	4	95.907	1032.2
20	14.00	40	4	97.589	1050
30	14.00	59	4	99.17	1066.8
40	14.00	79	4	100.81	1084.2
50	14.00	98	4	102.36	1100.5
60	14.00	118	4	103.95	1117.4
70	14.00	137	3	97.092	1050.2
80	14.00	157	3	98.544	1065.6
90	14.00	176	3	99.87	1079.6
100	14.00	196	3	101.2	1093.7

Table C.17 May results of power-MSF-AR configuration

AR load %	MSF units	AR units	NT	Fuel cost million $	CO_2 emissions ktonne
0	14.00	0	5	105.77	1131.56
10	14.00	36	5	108.92	1165
20	14.00	72	5	112.03	1197.9
30	14.00	107	5	114.99	1229.3
40	14.00	143	4	109.44	1176.1
50	14.00	178	4	112.19	1205.2
60	14.00	214	4	114.89	1233.8
70	14.00	250	4	117.44	1260.8
80	14.00	286	4	119.82	1286
90	14.00	321	3	111.22	1200.6
100	14.00	357	3	114.32	1233.4

Table C.18 June results of power-MSF-AR configuration

AR load %	MSF units	AR units	NT	Fuel cost million $	CO_2 emissions ktonne
0	15.00	0	6	114.90	1225
10	15.00	40	6	118.3	1261.2
20	15.00	79	5	113.39	1214.7
30	15.00	119	5	116.66	1249.3
40	15.00	158	5	119.77	1282.2
50	15.00	198	5	122.86	1315
60	15.00	237	4	117.18	1260.3
70	15.00	276	4	119.73	1287.3
80	15.00	316	4	122.13	1312.6
90	15.00	355	3	114.95	1242.1
100	15.00	395	3	118.47	1279.3

Table C.19 July results of power-MSF-AR configuration

AR load %	MSF units	AR units	NT	Fuel cost million $	CO_2 emissions ktonne
0	14.00	0	6	114.18	1215.11
10	14.00	44	6	118.04	1255.9
20	14.00	88	6	121.83	1296.1
30	14.00	131	5	117	1250.5
40	14.00	175	5	120.58	1288.5
50	14.00	218	5	123.97	1324.4
60	14.00	262	4	118.25	1269.5
70	14.00	306	4	121.05	1299.1
80	14.00	349	4	123.48	1324.9
90	14.00	393	4	125.62	1347.5
100	14.00	436	3	121.92	1313.9

Table C.20 August results of power-MSF-AR configuration

AR load %	MSF units	AR units	NT	Fuel cost million $	CO_2 emissions ktonne
0	15.00	0	7	118.73	1266.10
10	15.00	47	6	122.85	1309.7
20	15.00	94	6	126.89	1352.5
30	15.00	140	5	122.29	1309.4
40	15.00	187	5	126.09	1349.6
50	15.00	233	5	129.67	1387.5
60	15.00	280	5	133.15	1424.4
70	15.00	326	5	136.35	1458.3
80	15.00	373	4	129.24	1388.7
90	15.00	420	4	131.31	1410.5
100	15.00	466	4	135.32	1453

Table C.21 September results of power-MSF-AR configuration

AR load %	MSF units	AR units	NT	Fuel cost million $	CO_2 emissions ktonne
0	14.00	0	6	110.50	1175.92
10	14.00	42	6	114.06	1213.6
20	14.00	84	5	109.4	1169.7
30	14.00	125	5	112.74	1205.1
40	14.00	167	5	116.07	1240.3
50	14.00	208	5	119.22	1273.7
60	14.00	250	4	113.65	1220.2
70	14.00	292	4	116.32	1248.4
80	14.00	334	4	118.72	1273.8
90	14.00	375	4	120.77	1295.5
100	14.00	417	3	115.07	1240.6

Table C.22 October results of power-MSF-AR configuration

AR load %	MSF units	AR units	NT	Fuel cost million $	CO_2 emissions ktonne
0	13.00	0	5	101.22	1080.58
10	13.00	25	5	103.41	1103.8
20	13.00	51	4	97.241	1044.1
30	13.00	76	4	99.373	1066.6
40	13.00	101	4	101.47	1088.8
50	13.00	126	4	103.52	1110.6
60	13.00	151	4	105.53	1131.9
70	13.00	177	4	107.72	1155.1
80	13.00	202	4	109.87	1177.8
90	13.00	227	3	103.78	1119
100	13.00	252	3	106.03	1142.8

Table C.23 November results of power-MSF-AR configuration

AR load %	MSF units	AR units	NT	Fuel cost million $	CO_2 emissions ktonne
0	13.00	0	4	89.81	964.86
10	13.00	13	4	90.912	976.58
20	13.00	25	4	91.927	987.33
30	13.00	38	3	84.862	917.93
40	13.00	50	3	85.855	928.45
50	13.00	63	3	86.92	939.73
60	13.00	75	3	87.891	950.01
70	13.00	88	3	88.929	961.01
80	13.00	100	3	89.873	971.01
90	13.00	113	3	90.88	981.68
100	13.00	125	3	91.89	992.37

C.5. Power-RO-AR Configuration

Table C.24 March results of power-RO-AR configuration

AR load %	RO units	AR units	NT	Fuel cost million $	CO_2 emissions ktonne
0	4	0	4	62.00	661.00
10	4	11	4	61.639	652.91
20	4	21	4	62.05	657.26
30	4	31	4	62.461	661.61
40	4	41	4	62.872	665.96
50	4	52	4	63.324	670.75
60	4	62	3	48.438	513.07
70	4	72	3	48.848	517.42
80	4	82	3	49.259	521.77
90	4	93	3	49.913	528.82
100	4	103	3	50.991	540.64

Table C.25 April results of power-RO-AR configuration

AR load %	RO units	AR units	NT	Fuel cost million $	CO_2 emissions ktonne
0	4	0	5	74.02	784.02
10	4	20	4	60.01	635.64
20	4	40	4	60.80	644.06
30	4	59	4	61.56	652.06
40	4	79	4	62.35	660.48
50	4	98	4	63.11	668.48
60	4	118	4	63.90	676.91
70	4	137	4	66.33	703.56
80	4	157	4	69.08	733.89
90	4	176	4	71.69	762.69
100	4	196	3	59.05	629.59

Table C.26 May results of power-RO-AR configuration

AR load %	RO units	AR units	NT	Fuel cost million $	CO_2 emissions ktonne
0	4	0	5	76.48	810.15
10	4	36	5	77.96	825.82
20	4	72	5	79.44	841.48
30	4	107	5	80.88	856.71
40	4	143	5	82.36	872.38
50	4	178	4	74.36	791.25
60	4	214	4	79.48	847.65
70	4	250	4	84.60	904.05
80	4	286	4	89.71	960.45
90	4	321	4	99.31	1066.28
100	4	357	4	110.09	1185.11

Table C.27 June results of power-RO-AR configuration

AR load %	RO units	AR units	NT	Fuel cost million $	CO_2 emissions ktonne
0	4	0	6	88.82	940.82
10	4	40	6	90.41	957.67
20	4	79	6	91.96	974.09
30	4	119	6	93.55	990.93
40	4	158	5	81.35	862.36
50	4	198	5	88.18	937.89
60	4	237	5	94.84	1011.54
70	4	276	4	85.44	914.31
80	4	316	4	95.35	1023.53
90	4	355	4	106.21	1143.23
100	4	395	4	118.34	1276.90

Table C.28 July results of power-RO-AR configuration

AR load %	RO units	AR units	NT	Fuel cost million $	CO_2 emissions ktonne
0	4	0	7	107.08	1134.20
10	4	44	6	93.59	991.33
20	4	88	6	95.40	1010.48
30	4	131	6	97.16	1029.19
40	4	175	5	87.06	924.28
50	4	218	5	94.65	1008.18
60	4	262	5	102.41	1094.04
70	4	306	4	96.97	1040.40
80	4	349	4	108.73	1170.03
90	4	393	4	121.91	1315.37
100	4	436	4	136.16	1472.49

Table C.29 August results of power-RO-AR configuration

AR load %	RO units	AR units	NT	Fuel cost million $	CO_2 emissions ktonne
0	4	0	7	107.08	1134.20
10	4	47	7	109.01	1154.66
20	4	94	6	95.64	1013.09
30	4	140	6	97.53	1033.10
40	4	187	6	100.66	1066.97
50	4	233	5	97.30	1037.45
60	4	280	5	105.59	1129.16
70	4	326	5	113.71	1218.92
80	4	373	4	118.20	1274.51
90	4	420	4	126.92	1370.54
100	4	466	4	142.16	1538.55

Table C.30 September results of power-RO-AR configuration

AR load %	RO units	AR units	NT	Fuel cost million $	CO_2 emissions ktonne
0	4	0	6	88.82	940.82
10	4	42	6	90.49	958.51
20	4	84	6	92.16	976.20
30	4	125	5	78.99	836.66
40	4	167	5	82.89	879.35
50	4	208	5	89.89	956.78
60	4	250	5	97.06	1036.09
70	4	292	4	87.65	938.57
80	4	334	4	102.74	1104.94
90	4	375	4	114.75	1237.35
100	4	417	4	122.28	1320.40

Table C.31 October results of power-RO-AR configuration

AR load %	RO units	AR units	NT	Fuel cost million $	CO_2 emissions ktonne
0	4	0	5	76.48	810.15
10	4	25	5	77.51	821.03
20	4	51	5	78.58	832.34
30	4	76	5	79.61	834.98
40	4	101	4	65.34	692.07
50	4	126	4	66.97	709.78
60	4	151	4	70.53	748.95
70	4	177	4	74.22	789.68
80	4	202	4	77.78	828.85
90	4	227	4	81.33	868.02
100	4	252	4	84.88	907.19

Table C.32 November results of power-RO-AR configuration

AR load %	RO units	AR units	NT	Fuel cost million $	CO_2 emissions ktonne
0	4	0	4	59.21	627.21
10	4	13	4	59.73	632.69
20	4	25	4	60.21	637.74
30	4	38	4	60.72	643.22
40	4	50	4	61.20	648.27
50	4	63	4	61.72	653.74
60	4	75	4	62.20	658.80
70	4	88	4	62.71	664.27
80	4	100	4	63.19	669.33
90	4	113	4	63.71	674.80
100	4	125	3	51.64	548.37

C.6. Power-MSF-RO-AR Configuration

March

Table C.33 Results of power-MSF-RO-AR Configuration for March at 10% AR load

RO load %	MSF demand m^3	RO demand m^3	MSF units	RO units	AR units	NT	Fuel cost million $	CO_2 emissions ktonne
5	1.04E+07	5.49E+05	11	1	11	3	76.25	821.74
10	9.88E+06	1.10E+06	11	1	11	3	76.25	821.74
15	9.33E+06	1.65E+06	10	1	11	3	71.70	770.76
20	8.78E+06	2.19E+06	10	1	11	3	71.70	770.76
25	8.23E+06	2.74E+06	9	1	11	3	67.16	719.77
30	7.68E+06	3.29E+06	9	1	11	3	67.16	719.77
35	7.13E+06	3.84E+06	8	2	11	3	62.61	668.78
40	6.58E+06	4.39E+06	8	2	11	3	62.61	668.78
45	6.04E+06	4.94E+06	7	2	11	3	58.06	617.80
50	5.49E+06	5.49E+06	7	2	11	3	58.06	617.80
55	4.94E+06	6.04E+06	6	2	11	3	53.51	566.81
60	4.39E+06	6.58E+06	5	2	11	3	53.51	566.81
65	3.84E+06	7.13E+06	5	3	11	3	53.51	566.81
70	3.29E+06	7.68E+06	4	3	11	3	53.51	566.81
75	2.74E+06	8.23E+06	4	3	11	3	53.51	566.81
80	2.19E+06	8.78E+06	3	3	11	3	53.51	566.81
85	1.65E+06	9.33E+06	3	3	11	3	53.51	566.81
90	1.10E+06	9.88E+06	2	3	11	3	53.51	566.81
95	5.49E+05	1.04E+07	2	4	11	4	71.03	752.34

Table C.34 Results of power-MSF-RO-AR Configuration for March at 20% AR load

RO load %	MSF demand m^3	RO demand m^3	MSF units	RO units	AR units	NT	Fuel cost million $	CO_2 emissions ktonne
5	1.04E+07	5.49E+05	11	1	21	3	77.13	830.99
10	9.88E+06	1.10E+06	11	1	21	3	77.13	830.99
15	9.33E+06	1.65E+06	10	1	21	3	72.58	780.00
20	8.78E+06	2.19E+06	10	1	21	3	72.58	780.00
25	8.23E+06	2.74E+06	9	1	21	3	68.03	729.02
30	7.68E+06	3.29E+06	9	1	21	3	68.03	729.02
35	7.13E+06	3.84E+06	8	2	21	3	63.48	678.03
40	6.58E+06	4.39E+06	8	2	21	3	63.48	678.03
45	6.04E+06	4.94E+06	7	2	21	3	58.93	627.04
50	5.49E+06	5.49E+06	7	2	21	3	58.93	627.04
55	4.94E+06	6.04E+06	6	2	21	3	54.38	576.06
60	4.39E+06	6.58E+06	5	2	21	3	54.38	576.06
65	3.84E+06	7.13E+06	5	3	21	3	54.38	576.06
70	3.29E+06	7.68E+06	4	3	21	3	54.38	576.06
75	2.74E+06	8.23E+06	4	3	21	3	54.38	576.06
80	2.19E+06	8.78E+06	3	3	21	3	54.38	576.06
85	1.65E+06	9.33E+06	3	3	21	3	54.38	576.06
90	1.10E+06	9.88E+06	2	3	21	3	54.38	576.06
95	5.49E+05	1.04E+07	2	4	21	4	71.90	761.61

Table C.35 Results of power-MSF-RO-AR Configuration for March at 30% AR load

RO load %	MSF demand m^3	RO demand m^3	MSF units	RO units	AR units	NT	Fuel cost million $	CO_2 emissions ktonne
5	1.04E+07	5.49E+05	11	1	31	3	77.99	840.17
10	9.88E+06	1.10E+06	11	1	31	3	77.99	840.17
15	9.33E+06	1.65E+06	10	1	31	3	73.44	789.19
20	8.78E+06	2.19E+06	10	1	31	3	73.44	789.19
25	8.23E+06	2.74E+06	9	1	31	3	68.90	738.20
30	7.68E+06	3.29E+06	9	1	31	3	68.90	738.20
35	7.13E+06	3.84E+06	8	2	31	3	64.35	687.21
40	6.58E+06	4.39E+06	8	2	31	3	64.35	687.21
45	6.04E+06	4.94E+06	7	2	31	3	59.80	636.23
50	5.49E+06	5.49E+06	7	2	31	3	59.80	636.23
55	4.94E+06	6.04E+06	6	2	31	3	55.25	585.24
60	4.39E+06	6.58E+06	5	2	31	3	55.25	585.24
65	3.84E+06	7.13E+06	5	3	31	3	55.25	585.24
70	3.29E+06	7.68E+06	4	3	31	3	55.25	585.24
75	2.74E+06	8.23E+06	4	3	31	3	55.25	585.24
80	2.19E+06	8.78E+06	3	3	31	3	55.25	585.24
85	1.65E+06	9.33E+06	3	3	31	3	55.25	585.24
90	1.10E+06	9.88E+06	2	3	31	3	55.25	585.24
95	5.49E+05	1.04E+07	2	4	31	4	72.77	770.84

Table C.36 Results of power-MSF-RO-AR Configuration for March at 40% AR load

RO load %	MSF demand m^3	RO demand m^3	MSF units	RO units	AR units	NT	Fuel cost million $	CO_2 emissions ktonne
5	1.04E+07	5.49E+05	11	1	41	3	78.85	849.29
10	9.88E+06	1.10E+06	11	1	41	3	78.85	849.29
15	9.33E+06	1.65E+06	10	1	41	3	74.30	798.30
20	8.78E+06	2.19E+06	10	1	41	3	74.30	798.30
25	8.23E+06	2.74E+06	9	1	41	3	69.76	747.31
30	7.68E+06	3.29E+06	9	1	41	3	69.76	747.31
35	7.13E+06	3.84E+06	8	2	41	3	65.21	696.33
40	6.58E+06	4.39E+06	8	2	41	3	65.21	696.33
45	6.04E+06	4.94E+06	7	2	41	3	60.66	645.34
50	5.49E+06	5.49E+06	7	2	41	3	60.66	645.34
55	4.94E+06	6.04E+06	6	2	41	3	56.11	594.36
60	4.39E+06	6.58E+06	5	2	41	3	56.11	594.36
65	3.84E+06	7.13E+06	5	3	41	3	56.11	594.36
70	3.29E+06	7.68E+06	4	3	41	3	56.11	594.36
75	2.74E+06	8.23E+06	4	3	41	3	56.11	594.36
80	2.19E+06	8.78E+06	3	3	41	3	56.11	594.36
85	1.65E+06	9.33E+06	3	3	41	3	56.11	594.36
90	1.10E+06	9.88E+06	2	3	41	3	56.11	594.36
95	5.49E+05	1.04E+07	2	4	41	4	73.64	780.02

Table C.37 Results of power-MSF-RO-AR Configuration for March at 50% AR load

RO load %	MSF demand m^3	RO demand m^3	MSF units	RO units	AR units	NT	Fuel cost million $	CO_2 emissions ktonne
5	1.04E+07	5.49E+05	11	1	52	3	79.79	859.23
10	9.88E+06	1.10E+06	11	1	52	3	79.79	859.23
15	9.33E+06	1.65E+06	10	1	52	3	75.24	808.24
20	8.78E+06	2.19E+06	10	1	52	3	75.24	808.24
25	8.23E+06	2.74E+06	9	1	52	3	70.70	757.26
30	7.68E+06	3.29E+06	9	1	52	3	70.70	757.26
35	7.13E+06	3.84E+06	8	2	52	3	66.15	706.27
40	6.58E+06	4.39E+06	8	2	52	3	66.15	706.27
45	6.04E+06	4.94E+06	7	2	52	3	61.60	655.29
50	5.49E+06	5.49E+06	7	2	52	3	61.60	655.29
55	4.94E+06	6.04E+06	6	2	52	3	57.05	604.30
60	4.39E+06	6.58E+06	5	2	52	3	57.05	604.30
65	3.84E+06	7.13E+06	5	3	52	3	57.05	604.30
70	3.29E+06	7.68E+06	4	3	52	3	57.05	604.30
75	2.74E+06	8.23E+06	4	3	52	3	57.05	604.30
80	2.19E+06	8.78E+06	3	3	52	3	57.05	604.30
85	1.65E+06	9.33E+06	3	3	52	3	57.05	604.30
90	1.10E+06	9.88E+06	2	3	52	3	57.05	604.30
95	5.49E+05	1.04E+07	2	4	52	4	74.59	790.05

Table C.38 Results of power-MSF-RO-AR Configuration for March at 60% AR load

RO load %	MSF demand m^3	RO demand m^3	MSF units	RO units	AR units	NT	Fuel cost million $	CO_2 emissions ktonne
5	1.04E+07	5.49E+05	11	1	62	3	80.64	868.19
10	9.88E+06	1.10E+06	11	1	62	3	80.64	868.19
15	9.33E+06	1.65E+06	10	1	62	3	76.09	817.20
20	8.78E+06	2.19E+06	10	1	62	3	76.09	817.20
25	8.23E+06	2.74E+06	9	1	62	3	71.54	766.21
30	7.68E+06	3.29E+06	9	1	62	3	71.54	766.21
35	7.13E+06	3.84E+06	8	2	62	3	66.99	715.23
40	6.58E+06	4.39E+06	8	2	62	3	66.99	715.23
45	6.04E+06	4.94E+06	7	2	62	3	62.44	664.24
50	5.49E+06	5.49E+06	7	2	62	3	62.44	664.24
55	4.94E+06	6.04E+06	6	2	62	3	57.90	613.26
60	4.39E+06	6.58E+06	5	2	62	3	57.90	613.26
65	3.84E+06	7.13E+06	5	3	62	3	57.90	613.26
70	3.29E+06	7.68E+06	4	3	62	3	57.90	613.26
75	2.74E+06	8.23E+06	4	3	62	3	57.90	613.26
80	2.19E+06	8.78E+06	3	3	62	3	57.90	613.26
85	1.65E+06	9.33E+06	3	3	62	3	57.90	613.26
90	1.10E+06	9.88E+06	2	3	62	3	57.90	613.26
95	5.49E+05	1.04E+07	2	4	62	3	57.90	613.26

Table C.39 Results of power-MSF-RO-AR Configuration for March at 70% AR load

RO load %	MSF demand m^3	RO demand m^3	MSF units	RO units	AR units	NT	Fuel cost million $	CO_2 emissions ktonne
5	1.04E+07	5.49E+05	11	1	72	3	81.47	877.06
10	9.88E+06	1.10E+06	11	1	72	3	81.47	877.06
15	9.33E+06	1.65E+06	10	1	72	3	76.93	826.07
20	8.78E+06	2.19E+06	10	1	72	3	76.93	826.07
25	8.23E+06	2.74E+06	9	1	72	3	72.38	775.09
30	7.68E+06	3.29E+06	9	1	72	3	72.38	775.09
35	7.13E+06	3.84E+06	8	2	72	3	67.83	724.10
40	6.58E+06	4.39E+06	8	2	72	3	67.83	724.10
45	6.04E+06	4.94E+06	7	2	72	3	63.28	673.12
50	5.49E+06	5.49E+06	7	2	72	3	63.28	673.12
55	4.94E+06	6.04E+06	6	2	72	3	58.73	622.13
60	4.39E+06	6.58E+06	5	2	72	3	58.73	622.13
65	3.84E+06	7.13E+06	5	3	72	3	58.73	622.13
70	3.29E+06	7.68E+06	4	3	72	3	58.73	622.13
75	2.74E+06	8.23E+06	4	3	72	3	58.73	622.13
80	2.19E+06	8.78E+06	3	3	72	3	58.73	622.13
85	1.65E+06	9.33E+06	3	3	72	3	58.73	622.13
90	1.10E+06	9.88E+06	2	3	72	3	58.73	622.13
95	5.49E+05	1.04E+07	2	4	72	3	58.73	622.13

Table C.40 Results of power-MSF-RO-AR Configuration for March at 80% AR load

RO load %	MSF demand m^3	RO demand m^3	MSF units	RO units	AR units	NT	Fuel cost million $	CO_2 emissions ktonne
5	1.04E+07	5.49E+05	11	1	82	3	82.30	885.84
10	9.88E+06	1.10E+06	11	1	82	3	82.30	885.84
15	9.33E+06	1.65E+06	10	1	82	3	77.76	834.86
20	8.78E+06	2.19E+06	10	1	82	3	77.76	834.86
25	8.23E+06	2.74E+06	9	1	82	3	73.21	783.87
30	7.68E+06	3.29E+06	9	1	82	3	73.21	783.87
35	7.13E+06	3.84E+06	8	2	82	3	68.66	732.89
40	6.58E+06	4.39E+06	8	2	82	3	68.66	732.89
45	6.04E+06	4.94E+06	7	2	82	3	64.11	681.90
50	5.49E+06	5.49E+06	7	2	82	3	64.11	681.90
55	4.94E+06	6.04E+06	6	2	82	3	59.56	630.91
60	4.39E+06	6.58E+06	5	2	82	3	59.56	630.91
65	3.84E+06	7.13E+06	5	3	82	3	59.56	630.91
70	3.29E+06	7.68E+06	4	3	82	3	59.56	630.91
75	2.74E+06	8.23E+06	4	3	82	3	59.56	630.91
80	2.19E+06	8.78E+06	3	3	82	3	59.56	630.91
85	1.65E+06	9.33E+06	3	3	82	3	59.56	630.91
90	1.10E+06	9.88E+06	2	3	82	3	59.56	630.91
95	5.49E+05	1.04E+07	2	4	82	3	59.56	630.91

Table C.41 Results of power-MSF-RO-AR Configuration for March at 90% AR load

RO load %	MSF demand m^3	RO demand m^3	MSF units	RO units	AR units	NT	Fuel cost million $	CO_2 emissions ktonne
5	1.04E+07	5.49E+05	11	1	93	3	83.21	895.39
10	9.88E+06	1.10E+06	11	1	93	3	83.21	895.39
15	9.33E+06	1.65E+06	10	1	93	3	78.66	844.41
20	8.78E+06	2.19E+06	10	1	93	3	78.66	844.41
25	8.23E+06	2.74E+06	9	1	93	3	74.11	793.42
30	7.68E+06	3.29E+06	9	1	93	3	74.11	793.42
35	7.13E+06	3.84E+06	8	2	93	3	69.56	742.44
40	6.58E+06	4.39E+06	8	2	93	3	69.56	742.44
45	6.04E+06	4.94E+06	7	2	93	3	65.01	691.45
50	5.49E+06	5.49E+06	7	2	93	3	65.01	691.45
55	4.94E+06	6.04E+06	6	2	93	3	60.46	640.46
60	4.39E+06	6.58E+06	5	2	93	3	60.46	640.46
65	3.84E+06	7.13E+06	5	3	93	3	60.46	640.46
70	3.29E+06	7.68E+06	4	3	93	3	60.46	640.46
75	2.74E+06	8.23E+06	4	3	93	3	60.46	640.46
80	2.19E+06	8.78E+06	3	3	93	3	60.46	640.46
85	1.65E+06	9.33E+06	3	3	93	3	60.46	640.46
90	1.10E+06	9.88E+06	2	3	93	3	60.46	640.46
95	5.49E+05	1.04E+07	2	4	93	3	60.46	640.46

Table C.42 Results of power-MSF-RO-AR Configuration for March at 100% AR load

RO load %	MSF demand m^3	RO demand m^3	MSF units	RO units	AR units	NT	Fuel cost million $	CO_2 emissions ktonne
5	1.04E+07	5.49E+05	11	1	103	3	84.02	903.97
10	9.88E+06	1.10E+06	11	1	103	3	84.02	903.97
15	9.33E+06	1.65E+06	10	1	103	3	79.47	852.98
20	8.78E+06	2.19E+06	10	1	103	3	79.47	852.98
25	8.23E+06	2.74E+06	9	1	103	3	74.92	802.00
30	7.68E+06	3.29E+06	9	1	103	3	74.92	802.00
35	7.13E+06	3.84E+06	8	2	103	3	70.37	751.01
40	6.58E+06	4.39E+06	8	2	103	3	70.37	751.01
45	6.04E+06	4.94E+06	7	2	103	3	65.82	700.02
50	5.49E+06	5.49E+06	7	2	103	3	65.82	700.02
55	4.94E+06	6.04E+06	6	2	103	3	61.27	649.04
60	4.39E+06	6.58E+06	5	2	103	3	61.27	649.04
65	3.84E+06	7.13E+06	5	3	103	3	61.27	649.04
70	3.29E+06	7.68E+06	4	3	103	3	61.27	649.04
75	2.74E+06	8.23E+06	4	3	103	3	61.27	649.04
80	2.19E+06	8.78E+06	3	3	103	3	61.27	649.04
85	1.65E+06	9.33E+06	3	3	103	3	61.27	649.04
90	1.10E+06	9.88E+06	2	3	103	3	61.27	649.04
95	5.49E+05	1.04E+07	2	4	103	3	61.27	649.04

April

Table C.43 Results of power-MSF-RO-AR Configuration for April at 10% AR load

RO load %	MSF demand m^3	RO demand m^3	MSF units	RO units	AR units	NT	Fuel cost million $	CO_2 emissions ktonne
5	1.16E+07	6.10E+05	13	1	20	4	91.51	982.86
10	1.10E+07	1.22E+06	12	1	20	4	87.10	933.52
15	1.04E+07	1.83E+06	12	1	20	4	87.10	933.52
20	9.76E+06	2.44E+06	11	1	20	4	82.70	884.17
25	9.15E+06	3.05E+06	10	1	20	4	78.30	834.83
30	8.54E+06	3.66E+06	10	2	20	4	78.30	834.83
35	7.93E+06	4.27E+06	9	2	20	4	73.90	785.49
40	7.32E+06	4.88E+06	9	2	20	4	73.90	785.49
45	6.71E+06	5.49E+06	8	2	20	4	69.50	736.15
50	6.10E+06	6.10E+06	7	2	20	4	69.50	736.15
55	5.49E+06	6.71E+06	7	3	20	4	69.50	736.15
60	4.88E+06	7.32E+06	6	3	20	4	69.50	736.15
65	4.27E+06	7.93E+06	6	3	20	4	69.50	736.15
70	3.66E+06	8.54E+06	5	3	20	4	69.50	736.15
75	3.05E+06	9.15E+06	4	3	20	4	69.50	736.15
80	2.44E+06	9.76E+06	4	3	20	4	69.50	736.15
85	1.83E+06	1.04E+07	3	4	20	4	69.50	736.15
90	1.22E+06	1.10E+07	2	4	20	4	69.50	736.15
95	6.10E+05	1.16E+07	2	4	20	4	69.50	736.15

Table C.44 Results of power-MSF-RO-AR Configuration for April at 20% AR load

RO load %	MSF demand m^3	RO demand m^3	MSF units	RO units	AR units	NT	Fuel cost million $	CO_2 emissions ktonne
5	1.16E+07	6.10E+05	13	1	40	4	93.19	1000.70
10	1.10E+07	1.22E+06	12	1	40	4	88.79	951.33
15	1.04E+07	1.83E+06	12	1	40	4	88.79	951.33
20	9.76E+06	2.44E+06	11	1	40	4	84.38	901.99
25	9.15E+06	3.05E+06	10	1	40	4	79.98	852.65
30	8.54E+06	3.66E+06	10	2	40	4	79.98	852.65
35	7.93E+06	4.27E+06	9	2	40	4	75.58	803.31
40	7.32E+06	4.88E+06	9	2	40	4	75.58	803.31
45	6.71E+06	5.49E+06	8	2	40	4	71.18	753.97
50	6.10E+06	6.10E+06	7	2	40	4	71.18	753.97
55	5.49E+06	6.71E+06	7	3	40	4	71.18	753.97
60	4.88E+06	7.32E+06	6	3	40	4	71.18	753.97
65	4.27E+06	7.93E+06	6	3	40	4	71.18	753.97
70	3.66E+06	8.54E+06	5	3	40	4	71.18	753.97
75	3.05E+06	9.15E+06	4	3	40	4	71.18	753.97
80	2.44E+06	9.76E+06	4	3	40	4	71.18	753.97
85	1.83E+06	1.04E+07	3	4	40	4	71.18	753.97
90	1.22E+06	1.10E+07	2	4	40	4	71.18	753.97
95	6.10E+05	1.16E+07	2	4	40	4	71.18	753.97

Table C.45 Results of power-MSF-RO-AR Configuration for April at 30% AR load

RO load %	MSF demand m^3	RO demand m^3	MSF units	RO units	AR units	NT	Fuel cost million $	CO_2 emissions ktonne
5	1.16E+07	6.10E+05	13	1	59	4	94.77	1017.40
10	1.10E+07	1.22E+06	12	1	59	4	90.37	968.08
15	1.04E+07	1.83E+06	12	1	59	4	90.37	968.08
20	9.76E+06	2.44E+06	11	1	59	4	85.97	918.74
25	9.15E+06	3.05E+06	10	1	59	4	81.56	869.40
30	8.54E+06	3.66E+06	10	2	59	4	81.56	869.40
35	7.93E+06	4.27E+06	9	2	59	4	77.16	820.06
40	7.32E+06	4.88E+06	9	2	59	4	77.16	820.06
45	6.71E+06	5.49E+06	8	2	59	4	72.76	770.71
50	6.10E+06	6.10E+06	7	2	59	4	72.76	770.71
55	5.49E+06	6.71E+06	7	3	59	4	72.76	770.71
60	4.88E+06	7.32E+06	6	3	59	4	72.76	770.71
65	4.27E+06	7.93E+06	6	3	59	4	72.76	770.71
70	3.66E+06	8.54E+06	5	3	59	4	72.76	770.71
75	3.05E+06	9.15E+06	4	3	59	4	72.76	770.71
80	2.44E+06	9.76E+06	4	3	59	4	72.76	770.71
85	1.83E+06	1.04E+07	3	4	59	4	72.76	770.71
90	1.22E+06	1.10E+07	2	4	59	4	72.76	770.71
95	6.10E+05	1.16E+07	2	4	59	4	72.76	770.71

Table C.46 Results of power-MSF-RO-AR Configuration for April at 40% AR load

RO load %	MSF demand m^3	RO demand m^3	MSF units	RO units	AR units	NT	Fuel cost million $	CO_2 emissions ktonne
5	1.16E+07	6.10E+05	13	1	79	4	96.41	1034.80
10	1.10E+07	1.22E+06	12	1	79	4	92.01	985.50
15	1.04E+07	1.83E+06	12	1	79	4	92.01	985.50
20	9.76E+06	2.44E+06	11	1	79	4	87.61	936.15
25	9.15E+06	3.05E+06	10	1	79	4	83.21	886.81
30	8.54E+06	3.66E+06	10	2	79	4	83.21	886.81
35	7.93E+06	4.27E+06	9	2	79	4	78.81	837.47
40	7.32E+06	4.88E+06	9	2	79	4	78.81	837.47
45	6.71E+06	5.49E+06	8	2	79	4	74.41	788.13
50	6.10E+06	6.10E+06	7	2	79	4	74.41	788.13
55	5.49E+06	6.71E+06	7	3	79	4	74.41	788.13
60	4.88E+06	7.32E+06	6	3	79	4	74.41	788.13
65	4.27E+06	7.93E+06	6	3	79	4	74.41	788.13
70	3.66E+06	8.54E+06	5	3	79	4	74.41	788.13
75	3.05E+06	9.15E+06	4	3	79	4	74.41	788.13
80	2.44E+06	9.76E+06	4	3	79	4	74.41	788.13
85	1.83E+06	1.04E+07	3	4	79	4	74.41	788.13
90	1.22E+06	1.10E+07	2	4	79	4	74.41	788.13
95	6.10E+05	1.16E+07	2	4	79	4	74.41	788.13

Table C.47 Results of power-MSF-RO-AR Configuration for April at 50% AR load

RO load %	MSF demand m^3	RO demand m^3	MSF units	RO units	AR units	NT	Fuel cost million $	CO_2 emissions ktonne
5	1.16E+07	6.10E+05	13	1	98	4	97.95	1051.20
10	1.10E+07	1.22E+06	12	1	98	4	93.55	1001.80
15	1.04E+07	1.83E+06	12	1	98	4	93.55	1001.80
20	9.76E+06	2.44E+06	11	1	98	4	89.15	952.48
25	9.15E+06	3.05E+06	10	1	98	4	84.75	903.14
30	8.54E+06	3.66E+06	10	2	98	4	84.75	903.14
35	7.93E+06	4.27E+06	9	2	98	4	80.35	853.80
40	7.32E+06	4.88E+06	9	2	98	4	80.35	853.80
45	6.71E+06	5.49E+06	8	2	98	4	75.95	804.46
50	6.10E+06	6.10E+06	7	2	98	4	75.95	804.46
55	5.49E+06	6.71E+06	7	3	98	4	75.95	804.46
60	4.88E+06	7.32E+06	6	3	98	4	75.95	804.46
65	4.27E+06	7.93E+06	6	3	98	4	75.95	804.46
70	3.66E+06	8.54E+06	5	3	98	4	75.95	804.46
75	3.05E+06	9.15E+06	4	3	98	4	75.95	804.46
80	2.44E+06	9.76E+06	4	3	98	4	75.95	804.46
85	1.83E+06	1.04E+07	3	4	98	4	75.95	804.46
90	1.22E+06	1.10E+07	2	4	98	4	75.95	804.46
95	6.10E+05	1.16E+07	2	4	98	4	75.95	804.46

Table C.48 Results of power-MSF-RO-AR Configuration for April at 60% AR load

RO load %	MSF demand m^3	RO demand m^3	MSF units	RO units	AR units	NT	Fuel cost million $	CO_2 emissions ktonne
5	1.16E+07	6.10E+05	13	1	118	4	99.55	1068.10
10	1.10E+07	1.22E+06	12	1	118	4	95.15	1018.70
15	1.04E+07	1.83E+06	12	1	118	4	95.15	1018.70
20	9.76E+06	2.44E+06	11	1	118	4	90.75	969.41
25	9.15E+06	3.05E+06	10	1	118	4	86.35	920.07
30	8.54E+06	3.66E+06	10	2	118	4	86.35	920.07
35	7.93E+06	4.27E+06	9	2	118	4	81.95	870.72
40	7.32E+06	4.88E+06	9	2	118	4	81.95	870.72
45	6.71E+06	5.49E+06	8	2	118	4	77.54	821.38
50	6.10E+06	6.10E+06	7	2	118	4	77.54	821.38
55	5.49E+06	6.71E+06	7	3	118	4	77.54	821.38
60	4.88E+06	7.32E+06	6	3	118	4	77.54	821.38
65	4.27E+06	7.93E+06	6	3	118	4	77.54	821.38
70	3.66E+06	8.54E+06	5	3	118	4	77.54	821.38
75	3.05E+06	9.15E+06	4	3	118	4	77.54	821.38
80	2.44E+06	9.76E+06	4	3	118	4	77.54	821.38
85	1.83E+06	1.04E+07	3	4	118	4	77.54	821.38
90	1.22E+06	1.10E+07	2	4	118	4	77.54	821.38
95	6.10E+05	1.16E+07	2	4	118	4	77.54	821.38

Table C.49 Results of power-MSF-RO-AR Configuration for April at 70% AR load

RO load %	MSF demand m^3	RO demand m^3	MSF units	RO units	AR units	NT	Fuel cost million $	CO_2 emissions ktonne
5	1.16E+07	6.10E+05	13	1	137	4	101.04	1083.90
10	1.10E+07	1.22E+06	12	1	137	4	96.64	1034.60
15	1.04E+07	1.83E+06	12	1	137	4	96.64	1034.60
20	9.76E+06	2.44E+06	11	1	137	4	92.24	985.22
25	9.15E+06	3.05E+06	10	1	137	4	87.84	935.88
30	8.54E+06	3.66E+06	10	2	137	4	87.84	935.88
35	7.93E+06	4.27E+06	9	2	137	4	83.44	886.53
40	7.32E+06	4.88E+06	9	2	137	4	83.44	886.53
45	6.71E+06	5.49E+06	8	2	137	4	79.04	837.19
50	6.10E+06	6.10E+06	7	2	137	4	79.04	837.19
55	5.49E+06	6.71E+06	7	3	137	4	79.04	837.19
60	4.88E+06	7.32E+06	6	3	137	4	79.04	837.19
65	4.27E+06	7.93E+06	6	3	137	4	79.04	837.19
70	3.66E+06	8.54E+06	5	3	137	4	79.04	837.19
75	3.05E+06	9.15E+06	4	3	137	4	79.04	837.19
80	2.44E+06	9.76E+06	4	3	137	4	79.04	837.19
85	1.83E+06	1.04E+07	3	4	137	4	79.04	837.19
90	1.22E+06	1.10E+07	2	4	137	4	79.04	837.19
95	6.10E+05	1.16E+07	2	4	137	4	79.04	837.19

Table C.50 Results of power-MSF-RO-AR Configuration for April at 80% AR load

RO load %	MSF demand m^3	RO demand m^3	MSF units	RO units	AR units	NT	Fuel cost million $	CO_2 emissions ktonne
5	1.16E+07	6.10E+05	13	1	157	3	94.14	1016.20
10	1.10E+07	1.22E+06	12	1	157	3	89.74	966.89
15	1.04E+07	1.83E+06	12	1	157	3	89.74	966.89
20	9.76E+06	2.44E+06	11	1	157	3	85.34	917.55
25	9.15E+06	3.05E+06	10	1	157	3	80.94	868.21
30	8.54E+06	3.66E+06	10	2	157	4	89.38	952.20
35	7.93E+06	4.27E+06	9	2	157	4	84.98	902.86
40	7.32E+06	4.88E+06	9	2	157	4	84.98	902.86
45	6.71E+06	5.49E+06	8	2	157	4	80.58	853.52
50	6.10E+06	6.10E+06	7	2	157	4	80.58	853.52
55	5.49E+06	6.71E+06	7	3	157	4	80.58	853.52
60	4.88E+06	7.32E+06	6	3	157	4	80.58	853.52
65	4.27E+06	7.93E+06	6	3	157	4	80.58	853.52
70	3.66E+06	8.54E+06	5	3	157	4	80.58	853.52
75	3.05E+06	9.15E+06	4	3	157	4	80.58	853.52
80	2.44E+06	9.76E+06	4	3	157	4	80.58	853.52
85	1.83E+06	1.04E+07	3	4	157	4	80.58	853.52
90	1.22E+06	1.10E+07	2	4	157	4	80.58	853.52
95	6.10E+05	1.16E+07	2	4	157	4	80.58	853.52

Table C.51 Results of power-MSF-RO-AR Configuration for April at 90% AR load

RO load %	MSF demand m^3	RO demand m^3	MSF units	RO units	AR units	NT	Fuel cost million $	CO_2 emissions ktonne
5	1.16E+07	6.10E+05	13	1	176	3	95.47	1030.30
10	1.10E+07	1.22E+06	12	1	176	3	91.07	980.94
15	1.04E+07	1.83E+06	12	1	176	3	91.07	980.94
20	9.76E+06	2.44E+06	11	1	176	3	86.67	931.60
25	9.15E+06	3.05E+06	10	1	176	3	82.27	882.26
30	8.54E+06	3.66E+06	10	2	176	3	82.27	882.26
35	7.93E+06	4.27E+06	9	2	176	3	77.86	832.92
40	7.32E+06	4.88E+06	9	2	176	3	77.86	832.92
45	6.71E+06	5.49E+06	8	2	176	3	73.46	783.58
50	6.10E+06	6.10E+06	7	2	176	3	69.06	734.23
55	5.49E+06	6.71E+06	7	3	176	4	82.01	868.70
60	4.88E+06	7.32E+06	6	3	176	4	82.01	868.70
65	4.27E+06	7.93E+06	6	3	176	4	82.01	868.70
70	3.66E+06	8.54E+06	5	3	176	4	82.01	868.70
75	3.05E+06	9.15E+06	4	3	176	4	82.01	868.70
80	2.44E+06	9.76E+06	4	3	176	4	82.01	868.70
85	1.83E+06	1.04E+07	3	4	176	4	82.01	868.70
90	1.22E+06	1.10E+07	2	4	176	4	82.01	868.70
95	6.10E+05	1.16E+07	2	4	176	4	82.01	868.70

Table C.52 Results of power-MSF-RO-AR Configuration for April at 100% AR load

RO load %	MSF demand m^3	RO demand m^3	MSF units	RO units	AR units	NT	Fuel cost million $	CO_2 emissions ktonne
5	1.16E+07	6.10E+05	13	1	196	3	96.80	1044.40
10	1.10E+07	1.22E+06	12	1	196	3	92.40	995.05
15	1.04E+07	1.83E+06	12	1	196	3	92.40	995.05
20	9.76E+06	2.44E+06	11	1	196	3	88.00	945.71
25	9.15E+06	3.05E+06	10	1	196	3	83.60	896.37
30	8.54E+06	3.66E+06	10	2	196	3	83.60	896.37
35	7.93E+06	4.27E+06	9	2	196	3	79.20	847.03
40	7.32E+06	4.88E+06	9	2	196	3	79.20	847.03
45	6.71E+06	5.49E+06	8	2	196	3	74.79	797.69
50	6.10E+06	6.10E+06	7	2	196	3	70.39	748.35
55	5.49E+06	6.71E+06	7	3	196	3	70.39	748.35
60	4.88E+06	7.32E+06	6	3	196	3	65.99	699.00
65	4.27E+06	7.93E+06	6	3	196	3	65.99	699.00
70	3.66E+06	8.54E+06	5	3	196	3	65.99	699.00
75	3.05E+06	9.15E+06	4	3	196	3	65.99	699.00
80	2.44E+06	9.76E+06	4	3	196	3	65.99	699.00
85	1.83E+06	1.04E+07	3	4	196	3	65.99	699.00
90	1.22E+06	1.10E+07	2	4	196	3	65.99	699.00
95	6.10E+05	1.16E+07	2	4	196	3	65.99	699.00

May

Table C.53 Results of power-MSF-RO-AR Configuration for May at 10% AR load

RO load %	MSF demand m^3	RO demand m^3	MSF units	RO units	AR units	NT	Fuel cost million $	CO_2 emissions ktonne
5	1.26E+07	6.63E+05	14	1	36	5	108.92	1165.00
10	1.19E+07	1.33E+06	13	1	36	5	104.37	1114.00
15	1.13E+07	1.99E+06	12	1	36	5	99.82	1063.00
20	1.06E+07	2.65E+06	12	1	36	5	99.82	1063.00
25	9.95E+06	3.32E+06	11	1	36	5	95.28	1012.00
30	9.28E+06	3.98E+06	10	2	36	5	90.73	961.02
35	8.62E+06	4.64E+06	10	2	36	5	90.73	961.02
40	7.96E+06	5.31E+06	9	2	36	5	90.73	961.02
45	7.29E+06	5.97E+06	8	2	36	5	90.73	961.02
50	6.63E+06	6.63E+06	8	2	36	5	90.73	961.02
55	5.97E+06	7.29E+06	7	3	36	5	90.73	961.02
60	5.31E+06	7.96E+06	6	3	36	5	90.73	961.02
65	4.64E+06	8.62E+06	6	3	36	5	90.73	961.02
70	3.98E+06	9.28E+06	5	3	36	5	90.73	961.02
75	3.32E+06	9.95E+06	4	3	36	5	90.73	961.02
80	2.65E+06	1.06E+07	4	4	36	5	90.73	961.02
85	1.99E+06	1.13E+07	3	4	36	5	90.73	961.02
90	1.33E+06	1.19E+07	2	4	36	5	90.73	961.02
95	6.63E+05	1.26E+07	2	4	36	5	90.73	961.02

Table C.54 Results of power-MSF-RO-AR Configuration for May at 20% AR load

RO load %	MSF demand m^3	RO demand m^3	MSF units	RO units	AR units	NT	Fuel cost million $	CO_2 emissions ktonne
5	1.26E+07	6.63E+05	14	1	72	5	112.03	1197.90
10	1.19E+07	1.33E+06	13	1	72	5	107.48	1146.90
15	1.13E+07	1.99E+06	12	1	72	5	102.93	1095.90
20	1.06E+07	2.65E+06	12	1	72	5	102.93	1095.90
25	9.95E+06	3.32E+06	11	1	72	5	98.38	1044.90
30	9.28E+06	3.98E+06	10	2	72	5	93.83	993.92
35	8.62E+06	4.64E+06	10	2	72	5	93.83	993.92
40	7.96E+06	5.31E+06	9	2	72	5	93.83	993.92
45	7.29E+06	5.97E+06	8	2	72	5	93.83	993.92
50	6.63E+06	6.63E+06	8	2	72	5	93.83	993.92
55	5.97E+06	7.29E+06	7	3	72	5	93.83	993.92
60	5.31E+06	7.96E+06	6	3	72	5	93.83	993.92
65	4.64E+06	8.62E+06	6	3	72	5	93.83	993.92
70	3.98E+06	9.28E+06	5	3	72	5	93.83	993.92
75	3.32E+06	9.95E+06	4	3	72	5	93.83	993.92
80	2.65E+06	1.06E+07	4	4	72	5	93.83	993.92
85	1.99E+06	1.13E+07	3	4	72	5	93.83	993.92
90	1.33E+06	1.19E+07	2	4	72	5	93.83	993.92
95	6.63E+05	1.26E+07	2	4	72	5	93.83	993.92

Table C.55 Results of power-MSF-RO-AR Configuration for May at 30% AR load

RO load %	MSF demand m^3	RO demand m^3	MSF units	RO units	AR units	NT	Fuel cost million $	CO_2 emissions ktonne
5	1.26E+07	6.63E+05	14	1	107	5	114.99	1229.30
10	1.19E+07	1.33E+06	13	1	107	5	110.45	1178.30
15	1.13E+07	1.99E+06	12	1	107	5	105.90	1127.30
20	1.06E+07	2.65E+06	12	1	107	5	105.90	1127.30
25	9.95E+06	3.32E+06	11	1	107	5	101.35	1076.30
30	9.28E+06	3.98E+06	10	2	107	5	96.80	1025.40
35	8.62E+06	4.64E+06	10	2	107	5	96.80	1025.40
40	7.96E+06	5.31E+06	9	2	107	5	96.80	1025.40
45	7.29E+06	5.97E+06	8	2	107	5	96.80	1025.40
50	6.63E+06	6.63E+06	8	2	107	5	96.80	1025.40
55	5.97E+06	7.29E+06	7	3	107	5	96.80	1025.40
60	5.31E+06	7.96E+06	6	3	107	5	96.80	1025.40
65	4.64E+06	8.62E+06	6	3	107	5	96.80	1025.40
70	3.98E+06	9.28E+06	5	3	107	5	96.80	1025.40
75	3.32E+06	9.95E+06	4	3	107	5	96.80	1025.40
80	2.65E+06	1.06E+07	4	4	107	5	96.80	1025.40
85	1.99E+06	1.13E+07	3	4	107	5	96.80	1025.40
90	1.33E+06	1.19E+07	2	4	107	5	96.80	1025.40
95	6.63E+05	1.26E+07	2	4	107	5	96.80	1025.40

Table C.56 Results of power-MSF-RO-AR Configuration for May at 40% AR load

RO load %	MSF demand m^3	RO demand m^3	MSF units	RO units	AR units	NT	Fuel cost million $	CO_2 emissions ktonne
5	1.26E+07	6.63E+05	14	1	143	4	109.44	1176.10
10	1.19E+07	1.33E+06	13	1	143	4	104.89	1125.10
15	1.13E+07	1.99E+06	12	1	143	4	100.35	1074.10
20	1.06E+07	2.65E+06	12	1	143	4	100.35	1074.10
25	9.95E+06	3.32E+06	11	1	143	4	95.80	1023.20
30	9.28E+06	3.98E+06	10	2	143	5	99.79	1057.00
35	8.62E+06	4.64E+06	10	2	143	5	99.79	1057.00
40	7.96E+06	5.31E+06	9	2	143	5	99.79	1057.00
45	7.29E+06	5.97E+06	8	2	143	5	99.79	1057.00
50	6.63E+06	6.63E+06	8	2	143	5	99.79	1057.00
55	5.97E+06	7.29E+06	7	3	143	5	99.79	1057.00
60	5.31E+06	7.96E+06	6	3	143	5	99.79	1057.00
65	4.64E+06	8.62E+06	6	3	143	5	99.79	1057.00
70	3.98E+06	9.28E+06	5	3	143	5	99.79	1057.00
75	3.32E+06	9.95E+06	4	3	143	5	99.79	1057.00
80	2.65E+06	1.06E+07	4	4	143	5	99.79	1057.00
85	1.99E+06	1.13E+07	3	4	143	5	99.79	1057.00
90	1.33E+06	1.19E+07	2	4	143	5	99.79	1057.00
95	6.63E+05	1.26E+07	2	4	143	5	99.79	1057.00

Table C.57 Results of power-MSF-RO-AR Configuration for May at 50% AR load

RO load %	MSF demand m^3	RO demand m^3	MSF units	RO units	AR units	NT	Fuel cost million $	CO_2 emissions ktonne
5	1.26E+07	6.63E+05	14	1	178	4	112.19	1205.20
10	1.19E+07	1.33E+06	13	1	178	4	107.64	1154.20
15	1.13E+07	1.99E+06	12	1	178	4	103.09	1103.20
20	1.06E+07	2.65E+06	12	1	178	4	103.09	1103.20
25	9.95E+06	3.32E+06	11	1	178	4	98.54	1052.20
30	9.28E+06	3.98E+06	10	2	178	4	94.00	1001.30
35	8.62E+06	4.64E+06	10	2	178	4	94.00	1001.30
40	7.96E+06	5.31E+06	9	2	178	4	89.45	950.28
45	7.29E+06	5.97E+06	8	2	178	4	84.90	899.29
50	6.63E+06	6.63E+06	8	2	178	4	84.90	899.29
55	5.97E+06	7.29E+06	7	3	178	4	84.90	899.29
60	5.31E+06	7.96E+06	6	3	178	4	84.90	899.29
65	4.64E+06	8.62E+06	6	3	178	4	84.90	899.29
70	3.98E+06	9.28E+06	5	3	178	4	84.90	899.29
75	3.32E+06	9.95E+06	4	3	178	4	84.90	899.29
80	2.65E+06	1.06E+07	4	4	178	4	84.90	899.29
85	1.99E+06	1.13E+07	3	4	178	4	84.90	899.29
90	1.33E+06	1.19E+07	2	4	178	4	84.90	899.29
95	6.63E+05	1.26E+07	2	4	178	4	84.90	899.29

Table C.58 Results of power-MSF-RO-AR Configuration for May at 60% AR load

RO load %	MSF demand m^3	RO demand m^3	MSF units	RO units	AR units	NT	Fuel cost million $	CO_2 emissions ktonne
5	1.26E+07	6.63E+05	14	1	214	4	114.89	1233.80
10	1.19E+07	1.33E+06	13	1	214	4	110.34	1182.80
15	1.13E+07	1.99E+06	12	1	214	4	105.79	1131.80
20	1.06E+07	2.65E+06	12	1	214	4	105.79	1131.80
25	9.95E+06	3.32E+06	11	1	214	4	101.25	1080.90
30	9.28E+06	3.98E+06	10	2	214	4	96.70	1029.90
35	8.62E+06	4.64E+06	10	2	214	4	96.70	1029.90
40	7.96E+06	5.31E+06	9	2	214	4	92.15	978.89
45	7.29E+06	5.97E+06	8	2	214	4	87.60	927.90
50	6.63E+06	6.63E+06	8	2	214	4	87.60	927.90
55	5.97E+06	7.29E+06	7	3	214	4	87.60	927.90
60	5.31E+06	7.96E+06	6	3	214	4	87.60	927.90
65	4.64E+06	8.62E+06	6	3	214	4	87.60	927.90
70	3.98E+06	9.28E+06	5	3	214	4	87.60	927.90
75	3.32E+06	9.95E+06	4	3	214	4	87.60	927.90
80	2.65E+06	1.06E+07	4	4	214	4	87.60	927.90
85	1.99E+06	1.13E+07	3	4	214	4	87.60	927.90
90	1.33E+06	1.19E+07	2	4	214	4	87.60	927.90
95	6.63E+05	1.26E+07	2	4	214	4	87.60	927.90

Table C.59 Results of power-MSF-RO-AR Configuration for May at 70% AR load

RO load %	MSF demand m^3	RO demand m^3	MSF units	RO units	AR units	NT	Fuel cost million $	CO_2 emissions ktonne
5	1.26E+07	6.63E+05	14	1	250	4	117.44	1260.80
10	1.19E+07	1.33E+06	13	1	250	4	112.89	1209.90
15	1.13E+07	1.99E+06	12	1	250	4	108.35	1158.90
20	1.06E+07	2.65E+06	12	1	250	4	108.35	1158.90
25	9.95E+06	3.32E+06	11	1	250	4	103.80	1107.90
30	9.28E+06	3.98E+06	10	2	250	4	99.25	1056.90
35	8.62E+06	4.64E+06	10	2	250	4	99.25	1056.90
40	7.96E+06	5.31E+06	9	2	250	4	94.70	1005.90
45	7.29E+06	5.97E+06	8	2	250	4	90.15	954.93
50	6.63E+06	6.63E+06	8	2	250	4	90.15	954.93
55	5.97E+06	7.29E+06	7	3	250	4	90.15	954.93
60	5.31E+06	7.96E+06	6	3	250	4	90.15	954.93
65	4.64E+06	8.62E+06	6	3	250	4	90.15	954.93
70	3.98E+06	9.28E+06	5	3	250	4	90.15	954.93
75	3.32E+06	9.95E+06	4	3	250	4	90.15	954.93
80	2.65E+06	1.06E+07	4	4	250	4	90.15	954.93
85	1.99E+06	1.13E+07	3	4	250	4	90.15	954.93
90	1.33E+06	1.19E+07	2	4	250	4	90.15	954.93
95	6.63E+05	1.26E+07	2	4	250	4	90.15	954.93

Table C.60 Results of power-MSF-RO-AR Configuration for May at 80% AR load

RO load %	MSF demand m^3	RO demand m^3	MSF units	RO units	AR units	NT	Fuel cost million $	CO_2 emissions ktonne
5	1.26E+07	6.63E+05	14	1	286	4	119.82	1286.00
10	1.19E+07	1.33E+06	13	1	286	4	115.27	1235.00
15	1.13E+07	1.99E+06	12	1	286	4	110.72	1184.10
20	1.06E+07	2.65E+06	12	1	286	4	110.72	1184.10
25	9.95E+06	3.32E+06	11	1	286	4	106.17	1133.10
30	9.28E+06	3.98E+06	10	2	286	4	101.63	1082.10
35	8.62E+06	4.64E+06	10	2	286	4	101.63	1082.10
40	7.96E+06	5.31E+06	9	2	286	4	97.08	1031.10
45	7.29E+06	5.97E+06	8	2	286	4	92.53	980.11
50	6.63E+06	6.63E+06	8	2	286	4	92.53	980.11
55	5.97E+06	7.29E+06	7	3	286	4	92.53	980.11
60	5.31E+06	7.96E+06	6	3	286	4	92.53	980.11
65	4.64E+06	8.62E+06	6	3	286	4	92.53	980.11
70	3.98E+06	9.28E+06	5	3	286	4	92.53	980.11
75	3.32E+06	9.95E+06	4	3	286	4	92.53	980.11
80	2.65E+06	1.06E+07	4	4	286	4	92.53	980.11
85	1.99E+06	1.13E+07	3	4	286	4	92.53	980.11
90	1.33E+06	1.19E+07	2	4	286	4	92.53	980.11
95	6.63E+05	1.26E+07	2	4	286	4	92.53	980.11

Table C.61 Results of power-MSF-RO-AR Configuration for May at 90% AR load

RO load %	MSF demand m^3	RO demand m^3	MSF units	RO units	AR units	NT	Fuel cost million $	CO_2 emissions ktonne
5	1.26E+07	6.63E+05	14	1	321	3	111.22	1200.60
10	1.19E+07	1.33E+06	13	1	321	3	106.67	1149.60
15	1.13E+07	1.99E+06	12	1	321	3	102.12	1098.60
20	1.06E+07	2.65E+06	12	1	321	3	102.12	1098.60
25	9.95E+06	3.32E+06	11	1	321	3	97.57	1047.60
30	9.28E+06	3.98E+06	10	2	321	4	103.75	1104.50
35	8.62E+06	4.64E+06	10	2	321	4	103.75	1104.50
40	7.96E+06	5.31E+06	9	2	321	4	99.20	1053.60
45	7.29E+06	5.97E+06	8	2	321	4	94.65	1002.60
50	6.63E+06	6.63E+06	8	2	321	4	94.65	1002.60
55	5.97E+06	7.29E+06	7	3	321	4	94.65	1002.60
60	5.31E+06	7.96E+06	6	3	321	4	94.65	1002.60
65	4.64E+06	8.62E+06	6	3	321	4	94.65	1002.60
70	3.98E+06	9.28E+06	5	3	321	4	94.65	1002.60
75	3.32E+06	9.95E+06	4	3	321	4	94.65	1002.60
80	2.65E+06	1.06E+07	4	4	321	4	94.65	1002.60
85	1.99E+06	1.13E+07	3	4	321	4	94.65	1002.60
90	1.33E+06	1.19E+07	2	4	321	4	94.65	1002.60
95	6.63E+05	1.26E+07	2	4	321	4	94.65	1002.60

Table C.62 Results of power-MSF-RO-AR Configuration for May at 100% AR load

RO load %	MSF demand m^3	RO demand m^3	MSF units	RO units	AR units	NT	Fuel cost million $	CO_2 emissions ktonne
5	1.26E+07	6.63E+05	14	1	357	3	112.43	1213.40
10	1.19E+07	1.33E+06	13	1	357	3	107.88	1162.40
15	1.13E+07	1.99E+06	12	1	357	3	103.33	1111.40
20	1.06E+07	2.65E+06	12	1	357	3	103.33	1111.40
25	9.95E+06	3.32E+06	11	1	357	3	98.79	1060.40
30	9.28E+06	3.98E+06	10	2	357	3	94.24	1009.40
35	8.62E+06	4.64E+06	10	2	357	3	94.24	1009.40
40	7.96E+06	5.31E+06	9	2	357	3	89.69	958.45
45	7.29E+06	5.97E+06	8	2	357	3	85.14	907.46
50	6.63E+06	6.63E+06	8	2	357	3	85.14	907.46
55	5.97E+06	7.29E+06	7	3	357	3	80.59	856.48
60	5.31E+06	7.96E+06	6	3	357	3	76.04	805.49
65	4.64E+06	8.62E+06	6	3	357	3	76.04	805.49
70	3.98E+06	9.28E+06	5	3	357	3	76.04	805.49
75	3.32E+06	9.95E+06	4	3	357	3	76.04	805.49
80	2.65E+06	1.06E+07	4	4	357	4	96.61	1023.30
85	1.99E+06	1.13E+07	3	4	357	4	96.61	1023.30
90	1.33E+06	1.19E+07	2	4	357	4	96.61	1023.30
95	6.63E+05	1.26E+07	2	4	357	4	96.61	1023.30

June

Table C.63 Results of power-MSF-RO-AR Configuration for June at 10% AR load

RO load %	MSF demand m^3	RO demand m^3	MSF units	RO units	AR units	NT	Fuel cost million $	CO_2 emissions ktonne
5	1.26E+07	6.63E+05	14	1	395	3	135.00	1451.70
10	1.19E+07	1.33E+06	13	1	395	3	130.60	1402.40
15	1.13E+07	1.99E+06	13	1	395	3	130.60	1402.40
20	1.06E+07	2.65E+06	12	1	395	3	126.20	1353.00
25	9.95E+06	3.32E+06	11	2	395	3	121.79	1303.70
30	9.28E+06	3.98E+06	11	2	395	3	121.79	1303.70
35	8.62E+06	4.64E+06	10	2	395	3	117.39	1254.30
40	7.96E+06	5.31E+06	9	2	395	3	112.99	1205.00
45	7.29E+06	5.97E+06	9	2	395	3	112.99	1205.00
50	6.63E+06	6.63E+06	8	3	395	3	108.59	1155.70
55	5.97E+06	7.29E+06	7	3	395	3	104.19	1106.30
60	5.31E+06	7.96E+06	7	3	395	3	104.19	1106.30
65	4.64E+06	8.62E+06	6	3	395	3	99.79	1057.00
70	3.98E+06	9.28E+06	5	3	395	3	99.79	1057.00
75	3.32E+06	9.95E+06	5	4	395	4	95.25	1008.90
80	2.65E+06	1.06E+07	4	4	395	4	95.25	1008.90
85	1.99E+06	1.13E+07	3	4	395	4	95.25	1008.90
90	1.33E+06	1.19E+07	3	4	395	4	95.25	1008.90
95	6.63E+05	1.26E+07	2	4	395	4	95.25	1008.90

Table C.64 Results of power-MSF-RO-AR Configuration for June at 20% AR load

RO load %	MSF demand m^3	RO demand m^3	MSF units	RO units	AR units	NT	Fuel cost million $	CO_2 emissions ktonne
5	1.26E+07	6.63E+05	14	1	79	5	108.99	1165.40
10	1.19E+07	1.33E+06	13	1	79	5	104.59	1116.00
15	1.13E+07	1.99E+06	13	1	79	5	104.59	1116.00
20	1.06E+07	2.65E+06	12	1	79	5	100.19	1066.70
25	9.95E+06	3.32E+06	11	2	79	6	108.35	1147.70
30	9.28E+06	3.98E+06	11	2	79	6	108.35	1147.70
35	8.62E+06	4.64E+06	10	2	79	6	108.35	1147.70
40	7.96E+06	5.31E+06	9	2	79	6	108.35	1147.70
45	7.29E+06	5.97E+06	9	2	79	6	108.35	1147.70
50	6.63E+06	6.63E+06	8	3	79	6	108.35	1147.70
55	5.97E+06	7.29E+06	7	3	79	6	108.35	1147.70
60	5.31E+06	7.96E+06	7	3	79	6	108.35	1147.70
65	4.64E+06	8.62E+06	6	3	79	6	108.35	1147.70
70	3.98E+06	9.28E+06	5	3	79	6	108.35	1147.70
75	3.32E+06	9.95E+06	5	4	79	6	108.35	1147.70
80	2.65E+06	1.06E+07	4	4	79	6	108.35	1147.70
85	1.99E+06	1.13E+07	3	4	79	6	108.35	1147.70
90	1.33E+06	1.19E+07	3	4	79	6	108.35	1147.70
95	6.63E+05	1.26E+07	2	4	79	6	108.35	1147.70

Table C.65 Results of power-MSF-RO-AR Configuration for June at 30% AR load

RO load %	MSF demand m^3	RO demand m^3	MSF units	RO units	AR units	NT	Fuel cost million $	CO_2 emissions ktonne
5	1.26E+07	6.63E+05	14	1	119	5	112.26	1199.90
10	1.19E+07	1.33E+06	13	1	119	5	107.86	1150.60
15	1.13E+07	1.99E+06	13	1	119	5	107.86	1150.60
20	1.06E+07	2.65E+06	12	1	119	5	103.45	1101.30
25	9.95E+06	3.32E+06	11	2	119	5	99.05	1051.90
30	9.28E+06	3.98E+06	11	2	119	5	99.05	1051.90
35	8.62E+06	4.64E+06	10	2	119	5	94.65	1002.60
40	7.96E+06	5.31E+06	9	2	119	5	94.65	1002.60
45	7.29E+06	5.97E+06	9	2	119	5	94.65	1002.60
50	6.63E+06	6.63E+06	8	3	119	5	94.65	1002.60
55	5.97E+06	7.29E+06	7	3	119	5	94.65	1002.60
60	5.31E+06	7.96E+06	7	3	119	5	94.65	1002.60
65	4.64E+06	8.62E+06	6	3	119	5	94.65	1002.60
70	3.98E+06	9.28E+06	5	3	119	5	94.65	1002.60
75	3.32E+06	9.95E+06	5	4	119	5	94.65	1002.60
80	2.65E+06	1.06E+07	4	4	119	5	94.65	1002.60
85	1.99E+06	1.13E+07	3	4	119	5	94.65	1002.60
90	1.33E+06	1.19E+07	3	4	119	5	94.65	1002.60
95	6.63E+05	1.26E+07	2	4	119	5	94.65	1002.60

Table C.66 Results of power-MSF-RO-AR Configuration for June at 40% AR load

RO load %	MSF demand m^3	RO demand m^3	MSF units	RO units	AR units	NT	Fuel cost million $	CO_2 emissions ktonne
5	1.26E+07	6.63E+05	14	1	158	5	115.37	1232.90
10	1.19E+07	1.33E+06	13	1	158	5	110.96	1183.50
15	1.13E+07	1.99E+06	13	1	158	5	110.96	1183.50
20	1.06E+07	2.65E+06	12	1	158	5	106.56	1134.20
25	9.95E+06	3.32E+06	11	2	158	5	102.16	1084.80
30	9.28E+06	3.98E+06	11	2	158	5	102.16	1084.80
35	8.62E+06	4.64E+06	10	2	158	5	97.76	1035.50
40	7.96E+06	5.31E+06	9	2	158	5	97.76	1035.50
45	7.29E+06	5.97E+06	9	2	158	5	97.76	1035.50
50	6.63E+06	6.63E+06	8	3	158	5	97.76	1035.50
55	5.97E+06	7.29E+06	7	3	158	5	97.76	1035.50
60	5.31E+06	7.96E+06	7	3	158	5	97.76	1035.50
65	4.64E+06	8.62E+06	6	3	158	5	97.76	1035.50
70	3.98E+06	9.28E+06	5	3	158	5	97.76	1035.50
75	3.32E+06	9.95E+06	5	4	158	5	97.76	1035.50
80	2.65E+06	1.06E+07	4	4	158	5	97.76	1035.50
85	1.99E+06	1.13E+07	3	4	158	5	97.76	1035.50
90	1.33E+06	1.19E+07	3	4	158	5	97.76	1035.50
95	6.63E+05	1.26E+07	2	4	158	5	97.76	1035.50

Table C.67 Results of power-MSF-RO-AR Configuration for June at 50% AR load

RO load %	MSF demand m^3	RO demand m^3	MSF units	RO units	AR units	NT	Fuel cost million $	CO_2 emissions ktonne
5	1.26E+07	6.63E+05	14	1	198	5	118.46	1265.70
10	1.19E+07	1.33E+06	13	1	198	5	114.06	1216.30
15	1.13E+07	1.99E+06	13	1	198	5	114.06	1216.30
20	1.06E+07	2.65E+06	12	1	198	5	109.66	1167.00
25	9.95E+06	3.32E+06	11	2	198	5	105.26	1117.70
30	9.28E+06	3.98E+06	11	2	198	5	105.26	1117.70
35	8.62E+06	4.64E+06	10	2	198	5	100.86	1068.30
40	7.96E+06	5.31E+06	9	2	198	5	100.86	1068.30
45	7.29E+06	5.97E+06	9	2	198	5	100.86	1068.30
50	6.63E+06	6.63E+06	8	3	198	5	100.86	1068.30
55	5.97E+06	7.29E+06	7	3	198	5	100.86	1068.30
60	5.31E+06	7.96E+06	7	3	198	5	100.86	1068.30
65	4.64E+06	8.62E+06	6	3	198	5	100.86	1068.30
70	3.98E+06	9.28E+06	5	3	198	5	100.86	1068.30
75	3.32E+06	9.95E+06	5	4	198	5	100.86	1068.30
80	2.65E+06	1.06E+07	4	4	198	5	100.86	1068.30
85	1.99E+06	1.13E+07	3	4	198	5	100.86	1068.30
90	1.33E+06	1.19E+07	3	4	198	5	100.86	1068.30
95	6.63E+05	1.26E+07	2	4	198	5	100.86	1068.30

Table C.68 Results of power-MSF-RO-AR Configuration for June at 60% AR load

RO load %	MSF demand m^3	RO demand m^3	MSF units	RO units	AR units	NT	Fuel cost million $	CO_2 emissions ktonne
5	1.26E+07	6.63E+05	14	1	237	4	112.78	1210.90
10	1.19E+07	1.33E+06	13	1	237	4	108.38	1161.60
15	1.13E+07	1.99E+06	13	1	237	4	108.38	1161.60
20	1.06E+07	2.65E+06	12	1	237	4	103.98	1112.20
25	9.95E+06	3.32E+06	11	2	237	4	99.58	1062.90
30	9.28E+06	3.98E+06	11	2	237	4	99.58	1062.90
35	8.62E+06	4.64E+06	10	2	237	4	95.17	1013.60
40	7.96E+06	5.31E+06	9	2	237	4	90.77	964.22
45	7.29E+06	5.97E+06	9	2	237	4	90.77	964.22
50	6.63E+06	6.63E+06	8	3	237	5	103.77	1099.20
55	5.97E+06	7.29E+06	7	3	237	5	103.77	1099.20
60	5.31E+06	7.96E+06	7	3	237	5	103.77	1099.20
65	4.64E+06	8.62E+06	6	3	237	5	103.77	1099.20
70	3.98E+06	9.28E+06	5	3	237	5	103.77	1099.20
75	3.32E+06	9.95E+06	5	4	237	5	103.77	1099.20
80	2.65E+06	1.06E+07	4	4	237	5	103.77	1099.20
85	1.99E+06	1.13E+07	3	4	237	5	103.77	1099.20
90	1.33E+06	1.19E+07	3	4	237	5	103.77	1099.20
95	6.63E+05	1.26E+07	2	4	237	5	103.77	1099.20

Table C.69 Results of power-MSF-RO-AR Configuration for June at 70% AR load

RO load %	MSF demand m^3	RO demand m^3	MSF units	RO units	AR units	NT	Fuel cost million $	CO_2 emissions ktonne
5	1.26E+07	6.63E+05	14	1	276	4	115.33	1238.00
10	1.19E+07	1.33E+06	13	1	276	4	110.93	1188.60
15	1.13E+07	1.99E+06	13	1	276	4	110.93	1188.60
20	1.06E+07	2.65E+06	12	1	276	4	106.53	1139.30
25	9.95E+06	3.32E+06	11	2	276	4	102.13	1089.90
30	9.28E+06	3.98E+06	11	2	276	4	102.13	1089.90
35	8.62E+06	4.64E+06	10	2	276	4	97.73	1040.60
40	7.96E+06	5.31E+06	9	2	276	4	93.33	991.26
45	7.29E+06	5.97E+06	9	2	276	4	93.33	991.26
50	6.63E+06	6.63E+06	8	3	276	4	88.92	941.92
55	5.97E+06	7.29E+06	7	3	276	4	88.92	941.92
60	5.31E+06	7.96E+06	7	3	276	4	88.92	941.92
65	4.64E+06	8.62E+06	6	3	276	4	88.92	941.92
70	3.98E+06	9.28E+06	5	3	276	4	88.92	941.92
75	3.32E+06	9.95E+06	5	4	276	4	88.92	941.92
80	2.65E+06	1.06E+07	4	4	276	4	88.92	941.92
85	1.99E+06	1.13E+07	3	4	276	4	88.92	941.92
90	1.33E+06	1.19E+07	3	4	276	4	88.92	941.92
95	6.63E+05	1.26E+07	2	4	276	4	88.92	941.92

Table C.70 Results of power-MSF-RO-AR Configuration for June at 80% AR load

RO load %	MSF demand m^3	RO demand m^3	MSF units	RO units	AR units	NT	Fuel cost million $	CO_2 emissions ktonne
5	1.26E+07	6.63E+05	14	1	316	4	117.72	1263.30
10	1.19E+07	1.33E+06	13	1	316	4	113.32	1214.00
15	1.13E+07	1.99E+06	13	1	316	4	113.32	1214.00
20	1.06E+07	2.65E+06	12	1	316	4	108.92	1164.60
25	9.95E+06	3.32E+06	11	2	316	4	104.52	1115.30
30	9.28E+06	3.98E+06	11	2	316	4	104.52	1115.30
35	8.62E+06	4.64E+06	10	2	316	4	100.12	1065.90
40	7.96E+06	5.31E+06	9	2	316	4	95.72	1016.60
45	7.29E+06	5.97E+06	9	2	316	4	95.72	1016.60
50	6.63E+06	6.63E+06	8	3	316	4	91.32	967.25
55	5.97E+06	7.29E+06	7	3	316	4	91.32	967.25
60	5.31E+06	7.96E+06	7	3	316	4	91.32	967.25
65	4.64E+06	8.62E+06	6	3	316	4	91.32	967.25
70	3.98E+06	9.28E+06	5	3	316	4	91.32	967.25
75	3.32E+06	9.95E+06	5	4	316	4	91.32	967.25
80	2.65E+06	1.06E+07	4	4	316	4	91.32	967.25
85	1.99E+06	1.13E+07	3	4	316	4	91.32	967.25
90	1.33E+06	1.19E+07	3	4	316	4	91.32	967.25
95	6.63E+05	1.26E+07	2	4	316	4	91.32	967.25

Table C.71 Results of power-MSF-RO-AR Configuration for June at 90% AR load

RO load %	MSF demand m^3	RO demand m^3	MSF units	RO units	AR units	NT	Fuel cost million $	CO_2 emissions ktonne
5	1.26E+07	6.63E+05	14	1	355	4	119.80	1285.30
10	1.19E+07	1.33E+06	13	1	355	4	115.40	1236.00
15	1.13E+07	1.99E+06	13	1	355	4	115.40	1236.00
20	1.06E+07	2.65E+06	12	1	355	4	111.00	1186.60
25	9.95E+06	3.32E+06	11	2	355	4	106.60	1137.30
30	9.28E+06	3.98E+06	11	2	355	4	106.60	1137.30
35	8.62E+06	4.64E+06	10	2	355	4	102.20	1088.00
40	7.96E+06	5.31E+06	9	2	355	4	97.80	1038.60
45	7.29E+06	5.97E+06	9	2	355	4	97.80	1038.60
50	6.63E+06	6.63E+06	8	3	355	4	93.40	989.28
55	5.97E+06	7.29E+06	7	3	355	4	93.40	989.28
60	5.31E+06	7.96E+06	7	3	355	4	93.40	989.28
65	4.64E+06	8.62E+06	6	3	355	4	93.40	989.28
70	3.98E+06	9.28E+06	5	3	355	4	93.40	989.28
75	3.32E+06	9.95E+06	5	4	355	4	93.40	989.28
80	2.65E+06	1.06E+07	4	4	355	4	93.40	989.28
85	1.99E+06	1.13E+07	3	4	355	4	93.40	989.28
90	1.33E+06	1.19E+07	3	4	355	4	93.40	989.28
95	6.63E+05	1.26E+07	2	4	355	4	93.40	989.28

Table C.72 Results of power-MSF-RO-AR Configuration for June at 100% AR load

RO load %	MSF demand m^3	RO demand m^3	MSF units	RO units	AR units	NT	Fuel cost million $	CO_2 emissions ktonne
5	1.26E+07	6.63E+05	14	1	395	3	135.00	1451.70
10	1.19E+07	1.33E+06	13	1	395	3	130.60	1402.40
15	1.13E+07	1.99E+06	13	1	395	3	130.60	1402.40
20	1.06E+07	2.65E+06	12	1	395	3	126.20	1353.00
25	9.95E+06	3.32E+06	11	2	395	3	121.79	1303.70
30	9.28E+06	3.98E+06	11	2	395	3	121.79	1303.70
35	8.62E+06	4.64E+06	10	2	395	3	117.39	1254.30
40	7.96E+06	5.31E+06	9	2	395	3	112.99	1205.00
45	7.29E+06	5.97E+06	9	2	395	3	112.99	1205.00
50	6.63E+06	6.63E+06	8	3	395	3	108.59	1155.70
55	5.97E+06	7.29E+06	7	3	395	3	104.19	1106.30
60	5.31E+06	7.96E+06	7	3	395	3	104.19	1106.30
65	4.64E+06	8.62E+06	6	3	395	3	99.79	1057.00
70	3.98E+06	9.28E+06	5	3	395	3	99.79	1057.00
75	3.32E+06	9.95E+06	5	4	395	4	95.25	1008.90
80	2.65E+06	1.06E+07	4	4	395	4	95.25	1008.90
85	1.99E+06	1.13E+07	3	4	395	4	95.25	1008.90
90	1.33E+06	1.19E+07	3	4	395	4	95.25	1008.90
95	6.63E+05	1.26E+07	2	4	395	4	95.25	1008.90

July

Table C.73 Results of power-MSF-RO-AR Configuration for July at 10% AR load

RO load %	MSF demand m^3	RO demand m^3	MSF units	RO units	AR units	NT	Fuel cost million $	CO_2 emissions ktonne
5	1.28E+07	6.75E+05	14	1	44	6	118.04	1255.90
10	1.22E+07	1.35E+06	13	1	44	6	113.49	1204.90
15	1.15E+07	2.03E+06	13	1	44	6	113.49	1204.90
20	1.08E+07	2.70E+06	12	1	44	6	108.94	1154.00
25	1.01E+07	3.38E+06	11	1	44	6	108.94	1154.00
30	9.45E+06	4.05E+06	10	2	44	6	108.94	1154.00
35	8.78E+06	4.73E+06	10	2	44	6	108.94	1154.00
40	8.10E+06	5.40E+06	9	2	44	6	108.94	1154.00
45	7.43E+06	6.08E+06	8	2	44	6	108.94	1154.00
50	6.75E+06	6.75E+06	8	2	44	6	108.94	1154.00
55	6.08E+06	7.43E+06	7	3	44	6	108.94	1154.00
60	5.40E+06	8.10E+06	6	3	44	6	108.94	1154.00
65	4.73E+06	8.78E+06	6	3	44	6	108.94	1154.00
70	4.05E+06	9.45E+06	5	3	44	6	108.94	1154.00
75	3.38E+06	1.01E+07	4	3	44	6	108.94	1154.00
80	2.70E+06	1.08E+07	4	4	44	6	108.94	1154.00
85	2.03E+06	1.15E+07	3	4	44	6	108.94	1154.00
90	1.35E+06	1.22E+07	2	4	44	6	108.94	1154.00
95	6.75E+05	1.28E+07	2	4	44	6	108.94	1154.00

Table C.74 Results of power-MSF-RO-AR Configuration for July at 20% AR load

RO load %	MSF demand m^3	RO demand m^3	MSF units	RO units	AR units	NT	Fuel cost million $	CO_2 emissions ktonne
5	1.28E+07	6.75E+05	14	1	88	6	121.83	1296.10
10	1.22E+07	1.35E+06	13	1	88	6	117.28	1245.10
15	1.15E+07	2.03E+06	13	1	88	6	117.28	1245.10
20	1.08E+07	2.70E+06	12	1	88	6	112.74	1194.20
25	1.01E+07	3.38E+06	11	1	88	6	112.74	1194.20
30	9.45E+06	4.05E+06	10	2	88	6	112.74	1194.20
35	8.78E+06	4.73E+06	10	2	88	6	112.74	1194.20
40	8.10E+06	5.40E+06	9	2	88	6	112.74	1194.20
45	7.43E+06	6.08E+06	8	2	88	6	112.74	1194.20
50	6.75E+06	6.75E+06	8	2	88	6	112.74	1194.20
55	6.08E+06	7.43E+06	7	3	88	6	112.74	1194.20
60	5.40E+06	8.10E+06	6	3	88	6	112.74	1194.20
65	4.73E+06	8.78E+06	6	3	88	6	112.74	1194.20
70	4.05E+06	9.45E+06	5	3	88	6	112.74	1194.20
75	3.38E+06	1.01E+07	4	3	88	6	112.74	1194.20
80	2.70E+06	1.08E+07	4	4	88	6	112.74	1194.20
85	2.03E+06	1.15E+07	3	4	88	6	112.74	1194.20
90	1.35E+06	1.22E+07	2	4	88	6	112.74	1194.20
95	6.75E+05	1.28E+07	2	4	88	6	112.74	1194.20

Table C.75 Results of power-MSF-RO-AR Configuration for July at 30% AR load

RO load %	MSF demand m^3	RO demand m^3	MSF units	RO units	AR units	NT	Fuel cost million $	CO_2 emissions ktonne
5	1.28E+07	6.75E+05	14	1	131	5	117.00	1250.50
10	1.22E+07	1.35E+06	13	1	131	5	112.45	1199.50
15	1.15E+07	2.03E+06	13	1	131	5	112.45	1199.50
20	1.08E+07	2.70E+06	12	1	131	5	107.90	1148.50
25	1.01E+07	3.38E+06	11	1	131	5	103.35	1097.50
30	9.45E+06	4.05E+06	10	2	131	5	98.80	1046.60
35	8.78E+06	4.73E+06	10	2	131	5	98.80	1046.60
40	8.10E+06	5.40E+06	9	2	131	5	98.80	1046.60
45	7.43E+06	6.08E+06	8	2	131	5	98.80	1046.60
50	6.75E+06	6.75E+06	8	2	131	5	98.80	1046.60
55	6.08E+06	7.43E+06	7	3	131	6	116.38	1232.70
60	5.40E+06	8.10E+06	6	3	131	6	116.38	1232.70
65	4.73E+06	8.78E+06	6	3	131	6	116.38	1232.70
70	4.05E+06	9.45E+06	5	3	131	6	116.38	1232.70
75	3.38E+06	1.01E+07	4	3	131	6	116.38	1232.70
80	2.70E+06	1.08E+07	4	4	131	6	116.38	1232.70
85	2.03E+06	1.15E+07	3	4	131	6	116.38	1232.70
90	1.35E+06	1.22E+07	2	4	131	6	116.38	1232.70
95	6.75E+05	1.28E+07	2	4	131	6	116.38	1232.70

Table C.76 Results of power-MSF-RO-AR Configuration for July at 40% AR load

RO load %	MSF demand m^3	RO demand m^3	MSF units	RO units	AR units	NT	Fuel cost million $	CO_2 emissions ktonne
5	1.28E+07	6.75E+05	14	1	175	5	120.58	1288.50
10	1.22E+07	1.35E+06	13	1	175	5	116.04	1237.50
15	1.15E+07	2.03E+06	13	1	175	5	116.04	1237.50
20	1.08E+07	2.70E+06	12	1	175	5	111.49	1186.50
25	1.01E+07	3.38E+06	11	1	175	5	106.94	1135.60
30	9.45E+06	4.05E+06	10	2	175	5	102.39	1084.60
35	8.78E+06	4.73E+06	10	2	175	5	102.39	1084.60
40	8.10E+06	5.40E+06	9	2	175	5	102.39	1084.60
45	7.43E+06	6.08E+06	8	2	175	5	102.39	1084.60
50	6.75E+06	6.75E+06	8	2	175	5	102.39	1084.60
55	6.08E+06	7.43E+06	7	3	175	5	102.39	1084.60
60	5.40E+06	8.10E+06	6	3	175	5	102.39	1084.60
65	4.73E+06	8.78E+06	6	3	175	5	102.39	1084.60
70	4.05E+06	9.45E+06	5	3	175	5	102.39	1084.60
75	3.38E+06	1.01E+07	4	3	175	5	102.39	1084.60
80	2.70E+06	1.08E+07	4	4	175	5	102.39	1084.60
85	2.03E+06	1.15E+07	3	4	175	5	102.39	1084.60
90	1.35E+06	1.22E+07	2	4	175	5	102.39	1084.60
95	6.75E+05	1.28E+07	2	4	175	5	102.39	1084.60

Table C.77 Results of power-MSF-RO-AR Configuration for July at 50% AR load

RO load %	MSF demand m^3	RO demand m^3	MSF units	RO units	AR units	NT	Fuel cost million $	CO_2 emissions ktonne
5	1.28E+07	6.75E+05	14	1	218	5	123.97	1324.40
10	1.22E+07	1.35E+06	13	1	218	5	119.42	1273.40
15	1.15E+07	2.03E+06	13	1	218	5	119.42	1273.40
20	1.08E+07	2.70E+06	12	1	218	5	114.87	1222.40
25	1.01E+07	3.38E+06	11	1	218	5	110.33	1171.40
30	9.45E+06	4.05E+06	10	2	218	5	105.78	1120.40
35	8.78E+06	4.73E+06	10	2	218	5	105.78	1120.40
40	8.10E+06	5.40E+06	9	2	218	5	105.78	1120.40
45	7.43E+06	6.08E+06	8	2	218	5	105.78	1120.40
50	6.75E+06	6.75E+06	8	2	218	5	105.78	1120.40
55	6.08E+06	7.43E+06	7	3	218	5	105.78	1120.40
60	5.40E+06	8.10E+06	6	3	218	5	105.78	1120.40
65	4.73E+06	8.78E+06	6	3	218	5	105.78	1120.40
70	4.05E+06	9.45E+06	5	3	218	5	105.78	1120.40
75	3.38E+06	1.01E+07	4	3	218	5	105.78	1120.40
80	2.70E+06	1.08E+07	4	4	218	5	105.78	1120.40
85	2.03E+06	1.15E+07	3	4	218	5	105.78	1120.40
90	1.35E+06	1.22E+07	2	4	218	5	105.78	1120.40
95	6.75E+05	1.28E+07	2	4	218	5	105.78	1120.40

Table C.78 Results of power-MSF-RO-AR Configuration for July at 60% AR load

RO load %	MSF demand m^3	RO demand m^3	MSF units	RO units	AR units	NT	Fuel cost million $	CO_2 emissions ktonne
5	1.28E+07	6.75E+05	14	1	262	5	127.29	1359.50
10	1.22E+07	1.35E+06	13	1	262	5	122.74	1308.60
15	1.15E+07	2.03E+06	13	1	262	5	122.74	1308.60
20	1.08E+07	2.70E+06	12	1	262	5	118.19	1257.60
25	1.01E+07	3.38E+06	11	1	262	5	113.65	1206.60
30	9.45E+06	4.05E+06	10	2	262	5	109.10	1155.60
35	8.78E+06	4.73E+06	10	2	262	5	109.10	1155.60
40	8.10E+06	5.40E+06	9	2	262	5	109.10	1155.60
45	7.43E+06	6.08E+06	8	2	262	5	109.10	1155.60
50	6.75E+06	6.75E+06	8	2	262	5	109.10	1155.60
55	6.08E+06	7.43E+06	7	3	262	5	109.10	1155.60
60	5.40E+06	8.10E+06	6	3	262	5	109.10	1155.60
65	4.73E+06	8.78E+06	6	3	262	5	109.10	1155.60
70	4.05E+06	9.45E+06	5	3	262	5	109.10	1155.60
75	3.38E+06	1.01E+07	4	3	262	5	109.10	1155.60
80	2.70E+06	1.08E+07	4	4	262	5	109.10	1155.60
85	2.03E+06	1.15E+07	3	4	262	5	109.10	1155.60
90	1.35E+06	1.22E+07	2	4	262	5	109.10	1155.60
95	6.75E+05	1.28E+07	2	4	262	5	109.10	1155.60

Table C.79 Results of power-MSF-RO-AR Configuration for July at 70% AR load

RO load %	MSF demand m^3	RO demand m^3	MSF units	RO units	AR units	NT	Fuel cost million $	CO_2 emissions ktonne
5	1.28E+07	6.75E+05	14	1	306	4	121.05	1299.10
10	1.22E+07	1.35E+06	13	1	306	4	116.51	1248.10
15	1.15E+07	2.03E+06	13	1	306	4	116.51	1248.10
20	1.08E+07	2.70E+06	12	1	306	4	111.96	1197.10
25	1.01E+07	3.38E+06	11	1	306	4	107.41	1146.20
30	9.45E+06	4.05E+06	10	2	306	4	102.86	1095.20
35	8.78E+06	4.73E+06	10	2	306	4	102.86	1095.20
40	8.10E+06	5.40E+06	9	2	306	4	98.31	1044.20
45	7.43E+06	6.08E+06	8	2	306	4	93.77	993.20
50	6.75E+06	6.75E+06	8	2	306	4	93.77	993.20
55	6.08E+06	7.43E+06	7	3	306	4	93.77	993.20
60	5.40E+06	8.10E+06	6	3	306	4	93.77	993.20
65	4.73E+06	8.78E+06	6	3	306	4	93.77	993.20
70	4.05E+06	9.45E+06	5	3	306	4	93.77	993.20
75	3.38E+06	1.01E+07	4	3	306	4	93.77	993.20
80	2.70E+06	1.08E+07	4	4	306	4	93.77	993.20
85	2.03E+06	1.15E+07	3	4	306	4	93.77	993.20
90	1.35E+06	1.22E+07	2	4	306	4	93.77	993.20
95	6.75E+05	1.28E+07	2	4	306	4	93.77	993.20

Table C.80 Results of power-MSF-RO-AR Configuration for July at 80% AR load

RO load %	MSF demand m^3	RO demand m^3	MSF units	RO units	AR units	NT	Fuel cost million $	CO_2 emissions ktonne
5	1.28E+07	6.75E+05	14	1	349	4	123.48	1324.90
10	1.22E+07	1.35E+06	13	1	349	4	118.94	1273.90
15	1.15E+07	2.03E+06	13	1	349	4	118.94	1273.90
20	1.08E+07	2.70E+06	12	1	349	4	114.39	1222.90
25	1.01E+07	3.38E+06	11	1	349	4	109.84	1171.90
30	9.45E+06	4.05E+06	10	2	349	4	105.29	1120.90
35	8.78E+06	4.73E+06	10	2	349	4	105.29	1120.90
40	8.10E+06	5.40E+06	9	2	349	4	100.74	1069.90
45	7.43E+06	6.08E+06	8	2	349	4	96.20	1018.90
50	6.75E+06	6.75E+06	8	2	349	4	96.20	1018.90
55	6.08E+06	7.43E+06	7	3	349	4	96.20	1018.90
60	5.40E+06	8.10E+06	6	3	349	4	96.20	1018.90
65	4.73E+06	8.78E+06	6	3	349	4	96.20	1018.90
70	4.05E+06	9.45E+06	5	3	349	4	96.20	1018.90
75	3.38E+06	1.01E+07	4	3	349	4	96.20	1018.90
80	2.70E+06	1.08E+07	4	4	349	4	96.20	1018.90
85	2.03E+06	1.15E+07	3	4	349	4	96.20	1018.90
90	1.35E+06	1.22E+07	2	4	349	4	96.20	1018.90
95	6.75E+05	1.28E+07	2	4	349	4	96.20	1018.90

Table C.81 Results of power-MSF-RO-AR Configuration for July at 90% AR load

RO load %	MSF demand m^3	RO demand m^3	MSF units	RO units	AR units	NT	Fuel cost million $	CO_2 emissions ktonne
5	1.28E+07	6.75E+05	14	1	393	4	125.62	1347.50
10	1.22E+07	1.35E+06	13	1	393	4	121.08	1296.50
15	1.15E+07	2.03E+06	13	1	393	4	121.08	1296.50
20	1.08E+07	2.70E+06	12	1	393	4	116.53	1245.60
25	1.01E+07	3.38E+06	11	1	393	4	111.98	1194.60
30	9.45E+06	4.05E+06	10	2	393	4	107.43	1143.60
35	8.78E+06	4.73E+06	10	2	393	4	107.43	1143.60
40	8.10E+06	5.40E+06	9	2	393	4	102.88	1092.60
45	7.43E+06	6.08E+06	8	2	393	4	98.34	1041.60
50	6.75E+06	6.75E+06	8	2	393	4	98.34	1041.60
55	6.08E+06	7.43E+06	7	3	393	4	98.34	1041.60
60	5.40E+06	8.10E+06	6	3	393	4	98.34	1041.60
65	4.73E+06	8.78E+06	6	3	393	4	98.34	1041.60
70	4.05E+06	9.45E+06	5	3	393	4	98.34	1041.60
75	3.38E+06	1.01E+07	4	3	393	4	98.34	1041.60
80	2.70E+06	1.08E+07	4	4	393	4	98.34	1041.60
85	2.03E+06	1.15E+07	3	4	393	4	98.34	1041.60
90	1.35E+06	1.22E+07	2	4	393	4	98.34	1041.60
95	6.75E+05	1.28E+07	2	4	393	4	98.34	1041.60

Table C.82 Results of power-MSF-RO-AR Configuration for July at 100% AR load

RO load %	MSF demand m^3	RO demand m^3	MSF units	RO units	AR units	NT	Fuel cost million $	CO_2 emissions ktonne
5	1.28E+07	6.75E+05	14	1	436	3	114.13	1231.40
10	1.22E+07	1.35E+06	13	1	436	3	109.58	1180.40
15	1.15E+07	2.03E+06	13	1	436	3	109.58	1180.40
20	1.08E+07	2.70E+06	12	1	436	3	105.03	1129.40
25	1.01E+07	3.38E+06	11	1	436	3	100.48	1078.40
30	9.45E+06	4.05E+06	10	2	436	3	95.93	1027.40
35	8.78E+06	4.73E+06	10	2	436	3	95.93	1027.40
40	8.10E+06	5.40E+06	9	2	436	3	91.39	976.43
45	7.43E+06	6.08E+06	8	2	436	3	86.84	925.45
50	6.75E+06	6.75E+06	8	2	436	3	86.84	925.45
55	6.08E+06	7.43E+06	7	3	436	4	100.08	1060.00
60	5.40E+06	8.10E+06	6	3	436	4	100.08	1060.00
65	4.73E+06	8.78E+06	6	3	436	4	100.08	1060.00
70	4.05E+06	9.45E+06	5	3	436	4	100.08	1060.00
75	3.38E+06	1.01E+07	4	3	436	4	100.08	1060.00
80	2.70E+06	1.08E+07	4	4	436	4	100.08	1060.00
85	2.03E+06	1.15E+07	3	4	436	4	100.08	1060.00
90	1.35E+06	1.22E+07	2	4	436	4	100.08	1060.00
95	6.75E+05	1.28E+07	2	4	436	4	100.08	1060.00

August

Table C.83 Results of power-MSF-RO-AR Configuration for August at 10% AR load

RO load %	MSF demand m^3	RO demand m^3	MSF units	RO units	AR units	NT	Fuel cost million $	CO_2 emissions ktonne
5	1.30E+07	6.83E+05	14	1	47	6	118.30	1258.70
10	1.23E+07	1.37E+06	13	1	47	6	113.75	1207.70
15	1.16E+07	2.05E+06	13	1	47	6	113.75	1207.70
20	1.09E+07	2.73E+06	12	1	47	6	109.20	1156.70
25	1.02E+07	3.42E+06	11	2	47	6	109.20	1156.70
30	9.56E+06	4.10E+06	11	2	47	6	109.20	1156.70
35	8.88E+06	4.78E+06	10	2	47	6	109.20	1156.70
40	8.20E+06	5.46E+06	9	2	47	6	109.20	1156.70
45	7.51E+06	6.15E+06	9	2	47	6	109.20	1156.70
50	6.83E+06	6.83E+06	8	3	47	6	109.20	1156.70
55	6.15E+06	7.51E+06	7	3	47	6	109.20	1156.70
60	5.46E+06	8.20E+06	7	3	47	6	109.20	1156.70
65	4.78E+06	8.88E+06	6	3	47	6	109.20	1156.70
70	4.10E+06	9.56E+06	5	3	47	6	109.20	1156.70
75	3.42E+06	1.02E+07	5	3	47	6	109.20	1156.70
80	2.73E+06	1.09E+07	4	4	47	6	109.20	1156.70
85	2.05E+06	1.16E+07	3	4	47	6	109.20	1156.70
90	1.37E+06	1.23E+07	3	4	47	6	109.20	1156.70
95	6.83E+05	1.30E+07	2	4	47	6	109.20	1156.70

Table C.84 Results of power-MSF-RO-AR Configuration for August at 20% AR load

RO load %	MSF demand m^3	RO demand m^3	MSF units	RO units	AR units	NT	Fuel cost million $	CO_2 emissions ktonne
5	1.30E+07	6.83E+05	14	1	94	6	122.35	1301.60
10	1.23E+07	1.37E+06	13	1	94	6	117.80	1250.60
15	1.16E+07	2.05E+06	13	1	94	6	117.80	1250.60
20	1.09E+07	2.73E+06	12	1	94	6	113.25	1199.60
25	1.02E+07	3.42E+06	11	2	94	6	113.25	1199.60
30	9.56E+06	4.10E+06	11	2	94	6	113.25	1199.60
35	8.88E+06	4.78E+06	10	2	94	6	113.25	1199.60
40	8.20E+06	5.46E+06	9	2	94	6	113.25	1199.60
45	7.51E+06	6.15E+06	9	2	94	6	113.25	1199.60
50	6.83E+06	6.83E+06	8	3	94	6	113.25	1199.60
55	6.15E+06	7.51E+06	7	3	94	6	113.25	1199.60
60	5.46E+06	8.20E+06	7	3	94	6	113.25	1199.60
65	4.78E+06	8.88E+06	6	3	94	6	113.25	1199.60
70	4.10E+06	9.56E+06	5	3	94	6	113.25	1199.60
75	3.42E+06	1.02E+07	5	3	94	6	113.25	1199.60
80	2.73E+06	1.09E+07	4	4	94	6	113.25	1199.60
85	2.05E+06	1.16E+07	3	4	94	6	113.25	1199.60
90	1.37E+06	1.23E+07	3	4	94	6	113.25	1199.60
95	6.83E+05	1.30E+07	2	4	94	6	113.25	1199.60

Table C.85 Results of power-MSF-RO-AR Configuration for August at 30% AR load

RO load %	MSF demand m^3	RO demand m^3	MSF units	RO units	AR units	NT	Fuel cost million $	CO_2 emissions ktonne
5	1.30E+07	6.83E+05	14	1	140	6	126.23	1342.70
10	1.23E+07	1.37E+06	13	1	140	6	121.68	1291.70
15	1.16E+07	2.05E+06	13	1	140	6	121.68	1291.70
20	1.09E+07	2.73E+06	12	1	140	6	117.13	1240.70
25	1.02E+07	3.42E+06	11	2	140	6	117.13	1240.70
30	9.56E+06	4.10E+06	11	2	140	6	117.13	1240.70
35	8.88E+06	4.78E+06	10	2	140	6	117.13	1240.70
40	8.20E+06	5.46E+06	9	2	140	6	117.13	1240.70
45	7.51E+06	6.15E+06	9	2	140	6	117.13	1240.70
50	6.83E+06	6.83E+06	8	3	140	6	117.13	1240.70
55	6.15E+06	7.51E+06	7	3	140	6	117.13	1240.70
60	5.46E+06	8.20E+06	7	3	140	6	117.13	1240.70
65	4.78E+06	8.88E+06	6	3	140	6	117.13	1240.70
70	4.10E+06	9.56E+06	5	3	140	6	117.13	1240.70
75	3.42E+06	1.02E+07	5	3	140	6	117.13	1240.70
80	2.73E+06	1.09E+07	4	4	140	6	117.13	1240.70
85	2.05E+06	1.16E+07	3	4	140	6	117.13	1240.70
90	1.37E+06	1.23E+07	3	4	140	6	117.13	1240.70
95	6.83E+05	1.30E+07	2	4	140	6	117	1241

Table C.86 Results of power-MSF-RO-AR Configuration for August at 40% AR load

RO load %	MSF demand m^3	RO demand m^3	MSF units	RO units	AR units	NT	Fuel cost million $	CO_2 emissions ktonne
5	1.30E+07	6.83E+05	14	1	187	5	121.54	1298.70
10	1.23E+07	1.37E+06	13	1	187	5	116.99	1247.70
15	1.16E+07	2.05E+06	13	1	187	5	116.99	1247.70
20	1.09E+07	2.73E+06	12	1	187	5	112.45	1196.70
25	1.02E+07	3.42E+06	11	2	187	5	107.90	1145.70
30	9.56E+06	4.10E+06	11	2	187	5	107.90	1145.70
35	8.88E+06	4.78E+06	10	2	187	5	103.35	1094.70
40	8.20E+06	5.46E+06	9	2	187	5	103.35	1094.70
45	7.51E+06	6.15E+06	9	2	187	5	103.35	1094.70
50	6.83E+06	6.83E+06	8	3	187	5	103.35	1094.70
55	6.15E+06	7.51E+06	7	3	187	5	103.35	1094.70
60	5.46E+06	8.20E+06	7	3	187	5	103.35	1094.70
65	4.78E+06	8.88E+06	6	3	187	5	103.35	1094.70
70	4.10E+06	9.56E+06	5	3	187	5	103.35	1094.70
75	3.42E+06	1.02E+07	5	3	187	5	103.35	1094.70
80	2.73E+06	1.09E+07	4	4	187	5	103.35	1094.70
85	2.05E+06	1.16E+07	3	4	187	5	103.35	1094.70
90	1.37E+06	1.23E+07	3	4	187	5	103.35	1094.70
95	6.83E+05	1.30E+07	2	4	187	5	103.35	1094.70

Table C.87 Results of power-MSF-RO-AR Configuration for August at 50% AR load

RO load %	MSF demand m^3	RO demand m^3	MSF units	RO units	AR units	NT	Fuel cost million $	CO_2 emissions ktonne
5	1.30E+07	6.83E+05	14	1	233	5	125.12	1336.60
10	1.23E+07	1.37E+06	13	1	233	5	120.57	1285.60
15	1.16E+07	2.05E+06	13	1	233	5	120.57	1285.60
20	1.09E+07	2.73E+06	12	1	233	5	116.02	1234.60
25	1.02E+07	3.42E+06	11	2	233	5	111.48	1183.60
30	9.56E+06	4.10E+06	11	2	233	5	111.48	1183.60
35	8.88E+06	4.78E+06	10	2	233	5	106.93	1132.60
40	8.20E+06	5.46E+06	9	2	233	5	106.93	1132.60
45	7.51E+06	6.15E+06	9	2	233	5	106.93	1132.60
50	6.83E+06	6.83E+06	8	3	233	5	106.93	1132.60
55	6.15E+06	7.51E+06	7	3	233	5	106.93	1132.60
60	5.46E+06	8.20E+06	7	3	233	5	106.93	1132.60
65	4.78E+06	8.88E+06	6	3	233	5	106.93	1132.60
70	4.10E+06	9.56E+06	5	3	233	5	106.93	1132.60
75	3.42E+06	1.02E+07	5	3	233	5	106.93	1132.60
80	2.73E+06	1.09E+07	4	4	233	5	106.93	1132.60
85	2.05E+06	1.16E+07	3	4	233	5	106.93	1132.60
90	1.37E+06	1.23E+07	3	4	233	5	106.93	1132.60
95	6.83E+05	1.30E+07	2	4	233	5	106.93	1132.60

Table C.88 Results of power-MSF-RO-AR Configuration for August at 60% AR load

RO load %	MSF demand m^3	RO demand m^3	MSF units	RO units	AR units	NT	Fuel cost million $	CO_2 emissions ktonne
5	1.30E+07	6.83E+05	14	1	280	5	128.60	1373.40
10	1.23E+07	1.37E+06	13	1	280	5	124.05	1322.40
15	1.16E+07	2.05E+06	13	1	280	5	124.05	1322.40
20	1.09E+07	2.73E+06	12	1	280	5	119.50	1271.40
25	1.02E+07	3.42E+06	11	2	280	5	114.96	1220.50
30	9.56E+06	4.10E+06	11	2	280	5	114.96	1220.50
35	8.88E+06	4.78E+06	10	2	280	5	110.41	1169.50
40	8.20E+06	5.46E+06	9	2	280	5	110.41	1169.50
45	7.51E+06	6.15E+06	9	2	280	5	110.41	1169.50
50	6.83E+06	6.83E+06	8	3	280	5	110.41	1169.50
55	6.15E+06	7.51E+06	7	3	280	5	110.41	1169.50
60	5.46E+06	8.20E+06	7	3	280	5	110.41	1169.50
65	4.78E+06	8.88E+06	6	3	280	5	110.41	1169.50
70	4.10E+06	9.56E+06	5	3	280	5	110.41	1169.50
75	3.42E+06	1.02E+07	5	3	280	5	110.41	1169.50
80	2.73E+06	1.09E+07	4	4	280	5	110.41	1169.50
85	2.05E+06	1.16E+07	3	4	280	5	110.41	1169.50
90	1.37E+06	1.23E+07	3	4	280	5	110.41	1169.50
95	6.83E+05	1.30E+07	2	4	280	5	110.41	1169.50

Table C.89 Results of power-MSF-RO-AR Configuration for August at 70% AR load

RO load %	MSF demand m^3	RO demand m^3	MSF units	RO units	AR units	NT	Fuel cost million $	CO_2 emissions ktonne
5	1.30E+07	6.83E+05	14	1	326	4	154.82	1656.80
10	1.23E+07	1.37E+06	13	1	326	4	150.27	1605.80
15	1.16E+07	2.05E+06	13	1	326	4	150.27	1605.80
20	1.09E+07	2.73E+06	12	1	326	4	145.72	1554.80
25	1.02E+07	3.42E+06	11	2	326	4	141.18	1503.80
30	9.56E+06	4.10E+06	11	2	326	4	141.18	1503.80
35	8.88E+06	4.78E+06	10	2	326	4	136.63	1452.80
40	8.20E+06	5.46E+06	9	2	326	4	132.08	1401.90
45	7.51E+06	6.15E+06	9	2	326	4	132.08	1401.90
50	6.83E+06	6.83E+06	8	3	326	4	127.53	1350.90
55	6.15E+06	7.51E+06	7	3	326	4	127.53	1350.90
60	5.46E+06	8.20E+06	7	3	326	4	127.53	1350.90
65	4.78E+06	8.88E+06	6	3	326	4	127.53	1350.90
70	4.10E+06	9.56E+06	5	3	326	4	127.53	1350.90
75	3.42E+06	1.02E+07	5	3	326	4	127.53	1350.90
80	2.73E+06	1.09E+07	4	4	326	5	113.61	1203.40
85	2.05E+06	1.16E+07	3	4	326	5	113.61	1203.40
90	1.37E+06	1.23E+07	3	4	326	5	113.61	1203.40
95	6.83E+05	1.30E+07	2	4	326	5	113.61	1203.40

Table C.90 Results of power-MSF-RO-AR Configuration for August at 80% AR load

RO load %	MSF demand m^3	RO demand m^3	MSF units	RO units	AR units	NT	Fuel cost million $	CO_2 emissions ktonne
5	1.30E+07	6.83E+05	14	1	373	4	124.70	1337.70
10	1.23E+07	1.37E+06	13	1	373	4	120.15	1286.70
15	1.16E+07	2.05E+06	13	1	373	4	120.15	1286.70
20	1.09E+07	2.73E+06	12	1	373	4	115.60	1235.70
25	1.02E+07	3.42E+06	11	2	373	4	111.05	1184.70
30	9.56E+06	4.10E+06	11	2	373	4	111.05	1184.70
35	8.88E+06	4.78E+06	10	2	373	4	106.50	1133.80
40	8.20E+06	5.46E+06	9	2	373	4	101.96	1082.80
45	7.51E+06	6.15E+06	9	2	373	4	101.96	1082.80
50	6.83E+06	6.83E+06	8	3	373	4	97.41	1031.80
55	6.15E+06	7.51E+06	7	3	373	4	97.41	1031.80
60	5.46E+06	8.20E+06	7	3	373	4	97.41	1031.80
65	4.78E+06	8.88E+06	6	3	373	4	97.41	1031.80
70	4.10E+06	9.56E+06	5	3	373	4	97.41	1031.80
75	3.42E+06	1.02E+07	5	3	373	4	97.41	1031.80
80	2.73E+06	1.09E+07	4	4	373	4	97.41	1031.80
85	2.05E+06	1.16E+07	3	4	373	4	97.41	1031.80
90	1.37E+06	1.23E+07	3	4	373	4	97.41	1031.80
95	6.83E+05	1.30E+07	2	4	373	4	97.41	1031.80

Table C.91 Results of power-MSF-RO-AR Configuration for August at 90% AR load

RO load %	MSF demand m^3	RO demand m^3	MSF units	RO units	AR units	NT	Fuel cost million $	CO_2 emissions ktonne
5	1.30E+07	6.83E+05	14	1	420	4	126.76	1359.50
10	1.23E+07	1.37E+06	13	1	420	4	122.21	1308.50
15	1.16E+07	2.05E+06	13	1	420	4	122.21	1308.50
20	1.09E+07	2.73E+06	12	1	420	4	117.66	1257.60
25	1.02E+07	3.42E+06	11	2	420	4	113.11	1206.60
30	9.56E+06	4.10E+06	11	2	420	4	113.11	1206.60
35	8.88E+06	4.78E+06	10	2	420	4	108.56	1155.60
40	8.20E+06	5.46E+06	9	2	420	4	104.02	1104.60
45	7.51E+06	6.15E+06	9	2	420	4	104.02	1104.60
50	6.83E+06	6.83E+06	8	3	420	4	99.47	1053.60
55	6.15E+06	7.51E+06	7	3	420	4	99.47	1053.60
60	5.46E+06	8.20E+06	7	3	420	4	99.47	1053.60
65	4.78E+06	8.88E+06	6	3	420	4	99.47	1053.60
70	4.10E+06	9.56E+06	5	3	420	4	99.47	1053.60
75	3.42E+06	1.02E+07	5	3	420	4	99.47	1053.60
80	2.73E+06	1.09E+07	4	4	420	4	99.47	1053.60
85	2.05E+06	1.16E+07	3	4	420	4	99.47	1053.60
90	1.37E+06	1.23E+07	3	4	420	4	99.47	1053.60
95	6.83E+05	1.30E+07	2	4	420	4	99.47	1053.60

Table C.92 Results of power-MSF-RO-AR Configuration for Augustat 100% AR load

RO load %	MSF demand m^3	RO demand m^3	MSF units	RO units	AR units	NT	Fuel cost million $	CO_2 emissions ktonne
5	1.30E+07	6.83E+05	14	1	466	3	145.22	1560.70
10	1.23E+07	1.37E+06	13	1	466	3	140.67	1509.70
15	1.16E+07	2.05E+06	13	1	466	3	140.67	1509.70
20	1.09E+07	2.73E+06	12	1	466	3	136.12	1458.70
25	1.02E+07	3.42E+06	11	2	466	3	131.57	1407.70
30	9.56E+06	4.10E+06	11	2	466	3	131.57	1407.70
35	8.88E+06	4.78E+06	10	2	466	3	127.02	1356.70
40	8.20E+06	5.46E+06	9	2	466	3	122.47	1305.70
45	7.51E+06	6.15E+06	9	2	466	3	122.47	1305.70
50	6.83E+06	6.83E+06	8	3	466	4	103.48	1096.10
55	6.15E+06	7.51E+06	7	3	466	4	103.48	1096.10
60	5.46E+06	8.20E+06	7	3	466	4	103.48	1096.10
65	4.78E+06	8.88E+06	6	3	466	4	103.48	1096.10
70	4.10E+06	9.56E+06	5	3	466	4	103.48	1096.10
75	3.42E+06	1.02E+07	5	3	466	4	103.48	1096.10
80	2.73E+06	1.09E+07	4	4	466	4	103.48	1096.10
85	2.05E+06	1.16E+07	3	4	466	4	103.48	1096.10
90	1.37E+06	1.23E+07	3	4	466	4	103.48	1096.10
95	6.83E+05	1.30E+07	2	4	466	4	103.48	1096.10

September

Table C.93 Results of power-MSF-RO-AR Configuration for September at 10% AR load

RO load %	MSF demand m^3	RO demand m^3	MSF units	RO units	AR units	NT	Fuel cost million $	CO_2 emissions ktonne
5	1.21E+07	6.39E+05	13	1	42	6	109.66	1164.30
10	1.15E+07	1.28E+06	13	1	42	6	109.66	1164.30
15	1.09E+07	1.92E+06	12	1	42	6	105.26	1114.90
20	1.02E+07	2.55E+06	12	1	42	6	105.26	1114.90
25	9.58E+06	3.19E+06	11	1	42	6	105.26	1114.90
30	8.94E+06	3.83E+06	10	2	42	6	105.26	1114.90
35	8.30E+06	4.47E+06	10	2	42	6	105.26	1114.90
40	7.66E+06	5.11E+06	9	2	42	6	105.26	1114.90
45	7.02E+06	5.75E+06	8	2	42	6	105.26	1114.90
50	6.39E+06	6.39E+06	8	2	42	6	105.26	1114.90
55	5.75E+06	7.02E+06	7	3	42	6	105.26	1114.90
60	5.11E+06	7.66E+06	6	3	42	6	105.26	1114.90
65	4.47E+06	8.30E+06	6	3	42	6	105.26	1114.90
70	3.83E+06	8.94E+06	5	3	42	6	105.26	1114.90
75	3.19E+06	9.58E+06	4	3	42	6	105.26	1114.90
80	2.55E+06	1.02E+07	4	4	42	6	105.26	1114.90
85	1.92E+06	1.09E+07	3	4	42	6	105.26	1114.90
90	1.28E+06	1.15E+07	2	4	42	6	105.26	1114.90
95	6.39E+05	1.21E+07	2	4	42	6	105.26	1114.90

Table C.94 Results of power-MSF-RO-AR Configuration for September at 20% AR load

RO load %	MSF demand m^3	RO demand m^3	MSF units	RO units	AR units	NT	Fuel cost million $	CO_2 emissions ktonne
5	1.21E+07	6.39E+05	13	1	84	5	105.00	1120.40
10	1.15E+07	1.28E+06	13	1	84	5	105.00	1120.40
15	1.09E+07	1.92E+06	12	1	84	5	100.60	1071.00
20	1.02E+07	2.55E+06	12	1	84	5	100.60	1071.00
25	9.58E+06	3.19E+06	11	1	84	5	96.20	1021.70
30	8.94E+06	3.83E+06	10	2	84	5	91.80	972.35
35	8.30E+06	4.47E+06	10	2	84	5	91.80	972.35
40	7.66E+06	5.11E+06	9	2	84	5	91.80	972.35
45	7.02E+06	5.75E+06	8	2	84	5	91.80	972.35
50	6.39E+06	6.39E+06	8	2	84	5	91.80	972.35
55	5.75E+06	7.02E+06	7	3	84	6	108.77	1152.10
60	5.11E+06	7.66E+06	6	3	84	6	108.77	1152.10
65	4.47E+06	8.30E+06	6	3	84	6	108.77	1152.10
70	3.83E+06	8.94E+06	5	3	84	6	108.77	1152.10
75	3.19E+06	9.58E+06	4	3	84	6	108.77	1152.10
80	2.55E+06	1.02E+07	4	4	84	6	108.77	1152.10
85	1.92E+06	1.09E+07	3	4	84	6	108.77	1152.10
90	1.28E+06	1.15E+07	2	4	84	6	108.77	1152.10
95	6.39E+05	1.21E+07	2	4	84	6	108.77	1152.10

Table C.95 Results of power-MSF-RO-AR Configuration for September at 30% AR load

RO load %	MSF demand m^3	RO demand m^3	MSF units	RO units	AR units	NT	Fuel cost million $	CO_2 emissions ktonne
5	1.21E+07	6.39E+05	13	1	125	5	108.34	1155.70
10	1.15E+07	1.28E+06	13	1	125	5	108.34	1155.70
15	1.09E+07	1.92E+06	12	1	125	5	103.94	1106.40
20	1.02E+07	2.55E+06	12	1	125	5	103.94	1106.40
25	9.58E+06	3.19E+06	11	1	125	5	99.54	1057.00
30	8.94E+06	3.83E+06	10	2	125	5	95.13	1007.70
35	8.30E+06	4.47E+06	10	2	125	5	95.13	1007.70
40	7.66E+06	5.11E+06	9	2	125	5	95.13	1007.70
45	7.02E+06	5.75E+06	8	2	125	5	95.13	1007.70
50	6.39E+06	6.39E+06	8	2	125	5	95.13	1007.70
55	5.75E+06	7.02E+06	7	3	125	5	95.13	1007.70
60	5.11E+06	7.66E+06	6	3	125	5	95.13	1007.70
65	4.47E+06	8.30E+06	6	3	125	5	95.13	1007.70
70	3.83E+06	8.94E+06	5	3	125	5	95.13	1007.70
75	3.19E+06	9.58E+06	4	3	125	5	95.13	1007.70
80	2.55E+06	1.02E+07	4	4	125	5	95.13	1007.70
85	1.92E+06	1.09E+07	3	4	125	5	95.13	1007.70
90	1.28E+06	1.15E+07	2	4	125	5	95.13	1007.70
95	6.39E+05	1.21E+07	2	4	125	5	95.13	1007.70

Table C.96 Results of power-MSF-RO-AR Configuration for September at 40% AR load

RO load %	MSF demand m^3	RO demand m^3	MSF units	RO units	AR units	NT	Fuel cost million $	CO_2 emissions ktonne
5	1.21E+07	6.39E+05	13	1	167	5	111.67	1191.00
10	1.15E+07	1.28E+06	13	1	167	5	111.67	1191.00
15	1.09E+07	1.92E+06	12	1	167	5	107.27	1141.70
20	1.02E+07	2.55E+06	12	1	167	5	107.27	1141.70
25	9.58E+06	3.19E+06	11	1	167	5	102.87	1092.30
30	8.94E+06	3.83E+06	10	2	167	5	98.47	1043.00
35	8.30E+06	4.47E+06	10	2	167	5	98.47	1043.00
40	7.66E+06	5.11E+06	9	2	167	5	98.47	1043.00
45	7.02E+06	5.75E+06	8	2	167	5	98.47	1043.00
50	6.39E+06	6.39E+06	8	2	167	5	98.47	1043.00
55	5.75E+06	7.02E+06	7	3	167	5	98.47	1043.00
60	5.11E+06	7.66E+06	6	3	167	5	98.47	1043.00
65	4.47E+06	8.30E+06	6	3	167	5	98.47	1043.00
70	3.83E+06	8.94E+06	5	3	167	5	98.47	1043.00
75	3.19E+06	9.58E+06	4	3	167	5	98.47	1043.00
80	2.55E+06	1.02E+07	4	4	167	5	98.47	1043.00
85	1.92E+06	1.09E+07	3	4	167	5	98.47	1043.00
90	1.28E+06	1.15E+07	2	4	167	5	98.47	1043.00
95	6.39E+05	1.21E+07	2	4	167	5	98.47	1043.00

Table C.97 Results of power-MSF-RO-AR Configuration for September at 50% AR load

RO load %	MSF demand m^3	RO demand m^3	MSF units	RO units	AR units	NT	Fuel cost million $	CO_2 emissions ktonne
5	1.21E+07	6.39E+05	13	1	208	5	114.82	1224.40
10	1.15E+07	1.28E+06	13	1	208	5	114.82	1224.40
15	1.09E+07	1.92E+06	12	1	208	5	110.42	1175.00
20	1.02E+07	2.55E+06	12	1	208	5	110.42	1175.00
25	9.58E+06	3.19E+06	11	1	208	5	106.02	1125.70
30	8.94E+06	3.83E+06	10	2	208	5	101.61	1076.30
35	8.30E+06	4.47E+06	10	2	208	5	101.61	1076.30
40	7.66E+06	5.11E+06	9	2	208	5	101.61	1076.30
45	7.02E+06	5.75E+06	8	2	208	5	101.61	1076.30
50	6.39E+06	6.39E+06	8	2	208	5	101.61	1076.30
55	5.75E+06	7.02E+06	7	3	208	5	101.61	1076.30
60	5.11E+06	7.66E+06	6	3	208	5	101.61	1076.30
65	4.47E+06	8.30E+06	6	3	208	5	101.61	1076.30
70	3.83E+06	8.94E+06	5	3	208	5	101.61	1076.30
75	3.19E+06	9.58E+06	4	3	208	5	101.61	1076.30
80	2.55E+06	1.02E+07	4	4	208	5	101.61	1076.30
85	1.92E+06	1.09E+07	3	4	208	5	101.61	1076.30
90	1.28E+06	1.15E+07	2	4	208	5	101.61	1076.30
95	6.39E+05	1.21E+07	2	4	208	5	101.61	1076.30

Table C.98 Results of power-MSF-RO-AR Configuration for September at 60% AR load

RO load %	MSF demand m^3	RO demand m^3	MSF units	RO units	AR units	NT	Fuel cost million $	CO_2 emissions ktonne
5	1.21E+07	6.39E+05	13	1	250	4	109.25	1170.80
10	1.15E+07	1.28E+06	13	1	250	4	109.25	1170.80
15	1.09E+07	1.92E+06	12	1	250	4	104.85	1121.50
20	1.02E+07	2.55E+06	12	1	250	4	104.85	1121.50
25	9.58E+06	3.19E+06	11	1	250	4	100.45	1072.20
30	8.94E+06	3.83E+06	10	2	250	4	96.05	1022.80
35	8.30E+06	4.47E+06	10	2	250	4	96.05	1022.80
40	7.66E+06	5.11E+06	9	2	250	4	91.65	973.47
45	7.02E+06	5.75E+06	8	2	250	4	87.24	924.13
50	6.39E+06	6.39E+06	8	2	250	4	87.24	924.13
55	5.75E+06	7.02E+06	7	3	250	5	104.72	1109.20
60	5.11E+06	7.66E+06	6	3	250	5	104.72	1109.20
65	4.47E+06	8.30E+06	6	3	250	5	104.72	1109.20
70	3.83E+06	8.94E+06	5	3	250	5	104.72	1109.20
75	3.19E+06	9.58E+06	4	3	250	5	104.72	1109.20
80	2.55E+06	1.02E+07	4	4	250	5	104.72	1109.20
85	1.92E+06	1.09E+07	3	4	250	5	104.72	1109.20
90	1.28E+06	1.15E+07	2	4	250	5	104.72	1109.20
95	6.39E+05	1.21E+07	2	4	250	5	104.72	1109.20

Table C.99 Results of power-MSF-RO-AR Configuration for September at 70% AR load

RO load %	MSF demand m^3	RO demand m^3	MSF units	RO units	AR units	NT	Fuel cost million $	CO_2 emissions ktonne
5	1.21E+07	6.39E+05	13	1	292	4	111.92	1199.10
10	1.15E+07	1.28E+06	13	1	292	4	111.92	1199.10
15	1.09E+07	1.92E+06	12	1	292	4	107.52	1149.70
20	1.02E+07	2.55E+06	12	1	292	4	107.52	1149.70
25	9.58E+06	3.19E+06	11	1	292	4	103.11	1100.40
30	8.94E+06	3.83E+06	10	2	292	4	98.71	1051.00
35	8.30E+06	4.47E+06	10	2	292	4	98.71	1051.00
40	7.66E+06	5.11E+06	9	2	292	4	94.31	1001.70
45	7.02E+06	5.75E+06	8	2	292	4	89.91	952.37
50	6.39E+06	6.39E+06	8	2	292	4	89.91	952.37
55	5.75E+06	7.02E+06	7	3	292	4	89.91	952.37
60	5.11E+06	7.66E+06	6	3	292	4	89.91	952.37
65	4.47E+06	8.30E+06	6	3	292	4	89.91	952.37
70	3.83E+06	8.94E+06	5	3	292	4	89.91	952.37
75	3.19E+06	9.58E+06	4	3	292	4	89.91	952.37
80	2.55E+06	1.02E+07	4	4	292	4	89.91	952.37
85	1.92E+06	1.09E+07	3	4	292	4	89.91	952.37
90	1.28E+06	1.15E+07	2	4	292	4	89.91	952.37
95	6.39E+05	1.21E+07	2	4	292	4	89.91	952.37

Table C.100 Results of power-MSF-RO-AR Configuration for September at 80% AR load

RO load %	MSF demand m^3	RO demand m^3	MSF units	RO units	AR units	NT	Fuel cost million $	CO_2 emissions ktonne
5	1.21E+07	6.39E+05	13	1	334	4	114.31	1224.50
10	1.15E+07	1.28E+06	13	1	334	4	114.31	1224.50
15	1.09E+07	1.92E+06	12	1	334	4	109.91	1175.10
20	1.02E+07	2.55E+06	12	1	334	4	109.91	1175.10
25	9.58E+06	3.19E+06	11	1	334	4	105.51	1125.80
30	8.94E+06	3.83E+06	10	2	334	4	101.11	1076.40
35	8.30E+06	4.47E+06	10	2	334	4	101.11	1076.40
40	7.66E+06	5.11E+06	9	2	334	4	96.71	1027.10
45	7.02E+06	5.75E+06	8	2	334	4	92.31	977.76
50	6.39E+06	6.39E+06	8	2	334	4	92.31	977.76
55	5.75E+06	7.02E+06	7	3	334	4	92.31	977.76
60	5.11E+06	7.66E+06	6	3	334	4	92.31	977.76
65	4.47E+06	8.30E+06	6	3	334	4	92.31	977.76
70	3.83E+06	8.94E+06	5	3	334	4	92.31	977.76
75	3.19E+06	9.58E+06	4	3	334	4	92.31	977.76
80	2.55E+06	1.02E+07	4	4	334	4	92.31	977.76
85	1.92E+06	1.09E+07	3	4	334	4	92.31	977.76
90	1.28E+06	1.15E+07	2	4	334	4	92.31	977.76
95	6.39E+05	1.21E+07	2	4	334	4	92.31	977.76

Table C.101 Results of power-MSF-RO-AR Configuration for September at 90% AR load

RO load %	MSF demand m^3	RO demand m^3	MSF units	RO units	AR units	NT	Fuel cost million $	CO_2 emissions ktonne
5	1.21E+07	6.39E+05	13	1	375	4	116.37	1246.20
10	1.15E+07	1.28E+06	13	1	375	4	116.37	1246.20
15	1.09E+07	1.92E+06	12	1	375	4	111.96	1196.80
20	1.02E+07	2.55E+06	12	1	375	4	111.96	1196.80
25	9.58E+06	3.19E+06	11	1	375	4	107.56	1147.50
30	8.94E+06	3.83E+06	10	2	375	4	103.16	1098.20
35	8.30E+06	4.47E+06	10	2	375	4	103.16	1098.20
40	7.66E+06	5.11E+06	9	2	375	4	98.76	1048.80
45	7.02E+06	5.75E+06	8	2	375	4	94.36	999.48
50	6.39E+06	6.39E+06	8	2	375	4	94.36	999.48
55	5.75E+06	7.02E+06	7	3	375	4	94.36	999.48
60	5.11E+06	7.66E+06	6	3	375	4	94.36	999.48
65	4.47E+06	8.30E+06	6	3	375	4	94.36	999.48
70	3.83E+06	8.94E+06	5	3	375	4	94.36	999.48
75	3.19E+06	9.58E+06	4	3	375	4	94.36	999.48
80	2.55E+06	1.02E+07	4	4	375	4	94.36	999.48
85	1.92E+06	1.09E+07	3	4	375	4	94.36	999.48
90	1.28E+06	1.15E+07	2	4	375	4	94.36	999.48
95	6.39E+05	1.21E+07	2	4	375	4	94.36	999.48

Table C.102 Results of power-MSF-RO-AR Configuration for September at 100% AR load

RO load %	MSF demand m^3	RO demand m^3	MSF units	RO units	AR units	NT	Fuel cost million $	CO_2 emissions ktonne
5	1.21E+07	6.39E+05	13	1	417	3	132.06	1417.90
10	1.15E+07	1.28E+06	13	1	417	3	132.06	1417.90
15	1.09E+07	1.92E+06	12	1	417	3	127.66	1368.50
20	1.02E+07	2.55E+06	12	1	417	3	127.66	1368.50
25	9.58E+06	3.19E+06	11	1	417	3	123.26	1319.20
30	8.94E+06	3.83E+06	10	2	417	3	118.85	1269.80
35	8.30E+06	4.47E+06	10	2	417	3	118.85	1269.80
40	7.66E+06	5.11E+06	9	2	417	3	114.45	1220.50
45	7.02E+06	5.75E+06	8	2	417	3	110.05	1171.10
50	6.39E+06	6.39E+06	8	2	417	3	110.05	1171.10
55	5.75E+06	7.02E+06	7	3	417	3	105.65	1121.80
60	5.11E+06	7.66E+06	6	3	417	3	101.25	1072.50
65	4.47E+06	8.30E+06	6	3	417	3	101.25	1072.50
70	3.83E+06	8.94E+06	5	3	417	3	101.25	1072.50
75	3.19E+06	9.58E+06	4	3	417	3	101.25	1072.50
80	2.55E+06	1.02E+07	4	4	417	4	96.15	1018.40
85	1.92E+06	1.09E+07	3	4	417	4	96.15	1018.40
90	1.28E+06	1.15E+07	2	4	417	4	96.15	1018.40
95	6.39E+05	1.21E+07	2	4	417	4	96.15	1018.40

October

Table C.103 Results of power-MSF-RO-AR Configuration for October at 10% AR load

RO load %	MSF demand m^3	RO demand m^3	MSF units	RO units	AR units	NT	Fuel cost million $	CO_2 emissions ktonne
5	1.15E+07	6.04E+05	13	1	25	5	103.41	1103.80
10	1.09E+07	1.21E+06	12	1	25	5	98.86	1052.80
15	1.03E+07	1.81E+06	11	1	25	5	94.32	1001.80
20	9.67E+06	2.42E+06	11	1	25	5	94.32	1001.80
25	9.06E+06	3.02E+06	10	1	25	5	89.77	950.86
30	8.46E+06	3.63E+06	10	2	25	5	89.77	950.86
35	7.86E+06	4.23E+06	9	2	25	5	89.77	950.86
40	7.25E+06	4.83E+06	8	2	25	5	89.77	950.86
45	6.65E+06	5.44E+06	8	2	25	5	89.77	950.86
50	6.04E+06	6.04E+06	7	2	25	5	89.77	950.86
55	5.44E+06	6.65E+06	7	2	25	5	89.77	950.86
60	4.83E+06	7.25E+06	6	3	25	5	89.77	950.86
65	4.23E+06	7.86E+06	5	3	25	5	89.77	950.86
70	3.63E+06	8.46E+06	5	3	25	5	89.77	950.86
75	3.02E+06	9.06E+06	4	3	25	5	89.77	950.86
80	2.42E+06	9.67E+06	4	3	25	5	89.77	950.86
85	1.81E+06	1.03E+07	3	4	25	5	89.77	950.86
90	1.21E+06	1.09E+07	2	4	25	5	89.77	950.86
95	6.04E+05	1.15E+07	2	4	25	5	89.77	950.86

Table C.104 Results of power-MSF-RO-AR Configuration for October at 20% AR load

RO load %	MSF demand m^3	RO demand m^3	MSF units	RO units	AR units	NT	Fuel cost million $	CO_2 emissions ktonne
5	1.15E+07	6.04E+05	13	1	51	4	97.24	1044.10
10	1.09E+07	1.21E+06	12	1	51	4	92.69	993.09
15	1.03E+07	1.81E+06	11	1	51	4	88.15	942.10
20	9.67E+06	2.42E+06	11	1	51	4	88.15	942.10
25	9.06E+06	3.02E+06	10	1	51	4	83.60	891.11
30	8.46E+06	3.63E+06	10	2	51	5	92.03	974.79
35	7.86E+06	4.23E+06	9	2	51	5	92.03	974.79
40	7.25E+06	4.83E+06	8	2	51	5	92.03	974.79
45	6.65E+06	5.44E+06	8	2	51	5	92.03	974.79
50	6.04E+06	6.04E+06	7	2	51	5	92.03	974.79
55	5.44E+06	6.65E+06	7	2	51	5	92.03	974.79
60	4.83E+06	7.25E+06	6	3	51	5	92.03	974.79
65	4.23E+06	7.86E+06	5	3	51	5	92.03	974.79
70	3.63E+06	8.46E+06	5	3	51	5	92.03	974.79
75	3.02E+06	9.06E+06	4	3	51	5	92.03	974.79
80	2.42E+06	9.67E+06	4	3	51	5	92.03	974.79
85	1.81E+06	1.03E+07	3	4	51	5	92.03	974.79
90	1.21E+06	1.09E+07	2	4	51	5	92.03	974.79
95	6.04E+05	1.15E+07	2	4	51	5	92.03	974.79

Table C.105 Results of power-MSF-RO-AR Configuration for October at 30% AR load

RO load %	MSF demand m^3	RO demand m^3	MSF units	RO units	AR units	NT	Fuel cost million $	CO_2 emissions ktonne
5	1.15E+07	6.04E+05	13	1	76	4	99.37	1066.60
10	1.09E+07	1.21E+06	12	1	76	4	94.83	1015.70
15	1.03E+07	1.81E+06	11	1	76	4	90.28	964.68
20	9.67E+06	2.42E+06	11	1	76	4	90.28	964.68
25	9.06E+06	3.02E+06	10	1	76	4	85.73	913.69
30	8.46E+06	3.63E+06	10	2	76	4	85.73	913.69
35	7.86E+06	4.23E+06	9	2	76	4	81.18	862.70
40	7.25E+06	4.83E+06	8	2	76	4	76.63	811.72
45	6.65E+06	5.44E+06	8	2	76	4	76.63	811.72
50	6.04E+06	6.04E+06	7	2	76	4	76.63	811.72
55	5.44E+06	6.65E+06	7	2	76	4	76.63	811.72
60	4.83E+06	7.25E+06	6	3	76	5	94.18	997.54
65	4.23E+06	7.86E+06	5	3	76	5	94.18	997.54
70	3.63E+06	8.46E+06	5	3	76	5	94.18	997.54
75	3.02E+06	9.06E+06	4	3	76	5	94.18	997.54
80	2.42E+06	9.67E+06	4	3	76	5	94.18	997.54
85	1.81E+06	1.03E+07	3	4	76	5	94.18	997.54
90	1.21E+06	1.09E+07	2	4	76	5	94.18	997.54
95	6.04E+05	1.15E+07	2	4	76	5	94.18	997.54

Table C.106 Results of power-MSF-RO-AR Configuration for October at 40% AR load

RO load %	MSF demand m^3	RO demand m^3	MSF units	RO units	AR units	NT	Fuel cost million $	CO_2 emissions ktonne
5	1.15E+07	6.04E+05	13	1	101	4	101.47	1088.80
10	1.09E+07	1.21E+06	12	1	101	4	96.92	1037.90
15	1.03E+07	1.81E+06	11	1	101	4	92.37	986.87
20	9.67E+06	2.42E+06	11	1	101	4	92.37	986.87
25	9.06E+06	3.02E+06	10	1	101	4	87.82	935.88
30	8.46E+06	3.63E+06	10	2	101	4	87.82	935.88
35	7.86E+06	4.23E+06	9	2	101	4	83.28	884.90
40	7.25E+06	4.83E+06	8	2	101	4	78.73	833.91
45	6.65E+06	5.44E+06	8	2	101	4	78.73	833.91
50	6.04E+06	6.04E+06	7	2	101	4	78.73	833.91
55	5.44E+06	6.65E+06	7	2	101	4	78.73	833.91
60	4.83E+06	7.25E+06	6	3	101	4	78.73	833.91
65	4.23E+06	7.86E+06	5	3	101	4	78.73	833.91
70	3.63E+06	8.46E+06	5	3	101	4	78.73	833.91
75	3.02E+06	9.06E+06	4	3	101	4	78.73	833.91
80	2.42E+06	9.67E+06	4	3	101	4	78.73	833.91
85	1.81E+06	1.03E+07	3	4	101	4	78.73	833.91
90	1.21E+06	1.09E+07	2	4	101	4	78.73	833.91
95	6.04E+05	1.15E+07	2	4	101	4	78.73	833.91

Table C.107 Results of power-MSF-RO-AR Configuration for October at 50% AR load

RO load %	MSF demand m^3	RO demand m^3	MSF units	RO units	AR units	NT	Fuel cost million $	CO_2 emissions ktonne
5	1.15E+07	6.04E+05	13	1	126	4	103.52	1110.60
10	1.09E+07	1.21E+06	12	1	126	4	98.98	1059.60
15	1.03E+07	1.81E+06	11	1	126	4	94.43	1008.60
20	9.67E+06	2.42E+06	11	1	126	4	94.43	1008.60
25	9.06E+06	3.02E+06	10	1	126	4	89.88	957.65
30	8.46E+06	3.63E+06	10	2	126	4	89.88	957.65
35	7.86E+06	4.23E+06	9	2	126	4	85.33	906.66
40	7.25E+06	4.83E+06	8	2	126	4	80.78	855.68
45	6.65E+06	5.44E+06	8	2	126	4	80.78	855.68
50	6.04E+06	6.04E+06	7	2	126	4	80.78	855.68
55	5.44E+06	6.65E+06	7	2	126	4	80.78	855.68
60	4.83E+06	7.25E+06	6	3	126	4	80.78	855.68
65	4.23E+06	7.86E+06	5	3	126	4	80.78	855.68
70	3.63E+06	8.46E+06	5	3	126	4	80.78	855.68
75	3.02E+06	9.06E+06	4	3	126	4	80.78	855.68
80	2.42E+06	9.67E+06	4	3	126	4	80.78	855.68
85	1.81E+06	1.03E+07	3	4	126	4	80.78	855.68
90	1.21E+06	1.09E+07	2	4	126	4	80.78	855.68
95	6.04E+05	1.15E+07	2	4	126	4	80.78	855.68

Table C.108 Results of power-MSF-RO-AR Configuration for October at 60% AR load

RO load %	MSF demand m^3	RO demand m^3	MSF units	RO units	AR units	NT	Fuel cost million $	CO_2 emissions ktonne
5	1.15E+07	6.04E+05	13	1	151	4	105.53	1131.90
10	1.09E+07	1.21E+06	12	1	151	4	100.98	1080.90
15	1.03E+07	1.81E+06	11	1	151	4	96.44	1029.90
20	9.67E+06	2.42E+06	11	1	151	4	96.44	1029.90
25	9.06E+06	3.02E+06	10	1	151	4	91.89	978.92
30	8.46E+06	3.63E+06	10	2	151	4	91.89	978.92
35	7.86E+06	4.23E+06	9	2	151	4	87.34	927.93
40	7.25E+06	4.83E+06	8	2	151	4	82.79	876.95
45	6.65E+06	5.44E+06	8	2	151	4	82.79	876.95
50	6.04E+06	6.04E+06	7	2	151	4	82.79	876.95
55	5.44E+06	6.65E+06	7	2	151	4	82.79	876.95
60	4.83E+06	7.25E+06	6	3	151	4	82.79	876.95
65	4.23E+06	7.86E+06	5	3	151	4	82.79	876.95
70	3.63E+06	8.46E+06	5	3	151	4	82.79	876.95
75	3.02E+06	9.06E+06	4	3	151	4	82.79	876.95
80	2.42E+06	9.67E+06	4	3	151	4	82.79	876.95
85	1.81E+06	1.03E+07	3	4	151	4	82.79	876.95
90	1.21E+06	1.09E+07	2	4	151	4	82.79	876.95
95	6.04E+05	1.15E+07	2	4	151	4	82.79	876.95

Table C.109 Results of power-MSF-RO-AR Configuration for October at 70% AR load

RO load %	MSF demand m^3	RO demand m^3	MSF units	RO units	AR units	NT	Fuel cost million $	CO_2 emissions ktonne
5	1.15E+07	6.04E+05	13	1	177	4	107.56	1153.40
10	1.09E+07	1.21E+06	12	1	177	4	103.02	1102.40
15	1.03E+07	1.81E+06	11	1	177	4	98.47	1051.40
20	9.67E+06	2.42E+06	11	1	177	4	98.47	1051.40
25	9.06E+06	3.02E+06	10	1	177	4	93.92	1000.40
30	8.46E+06	3.63E+06	10	2	177	4	93.92	1000.40
35	7.86E+06	4.23E+06	9	2	177	4	89.37	949.46
40	7.25E+06	4.83E+06	8	2	177	4	84.82	898.48
45	6.65E+06	5.44E+06	8	2	177	4	84.82	898.48
50	6.04E+06	6.04E+06	7	2	177	4	84.82	898.48
55	5.44E+06	6.65E+06	7	2	177	4	84.82	898.48
60	4.83E+06	7.25E+06	6	3	177	4	84.82	898.48
65	4.23E+06	7.86E+06	5	3	177	4	84.82	898.48
70	3.63E+06	8.46E+06	5	3	177	4	84.82	898.48
75	3.02E+06	9.06E+06	4	3	177	4	84.82	898.48
80	2.42E+06	9.67E+06	4	3	177	4	84.82	898.48
85	1.81E+06	1.03E+07	3	4	177	4	84.82	898.48
90	1.21E+06	1.09E+07	2	4	177	4	84.82	898.48
95	6.04E+05	1.15E+07	2	4	177	4	84.82	898.48

Table C.110 Results of power-MSF-RO-AR Configuration for October at 80% AR load

RO load %	MSF demand m^3	RO demand m^3	MSF units	RO units	AR units	NT	Fuel cost million $	CO_2 emissions ktonne
5	1.15E+07	6.04E+05	13	1	202	4	109.46	1173.50
10	1.09E+07	1.21E+06	12	1	202	4	104.91	1122.50
15	1.03E+07	1.81E+06	11	1	202	4	100.36	1071.50
20	9.67E+06	2.42E+06	11	1	202	4	100.36	1071.50
25	9.06E+06	3.02E+06	10	1	202	4	95.81	1020.50
30	8.46E+06	3.63E+06	10	2	202	4	95.81	1020.50
35	7.86E+06	4.23E+06	9	2	202	4	91.26	969.51
40	7.25E+06	4.83E+06	8	2	202	4	86.72	918.53
45	6.65E+06	5.44E+06	8	2	202	4	86.72	918.53
50	6.04E+06	6.04E+06	7	2	202	4	86.72	918.53
55	5.44E+06	6.65E+06	7	2	202	4	86.72	918.53
60	4.83E+06	7.25E+06	6	3	202	4	86.72	918.53
65	4.23E+06	7.86E+06	5	3	202	4	86.72	918.53
70	3.63E+06	8.46E+06	5	3	202	4	86.72	918.53
75	3.02E+06	9.06E+06	4	3	202	4	86.72	918.53
80	2.42E+06	9.67E+06	4	3	202	4	86.72	918.53
85	1.81E+06	1.03E+07	3	4	202	4	86.72	918.53
90	1.21E+06	1.09E+07	2	4	202	4	86.72	918.53
95	6.04E+05	1.15E+07	2	4	202	4	86.72	918.53

Table C.111 Results of power-MSF-RO-AR Configuration for October at 90% AR load

RO load %	MSF demand m^3	RO demand m^3	MSF units	RO units	AR units	NT	Fuel cost million $	CO_2 emissions ktonne
5	1.15E+07	6.04E+05	13	1	227	3	102.01	1100.20
10	1.09E+07	1.21E+06	12	1	227	3	97.46	1049.20
15	1.03E+07	1.81E+06	11	1	227	3	92.91	998.23
20	9.67E+06	2.42E+06	11	1	227	3	92.91	998.23
25	9.06E+06	3.02E+06	10	1	227	3	88.37	947.25
30	8.46E+06	3.63E+06	10	2	227	3	88.37	947.25
35	7.86E+06	4.23E+06	9	2	227	3	83.82	896.26
40	7.25E+06	4.83E+06	8	2	227	3	79.27	845.27
45	6.65E+06	5.44E+06	8	2	227	3	79.27	845.27
50	6.04E+06	6.04E+06	7	2	227	3	74.72	794.29
55	5.44E+06	6.65E+06	7	2	227	3	74.72	794.29
60	4.83E+06	7.25E+06	6	3	227	4	88.54	937.86
65	4.23E+06	7.86E+06	5	3	227	4	88.54	937.86
70	3.63E+06	8.46E+06	5	3	227	4	88.54	937.86
75	3.02E+06	9.06E+06	4	3	227	4	88.54	937.86
80	2.42E+06	9.67E+06	4	3	227	4	88.54	937.86
85	1.81E+06	1.03E+07	3	4	227	4	88.54	937.86
90	1.21E+06	1.09E+07	2	4	227	4	88.54	937.86
95	6.04E+05	1.15E+07	2	4	227	4	88.54	937.86

Table C.112 Results of power-MSF-RO-AR Configuration for October at 100% AR load

RO load %	MSF demand m^3	RO demand m^3	MSF units	RO units	AR units	NT	Fuel cost million $	CO_2 emissions ktonne
5	1.15E+07	6.04E+05	13	1	252	3	103.46	1115.50
10	1.09E+07	1.21E+06	12	1	252	3	98.91	1064.60
15	1.03E+07	1.81E+06	11	1	252	3	94.36	1013.60
20	9.67E+06	2.42E+06	11	1	252	3	94.36	1013.60
25	9.06E+06	3.02E+06	10	1	252	3	89.81	962.59
30	8.46E+06	3.63E+06	10	2	252	3	89.81	962.59
35	7.86E+06	4.23E+06	9	2	252	3	85.27	911.60
40	7.25E+06	4.83E+06	8	2	252	3	80.72	860.61
45	6.65E+06	5.44E+06	8	2	252	3	80.72	860.61
50	6.04E+06	6.04E+06	7	2	252	3	76.17	809.63
55	5.44E+06	6.65E+06	7	2	252	3	76.17	809.63
60	4.83E+06	7.25E+06	6	3	252	3	71.62	758.64
65	4.23E+06	7.86E+06	5	3	252	3	71.62	758.64
70	3.63E+06	8.46E+06	5	3	252	3	71.62	758.64
75	3.02E+06	9.06E+06	4	3	252	3	71.62	758.64
80	2.42E+06	9.67E+06	4	3	252	3	71.62	758.64
85	1.81E+06	1.03E+07	3	4	252	4	90.29	956.38
90	1.21E+06	1.09E+07	2	4	252	4	90.29	956.38
95	6.04E+05	1.15E+07	2	4	252	4	90.29	956.38

November

Table C.113 Results of power-MSF-RO-AR Configuration for November at 10% AR load

RO load %	MSF demand m^3	RO demand m^3	MSF units	RO units	AR units	NT	Fuel cost million $	CO_2 emissions ktonne
5	1.13E+07	5.95E+05	13	1	13	4	90.91	976.58
10	1.07E+07	1.19E+06	12	1	13	4	86.51	927.24
15	1.01E+07	1.78E+06	11	1	13	4	82.11	877.90
20	9.52E+06	2.38E+06	11	1	13	4	82.11	877.90
25	8.92E+06	2.97E+06	10	1	13	4	77.71	828.55
30	8.33E+06	3.57E+06	10	2	13	4	77.71	828.55
35	7.73E+06	4.16E+06	9	2	13	4	73.31	779.21
40	7.14E+06	4.76E+06	8	2	13	4	68.91	729.87
45	6.54E+06	5.35E+06	8	2	13	4	68.91	729.87
50	5.95E+06	5.95E+06	7	2	13	4	68.91	729.87
55	5.35E+06	6.54E+06	7	2	13	4	68.91	729.87
60	4.76E+06	7.14E+06	6	3	13	4	68.91	729.87
65	4.16E+06	7.73E+06	5	3	13	4	68.91	729.87
70	3.57E+06	8.33E+06	5	3	13	4	68.91	729.87
75	2.97E+06	8.92E+06	4	3	13	4	68.91	729.87
80	2.38E+06	9.52E+06	4	3	13	4	68.91	729.87
85	1.78E+06	1.01E+07	3	4	13	4	68.91	729.87
90	1.19E+06	1.07E+07	2	4	13	4	68.91	729.87
95	5.95E+05	1.13E+07	2	4	13	4	68.91	729.87

Table C.114 Results of power-MSF-RO-AR Configuration for November at 20% AR load

RO load %	MSF demand m^3	RO demand m^3	MSF units	RO units	AR units	NT	Fuel cost million $	CO_2 emissions ktonne
5	1.13E+07	5.95E+05	13	1	25	3	83.78	906.43
10	1.07E+07	1.19E+06	12	1	25	3	79.38	857.09
15	1.01E+07	1.78E+06	11	1	25	3	74.97	807.74
20	9.52E+06	2.38E+06	11	1	25	3	74.97	807.74
25	8.92E+06	2.97E+06	10	1	25	3	70.57	758.40
30	8.33E+06	3.57E+06	10	2	25	4	78.72	839.31
35	7.73E+06	4.16E+06	9	2	25	4	74.32	789.96
40	7.14E+06	4.76E+06	8	2	25	4	69.92	740.62
45	6.54E+06	5.35E+06	8	2	25	4	69.92	740.62
50	5.95E+06	5.95E+06	7	2	25	4	69.92	740.62
55	5.35E+06	6.54E+06	7	2	25	4	69.92	740.62
60	4.76E+06	7.14E+06	6	3	25	4	69.92	740.62
65	4.16E+06	7.73E+06	5	3	25	4	69.92	740.62
70	3.57E+06	8.33E+06	5	3	25	4	69.92	740.62
75	2.97E+06	8.92E+06	4	3	25	4	69.92	740.62
80	2.38E+06	9.52E+06	4	3	25	4	69.92	740.62
85	1.78E+06	1.01E+07	3	4	25	4	69.92	740.62
90	1.19E+06	1.07E+07	2	4	25	4	69.92	740.62
95	5.95E+05	1.13E+07	2	4	25	4	69.92	740.62

Table C.115 Results of power-MSF-RO-AR Configuration for November at 30% AR load

RO load %	MSF demand m^3	RO demand m^3	MSF units	RO units	AR units	NT	Fuel cost million $	CO_2 emissions ktonne
5	1.13E+07	5.95E+05	13	1	38	3	84.86	917.93
10	1.07E+07	1.19E+06	12	1	38	3	80.46	868.59
15	1.01E+07	1.78E+06	11	1	38	3	76.06	819.25
20	9.52E+06	2.38E+06	11	1	38	3	76.06	819.25
25	8.92E+06	2.97E+06	10	1	38	3	71.66	769.91
30	8.33E+06	3.57E+06	10	2	38	4	79.82	850.88
35	7.73E+06	4.16E+06	9	2	38	4	75.41	801.54
40	7.14E+06	4.76E+06	8	2	38	4	71.01	752.19
45	6.54E+06	5.35E+06	8	2	38	4	71.01	752.19
50	5.95E+06	5.95E+06	7	2	38	4	71.01	752.19
55	5.35E+06	6.54E+06	7	2	38	4	71.01	752.19
60	4.76E+06	7.14E+06	6	3	38	4	71.01	752.19
65	4.16E+06	7.73E+06	5	3	38	4	71.01	752.19
70	3.57E+06	8.33E+06	5	3	38	4	71.01	752.19
75	2.97E+06	8.92E+06	4	3	38	4	71.01	752.19
80	2.38E+06	9.52E+06	4	3	38	4	71.01	752.19
85	1.78E+06	1.01E+07	3	4	38	4	71.01	752.19
90	1.19E+06	1.07E+07	2	4	38	4	71.01	752.19
95	5.95E+05	1.13E+07	2	4	38	4	71.01	752.19

Table C.116 Results of power-MSF-RO-AR Configuration for November at 40% AR load

RO load %	MSF demand m^3	RO demand m^3	MSF units	RO units	AR units	NT	Fuel cost million $	CO_2 emissions ktonne
5	1.13E+07	5.95E+05	13	1	50	3	85.86	928.45
10	1.07E+07	1.19E+06	12	1	50	3	81.45	879.11
15	1.01E+07	1.78E+06	11	1	50	3	77.05	829.77
20	9.52E+06	2.38E+06	11	1	50	3	77.05	829.77
25	8.92E+06	2.97E+06	10	1	50	3	72.65	780.43
30	8.33E+06	3.57E+06	10	2	50	4	80.82	861.49
35	7.73E+06	4.16E+06	9	2	50	4	76.42	812.15
40	7.14E+06	4.76E+06	8	2	50	4	72.01	762.80
45	6.54E+06	5.35E+06	8	2	50	4	72.01	762.80
50	5.95E+06	5.95E+06	7	2	50	4	72.01	762.80
55	5.35E+06	6.54E+06	7	2	50	4	72.01	762.80
60	4.76E+06	7.14E+06	6	3	50	4	72.01	762.80
65	4.16E+06	7.73E+06	5	3	50	4	72.01	762.80
70	3.57E+06	8.33E+06	5	3	50	4	72.01	762.80
75	2.97E+06	8.92E+06	4	3	50	4	72.01	762.80
80	2.38E+06	9.52E+06	4	3	50	4	72.01	762.80
85	1.78E+06	1.01E+07	3	4	50	4	72.01	762.80
90	1.19E+06	1.07E+07	2	4	50	4	72.01	762.80
95	5.95E+05	1.13E+07	2	4	50	4	72.01	762.80

Table C.117 Results of power-MSF-RO-AR Configuration for November at 50% AR load

RO load %	MSF demand m^3	RO demand m^3	MSF units	RO units	AR units	NT	Fuel cost million $	CO_2 emissions ktonne
5	1.13E+07	5.95E+05	13	1	63	3	86.92	939.73
10	1.07E+07	1.19E+06	12	1	63	3	82.52	890.38
15	1.01E+07	1.78E+06	11	1	63	3	78.12	841.04
20	9.52E+06	2.38E+06	11	1	63	3	78.12	841.04
25	8.92E+06	2.97E+06	10	1	63	3	73.72	791.70
30	8.33E+06	3.57E+06	10	2	63	3	73.72	791.70
35	7.73E+06	4.16E+06	9	2	63	3	69.31	742.36
40	7.14E+06	4.76E+06	8	2	63	3	64.91	693.02
45	6.54E+06	5.35E+06	8	2	63	3	64.91	693.02
50	5.95E+06	5.95E+06	7	2	63	3	60.51	643.68
55	5.35E+06	6.54E+06	7	2	63	3	60.51	643.68
60	4.76E+06	7.14E+06	6	3	63	4	73.09	774.22
65	4.16E+06	7.73E+06	5	3	63	4	73.09	774.22
70	3.57E+06	8.33E+06	5	3	63	4	73.09	774.22
75	2.97E+06	8.92E+06	4	3	63	4	73.09	774.22
80	2.38E+06	9.52E+06	4	3	63	4	73.09	774.22
85	1.78E+06	1.01E+07	3	4	63	4	73.09	774.22
90	1.19E+06	1.07E+07	2	4	63	4	73.09	774.22
95	5.95E+05	1.13E+07	2	4	63	4	73.09	774.22

Table C.118 Results of power-MSF-RO-AR Configuration for November at 60% AR load

RO load %	MSF demand m^3	RO demand m^3	MSF units	RO units	AR units	NT	Fuel cost million $	CO_2 emissions ktonne
5	1.13E+07	5.95E+05	13	1	75	3	87.89	950.01
10	1.07E+07	1.19E+06	12	1	75	3	83.49	900.67
15	1.01E+07	1.78E+06	11	1	75	3	79.09	851.33
20	9.52E+06	2.38E+06	11	1	75	3	79.09	851.33
25	8.92E+06	2.97E+06	10	1	75	3	74.69	801.99
30	8.33E+06	3.57E+06	10	2	75	3	74.69	801.99
35	7.73E+06	4.16E+06	9	2	75	3	70.29	752.64
40	7.14E+06	4.76E+06	8	2	75	3	65.88	703.30
45	6.54E+06	5.35E+06	8	2	75	3	65.88	703.30
50	5.95E+06	5.95E+06	7	2	75	3	61.48	653.96
55	5.35E+06	6.54E+06	7	2	75	3	61.48	653.96
60	4.76E+06	7.14E+06	6	3	75	4	74.08	784.67
65	4.16E+06	7.73E+06	5	3	75	4	74.08	784.67
70	3.57E+06	8.33E+06	5	3	75	4	74.08	784.67
75	2.97E+06	8.92E+06	4	3	75	4	74.08	784.67
80	2.38E+06	9.52E+06	4	3	75	4	74.08	784.67
85	1.78E+06	1.01E+07	3	4	75	4	74.08	784.67
90	1.19E+06	1.07E+07	2	4	75	4	74.08	784.67
95	5.95E+05	1.13E+07	2	4	75	4	74.08	784.67

Table C.119 Results of power-MSF-RO-AR Configuration for November at 70% AR load

RO load %	MSF demand m^3	RO demand m^3	MSF units	RO units	AR units	NT	Fuel cost million $	CO_2 emissions ktonne
5	1.13E+07	5.95E+05	13	1	88	3	88.93	961.01
10	1.07E+07	1.19E+06	12	1	88	3	84.53	911.67
15	1.01E+07	1.78E+06	11	1	88	3	80.13	862.32
20	9.52E+06	2.38E+06	11	1	88	3	80.13	862.32
25	8.92E+06	2.97E+06	10	1	88	3	75.72	812.98
30	8.33E+06	3.57E+06	10	2	88	3	75.72	812.98
35	7.73E+06	4.16E+06	9	2	88	3	71.32	763.64
40	7.14E+06	4.76E+06	8	2	88	3	66.92	714.30
45	6.54E+06	5.35E+06	8	2	88	3	66.92	714.30
50	5.95E+06	5.95E+06	7	2	88	3	62.52	664.96
55	5.35E+06	6.54E+06	7	2	88	3	62.52	664.96
60	4.76E+06	7.14E+06	6	3	88	3	58.12	615.62
65	4.16E+06	7.73E+06	5	3	88	3	58.12	615.62
70	3.57E+06	8.33E+06	5	3	88	3	58.12	615.62
75	2.97E+06	8.92E+06	4	3	88	3	58.12	615.62
80	2.38E+06	9.52E+06	4	3	88	3	58.12	615.62
85	1.78E+06	1.01E+07	3	4	88	4	75.14	795.89
90	1.19E+06	1.07E+07	2	4	88	4	75.14	795.89
95	5.95E+05	1.13E+07	2	4	88	4	75.14	795.89

Table C.120 Results of power-MSF-RO-AR Configuration for November at 80% AR load

RO load %	MSF demand m^3	RO demand m^3	MSF units	RO units	AR units	NT	Fuel cost million $	CO_2 emissions ktonne
5	1.13E+07	5.95E+05	13	1	100	3	89.87	971.01
10	1.07E+07	1.19E+06	12	1	100	3	85.47	921.67
15	1.01E+07	1.78E+06	11	1	100	3	81.07	872.33
20	9.52E+06	2.38E+06	11	1	100	3	81.07	872.33
25	8.92E+06	2.97E+06	10	1	100	3	76.67	822.99
30	8.33E+06	3.57E+06	10	2	100	3	76.67	822.99
35	7.73E+06	4.16E+06	9	2	100	3	72.27	773.65
40	7.14E+06	4.76E+06	8	2	100	3	67.87	724.31
45	6.54E+06	5.35E+06	8	2	100	3	67.87	724.31
50	5.95E+06	5.95E+06	7	2	100	3	63.47	674.96
55	5.35E+06	6.54E+06	7	2	100	3	63.47	674.96
60	4.76E+06	7.14E+06	6	3	100	3	59.06	625.62
65	4.16E+06	7.73E+06	5	3	100	3	59.06	625.62
70	3.57E+06	8.33E+06	5	3	100	3	59.06	625.62
75	2.97E+06	8.92E+06	4	3	100	3	59.06	625.62
80	2.38E+06	9.52E+06	4	3	100	3	59.06	625.62
85	1.78E+06	1.01E+07	3	4	100	4	76.11	806.16
90	1.19E+06	1.07E+07	2	4	100	4	76.11	806.16
95	5.95E+05	1.13E+07	2	4	100	4	76.11	806.16

Table C.121 Results of power-MSF-RO-AR Configuration for November at 90% AR load

RO load %	MSF demand m^3	RO demand m^3	MSF units	RO units	AR units	NT	Fuel cost million $	CO_2 emissions ktonne
5	1.13E+07	5.95E+05	13	1	113	3	90.88	981.68
10	1.07E+07	1.19E+06	12	1	113	3	86.48	932.34
15	1.01E+07	1.78E+06	11	1	113	3	82.08	883.00
20	9.52E+06	2.38E+06	11	1	113	3	82.08	883.00
25	8.92E+06	2.97E+06	10	1	113	3	77.68	833.66
30	8.33E+06	3.57E+06	10	2	113	3	77.68	833.66
35	7.73E+06	4.16E+06	9	2	113	3	73.28	784.31
40	7.14E+06	4.76E+06	8	2	113	3	68.87	734.97
45	6.54E+06	5.35E+06	8	2	113	3	68.87	734.97
50	5.95E+06	5.95E+06	7	2	113	3	64.47	685.63
55	5.35E+06	6.54E+06	7	2	113	3	64.47	685.63
60	4.76E+06	7.14E+06	6	3	113	3	60.07	636.29
65	4.16E+06	7.73E+06	5	3	113	3	60.07	636.29
70	3.57E+06	8.33E+06	5	3	113	3	60.07	636.29
75	2.97E+06	8.92E+06	4	3	113	3	60.07	636.29
80	2.38E+06	9.52E+06	4	3	113	3	60.07	636.29
85	1.78E+06	1.01E+07	3	4	113	4	77.15	817.18
90	1.19E+06	1.07E+07	2	4	113	4	77.15	817.18
95	5.95E+05	1.13E+07	2	4	113	4	77.15	817.18

Table C.122 Results of power-MSF-RO-AR Configuration for November at 100% AR load

RO load %	MSF demand m^3	RO demand m^3	MSF units	RO units	AR units	NT	Fuel cost million $	CO_2 emissions ktonne
5	1.13E+07	5.95E+05	13	1	125	3	91.79	991.36
10	1.07E+07	1.19E+06	12	1	125	3	87.39	942.01
15	1.01E+07	1.78E+06	11	1	125	3	82.99	892.67
20	9.52E+06	2.38E+06	11	1	125	3	82.99	892.67
25	8.92E+06	2.97E+06	10	1	125	3	78.59	843.33
30	8.33E+06	3.57E+06	10	2	125	3	78.59	843.33
35	7.73E+06	4.16E+06	9	2	125	3	74.19	793.99
40	7.14E+06	4.76E+06	8	2	125	3	69.79	744.65
45	6.54E+06	5.35E+06	8	2	125	3	69.79	744.65
50	5.95E+06	5.95E+06	7	2	125	3	65.39	695.31
55	5.35E+06	6.54E+06	7	2	125	3	65.39	695.31
60	4.76E+06	7.14E+06	6	3	125	3	60.98	645.97
65	4.16E+06	7.73E+06	5	3	125	3	60.98	645.97
70	3.57E+06	8.33E+06	5	3	125	3	60.98	645.97
75	2.97E+06	8.92E+06	4	3	125	3	60.98	645.97
80	2.38E+06	9.52E+06	4	3	125	3	60.98	645.97
85	1.78E+06	1.01E+07	3	4	125	3	60.98	645.97
90	1.19E+06	1.07E+07	2	4	125	3	60.98	645.97
95	5.95E+05	1.13E+07	2	4	125	3	60.98	645.97